

# Development and characterization of immunogenic genetically engineered mouse models of pancreatic cancer

By

Laurens J. Lambert

MSc, Medical Biology  
Radboud University, 2014

Submitted to the Department of Biology  
in Partial Fulfillment of the Requirements for the Degree of

Doctor of Philosophy  
at the

MASSACHUSETTS INSTITUTE OF TECHNOLOGY

September 2020

© 2020 Massachusetts Institute of Technology. All rights reserved.

Signature of Author.....

Laurens J. Lambert  
Department of Biology  
June 16, 2020

Certified by.....

Tyler Jacks  
David H. Koch Professor of Biology  
Investigator, Howard Hughes Medical Institute  
Thesis Supervisor

Accepted by.....

Stephen Bell  
Uncas and Helen Whitaker Professor of Biology  
Investigator, Howard Hughes Medical Institute  
Co-Director, Biology Graduate Committee



# Development and characterization of immunogenic genetically engineered mouse models of pancreatic cancer

By

Laurens J. Lambert

Submitted to the Department of Biology on June 16, 2020 in Partial Fulfillment of the Requirements for the Degree of Doctor of Philosophy in Biology

## Abstract

Insights into mechanisms of immune escape have fueled the clinical success of immunotherapy in many cancers. However, pancreatic cancer has remained largely refractory to checkpoint immunotherapy. To uncover mechanisms of immune escape, we have characterized two preclinical models of immunogenic pancreatic ductal adenocarcinoma (PDAC). In order to dissect the endogenous antigen-specific T cell response in PDAC, lentivirus encoding the Cre recombinase and a tumor specific antigen (SIINFEKL, OVA<sub>257-264</sub>) was delivered to *Kras*<sup>LSL-G12D/+</sup>; *Trp53*<sup>flox/flox</sup> (KP) mice. We demonstrate that KP tumors show distinct antigenic outcomes: a subset of PDAC tumors undergoes clearance or editing by a robust antigen-specific CD8<sup>+</sup> T cell response, while a fraction undergo immune escape.

Subsequently, we have developed an immunogenic pancreatic tumor organoid orthotopic transplant model. In this model, immunogenic pancreatic tumors manifest divergent tumor phenotypes; 40% of tumor organoids do not form tumors (“non-progressors”), whereas 50% of organoids form aggressive tumors despite maintaining antigen expression and a demonstrable T cell response (“progressors”). Additionally, a subset (10%) of tumors show an intermediate phenotype, possibly reflective of an immune equilibrium state. We have further phenotypically and transcriptionally characterized the CD8<sup>+</sup> T cell response to understand immune escape in this model. Our analyses reveal unexpected T cell heterogeneity, and acquisition of T cell dysfunctionality. Therapeutic combinatorial targeting of co-inhibitory receptors identified on dysfunctional antigen-specific CD8<sup>+</sup> T cells led to dramatic regression of aggressive pancreatic tumors. Finally, we demonstrate that human CD8<sup>+</sup> T cells isolated from pancreatic tumors co-express co-inhibitory receptors, suggesting that T cell dysfunction may be operational in human disease.

This is the first demonstration of immunoediting in an autochthonous and organoid-based model of pancreatic cancer. Further characterization of these preclinical model systems will enable rational design of novel clinical immunotherapeutic strategies for treatment of this devastating disease.

Thesis Advisor: Tyler Jacks

Title: Professor of Biology

# Curriculum vitae

## Laurens J. Lambert

### Education

---

2014 - Present **MASSACHUSETTS INSTITUTE OF TECHNOLOGY (CAMBRIDGE, MA, USA)**  
PhD, Department of Biology, The Jacks Lab

2009 - 2014 **RADBOD UNIVERSITY (NIJMEGEN, NETHERLANDS)**  
Bachelor of Science in Biology  
Master of Science in Medical Biology, Cum Laude

### Professional Experience

---

May 2015- Present **The David Koch Institute for Integrative Cancer Research, MIT (Tyler Jacks Laboratory)**  
**PhD Student**

- Developed novel pancreatic cancer mouse models and characterized the T cell response in these models.
- Discovered a therapeutic checkpoint combination with clinical translatability.
- Co-led a pancreas research team in the Jacks lab and coordinated with internal and external collaborators (Koch Institute, DFCI).
- Authored a chapter in a major textbook and submitted a manuscript to Nature (under review).

Jan. 2020- Present **MPM Capital (Cambridge, MA)**  
**Consultant**

- Supported key company-formation activities through the technical evaluation of scientific fields and identification of high priority development candidates.
- Presented progress in weekly strategy meetings with the founding team at MPM Capital.

April 2019- Dec. 2019 **Vida Ventures (Boston, MA)**  
**Fellow**

- Evaluated the scientific evidence, clinical paradigms, and commercial landscape to support 15+ investment decisions for the team at the Boston office.
- Performed technical diligence on a Vida investment (Kinnate Biopharma, Series B closed Dec. 2019).

Fall 2018     **Merrimack Pharmaceuticals (Cambridge, MA)**  
**Graduate Intern**

- Participated in the selective “Research Experience in Biopharma” course and interned at Merrimack Pharmaceuticals for the semester.
- Assisted in target validation of the TNFR1I preclinical immunology program (MM-401).

**Scientific Publications**

---

Freed-Pastor W\*, Lambert LJ\*, Mercer K, Pattada N, Garcia A, Ely Z, Hwang W, Lin L, Eng G, Westcott P, Yilmaz O, Jacks T (2020). Immunogenic models of pancreatic adenocarcinoma reveal the therapeutic benefit of novel checkpoint combinations. Manuscript under review (Nature). \*Co-authors

Lambert LJ, Muzumdar MD, Rideout III WM, Jacks T (2017). Chapter 15: Harnessing the Mouse for Biomedical Research, in Basic Science Methods for Clinical Researchers, ed. Jalali M, Saldanha FYL and Jalali M, Academic Press

Wefers C, Lambert LJ, Torensma R, Hato SV (2015). Cellular immunotherapy in ovarian cancer: Targeting the stem of recurrence. Gynecologic Oncology 137(2)

Lambert LJ, Walker S, Feltham J, Lee HJ, Reik W, Houseley J (2013). Etoposide Induces Nuclear Re-Localisation of AID. PLoS ONE 8(12)

**Teaching & Leadership Experience**

---

Sep. 2018- Present     **Co-Director, Industry Initiative team**  
MIT Biotech Group (MBG)

Fall 2017     **Teaching Assistant**, Hallmarks of Cancer (7.45/7.85), MIT

Fall 2015     **Teaching Assistant**, Introductory Biology (7.016), MIT

**Awards & Grants**

---

- Koch Institute Graduate Fellowship (2018)
- Praecis Pharmaceuticals MIT Presidential Fellowship (2014)
- Radboud University Excellence Grant (2012)
- Erasmus Lifelong Learning Training Grant (2011)

# Acknowledgments

I am extremely grateful for the past 6 years in the Jacks Lab. I have grown tremendously as a scientist, as a mentor, as an educator, and most of all as a person during my PhD. I firmly believe that the skills and life lessons instilled through my graduate training have prepared me well as I pursue the next chapter in my career.

In the Jacks Lab, I have had the privilege to work alongside an amazing group of smart and passionate people. I have benefited so much from the experience and scientific knowledge shared, and the friendships formed along the way. Without the tireless dedication of many people in and outside the lab, support and advice from many colleagues, friends and loved ones, the work in this thesis would not have been possible.

I have many people to thank...

First and foremost, I would like to thank my thesis supervisor, Tyler, for letting me join the lab and for incredible mentorship during my graduate studies. From the early days in the lab, you have given me the freedom to pursue my interests in immunotherapy, trusted me to fail and succeed when I needed to, and through it all challenged me to think “two steps ahead”. I have also appreciated that you have always had my career at heart, and have allowed me to explore my interests in biotech while completing my PhD. Your leadership, thoughtfulness, rigor and generosity are truly inspiring to me, and are qualities I will strive for in the rest of my career.

I would also like to thank my thesis committee members, Matt and Jackie. I have benefited tremendously from your scientific insights, guidance and mentorship during my time at MIT. It was always a pleasure to share the latest updates on my science with you during my committee meetings, and I will truly miss having these stimulating conversations moving forward. The classes I took as a TA in 7.45/7.85 Cancer Biology were one of the most memorable courses I took while at MIT-- thank you making them so fun and interactive, Matt.

I would also like to thank Vijay Kuchroo for agreeing to be my external thesis defense member, and I look forward to discussing pancreatic tumor immunology with a true leader in the field.

I would like to thank Will, for being an amazing collaborator and a great friend. Your incredible drive, intellect, and dedication has pushed our shared science to greater heights. Thank you for always being willing to do the crazy experiments, for challenging the status quo, and for your unrelenting excitement when making new discoveries. I will miss our comradery, wide-ranging discussions on anything pancreatic or immunology-related, and yes maybe even 4 am scRNA-seq harvests. Those were days...

I would like to thank the Jacks Lab members who keep our lab running: Judy, Karen, Kate, Kim, and Margaret. Thank you for helping me with countless things during my time in the lab, and for your selfless efforts to make sure the lab is clean, continued to operate

smoothly and remained in stable financial waters. I really appreciate everything you have done.

Thank you to Kim for your generosity, support, and friendship. Your dedication to the mouse colony and animal experiments over the last year(s) have made much of the work in this thesis possible. I particularly want to thank you for jumping in during the COVID-19 lockdown, which has allowed me to stay focused on completing my PhD.

Thank you to two incredible technicians, Nimisha and Ana. I have really appreciated your patience, countless technical contributions, and commitment to this project. It has been rewarding to see you grow as scientists during your time in the lab, and I look forward to following your paths as you chart out on bright futures.

Thank you to Zack for jumping into the deep with this pancreas project at full pace. I am incredibly grateful for your computational analyses that have pushed the science described here forward, and I am excited to see what you will achieve during your PhD.

Thank you to all current and past graduate students in the lab, in particular Sheng Rong, Rodrigo, Amy, David, Leah, Ryan, Grissel and Amanda. After “ascending” to becoming the most senior graduate student in the lab, I have come to realize that much of the experience during a PhD in the Jacks Lab is universal. I have tremendously benefited from your advice, support, comradery and expertise at many points during the past 6 years.

Thank you to all current and past postdoc students and staff in the lab, in particular Britt, Megan, Carla, Peter, Alex, Banu, Jason, Mandar, and Nik. Each one of you has helped me in a myriad of ways, be it through advice, sharing scientific insights and expertise, or even just perspectives on life—it has helped me grow as a person and allowed me to keep pushing the science forward.

Thank you to all the current and past technicians in the lab, for your dedication and hard work. Your energy and excitement for science is a big part of what makes the culture in the Jacks lab so great. I especially want to thank Grace, Sophie, Demi, Michelle, Caterina, and Da-Yae—I appreciate your willingness to always help me out and your friendship.

Thank you to the amazing MIT classmates I have been fortunate enough to call friends, in particular Santi, Nikola, Chris, Danny, Spencer, and Josh—for countless dinners, movies, parties, ski and hiking trips, being part of my wedding, and numerous other things! I know our friendship is bigger than a PhD, and that is incredibly special.

To my sisters Willemijn and Nora, and my parents Hein and Jannie. Thank you for your unconditional love and support. You have always been there for when I needed it most and much of this work is inspired by the lessons you have taught me. I hope this thesis makes you proud.

Last, but most importantly, to the love of my life, Alexandra: Thank you for always believing in me, for always encouraging me to do and be my best. Thank you for your enduring patience and understanding as I spent many weekends and late nights in the lab. I could not have done this without your love and support all these years, and I am so excited to welcome our first addition to the family in August.

Laurens Lambert  
June 2020



## Table of Contents

<b>Abstract</b> .....	<b>3</b>
<b>Curriculum vitae</b> .....	<b>4</b>
<b>Acknowledgments</b> .....	<b>6</b>
<b>1. Introduction</b> .....	<b>12</b>
<b>1.1. History of tumor immunology</b> .....	<b>13</b>
1.1.1. The early history of immunotherapy .....	13
1.1.2. Coley's toxins and the beginning of tumor immunology .....	15
1.1.3. The dawn of tumor transplantation models .....	18
1.1.4. Tumor antigens and the immunosurveillance hypothesis .....	20
1.1.5. Cellular immunology comes of age .....	23
1.1.6. The beginning of a modern era in tumor immunology.....	25
<b>1.2. The cancer immune response</b> .....	<b>28</b>
1.2.1 Tumor antigen release leads to the initiation of immune responses .....	29
1.2.2 Dendritic cells traffic to lymph node and interact with naïve T cells .....	31
1.2.3 T cell priming triggers clonal expansion and effector cell differentiation .....	31
1.2.4 T cells use chemotactic cues to migrate to the tumor microenvironment .....	33
1.2.5 T cells infiltrate into the tumor microenvironment.....	34
1.2.6 Effector T cells recognize cancer cells through antigen presentation .....	35
<b>1.3. Tumor-intrinsic mechanisms of immune escape</b> .....	<b>37</b>
1.3.1. Antigenicity is a critical determinant in immune escape.....	37
1.3.2. Immunoediting can mediate tumor immune escape .....	39
1.3.3. Oncogenic pathways drive T cell exclusion .....	41
<b>1.4. Tumor-extrinsic mechanisms of immune escape</b> .....	<b>44</b>
1.4.1. Endothelial cells .....	44

1.4.2.	Cancer-associated fibroblasts (CAFs).....	45
1.4.3.	Myeloid-derived suppressor cells (MDSCs) and tumor-associated macrophages (TAMs)..	47
1.4.4.	Tumor-associated macrophages (TAMs).....	48
1.4.5.	T cell-intrinsic dysfunction .....	49
1.4.6.	CD4+ T cells.....	56
1.4.7.	Tumor microenvironments can exist in distinct inflammatory states .....	58
<b>1.5.</b>	<b>Pancreatic cancer .....</b>	<b>59</b>
1.5.1.	The disease progression and the genetic basis of pancreatic adenocarcinoma.....	61
1.5.2.	The pancreatic tumor microenvironment.....	64
1.5.3.	Immunotherapy in pancreatic cancer .....	70
<b>1.6.</b>	<b>Synopsis .....</b>	<b>74</b>
<b>1.7.</b>	<b>References.....</b>	<b>77</b>
<b>2.</b>	<b>TIGIT-based therapy induces potent anti-tumor responses in pancreatic cancer.....</b>	<b>103</b>
<b>2.1</b>	<b>Abstract.....</b>	<b>104</b>
<b>2.2</b>	<b>Main results .....</b>	<b>105</b>
2.2.1	Preclinical modeling of immunogenic pancreatic cancer .....	105
2.2.2	Immune evasive pancreatic tumors retain antigen expression and presentation .....	109
2.2.3	Multiple classes of antigen-specific CD8 <sup>+</sup> TILs within immune evasive pancreatic tumors	114
2.2.4	TIGIT-directed combination immunotherapy as a novel therapeutic approach in PDAC...	119
<b>2.3</b>	<b>Discussion .....</b>	<b>122</b>
<b>2.4</b>	<b>Acknowledgements .....</b>	<b>123</b>
<b>2.5</b>	<b>Methods .....</b>	<b>124</b>
<b>2.6</b>	<b>References.....</b>	<b>144</b>

<b>3. Discussion.....</b>	<b>161</b>
3.1. Genetically engineered mouse models offer unique insights into tumor immunoediting 161	
3.2. Outlook – the potential of autochthonous models and outstanding questions.....	167
3.3. Organoid tumor immune escape may be mediated by tumor-extrinsic mechanisms of immune evasion.....	169
3.4. Transcriptional profiling of the antigen-specific T cell compartment revealed heterogenous effector states .....	173
3.5. Outlook – The future of immunotherapy in pancreatic ductal adenocarcinoma through the lens of genetically engineered mouse models .....	175
3.6. References .....	177
<b>Appendix I .....</b>	<b>180</b>
<b>Abstract .....</b>	<b>181</b>
<b>Main text .....</b>	<b>181</b>
<b>Discussion.....</b>	<b>183</b>
<b>Methods .....</b>	<b>184</b>
<b>Acknowledgments .....</b>	<b>188</b>
<b>References .....</b>	<b>189</b>

# 1. Introduction

It is now widely appreciated that the immune system plays a critical role in tumorigenesis, and is considered a “hallmark of cancer”<sup>1</sup>. Recent clinical successes with therapeutic agents that modulate the immune system, rather than the tumor itself, have truly revolutionized cancer treatment in recent years.

Given these clinical successes, it may come as a surprise that the tumor immunology field is over a century old, and for most of its recent scientific history, has been regarded with much skepticism. Prevailing dogma asserted that because cancers arise from the body’s own tissues, the immune system is unable to detect these cells and remains ignorant of the growing tumor. Beginning in the 1990s, this concept was slowly overturned by revisions to concept of cancer immunosurveillance<sup>2</sup>, the identification of human tumor antigens<sup>3</sup>, and the demonstration of immune checkpoint blockade efficacy in tumor transplantation models<sup>4</sup>. These findings have sparked an enthusiasm for the development of immunotherapeutic anti-cancer agents, which has led to regulatory approval of the first generation of immune checkpoint inhibitors (ICIs). The durable clinical remissions achieved with these therapies are arguably the most convincing evidence that the immune system can be mobilized to elicit anti-tumor responses<sup>5</sup>.

While immunotherapies have made tremendous clinical impact on many different types of cancer, pancreatic adenocarcinoma (PDAC) has remained largely treatment-refractory. The overall five-year survival rate of metastatic PDAC, which constitutes the majority of diagnosed pancreatic cancer cases, has not improved over the last decade. Therefore, novel therapies to combat this devastating disease are urgently needed. Genomic profiling has revealed that (a subset of) PDAC harbors high affinity

neoantigens<sup>6</sup>, suggesting that this cancer is not intrinsically resistant to anti-tumor T cell responses. Therefore, a deeper understanding of the tumor-immune microenvironment is necessary to dissect the mechanisms that may limit the efficacy of immunotherapeutic approaches.

This introductory chapter includes a historical overview of the field of tumor immunology, and reviews our current understanding of the anti-tumor immune response. Following this overview, the tumor-intrinsic and tumor-extrinsic mechanisms of immunoevasion are described. This chapter concludes with a summary of our current understanding of the genetic basis of pancreatic cancer, the role of the tumor microenvironment in PDAC progression, and the ongoing clinical efforts focused on harnessing immunotherapy for the treatment of pancreatic cancer.

## **1.1. History of tumor immunology**

### **1.1.1. The early history of immunotherapy**

The concept of utilizing the immune system to treat human disease, broadly referred to as ‘immunotherapy’, dates back millennia. The Greek philosopher and historian, Thucydides, first described a link between the survival of a disease, “the plague of Athens”, and the acquisition of immunity in 430 BC<sup>7</sup>. However, it would take many centuries for these observations to become actionable. During the 10<sup>th</sup> century, Chinese doctors noticed that “ripe pus” from smallpox patients could be transferred to other individuals on dried cotton tips, and that this sometimes conferred protection against the disease<sup>8</sup>. A Chinese text from 1597 suggested the use of “powdered cow ice” for the treatment of this deadly disease<sup>8</sup>.

The practice of these 'variolation' techniques (or inoculation) appears to have arisen independently in China, India, and Africa before slowly spreading to Europe and America. Lady Mary Wortley Montagu, wife of the British ambassador of the Ottoman Empire has been widely credited for introducing this idea into Western civilizations. Having witnessed the practice firsthand in Turkey, she had her son secretly variolated by the Scottish physician Charles Maitland in 1716<sup>8</sup>. When Maitland subsequently performed a successful variolation on Montagu's second child under the observation of prominent Royal Society physicians, he was granted a medical license to perform a "clinical trial". For his variolation experiment in 1721, Maitland chose 6 condemned prisoners whom he infected with smallpox pus. Much to his surprise, all individuals recovered from their symptoms, and even had subsequent immunity when exposed to smallpox patients<sup>8</sup>.

That same year, the city of Boston (U.S.) was plagued with a smallpox epidemic; nearly half of its 12,000 citizens developed the disease. Desperate to fight the spread of smallpox, the physician Zabdiel Boylston, and Reverend Cotton Mather, variolated nearly 300 Bostonians, and compared the disease outcomes of these treated individuals against the naturally infected patients<sup>9</sup>. In what is arguably one of the first examples of a rigorous clinical statistical analysis, they were able to show that smallpox variolation dramatically reduced subsequent disease mortality. However, the practice was vehemently opposed by townsmen; at some point 'anti-variolators' went as far as bombing Mather's house. While certainly a progressive medical thinker in his time, Mather's legacy is nowadays mired in controversy due his written justifications of the Salem witch trials.

The success from this large-scale variolation campaign did not go unnoticed at the time, and the practice became gradually commonplace across European nations and in

the U.S. throughout the 18<sup>th</sup> century. However, smallpox variolation was not without complications, as these “vaccines” were frequently contaminated and could cause syphilis. Moreover, (excessive) transfer of smallpox virus to nonimmunized individuals would sometimes result in active infection, as opposed to the protective immune response that the treatment was supposed to confer.

It would take until the turn of the 18<sup>th</sup> century before prophylactic vaccination against smallpox became safer. Growing up in the county of Berkeley (England), the physician Edward Jenner had heard stories about dairy milkmaids that were protected against smallpox after suffering from the milder cowpox disease. He decided to investigate these observations further, and in 1796 transferred cowpox from an infected maid to an 8-year-old boy<sup>10</sup>. When he subsequently inoculated the boy with smallpox, no disease developed. Buoyed by this finding, Jenner submitted a treatise to the Royal Society, which was abruptly rejected. After adding a few more cases, Jenner published a small booklet, in which he coined the practice of ‘vaccination’, derived from the cowpox-causing *Vaccinia virus*<sup>10</sup>. This proved enough to convince a number of leading British physicians, and as a result the procedure spread quickly throughout the country; it is estimated that over 100,000 people were vaccinated by 1801<sup>8</sup>. In 1840 the British government officially banned the practice of variolation. However, it would take another 176 years before global incidence of smallpox was completely reduced to zero.

### 1.1.2. Coley’s toxins and the beginning of tumor immunology

The concept that human diseases could be prevented through prophylactic vaccination undoubtedly laid the foundation for tumor immunology. Throughout the history

of medicine, individual cases of spontaneously regressing tumors have been reported, often accompanied by seemingly unrelated infections<sup>11</sup>. During the late 19<sup>th</sup> century, German physicians Wilhelm Busch and Friedrich Fehleisen independently noted a connection between an opportunistic bacterial skin infection (erysipelas) and tumor regression. Fehleisen identified the causative pathogen as the Gram-positive *Streptococcus pyogenes* bacterium. These observations led both physicians to experiment with the intentional induction of erysipelas in cancer patients, which reportedly led to tumor shrinkage<sup>12</sup>. The practice, however, was not widely adopted by other physicians at the time.

Frustrated by an inoperable case of head and neck sarcoma, a young American surgeon, William Coley, took note of these cases in 1891 and decided to perform his own experimentation in his cancer ward at the Memorial Hospital in New York. In a series of treatments on 6 inoperable sarcoma and 4 carcinoma patients, Coley administered *S. pyogenes* inoculations that he had received from Robert Koch's laboratory in Germany. The results were mixed: in 4 patients he was able to induce full erysipelas and observed robust tumor regressions. However, the condition of 4 other patients only temporarily improved, but they managed to achieve a fully developed infection. Worse yet, 2 patients did develop erysipelas, and actually succumbed to a pathogenic attack instead<sup>13,14</sup>. This led Coley to try combining heat-killed *S. pyogenes* with toxins from the Gram-negative bacterium *Serratia marcescens*, thereby creating the first ever mixed bacterial vaccine (MBV)<sup>13</sup>. Unbeknownst at the time, this combination of Gram-positive and Gram-negative bacteria creates a potent immunostimulatory cocktail, and is now thought to induce the release of multiple inflammatory cytokines, including interleukin-12 (IL-12)<sup>15</sup>.



Coley and colleagues at the Memorial Hospital in New York would go on to treat nearly 1200 patients with these “Coley’s toxins” over the next 40 years; 270 patients reportedly achieved long-term remissions with MBV, sometimes even lasting decades<sup>13,16</sup>. Many of the best responding tumors included soft tissue sarcomas, although responses in other tumor types were achieved as well<sup>16</sup>. These cases were carefully documented by Helen Coley Nauts (William Coley’s daughter). In honor of her late father, Nauts would establish the Cancer Research Institute (CRI) for advancement of tumor immunology in 1953.

However, the widespread adoption of MBV outside of New York was hampered by poor documentation of Coley’s practices and the limited potency of commercial preparations<sup>13</sup>. Coley frequently changed how he produced MBV and would inject the vaccines using various routes; many of these attempts were later shown to be ineffective<sup>16</sup>. Furthermore, the scientific field of tumor immunology was still in its infancy at the turn of the 20th century, and a mechanistic basis for the efficacy of Coley’s toxins was lacking. As radiation therapy and chemotherapy, which promised similar remission rates as MBV, became more popular for cancer treatment, Coley’s toxins fell out of favor. Ironically, James Ewing, one of Coley’s staunchest opponents and his director at Memorial Hospital, discovered a bone sarcoma (Ewing’s sarcoma) that could be effectively treated Coley’s toxins<sup>17</sup>. While MBV is no longer used in the clinic today, William Coley’s efforts undeniably set the practice of cancer immunotherapy in motion. He is now recognized as one of the founding fathers of the field.

### 1.1.3. The dawn of tumor transplantation models

It was the German physician Paul Ehrlich who was the first to formulate the concept that the human immune system is capable of recognizing and fighting off cancerous cells<sup>18</sup>. In his work published in 1909, Ehrlich suggested that “aberrant cells arising during fetal and post-fetal development” could remain latent due to the body’s “positive mechanisms”<sup>18</sup>. However, the scientific underpinnings of immunology at the time were not advanced enough to experimentally validate his hypothesis, nor was a connection made between Ehrlich’s theory and Coley’s toxins.

Instead, the nascent field of tumor immunology became fixated on understanding immune responses through tumor transplantation studies. Experiments performed around the turn of the 20<sup>th</sup> century by Loeb and Jensen showed that thyroid tumors and spontaneous alveolar carcinomas could sometimes be transplanted within the species they originated from, and that the growth of these transplants resulted directly from the transferred cells<sup>19</sup>. These results argued against one of the influential theories at that time, which stated that cancer was caused by an (unknown) etiologic agent and was essentially a “transmissible disease”<sup>19</sup>. Loeb and a number of his contemporaries then showed that tumor origin (“race”) was an important factor in determining the outcome of tumor transplantation<sup>20</sup>. Over ten years later, Clarence Little and Ernest Tyzzer at Harvard would revisit these studies by carefully examining the tumor transmissibility of inbred strains. Their work led to the discovery of a genetic basis for tumor transplantation, and importantly raised the question whether tumor transplant rejections were simply the result of transferring between “genetically impure” mouse strains<sup>20–22</sup>.

This issue would continue to frustrate tumor immunologists throughout the 1920s and 1930s<sup>22</sup>. In an expansive literature review, William Woglom gloomily concluded that “it would be as difficult to reject the right ear and leave the left ear intact as it is to immunize against cancer”<sup>23,24</sup>, a dogmatic belief that was shared by many geneticists around the time.

It would take until 1936 before further progress on the genetic basis of tumor transplantation was made. Through the ingenious use of human and rabbit antisera, Peter Gorer discovered the presence of distinct blood groups in mice of different inbred strains<sup>25</sup>. When Gorer transferred tumors originating from mice containing “blood group II” were transferred to mice with “blood group I”, these recipients rapidly rejected the tumor. This suggested to Gorer that the blood antigens were involved in mediating the resistance to tumor rejection. George Snell, working at the Jackson Laboratory, had similarly set out to pursue mapping of the genetic basis of tumor transplantation. As a classically trained geneticist, Snell approached the problem by generating a series of genetically identical mouse strains only differing in a single locus, so-called ‘congenic’ strains. Harnessing the antisera against “blood group II” on different congenic lines, Snell and Gorer were able to map the genetic site of tumor transplantation to the histocompatibility locus in 1948<sup>25,26</sup>. In recognition of the “blood group II” serum that led to its discovery, this locus became known as the histocompatibility locus II (*H-2*). As the *H-2* locus was shown to be the most critical determinant mediating tumor rejection, while in addition to being highly polymorphic in nature, it is referred to as the *major histocompatibility complex* (MHC) in mice. In 1980, George Snell shared the Nobel Prize

with Baruj Benacerraf for the discovery of the *H-2* locus; unfortunately, Peter Gorer had passed away 19 years prior.

A final insight into tumor transplantation came from the work of the British scientist, Peter Medawar, working in the separate field of transplantation immunology. Medawar focused his efforts on elucidating the basis of allogeneic skin graft rejection ('allografts'). In seminal papers published in 1953 and 1956, Medawar and Bellingham described the concept of 'acquired tolerance' by demonstrating that the immune system plays a fundamental role in the rejection of allogeneic transplants<sup>27-29</sup>. Medawar's work confirmed the earlier hypothesis formulated by Macfarlane Burnet in 1948, that the immune system (in Burnet's theory "antibodies") could acquire the ability to discriminate 'self' from 'non-self' during development<sup>30</sup>. Both scientists would be awarded the Nobel Prize in 1960.

#### 1.1.4. Tumor antigens and the immunosurveillance hypothesis

While the study of tumor transplantation models shaped much of the first 50 years of tumor immunology, leading to the discovery of the MHC locus and immunological tolerance, it did little to illuminate how the immune system could respond to tumors arising in its own host. To study this question, immunologists increasingly turned to the chemical carcinogen methylcholanthrene (MCA) to induce sporadic tumors in mice. In 1943 Polish scientist Ludwig Gross was the first to demonstrate that an MCA-induced sarcoma line from the inbred C3H strain was rejected by genetically identical C3H recipients<sup>31</sup>, suggesting that the sarcoma contained antigens that could be recognized by the host's immune system. However, his work left open the possibility that the sarcomas had acquired mutations during repeated transplantation. Edward Foley confirmed Gross'

observations in 1953 by demonstrating that methylcholanthrene-induced tumors were antigenic upon direct transplantation in isogenic animals<sup>32</sup>. Raymond Prehn and Joan Main would further extend these results through the characterization of several fibrosarcoma tumor lines that were rejected upon transplantation into isogenic strains<sup>33</sup>. However, these studies were viewed with skepticism, as they could still be explained by a lack of a genetically pure background between strains ('residual heterozygosity'). George Klein and colleagues would finally settle this debate by demonstrating that autochthonous tumors (in addition to syngeneic tumors) could be rejected upon pre-immunization of the hosts<sup>34</sup>.

Collectively, these studies raised the idea that the immune system is actively involved in the elimination of cancerous cells arising in the body. This led Macfarlane Burnet and Lewis Thomas to formulate their influential cancer immunosurveillance hypotheses in the late 1950s, echoing Paul Ehrlich's theory half a century earlier. Inspired by the concept of immune tolerance, Burnet focused on his hypothesis on the accumulation of "antigenic potentialities" (neoantigens) by cancer cells, which would be sufficiently different from the own body to trigger immune responses that restrained tumors from becoming clinically apparent<sup>35,36</sup>. Thomas' early theory was more evolutionary in nature, suggesting that multicellular organisms have developed mechanisms to protect against transformed cells in order to maintain tissue homeostasis, similar to the protection against foreign tissues (during allograft rejection)<sup>37,38</sup>. Experimental validation for these hypotheses soon followed with demonstrations that carcinogen-induced and oncoviral experimental models contained unique tumor

antigens<sup>39</sup>. However, evidence for the existence of human antigens was absent, and whether these models accurately reflected human cancer remained unclear.

The field of tumor immunology would soon face a setback that would again cause skepticism about the perceived ability of the immune system to ward off cancer cells. A logical extension of the cancer immunosurveillance hypothesis was an absence of immune function ('immunodepression') would result in higher incidence of tumor formation. The development of athymic (*Nu/Nu*) mice in the late 1960s made it possible to experimentally test this idea<sup>40,41</sup>, as these mice largely lacked mature T lymphocytes. Working with these 'nude' mice at Memorial Sloan Kettering, Osias Stutman demonstrated in the 1970s that MCA induction at birth did not lead to a statistically higher number of sarcomas in *Nu/Nu* mice compared to their normal, heterozygous counterparts (*Nu/+*)<sup>42,43</sup>. He concluded that his results did not support the immunosurveillance hypothesis. Additionally, no evidence of increased susceptibility to spontaneous tumors was found when 27 murine lines were systemically investigated by Harold Hewitt and colleagues<sup>44</sup>. Indeed, even Foley, Prehn, and Main, in their landmark papers during the 1950s, had noted the differences between carcinogen-induced and spontaneous tumor models<sup>32,33</sup>, raising doubts that the MCA-induced tumors were just an anomaly.

While these results certainly dampened the excitement around cancer immunotherapies over the next decade, we now know that Stutman's studies were flawed by several technical factors unknown to him. While athymic mice have severely compromised immune responses to infectious agents, some basal T cell functionality is maintained<sup>45-47</sup>. Additionally, natural killer (NK) cells, developing normally in these mice, can make significant contributions to anti-tumor immunity<sup>48-50</sup>. Finally, tumor induction

with MCA is highly efficient in the CBA/N strain (the only *Nu/Nu* model available to Stutman), raising the possibility that early tumor induction simply overwhelmed an immature immune system<sup>51</sup>. Indeed, later studies using mouse strains lacking T, B, and NK cells (*Rag2*<sup>-/-</sup>;  $\gamma$ *c*<sup>-/-</sup> mice), the interferon- $\gamma$  receptor (*Ifng1*<sup>-/-</sup>) or the cytotoxicity-mediating protein perforin (*Prf1*<sup>-/-</sup>) have shown elevated susceptibility to MCA-induced tumorigenesis<sup>52-55</sup>. Thus, Stutman's rejection of tumor immunity ultimately proved premature; rather, genetic murine models as well as epidemiological observations of elevated cancer incidence in immunocompromised humans have firmly cemented the immune system's role in cancer surveillance.

#### 1.1.5. Cellular immunology comes of age

While tumor immunology remained focused on experimental models of cancer, discoveries made in different immunological fields during the 1960s and 1970s would lay the foundation for our modern understanding of the cellular components of the anti-tumor response. Drawing upon Medawar's concepts of transplant tolerance, James Gowans and colleagues showed that thoracic duct lymphocytes (TDLs) were involved in the initiation of alloreactive immune responses, although they could not distinguish cellular from humoral responses<sup>56</sup>. Jacques Miller soon followed these results by demonstrating that neonatal thymectomized mice were unable to reject their skin grafts, which suggested that the thymus was the source of these reactive immune cells<sup>57,58</sup>. His results stood in stark contrast to the widely held belief that the thymus was simply a vestigial organ where lymphocyte would "go to die". Additionally, Miller found that adult thymectomized mice were unable to regenerate their lymphocytes upon total body irradiation or initiate immune

responses upon antigenic challenges with sheep erythrocytes, further solidifying the role of the thymus in immunocompetence<sup>59-61</sup>. In a series of experiments using irradiated CBA mice grafted with syngeneic thymi, TDLs, and allogeneic bone marrow, Mitchell and Miller then unequivocally proved that thymus-derived lymphocytes ('T cells') were immunologically distinct from bone marrow-derived lymphocytes ('B cells')<sup>62-65</sup>.

Subsequent use of different antisera helped to further distinguish these lymphocytic cell types by their respective cell surface markers<sup>66,67</sup>, and led to the subdivision of T cells into CD8+ (originally Ly-2, Ly-3) and CD4+ (Ly-4) cells<sup>68,69</sup>. The development of monoclonal antibodies in 1975 by Kohler and Milstein<sup>70</sup> would usher in a new age where lymphocytes could be studied in increasingly greater detail, particularly with the advent of flow cytometric methods<sup>71</sup>.

In an effort to dissect immune responses *in vitro*, Mishell and Dutton developed an assay during the 1960s that mixed antigens with splenic lymphocytes, which led to the realization that antibody formation required an additional cell type present in this mixture<sup>72</sup>. Working with these cultures in 1973, Steinman and Cohn first described the dendritic cell (DC) as the third cell type<sup>73,74</sup>. Steinman and colleagues would go on to decipher much of the biology of DCs over the next decades<sup>75-78</sup>, and establish a critical role for this antigen-presenting cell (APC) in the initiation of adaptive immune responses.

The structure of antibodies was uncovered in an influential set of studies during the 1950s and 1960s<sup>79,80</sup>, setting the stage for the discovery of immunoglobulin (Ig) rearrangement by Hozumi and Tonegawa<sup>81</sup>. By early 1980s it was well accepted that the B cells used Ig molecules to recognize soluble antigen, however the nature of the T cell receptor (TCR) and how T cells recognized antigens remained topics of debate<sup>82,83</sup>. The



latter was clarified by Zinkernagel and Doherty, who established that T cell recognition was governed by the MHC molecule of the syngeneic host, a concept that became known as ‘MHC restriction’<sup>84–86</sup>. Importantly, their results argued that a single TCR could recognize both antigen and MHC—a model proven correct when the first MHC peptide epitopes were uncovered<sup>87,88</sup>. The nature of the TCR was uncovered when Davis and Mak isolated the first murine and human TCR chains<sup>89,90</sup>, before rapidly cloning of the remaining TCR chains<sup>91–93</sup>. Collectively, these studies demonstrated that primary antigen sensing receptors (the TCR $\alpha,\beta$  chains) were part of a larger transmembrane protein complex that associated with  $\gamma$ ,  $\delta$ , and the two  $\epsilon$ ,  $\zeta$  polypeptide chains<sup>94,95</sup>.

Additional discoveries in cellular immunology made in the 1970s and 1980s included with the discovery of interleukin-2 (IL-2)<sup>96</sup>, which allowed the sustained *in vitro* culture of cytotoxic lymphocytes, and the generation of transgenic TCR mouse strains<sup>97</sup>. Together, these advancements would form the basis for novel immunotherapeutic strategies pioneered over the following decade, as the field of tumor immunology regained its former momentum.

#### 1.1.6. The beginning of a modern era in tumor immunology

While tumor immunologists still grappled with the implications of Stutman’s results throughout the 1980s, Thierry Boon’s work offered a glimmer of hope for the field. In 1982, Boon and van der Pel showed that vaccination with mutagenized leukemia clones could induce the immune rejection of spontaneous tumors of the same origin<sup>98</sup>, which suggested that these tumors, rather than lacking antigens, failed to stimulate strong immune responses. These findings called the results obtained with experimental models

in the decades before into question, and raised the possibility that human tumors could be antigenic as well. The Boon group would continue their focus on tumor antigens, which culminated with the identification of the first human T cell antigen in 1991, encoded by the *MAGE-1* gene<sup>3</sup>. MAGE proteins are part of a diverse group of cancer-testis antigens (CTAs), which are normally restricted to immunoprivileged reproductive organs, but become aberrantly expressed in many tumor types<sup>99</sup>. In the immediate years following the initial identification of *MAGE-1*, a wealth of other murine and human antigens were characterized, including *MAGE*, *BAGE*, *GAGE*, *RAGE* (all CTAs), Tyrosine, gp100/pmel 17 (differentiation antigens), *E7* (a viral antigen), *HER2/Neu* (an overexpression antigen), *CDK4*, and *β-catenin* (neoantigens)<sup>100</sup>.

Further mechanistic insights into the relationship between the immune response and cancer antigenicity were generated by Bob Schreiber and Lloyd Old. In a landmark study published in 2001, Schreiber, Old and Shankaran carefully compared the re-transplantation kinetics of MCA-induced sarcomas derived in the absence of an immune-selective environment (*Rag2*<sup>-/-</sup> mice), or derived in an immunocompetent environment (wild-type 129/SvEv mice)<sup>54</sup>. They were able to demonstrate that tumor immune escape was intimately linked to the prior elimination of immunogenic cancer clones by T cells. These experiments, together with data from genetic knockout mice that showed increased susceptibility to cancer formation, and the experimental demonstration of an intermediate state of “stasis” between the actions of immune cells and tumor emergence<sup>101</sup>, have led to the definition of the ‘cancer immunoediting’ process. Cancer immunoediting is thought to occur in three distinct phases: immune elimination, immune equilibrium, and finally immune escape<sup>2,38</sup>.

The 1990s would also set the stage for much of the clinical excitement around immune checkpoint inhibitors nearly two decades later. In a landmark study published in 1996, James Allison and Max Krummel demonstrated that the cytotoxic T-lymphocyte-associated protein 4 (CTLA-4) was a negative regulator of T cell responses in murine transplant models<sup>4</sup>. Just two years later, Tasuku Honjo and Hiroyuki Nishimura used a genetic *Pdcd-1* knockout mouse to elucidate the function of PD-1 in the maintenance of peripheral tolerance<sup>102</sup>. The discovery of these two ‘immune checkpoints’ has had enormous impact on the field. Research into the mechanisms of immune tumor detection, tumor immune evasion and efficacy of novel immunotherapies is now truly flourishing. Indeed, much of the biology described in the following sections of this introduction has only been fairly recently elucidated; a testament to incredible pace of discovery in this field.

## 1.2. The cancer immune response

The immune response to a growing tumor can be conceptualized as a multistep iterative process, termed the “cancer-immunity cycle” by Chen and Mellman<sup>103</sup>. As will be reviewed in detail below, this immunological sequence begins with the release of tumor antigens, which trigger immune recognition and the mobilization of a T cell response. This culminates in destruction of antigen-expressing cancer cells by effector T cells, which in turn liberates additional antigens and thus amplifies the existing response (**see Figure 1**).

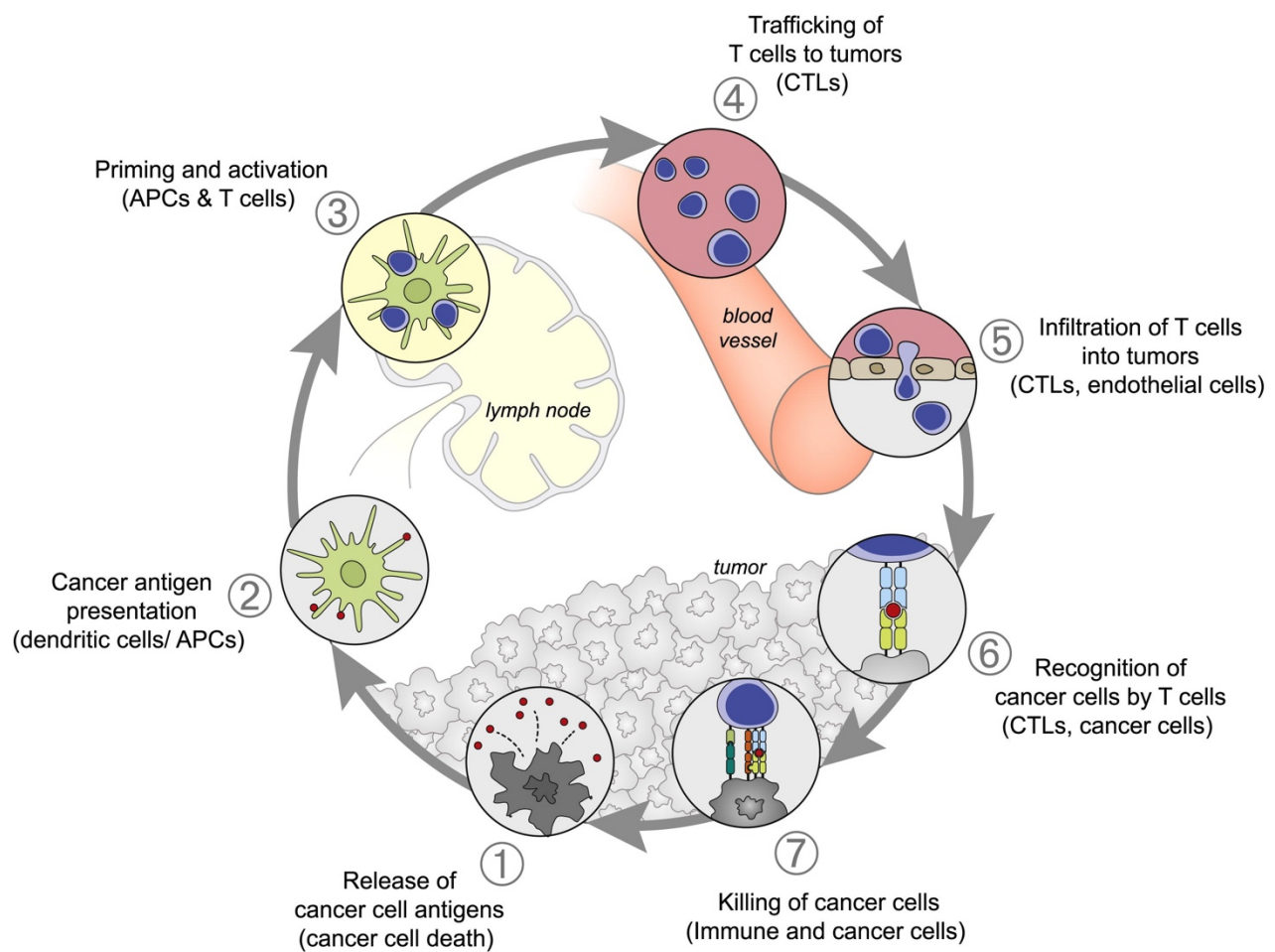


**Figure 1: The various stages of the anti-tumor immune response visualized as a cycle.** Source: Daniel S. Chen & Ira Mellman, *Immunity* (2013)

### 1.2.1 Tumor antigen release leads to the initiation of immune responses

The oncogenic transformation of normal cells is characterized by a number of altered cellular processes, including uncontrolled proliferation, altered metabolism, resistance to cell death and the acquisition of invasive motility<sup>1</sup>. Cancer cells often experience genetic instability over the course of neoplastic growth, leading to the acquisition of many single nucleotide variations (SNVs) and can even gain or lose whole chromosomes<sup>104</sup>. While this instability may seem detrimental to individual cells, these genomic alterations are thought to be beneficial to the bulk tumor by increasing clonal heterogeneity, which enables rapid selection of the “fittest” clones. However, as a consequence of mutagenic processes, cancer cells can also produce altered proteins that contain neoepitopes with strong binding affinity to MHC molecules<sup>105</sup>. As these ‘neoantigens’ essentially represent foreign peptides when presented to the human immune system, they are not subjected to immunological tolerance and can thus elicit a strong T cell attack. Indeed, accumulating evidence over the past decade has implicated neoantigens as a critical source for tumor-directed immune responses, both during endogenous immune recognition<sup>106,107</sup> as well as upon therapeutic modulation<sup>108–110</sup>. Many neoantigens identified through the use of high-throughput screening and T cell reactivity assays are contained in mutated proteins that are unlikely to fulfill oncogenic roles. However, on rare occasion, driver mutations have been found to generate neoepitopes capable of strongly binding HLA alleles (e.g. *KRAS*<sup>G12D</sup> on HLA-C\*08:02<sup>111</sup> and *TP53*<sup>R175H</sup> on HLA-A\*0201<sup>112</sup>). Targeting these driver neoantigens with immunotherapy is attractive, as these mutations are often highly clonal and T cell cytotoxicity can be precisely directed to cancer cells while sparing normal tissues.

Viral antigens constitute a different type of neoantigens and are foreign to the immune system as well. For example, the E6/7 oncoproteins that drive cervical and oropharyngeal carcinomas can mediate protective immunological responses in therapeutic settings<sup>113,114</sup>.

Finally, aside from neoantigens, several other classes of tumor antigens are present in many cancer types. These antigens are the result of aberrant re-expression of early lineage proteins (differentiation antigens), endogenous DNA viruses (retrovirus antigens), or the misexpression of proteins from immunoprivileged sites (cancer-testis antigens)<sup>115</sup>. These antigens derive their immunogenicity from a partial or complete lack of tolerance<sup>116</sup>.

It is clear that antigen release by tumor cells initiates the cancer-immunity cycle **(step 1, see Figure 1)**. Cellular stress (ER or oxidative stress) or therapeutic treatment (chemotherapy or radiotherapy) can trigger a type of 'immunogenic' cell death (ICD) that is distinct from apoptosis<sup>117,118</sup>. ICD results in the release of damage-associated molecular patterns (DAMPs, e.g. calreticulin, ATP, and HMGB1) into the microenvironment, which in turn induces phagocytotic activity and intracellular Toll-like receptor signaling in responding innate immune cells<sup>119</sup>. This allows antigen-presenting cells, such as dendritic cells (DCs), to capture and process tumor antigens, and undergo maturation to upregulate co-stimulatory surface ligands (CD80, CD86, MHC class II)<sup>120</sup>. Dendritic maturation is critical for productive T cell engagement, as the absence of co-stimulation can lead to a T cell anergy and clonal deletion<sup>121</sup>. The inflammatory cues innate cells receive are thus critically important in determining the outcome of this early phase of cancer immunity.

### 1.2.2 Dendritic cells traffic to lymph node and interact with naïve T cells

DC maturation allows an APC to migrate to nearby lymph nodes, where they encounter naïve T cells cycling through lymph nodes via the circulation (**step 2, see Figure 1**). In the lymph node, the APC and T cells congregate in a discrete anatomical location (the ‘T cell zone’) supported by a network of reticular cells<sup>122</sup>. Each T cell carries a uniquely rearranged TCR capable of recognizing its ‘cognate’ antigen. It has been estimated that the odds of a “match” between an APC and T cell are on the order of 1 in  $10^5$ - $10^6$ , based on the precursor frequency of naïve antigen-specific CD8+ T cells<sup>123</sup>. Therefore, during this initial phase of antigen presentation, multiple T cells transiently engage with the APC; their motility resembling an unguided, random walks<sup>124</sup>. Rapid T cell scanning of the surface of APC increases the likelihood of successful T cell antigen encounter. Once a T cell has found its cognate antigen, the search pattern changes to more a directed movement<sup>124</sup>, and the process of T cell priming is initiated.

### 1.2.3 T cell priming triggers clonal expansion and effector cell differentiation

T cell recognition of cognate antigen leads to the formation of a stable immunological synapse with the APC, known as ‘signal 1’ in T cell priming (**step 3, see Figure 1**)<sup>125</sup>. The CD8 co-receptor is required to form a stable interaction with the MHC class I for antigen binding, while the CD4 co-receptor forms a complex with MHC class II. The immune synapse recruits the transmembrane phosphatase CD45 to the TCR protein complex, setting an intracellular signal transduction pathway in motion. CD45 activity at the synapse allows for the dephosphorylation of the basally active kinase Lck<sup>125</sup>, which in

turn phosphorylates the immunoreceptor tyrosine-based activation motif (ITAM) residues on the TCR. The ITAMs are then bound by ZAP70 kinase to initiate proximal TCR signaling and activation of the MAPK, PI3K, and NFAT pathways<sup>125,126</sup>.

While the interaction between TCR and peptide-bound MHC molecules (pMHC) is relatively low affinity (in the millimolar range), T cells are nonetheless exquisitely sensitive to cognate antigen stimulation; even 1 pMHC molecule can trigger cytokine secretion<sup>127</sup>. Although several models have been put forward to reconcile these seemingly paradoxical findings, the mode by which the TCR transduces signals remains a topic of debate<sup>125,128,129</sup>.

A second positive signal results from the interaction between co-stimulatory receptors on the T cell surface and the ligands expressed on the APC (CD80, and CD86). This 'signal 2' is required to achieve full activation of naïve T cells. The intracellular pathways engaged upon co-stimulatory receptor ligation largely overlap with TCR signaling, thereby reinforcing T cell activation, differentiation and acquisition of effector function<sup>130</sup>. Co-stimulatory receptor expression is regulated in a complex spatiotemporal manner; while certain receptors are found on naïve T cells (e.g. CD28, CD27), other receptors are induced upon activation and impact differentiation and effector functionality (e.g. OX40, HVEM)<sup>130</sup>.

To balance the activity of co-stimulatory receptors, co-inhibitory receptors also become upregulated upon T cell activation<sup>131</sup>. These receptors provide critical feedback inhibition by negatively impacting TCR signaling pathways. Co-inhibitory receptors are thus thought to act as 'immune checkpoints' to restrain excessive T cell proliferation, ensuring that T cell responses are inherently self-limited. Robust prolonged engagement



of T cell co-inhibition can render T cells dysfunctional, a state also termed 'T cell exhaustion'. This dysfunctional state will be further examined later in this chapter.

Following extended T cell priming and the engagement of proliferative, survival, and cellular differentiation pathways, T cells undergo a period of rapid cell divisions leading to clonal expansion. During clonal expansion, CD8<sup>+</sup> T cells receive significant cytokine support from CD4<sup>+</sup> T cells through the secretion of interleukin 2 (IL-2), as well as 'licensed' APCs. The majority of activated T cells ultimately acquire a terminal effector cell state, characterized by an ability to produce cytotoxic molecules (granzymes, perforin, FasL) to kill a pMHC-expressing target cell.

#### 1.2.4 T cells use chemotactic cues to migrate to the tumor microenvironment

T cell migration through the body is not a passive process, but instead finely tuned through the surface expression of cell-adhesion molecules and chemokine receptors. For example, expression of CCR7 and CD62L endows naïve T cells with the ability to home to lymphoid tissues<sup>132,133</sup>, where they can receive antigen stimulation. During the clonal expansion phase of the CD8<sup>+</sup> T cell response, a different homing profile is imprinted upon terminally differentiated cytotoxic T lymphocytes (CTLs). CTLs downregulate CCR7 and instead upregulate the chemokine receptor CXCR3, which allows re-entry into the circulation and migration to the tumor site (**step 4, in the cancer-immunity cycle, see Figure 1**)<sup>132</sup>. The canonical CXCR3 ligands CXCL9 and CXCL10 have been shown to correlate with increased T cell infiltration in several tumor types<sup>134–136</sup>, indicating that these chemokines also play a crucial role in guiding T cells to the tumor microenvironment (TME). Although other chemokine axes (e.g. CCR5-CCL5 and CCR2-CCL2) have also

been implicated in T cell migration, genetic evidence suggests that CXCR3 is absolutely required<sup>137</sup>.

#### 1.2.5 T cells infiltrate into the tumor microenvironment

As T cells access tumors through the circulation, the endothelial cells (ECs) lining blood vessels are critically important mediators of entry to the tumor microenvironment **(step 5, see Figure 1)**. The movement across endothelial cells ('diapedesis') is a coordinated, multistep process, where T cells first initiate rolling movements across the EC barrier, before arresting and adhering to ECs<sup>138,139</sup>. These cell-cell adhesions are guided by the interactions of lymphocyte integrin receptors (LFA-1, Mac-1, and VLA-4) with their respective endothelial ligands (ICAM-1, ICAM-2, and VCAM-1)<sup>138</sup>. Both T cells and endothelial cells subsequently undergo extensive intracellular cytoskeletal remodeling, which allows the extravasation of T cells through endothelial cell junctions ('paracellular migration') or even directly through individual endothelial cells ('transcellular migration')<sup>140,141</sup>.

Given the importance of chemotactic cues for proper immune cell homing to tumor sites, it is perhaps not surprising that cancer cells frequently deregulate chemokine expression<sup>132</sup>. By attracting immunosuppressive cell types such as myeloid-derived suppressor cells (MDSCs) and T regulatory cells (Tregs) and avoiding anti-tumorigenic effector T cells, cancer cells can shape the immune composition of the tumor microenvironment. These "immuno-evasive" strategies will be described in more detail later in this chapter.

### 1.2.6 Effector T cells recognize cancer cells through antigen presentation

Upon successfully crossing the endothelial barrier, the positioning of T cells in the tumor microenvironment depends on the presence of chemoattractive molecules ('chemokines'), stromal cells, and crucially, the extracellular matrix (ECM) (**step 6, see Figure 1**).

The ECM has well-established roles in sustaining tumor proliferation, invasive motility, maintenance of cancer stem cell niches, and drug resistance<sup>142</sup>. Although the composition and "stiffness" of the ECM can vary considerably between different tumors, components of the ECM include collagen, proteoglycans, laminin, and fibronectin<sup>143,144</sup>. Both cancer cells, as well as cancer-associated fibroblasts (CAFs), are active contributors to the ECM, which can make up 60 percent of the tumor mass by some estimates<sup>145</sup>. It was shown that ECM density of lung tumors plays an important role in the T cell localization: tumor islets that contained abundant ECM components, largely excluded T cells<sup>146</sup>. The initial movement of CTLs through the TME is believed to be largely random<sup>124,147</sup>. However, when effector T cells come in contact with tumor cells expressing their cognate antigen, migration halts and long-lasting connections between the two cells are formed<sup>147,148</sup>.

When cytotoxic T lymphocytes detect cognate antigens on a tumor, this triggers a series of cell-surface and intracellular cytoskeletal changes in the effector cell (**step 7, see Figure 1**). The first step involves the formation of an 'immunological synapse' between the CTL and the tumor cell, and tight clustering of TCR receptors (also referred to as the 'central supramolecular activation cluster'; cSMAC) with pMHC molecules on cancer cells<sup>149</sup>. The synapse is reinforced by a peripheral ring of adhesion receptors

(LFA-1 and talin proteins; the 'pSMAC')<sup>149</sup>. The intracellular cytoskeletal network of the T cell also undergoes dynamic rearrangement, leading to the positioning of the microtubule organizing center (MTOC) near the cortex of the cSMAC<sup>150</sup>. This allows for directed delivery of a "lethal hit" by the T cell, while preventing potential exposure of nearby cells to cytotoxic molecules. CTLs appear to be capable of cooperating in the killing of target cells and in some instances, can serially kill several target cells<sup>151</sup>.

Cytotoxic T cells employ two distinct mechanisms to kill their target cell. The Fas and TNF-related apoptosis-inducing ligand (TRAIL) pathways mediate cytotoxicity through the binding of complementary 'death receptor' ligands on the surface of target cells<sup>152</sup>. In contrast, the granule exocytosis pathway relies on disruption of the target plasma membrane by perforin molecules for intracellular delivery of toxic granzyme molecules<sup>153,154</sup>. After intracellular release in the target cell, granzymes are capable of triggering apoptotic cell death directly through proteolytic cleavage of the effector caspases 3 and 7, and indirectly through the mitochondrial intrinsic pathway and apoptosome formation<sup>153,154</sup>. The Fas and TRAIL pathway also converge on caspases 3 and 7 activation, but instead mediate signaling through the Fas-associated death domain (FADD) adaptor and procaspase 8 proteins<sup>152,153</sup>.

This final step in the cancer immunity cycle thus involves the killing of cancer cells. In the course of dying, cancer cells may release new tumor antigens in the TME. These tumor antigens are required to initiate the next cancer immunity cycle, and may also redirect T cell responses to different antigens, a process known as 'epitope spreading'.

While the immune cycle described in detail in the previous sections is an idealized example of an effective anti-tumor response, it nonetheless forms the basis of what most

cancer immunotherapies aim to achieve. However, cancer immunosurveillance appears defective in most, if not all, cancer types. This dysfunction can be driven by both tumor-intrinsic and tumor-extrinsic (microenvironmental) mechanisms, leading to tumor escape from immune pressure, and ultimately, the clinical manifestation of a tumor. In the sections below, several mechanisms that can suppress a productive anti-tumor response will be reviewed.

### **1.3. Tumor-intrinsic mechanisms of immune escape**

Robust evidence for extensive crosstalk between the immune system and human tumors has only recently accumulated. Many aspects of tumorigenesis appear to be shaped by selective immune pressure; and conversely, several tumor cell oncogenic pathways impact and disrupt immune function. These ‘tumor-intrinsic’ (cell-autonomous) mechanisms allow tumors to evade and escape detection of immune cells.

#### **1.3.1. Antigenicity is a critical determinant in immune escape**

Lack of tumor antigenicity was one of the earliest recognized mechanisms of immune escape<sup>155</sup>. As initiation of an effector T cell response fundamentally requires the presence of immunogenic peptides that are presented by APCs, a paucity or complete lack of antigens would naturally not lead to a T cell response. Several pathways have shown to be involved in driving a loss of tumor antigenicity, including loss of antigens, and deregulation of the antigen presentation machinery (APM). Tumor antigenicity can also be shaped by the immune response, which can lead to the escape of non-antigenic ‘immunoedited’ tumors.

As described in the previous section, many human antigens are simply the product of ‘neutral’ mutations (leading to neoantigens), deregulated transcription (cancer-testis antigens, differentiation antigens, endogenous retroviruses), or oncogenic viral etiology (viral antigens). Therefore, cancer cells can often repress or genetically delete these antigenic sequences without overtly affecting their cellular fitness. Indeed, many experimental cancer models have documented the emergence of ‘antigen-loss variants’ that evaded immune control<sup>106,156–159</sup>. More recently, antigen loss has also been documented in clinical settings; both treatment with TILs<sup>160</sup>, as well as chimeric antigen receptor (CAR)-T cell therapy<sup>161–163</sup> have led to patient relapses harboring antigen-negative tumors.

The surface presentation of antigens on tumors, and indeed on all nucleated cells, is a complex biological pathway involving peptide import into the ER by the TAP1/2 transporters, peptide loading on MHC- $\beta$ 2-microglobulin complexes, and the transport of pMHCs to the plasma membrane<sup>164</sup>. At steady state, a cell will constantly present many peptides resulting from protein turn-over in the cell; the vast majority of these will not provoke an immune response. Exposure of the cell to IFN- $\gamma$  can lead to upregulation of several components of the antigen presentation machinery (APM). Tumors have been shown to frequently deregulate components of their APM, including downregulation of HLA alleles through genomic hypermethylation<sup>165,166</sup>, acquisition of inactivating *B2M* mutations<sup>167–169</sup> and subsequent loss of heterozygosity of the  $\beta$ 2m region on chromosome 15q21<sup>170</sup>, and genetic loss of TAP transporter proteins<sup>164,171,172</sup>. Similarly, mutations in *JAK/STAT* transducers of the IFN- $\gamma$  pathway can dampen a cancer cell’s ability to present antigens through HLA molecules<sup>169</sup>. Further evidence of the impact of selective,

endogenous immune pressure comes from longitudinal studies documenting *B2M* loss in metastatic melanomas samples in the absence of immunotherapy<sup>173,174</sup>, and computational analyses showing frequent subclonal and focal HLA loss of heterozygosity in metastatic lung cancer sites<sup>175</sup>. Thus, frequent loss of antigen and wide-spread deregulation of antigen presentation across many cancers demonstrates that lack of tumor antigenicity is a major component in driving immune escape.

### 1.3.2. Immunoediting can mediate tumor immune escape

It is now well appreciated that structural alterations in antigenicity and the presentation machinery of cancer cells can arise as a result of immune cell pressure during the early phases of tumor growth. To explain how the immune system may target and “sculpt” tumor cell antigenicity, the process of ‘immunoediting’ was defined by Schreiber, Old, and Smyth. Immunoediting occurs through three distinct phases: elimination, equilibrium, and escape (the three “E’s”)<sup>2,38</sup>.

During the elimination phase, innate and adaptive immune cells cooperate to detect and kill antigenic tumors. One of the initiating factors of these anti-tumor responses is the immunogenic cell death of tumor cells, leading to the release of antigens and DAMPs<sup>119</sup>. Other factors, such as expression of stress-induced ligands that activate NK cells, may play a role in recruiting additional immune cells, and promote a tumor microenvironment that favors immune tumoricidal activity<sup>2,176</sup>. Direct evidence for the existence of an elimination phase in human cancer has been difficult to obtain, and instead has been drawn from different lines of correlative studies. First, the presence of tumor infiltrating lymphocytes (TILs) is associated with favorable disease prognoses in

many cancer types, including breast cancer<sup>177,178</sup>, melanoma<sup>179–181</sup>, and colorectal cancer<sup>182–184</sup> (reviewed in refs. <sup>185,186</sup>). Second, several retrospective studies have demonstrated correlations between increased cancer susceptibility and the use of immunosuppressive drugs in patients with organ transplants<sup>187–190</sup> or HIV/AIDS<sup>191–193</sup>. These associations suggest that the immune system at baseline is involved in elimination of (pre-)malignant clones before these cancer cells can manifest as a clinical disease. Finally, immune elimination has been inferred from the greater frequency of chemical-induced tumors or spontaneous tumor penetrance in mice lacking key components of the immune system (e.g. *Rag2*<sup>-/-</sup>, *Prf1*<sup>-/-</sup> (perforin), *IFNGR1*<sup>-/-</sup> (IFN- $\gamma$  receptor) and others, as summarized in ref. <sup>194</sup>).

The equilibrium phase is characterized by the continuous emergence of new tumor clones and subsequent immune cell removal of particularly antigenic clones, thereby gradually “sculpting” the immunogenicity of the tumor. Although the existence of a clinically non-apparent, dormant tumor state has not been observed in human disease, evidence from a number of experimental models suggests that the equilibrium phase can persist for extended periods. For example, in a model of low-dose MCA-treatment, only disruption of the immune system (through CD8<sup>+</sup> T cell or IFN- $\gamma$  depletion) led to rapid sarcoma formation, suggesting that cytotoxic T cells previously had controlled tumorigenesis<sup>101</sup>. Although it is still largely unknown which factors dictate the equilibrium state, the cytokine milieu in the TME<sup>195</sup>, and the balance between (anti-tumorigenic) CTLs, NK cells and  $\gamma\delta$  T cells and (pro-tumorigenic) monocytic MDSCs are likely to be important<sup>196</sup>.



The final phase of immunoediting, tumor escape, is initiated by the acquisition of immunoevasive alterations that completely curtail an existing anti-tumor response and allow for uncontrolled tumor growth. As described above, during the escape phase tumor may be entirely devoid of antigenicity, have downregulated MHC molecules, or have deregulated the antigen presentation pathway. Additionally, some tumors develop resistance to T cell cytotoxicity through the upregulation of antiapoptotic molecules<sup>197,198</sup> or mutate death receptors<sup>199,200</sup>. Alternatively, tumors can recruit immune-regulatory cells through the secretion of chemokines to the tumor microenvironment to promote a state of immunosuppression. These tumor-extrinsic mechanisms will be reviewed in detail in the next section 1.4.

### 1.3.3. Oncogenic pathways drive T cell exclusion

In addition to deregulation of tumor antigenicity, tumor cells may also escape immune pressure through the activation of oncogenic pathways that impact and disrupt immune function.

One of the pathways is the Wnt- $\beta$ -catenin signaling axis. Binding of the growth factor Wnt activates an intracellular signal transduction cascade that triggers the cytoplasmic release of the transcription factor  $\beta$ -catenin, and its subsequent translocation to the nucleus to activate a host of genes involved in diverse biological functions, including (cancer) stem cell renewal<sup>201</sup>. In a preclinical genetically engineered mouse model (GEMM) of melanoma expressing constitutively active  $\beta$ -catenin (*Braf*<sup>V600E</sup>, *Pten*<sup>-/-</sup>, *CAT-STA* mice), Wnt signaling repressed transcription of the *Ccl4* chemokine gene, leading to impaired recruitment of CD103+ dendritic cells into the TME<sup>202</sup>. As these cross-presenting

DCs are crucial for the initiation of adaptive immune responses<sup>120</sup>, T cells were actively excluded from the tumor microenvironment<sup>202,203</sup>. This immunosuppressive axis does not appear to operate solely in melanoma, as a number of other cancers with alterations in the Wnt- $\beta$ -catenin pathway have similarly revealed T cell exclusion phenotypes<sup>204</sup>.

The loss of the tumor suppressor PTEN can also mediate immunosuppressive functions through the PI3K-AKT pathway. PI3K pathway alterations are among the most frequently found alterations in human cancers, and impact a wide range of cellular processes, including cellular proliferation, metabolism, and motility (invasion)<sup>205</sup>. In an analysis of cutaneous melanoma samples collected in the Cancer Genome Atlas (TCGA) database, *PTEN* deletions or loss-of-function mutations were associated with reduced T cell number and function<sup>206</sup>. Mechanistically, immunosuppression through *PTEN* loss appeared to be mediated through increased expression of VEGF (which can promote endothelial barrier function, see 1.4.1) and reduced sensitivity to T cell cytotoxicity<sup>206</sup>.

In lung cancers, two oncogenic pathways have been identified that cooperate with *Kras*-driven adenocarcinomas. Activation of the oncogene *Myc* leads to stromal reprogramming through the tumor-derived cytokines CCL9 and IL-23, causing macrophage influx into the TME and immune exclusion of T cells, B cells, and NK cells<sup>207</sup>. Additionally, these macrophages appeared to be critically involved in mediation of an angiogenic switch that sustained further adenocarcinoma development<sup>207</sup>. A second oncogenic pathway involving *STK11/LKB1*, was examined in lung adenocarcinoma patients treated with PD-1 blockade. Genetic alterations in *STK11/LKB1* were significantly associated with poorer progression-free survival (PFS) and overall survival (OS)<sup>208</sup>. Furthermore, these alterations were enriched in PD-L1 negative patients with

intermediate or high mutational burden<sup>208</sup>, suggesting that loss of *STK11/LKB1* may operate as an immunosuppressive mechanism that distinct from PD-1-mediated pathways. In lung GEMMs, genetic ablation of this pathway leads to increased neutrophil recruitment through elevated IL-1a and IL-6 production<sup>209</sup> and repression of the cytoplasmic DNA-sensor STING<sup>210</sup>. LKB1 restoration leads to upregulation of PD-L1 expression on tumor organoids<sup>210</sup>. The therapeutic blockade of IL-6 significantly inhibits tumor progression, and improved survival<sup>209</sup>. Interestingly, checkpoint blockade with CTLA-4 or a combination of PD-1 and TIM-3 did not demonstrate any efficacy in this model<sup>209</sup>, further suggesting that STK11/LKB1-mediated immunosuppression is a unique mechanism of therapeutic resistance and immune escape.

A third oncogenic pathway that has received significant attention over the past few years, involves the cyclin-dependent kinases 4 and 6 (CDK4/6). CDK4/6 are critical regulators of cell-cycle progression: they cooperate with D-type cyclins to phosphorylate Rb (pRB), thereby releasing E2F to trigger transition from G1 into the S-phase<sup>211</sup>. It was shown recently that CDK4 promotes proteasomal degradation of PD-L1<sup>212</sup>. Additionally, downstream pRB was shown to transcriptionally repress PD-L1 through NF- $\kappa$ B signaling<sup>213</sup>. These studies suggest that restoration of CDK4/6 or Rb may promote tumor immunity. However, *in vivo* pharmacological inhibition of CDK4/6 in breast carcinoma, colorectal carcinoma and melanoma mouse models is associated with improved anti-tumor immunity, rather than resistance<sup>214–217</sup>. These effects appear mediated through tumor-intrinsic factors (increased antigen presentation and type III interferon signaling<sup>214</sup>) as well effects on T cells (NFAT potentiation of T cell activation)<sup>215,216</sup>. An open question is how increased PD-L1 expression impacts these therapeutic responses. The

paradoxical nature of these complex *in vivo* responses illustrates that there is undoubtedly more to learn about the role of the CDK4/6-Rb pathway in tumor immune escape.

## **1.4. Tumor-extrinsic mechanisms of immune escape**

Over the course of malignant progression, tumors modulate their surrounding microenvironment extensively to create favorable conditions for oncogenic growth. A key aspect of these adaptations involves the preferential recruitment of pro-tumorigenic immune cell subsets, and suppression of anti-tumorigenic T cells and NK cells. In the next sections, the different aspects of the tumor microenvironment intimately involved in the creating immunosuppression will be described.

### **1.4.1. Endothelial cells**

Cancer cells extensively modulate the surrounding blood vasculature to access critical nutrient supplies that sustain rapid tumor proliferation<sup>218</sup>. Compared to healthy tissue vasculature, tumor vessels exhibit several abnormal morphological features, including erratic branching (“tortuous” vessels), loose endothelial lining, and sparse coverage of pericytes that control vascular permeability<sup>219,220</sup>. Consequently, tumor vessels are highly “leaky” and blood flow is irregular, contributing low-oxygen environment (known as ‘hypoxia’). Hypoxia in turn drives the secretion of vascular endothelial growth factor (VEGF) by tumor cells<sup>221</sup> and cells in the TME<sup>222</sup>, which binds VEGF receptors on nearby endothelial cells to stimulate “sprouting” of new blood vessels (‘neo-angiogenesis’)<sup>223</sup>. As T cells critically depend on coordinated interactions with the

endothelial vasculature to facilitate T cell migration into the TME, these aberrant tumor blood vessels may be more difficult to navigate for lymphocytes.

VEGF (and fibroblast growth factor) may also directly exert immunosuppressive functions through the promotion of endothelial barrier function and upregulation of FasL. VEGF leads to downregulation of ICAM-1/2, VCAM-1, and CD34 on endothelial cells<sup>224</sup>, referred to as 'anergic ECs'. EC anergy prevents the engagement of T cell integrin adhesion receptors (LFA-1, Mac-1, and VLA-4) that participate in endothelial extravasation<sup>138</sup>. VEGF can also upregulate the Fas ligand (FasL) on endothelial cells as an additional mechanism to stave off anti-tumorigenic T cells<sup>225</sup>. Recent effector CD8+ T cells may be particularly sensitive to endothelial FasL, as the death receptor Fas becomes upregulated during T cell activation<sup>226</sup>. Certain tissues (for example, the eye) actively exclude immune cells through FasL expression<sup>227</sup>, which has led to the suggestion that tumor sites acquire a degree of "immune privilege"<sup>228</sup>.

The endothelial B receptor (ET<sub>B</sub>R) pathway has been implicated in suppressing T cell adhesion to ECs as well<sup>229</sup>. ET<sub>B</sub>R expression was shown to be inversely correlated with the presence of tumor-infiltrating lymphocytes (TILs) in ovarian carcinomas, while pharmacological inhibition of ET<sub>B</sub>R led to improved T cell vessel adhesion<sup>138</sup>.

Tumors thus extensively impact T cell migration through aberrant vasculature and promotion of endothelial barrier function.

#### 1.4.2. Cancer-associated fibroblasts (CAFs)

Cancer-associated fibroblasts (CAFs) are abundant stromal cells in the tumor microenvironment, and can even outnumber cancer cells in certain tumors. Their role in

supporting cancer progression is highly pleiotropic in nature, and includes enabling tumor metabolic adaptation to hypoxia, facilitating cancer motility and invasion through remodeling of the ECM, promoting therapy resistance, and suppressing immune function<sup>230</sup>. As a result of continuous mechanical tissue disruption by growing cancer cells, tissue repair responses are typically chronically activated in the tumor parenchyma (cancers are a “wounds that never heal”). As a result, normal fibroblasts participating in tissue repair of the tumor microenvironment irreversibly differentiate into CAFs in response to chronic stimuli, which increases their migratory capacity and alters their secretome<sup>230</sup>. Attempts at defining several subtypes of CAFs with specialized functions have been made, however there is considerable heterogeneity based on their cellular origin<sup>231,232</sup>. To add to this complexity, a number of fibroblast subtypes can perform overlapping tumor-supportive functions.

Cancer-associated fibroblasts may exert both direct and indirect effects on the surrounding immune cell infiltrate. CAFs are known to secrete a plethora of different cytokines, chemokines, and pro-angiogenic factors that can have extensive effects on nearby innate immune cell polarization and T cell function. A comprehensive description of these factors is beyond the scope of this thesis, but is well summarized in a recent review<sup>231</sup>. Instead, a few key CAF-secreted factors will be highlighted below.

CAF are a major source of transforming growth factor  $\beta$  (TGF- $\beta$ ), which, aside from context-dependent roles in cancer progression<sup>233</sup>, can suppress the effector function of NK and T cells<sup>234,235</sup>, impair T cell memory responses<sup>236</sup>, and promote T cell exclusion<sup>237–239</sup>. Additionally, TGF- $\beta$  can promote CD4+ T cell transdifferentiation into T regulatory cells<sup>240</sup>. TGF- $\beta$ , and the CXCL12 chemokine can also recruit

immunosuppressive M2-polarized macrophages to the tumor microenvironment<sup>241–243</sup>, and thereby indirectly impact T cell function. CAFs also secrete abundant IL-6, which can impair dendritic cell maturation and antigen presentation capacity<sup>244,245</sup>, and skews monocyte differentiation towards macrophage fates<sup>246</sup>. Finally, modulation of the ECM by CAFs through the deposition of fibronectin, hyaluronic acid and collagens can lead to poor T cell infiltration and stromal trapping, as well as enhance M2-polarized macrophage migration into the TME<sup>146,247,248</sup>.

#### 1.4.3. Myeloid-derived suppressor cells (MDSCs) and tumor-associated macrophages (TAMs)

Myeloid-derived suppressor cells (MDSCs) are a heterogenous and highly plastic population of bone marrow-derived myeloid precursor cells. At least two distinct types of MDSCs exist in mice and humans: polymorphonuclear MDSCs (PMN-MDSCs), which are more closely related to neutrophils, and monocytic MDSCs (M-MDSCs), which are related to monocytes<sup>249</sup>. While both PMN-MDSCs and M-MDSCs are thought to mediate immunosuppressive roles during immune responses, PMN-MDSCs are typically localized to peripheral lymphoid organs, where they function to maintain immune tolerance<sup>249</sup>. In contrast, M-MDSCs migrate to tumors, where they can further acquire tumor-associated macrophage fates<sup>249</sup>. MDSCs are actively recruited by tumors through the secretion of a number of chemokines, including CCL2, CXCL1, and CXCL12<sup>250–253</sup>. In the tumor microenvironment MDSCs fulfill potent, but largely non-specific immunosuppressive roles. Persistent inflammation and hypoxia in tumors induces the upregulation of arginine 1 (Arg1) and inducible nitric oxide synthase 2 (iNOS2) proteins, which leads to local L-

arginine depletion and inhibition of IL-2 signaling through nitric oxide<sup>249,254</sup>. Furthermore, MDSCs can also deplete tryptophan levels through IDO1 expression<sup>255</sup>, can directly upregulate PD-L1<sup>256</sup>, and recruit CCR5+ T regulatory cells through the release of CCL3 and CCL4<sup>257</sup>.

#### 1.4.4. Tumor-associated macrophages (TAMs)

Macrophages are phagocytic cells that mediate key roles in the clearance of infectious agents, and maintenance of tissue homeostasis<sup>258</sup>. In tumors, macrophages are thought to derive from circulatory conventional monocytes or monocytic myeloid-derived suppressor cells<sup>259</sup>. Macrophage fate is highly plastic, and context-dependent, referred to as 'polarization'. In describing the different roles of tumor-associated macrophages (TAMs), a distinction between M1 (anti-tumorigenic) and M2 (pro-tumorigenic) has historically been made. However, it is now appreciated that macrophage polarization represents a spectrum<sup>260</sup>.

TAMs exert clear immunosuppressive roles in the primary tumor microenvironment, and can promote metastatic tumor dissemination. Their recruitment is mediated through chemokines (including CCL2 and CCL5), and cytokines (CSF-1 and VEGF)<sup>259,261,262</sup>. CSF-1 plays a particularly important role in attracting and polarizing TAMs to a "M-2-like" state<sup>262–264</sup>. TAMs promote tumor growth and immunosuppression of effector T cell responses through a number of different pathways. TAM stimulation by IL-4 and Wnt7 $\beta$  promotes an angiogenic switch through the release of VEGF, leading to the *de novo* development of blood vasculature in tumors<sup>265–267</sup>. TAMs are also known to



directly aid extravasation of invasive mammary cancer cells into the circulation<sup>268</sup>, and can remodel the ECM to further promote tumor migration<sup>269</sup>.

In addition to these tumor promoting functions, TAMs also exert a myriad of immune-regulatory roles through direct and indirect inhibition of T cell and NK cell anti-tumor responses. Direct mechanisms include expression of the nonclassical MHC class I molecules (HLA-G) which functions to inhibit T cells and NK cells<sup>270,271</sup>, cell-surface upregulation of PD-L1 and the alternate B7-H4 receptor<sup>272–276</sup>, and expression of the TRAIL death receptor<sup>277</sup>. Indirect mechanisms include the depletion of L-arginine (through Arg1)<sup>278–280</sup>, recruitment of T regulatory cells through CCL20 and CCL22<sup>281,282</sup>, and the secretion IL-10 and TGF- $\beta$  which may locally convert convention CD4+ into T regulatory cells<sup>283,284</sup>.

#### 1.4.5. T cell-intrinsic dysfunction

Upon cognate antigen stimulation in the lymph node by an APC, CD8+ and CD4+ T cells rapidly upregulate a number co-stimulatory (SRs) and co-inhibitory receptors (IRs)<sup>130</sup>. As T cells must “pass” these co-inhibitory functions in order to acquire full effector functionality, IRs are sometimes referred to as ‘immune checkpoints’. The spatiotemporal relationship between SR and IR expression has been conceptualized as a “tidal wave”<sup>285</sup>. In this model, a “wave” of signals triggered by SR engagement pulls naïve and recently activated T cells into a proliferative state. The peak of the wave is balanced by the opposing actions of SR and IR signals, before the wave recedes when the balance shifts to inhibitory signals<sup>130,285</sup>. Therefore, T cell responses are inherently self-limited in nature to control immune homeostasis. Furthermore, IR expression on CD4+ T regulatory cells

ensures that peripheral tolerance is maintained to restrain pathogenic host-directed adaptive immunological responses. Indeed, mutation or deficiency of several co-inhibitory receptors is associated with the development of murine and human autoimmune disorders<sup>102,286–289</sup>.

It has long been appreciated that T cells fail to clear certain experimental viral infections (e.g. lymphocytic choriomeningitis virus (LCMV) clone 13) and instead acquire impairments in their effector, proliferative and memory-formation capacities<sup>290–293</sup>. This distinct state has been defined as ‘T cell exhaustion’, and is thought to be driven by an aberrant differentiation program in the context of pathogen persistence, immunosuppressive cytokines, and lack of CD4+ T cell help<sup>294</sup>. Exhausted T cells in chronic LCMV exhibit several characteristics, including the sustained transcriptional upregulation of several IRs (*Pcd-1*, *Ctla-4*, *Lag-3*, *2b4*, *Gp49b*, and others), defects in cytokine production (IFN- $\gamma$ , TNF- $\alpha$ , IL-2), upregulation of chemokine genes (*Ccl3*, *Ccl4*, *Cxcl5*), transcription factors (T-bet, Eomes, Blimp-1, and Tcf-1), and altered cellular metabolism (bioenergetic deficiency)<sup>295</sup>. Epigenetic profiling of exhausted T cells has reinforced the idea that these cells exhibit distinct differentiation from effector or memory T cells<sup>296,297</sup>. Recently, the transcription factor *Tox* was identified as a key regulator of this epigenetic program in chronic LCMV<sup>298–300</sup> and a mouse model of cancer<sup>301</sup>.

As T cells experience persistent antigen load, they gradually become impaired in several effector functions<sup>302</sup>. High proliferative capacity, IL-2 production and *ex vivo* cytotoxicity are impaired first, before TNF- $\alpha$  production, and finally IFN- $\gamma$  production and the ability to degranulate<sup>302</sup>. Severely exhausted T cells that have lost effector functionality may get physically deleted from the host<sup>291–293</sup>. Although these progressive

impairments highlight that T cell responses can become highly dysfunctional, it is important to note that T cell exhaustion is a crucial safeguard against rampant pathological inflammatory reactions, and exhausted T cells are capable of maintaining some control over the infection<sup>302,303</sup>. Furthermore, exhaustion is not irreversible, as T cell functionality can be restored by a therapeutic blockade of PD-1-PD-L1 axis, which has been shown to decrease systemic viral load<sup>304</sup>.

Several lines of evidence demonstrate that T cells acquire a dysfunctional program in tumors that is analogous to T cell exhaustion. Tumor-specific T cells isolated from multiple types of cancers upregulate multiple IRs, including PD-1, CTLA-4, LAG-3, and TIM-3<sup>305–307</sup>. Furthermore, tumor-specific T cells are impaired in their ability to produce cytokines (IFN- $\gamma$ , TNF- $\alpha$ ) in multiple human tumors<sup>305–311</sup>. T cell proliferative capacity is another functional attribute that appears to decrease as intratumoral T cells become more dysfunctional, as early progenitor T cells exhibit more cell-cycle gene expression and Ki67 marker positivity than more dysfunctional T cells<sup>312</sup>.

Similar to T cell exhaustion, T cell tumor dysfunctionality is thought to be driven by chronic antigen exposure, and may be acquired early during tumorigenesis<sup>313</sup>. However, it is not a fixed state, and rather phenotypically heterogeneous, as evidenced by several reports over the past few years<sup>314–316</sup>. Several attempts at defining precursor states (“pre-dysfunctional”, “transitional” or “progenitor exhausted” cells) have been made by the gene expression patterns of unique genes (e.g. *GZMK*, *TCF-7*, *IL7R*, *ZNF683* and others) and the surface (co-)expression of different IRs (reviewed in <sup>317</sup>). For example, pre-dysfunctional T cells in a mouse model of melanoma are marked by Slamf6+TIM-3-TCF-1+, and can give rise to Slamf6-TIM-3+TCF-1 dysfunctional T cells (but not vice versa)<sup>318</sup>.

The impact of a number of transcription factors on the T cell dysfunctional program has also been extensively investigated in murine and human cancer. The pre-dysfunctional responsive state appears maintained by Tcf-1<sup>318–320</sup>, while dysfunctionality is driven by Tox<sup>301</sup>. A number of other transcription factors, such as Gata3, Blimp-1/Prdm1, c-Maf, T-bet, and Eomes appear play roles in maintaining this state as well<sup>321–323</sup>.

A more detailed review of the biology of the major co-inhibitory receptors is provided in the sections that follow:

#### CTLA-4

Although the cytotoxic T-lymphocyte associated protein 4 (CTLA-4) was originally thought to be a potentiator of T cell activity, research in the 1990s demonstrated that it was a negative regulator<sup>4</sup>. The expression of CTLA-4 is driven the NFAT transcription factor, which is activated by TCR and CD28 stimulation during T cell activation<sup>324</sup>. Upon expression, CTLA-4 locates to the TCR proximal plasma membrane, where it is subject to constitutive endocytosis. As a result ~90% of CTLA-4 is intracellular<sup>325</sup>. At the cell surface, CTLA-4 has high affinity for the CD80 (B7.1) and CD86 (B7.2) molecules on mature APCs<sup>326</sup>, and can form bivalent interfaces with both ligands, which allows it to outcompete CD28 binding<sup>327,328</sup>. CTLA-4 may also exert cell-extrinsic negative regulation through the trans-endocytosis of CD80 and CD86<sup>329,330</sup>. Through these actions, CTLA-4 counteracts CD28-mediated PI3K-AKT and RAS-MAPK signaling. Surprisingly, the intracellular pathways downstream of CTLA-4 receptor engagement are not fully elucidated (reviewed in <sup>331</sup>); conflicting data exists on whether CTLA-4 can

dephosphorylate proximal TCR complex components, recruit of SHP2 through YVKM sequence in the CTLA-4 cytoplasmic tail or directly inhibits PI3K-AKT pathway signaling. It is clear however that CTLA-4 plays a critical role as a negative regulator during T cell priming.

### PD-1

Programmed cell death protein 1 (PD-1) principally functions to maintain peripheral tolerance and restrain excessive inflammatory responses to preserve tissue homeostasis. PD-1 is upregulated on activated effector CD8<sup>+</sup> and CD4<sup>+</sup> T cells<sup>332</sup>, and PD-1 expression is sustained in the context of chronic antigen exposure<sup>304</sup>. A number of transcription factors (NFAT, FOXO1, T-Bet, and BLIMP-1) have been shown to regulate PD-1 expression<sup>333</sup>. PD-1 interacts with the PD-L1 and PD-L2 molecules in peripheral tissues. PD-L1 is widely expressed on both hematopoietic (T cells, B cells, macrophages, DCs, and mast cells) and non-hematopoietic cells (e.g. tumor, endothelial, corneal epithelial, placental syncytiotrophoblast, and pancreatic islet cells, as well as keratinocytes and astrocytes)<sup>334</sup>. In contrast, PD-L2 expression is restricted to macrophages, DCs, and mast cells. PD-L1 and (to a lesser degree) PD-L2 upregulation can be induced by IFN- $\gamma$  signaling<sup>335,336</sup>. PD-1-PD-L1 signaling has inhibitory effects on proximal TCR signaling components through the direct recruitment of the SHP2 phosphatase to the PD-1 cytoplasmic tail, and downregulates signaling outputs of CD28-mediated pathways<sup>337</sup>. The latter may represent a central axis of co-inhibitory regulation that is shared between CTLA-4 and PD-1<sup>338</sup>. Thus, PD-1 broadly acts to decrease T cell

activation, affecting cell survival, proliferation, and cytokine production as well as altering the cellular metabolism of effector T cells<sup>333,339</sup>.

### TIGIT

The T cell immunoglobulin and ITIM domain (TIGIT) is a relative recent addition to the co-inhibitory receptor family, after being discovered on effector T cells, Tregs and NK cells by several groups<sup>340–343</sup>. TIGIT is expressed on effector and memory T cells, Tregs, follicular T helper cells, and NK cells<sup>340–345</sup>. Tumor-specific T cells have been shown to co-express TIGIT with PD-1, which is thought to mark a dysfunctional CD8+ subset<sup>346,347</sup>. TIGIT binds two ligands, poliovirus receptor (PVR; CD155) and PVRL2 (CD122), although its affinity for PVR is 100-fold higher affinity than PVRL2<sup>348</sup>. Crystal structures of the TIGIT-PVR interaction have demonstrated that the complex exists in a tetrameric state, with each surface protein contributing *cis*-homodimers<sup>349</sup>.

TIGIT (and the Tactile/CD96 receptor) functions in opposition of the co-stimulatory receptor DNAM-1 (CD226), which also binds PVR, albeit with lower affinity than TIGIT<sup>350</sup>. TIGIT may counteract DNAM-1 through several mechanisms. First, TIGIT is capable of outcompeting DNAM-1 for PVR binding on the cell surface<sup>350</sup>, similarly to CTLA-4 and CD28. Second, TIGIT may regulate DNAM-1 in *cis* by impairing homodimerization of this receptor<sup>351</sup> and can mediate signals in *trans* through the ITIM motif in the cytoplasmic tail of PVR<sup>342</sup>. Finally, and perhaps most crucially, PVR binding leads to Grb2-SHIP2 sequestration to the cytoplasmic tail of TIGIT in NK cells, preventing downstream PI3K-AKT, MAPK, NF- $\kappa$ B signaling<sup>348</sup>. TIGIT thus broadly impacts T cell activation, proliferation and differentiation programs. However, TIGIT can also have positive roles, including the

promotion of cell survival through upregulation of IL-2R, IL-7R, and IL-15R and the anti-apoptotic Bcl-x<sub>L</sub> protein<sup>344</sup>.

In addition to roles on effector T cells and NK cells, TIGIT also promotes the functionality of T regulatory cells. The *TIGIT* gene is transcriptionally regulated by the Treg-lineage defining transcription factor Foxp3<sup>352</sup>. TIGIT<sup>+</sup> Tregs are more activated, as indicated by increased Foxp3, CD25, CTLA-4, and Fgl2, which mediates suppression of T<sub>H</sub>1 and T<sub>H</sub>17 responses<sup>345,353</sup>.

### TIM-3

T cell immunoglobulin-3 (TIM-3) is a co-inhibitory receptor that is part of a larger family of TIM proteins, which also encompasses TIM-1 and TIM-4. TIM-3 is expressed on activated T<sub>H</sub>1 CD4<sup>+</sup> T cells, effector CD8<sup>+</sup> T cells, T regulatory cells, dendritic cells, monocytes and NK cells. TIM-3 is upregulated on intratumoral T cells, where it is thought to mark severely impaired effector T cells. Tumor-resident TIM-3<sup>+</sup> Tregs are thought to be more immunosuppressive, and have increased expression of Foxp3, IL-10, granzymes, and Perforin. Several TIM-3 ligands have been identified, including Galectin-9, Ceacam-1, phosphatidyl serine (PtdSer), and HMGB1, although the latter two appear important for interactions on TIM-3<sup>+</sup> innate immune cells.

Similar to LAG-3 (see section below), TIM-3's cytoplasmic domain does not contain any canonical immunoreceptor tyrosine-based inhibitory motifs (ITIMs). Instead, several evolutionary conserved tyrosine residues (Y256 and Y263) have been implicated in recruiting Bat3 (in the absence of ligand) or Fyn (upon Galactin-9, CEACAM-1 binding).

Upon association with the cytoplasmic tail of TIM-3, Fyn recruits the Csk kinase, which, through sequestration of Lck, can inhibit proximal TCR signaling.

### LAG-3

Lymphocyte activation gene 3 (LAG-3) was discovered three decades ago<sup>354</sup>, and encodes a co-inhibitory receptor expressed on activated CD8+ and CD4+ T cells, T regulatory cells, NK cells<sup>354,355</sup>, murine plasmacytoid dendritic cells<sup>356</sup>, B cells<sup>357</sup>, and even neurons<sup>358</sup>. LAG-3 expression on T regulatory cells is associated with an activated phenotype, and LAG-3+ Tregs may play a role in T cell homeostasis<sup>355,359</sup>. LAG-3 is capable of binding several ligands, including MHC class II molecules, galectin-3, LSECtin, and  $\alpha$ -synuclein<sup>358,360,361</sup>. As LAG-3 is structurally similar to the CD4 co-receptor<sup>362</sup>, the interaction with MHC class II has been a major focus of investigation. The biophysical nature of this interaction however still remains poorly defined. The recent identification of fibrinogen-like protein 1 (FGL1) as a cognate ligand suggests that LAG-3 may have functions in immune cells do not typically interact with MHC class II molecules<sup>363</sup>.

LAG-3 closely associates with CD3 chains, which is thought to drive inhibition of T cell proliferation, cytokine production, and calcium flux<sup>364</sup>. However, as the cytoplasmic tail of LAG-3 contains poorly characterized motifs<sup>355</sup>, LAG-3 downstream intracellular signaling remains to be fully elucidated.

#### 1.4.6. CD4+ T cells

CD4+ T cells are critically involved in orchestrating immune responses, and can adopt many effector lineages upon antigen stimulation through MHC class II molecules.



In addition to stimulating antibody-production responses, CD4<sup>+</sup> T cells can provide “help” during effector CD8<sup>+</sup> T cell differentiation, regulate macrophage polarization, maintain tissue homeostasis and peripheral tolerance<sup>365</sup>. These effector functions are achieved by cellular differentiation into distinct fates, including T<sub>H</sub>1, T<sub>H</sub>2, T<sub>H</sub>17, T<sub>FH</sub>, and T regulatory cells fates. Each of these CD4<sup>+</sup> “helper” lineages are further characterized by the production of certain cytokines: T<sub>H</sub>1 CD4<sup>+</sup> predominantly produce IFN- $\gamma$ , TNF- $\alpha$ , CCL2 and CCL3, T<sub>H</sub>2 produce IL-4, IL-5, and IL-13, T<sub>H</sub>17 produce IL-17A and IL17F, T<sub>FH</sub> produce IL21, and Tregs produce IL-10, IL-35 and TGF- $\beta$ <sup>366,367</sup>. While a number of T<sub>H</sub> CD4<sup>+</sup> T cells can exert anti-tumorigenic roles, these functions are highly context-dependent (reviewed in <sup>366</sup>).

T regulatory cells are critical mediators of peripheral tolerance, and function to suppress excessive host-directed immune responses<sup>368</sup>. T regulatory cell lineage is defined by the transcription factor forkhead box protein P3 (Foxp3). A role for Tregs in peripheral tolerance further supported by mice strains carrying mutations in the *Foxp3* gene (“scurfy” mice) that develop rapid, lethal autoimmune responses<sup>369</sup>. Tregs can play a crucial roles at multiple stages of the anti-tumor immune response, notably during T cell priming and during the effector response in peripheral tissues. During antigen presentation in lymph nodes, Tregs can act as a “cytokine sink” by sequestering available T cell growth factor (IL-2)<sup>370,371</sup>, and can suppress antigen stimulation through upregulation of the co-inhibitory receptor CTLA-4<sup>372,373</sup>. Both tumors and macrophages have been shown to actively recruit T regulatory cells to the TME through the secretion of inflammatory cytokines CCL2, CCL21, and CCL22<sup>281,374,375</sup>. In the tumor tissue Tregs can effectively suppress effector CD8<sup>+</sup> T cell responses through direct inhibition or even

killing of CTLs (through perforin and granzymes)<sup>376</sup>, the production of T cell inhibitory metabolites (adenosine)<sup>377,378</sup>, and the secretion of a number of immunoregulatory cytokines (IL-10, IL-35 and TGF- $\beta$ ) that further dampen T cell activity<sup>379–382</sup>. Tumor-infiltrating T regulatory cells have been shown to be “activated”, and upregulate a number of IRs and SRs upon activation (PD-1, TIGIT, TIM-3, LAG-3, ICOS, and OX40)<sup>383</sup>. It has been suggested that Treg activation is mediated by the (abundant) release of self-antigens in the tumor microenvironment<sup>384</sup>, however the precise mechanisms remain to be established.

#### 1.4.7. Tumor microenvironments can exist in distinct inflammatory states

The previous sections illustrated that cancer cells, stromal cells and immune cells collectively influence the inflammatory state of the tumor microenvironment. Based on localization and density of lymphocytic infiltrates and presence of immune-associated soluble factors, a distinction between ‘cold’ (non-T cell-inflamed), ‘altered’, and ‘hot’ (T-cell inflamed) tumor microenvironments has been made<sup>385,386</sup>.

Non-T cell-inflamed tumors largely lack infiltrating T cells, but may still harbor macrophages and vascular endothelial cells<sup>386</sup>. Defective T cell priming is thought to underlie the absence of T cells in these cold tumors, however these priming defects cannot be explained by a lack of tumor antigens (at least in the case of melanoma)<sup>386,387</sup>. As described in 1.3.3, oncogenic alterations in Wnt/ $\beta$ -catenin or PTEN pathways may promote a non-T cell-inflamed microenvironment. Patients with immunologically cold tumors typically respond poorly to current approved immune checkpoint inhibitors<sup>385</sup>,

suggesting that fundamentally different strategies such as dendritic cell vaccination may be required to initiate and enhance anti-tumor immune responses.

In altered (or immune excluded) tumor microenvironments, effector T cells are confined to the invasive margins of the tumor bed. Several tumor-intrinsic and tumor-extrinsic factors can promote T cell exclusion, including altered chemokine signaling, presence of immunosuppressive innate immune cells, and stromal barriers (e.g. severe hypoxia in the tumor core, an impenetrable ECM, or abnormal endothelial vessels)<sup>388–390</sup>.

Finally, in a hot tumor microenvironment, cytotoxic T cells are abundantly present, and several soluble factors and cytokines (IFN- $\gamma$ , IDO1) indicate significant T cell reactivity. However, persistent antigen load as well as the presence of immune-regulatory subsets in the tumor microenvironment renders most of these effector T cells dysfunctional. Dysfunctional T cells may express a number of co-inhibitory surface markers, including CTLA-4, PD-1, TIGIT, TIM3, LAG-3, and CD39. These T cell dysfunctional programs are driven by transcription factor such as TOX. Patients with these hot tumor microenvironments are typically respond well to immune checkpoint inhibitors, and are most likely to derive clinically durable benefit from these immune-based therapies.

## **1.5. Pancreatic cancer**

Pancreatic cancer is a deadly malignant disease in one of the body's major digestive organs. The pancreas has both exocrine functions (secretion of enzymes such as trypsin, chymotrypsin, and lipase) and endocrine functions (regulation of glucose homeostasis). These functions are carried out by specialized cells contained in the

pancreatic parenchyma. Acinar cells are the major producers of digestive enzymes, which are released into tubular networks formed by ductal cells. Acinar cells constitute the bulk of the pancreatic tissue (80%), while islets of Langerhans lay interspersed in the parenchyma<sup>391</sup>. Islets contain several hormone-producing cell types, including  $\alpha$  cells (glucagon),  $\beta$  cells (insulin),  $\delta$  cells (somatostatin),  $\epsilon$  cells (ghrelin), and pancreatic polypeptide (PP) cells. Accordingly, tumors arising from either the exocrine or endocrine tissue have distinct classifications; pancreatic ductal adenocarcinomas (PDACs) are by far the most common (exocrine) pancreatic tumors, while pancreatic neuroendocrine tumors (pNETs) are relatively rare (endocrine) tumors (~7% of all pancreatic cancer cases)<sup>392</sup>.

Pancreatic cancer accounts for an estimated 57,600 new cases in 2020 in the U.S. alone, and for 47,050 deaths. It is the 10<sup>th</sup> most commonly diagnosed cancer, but the 4<sup>th</sup> leading cause of cancer death<sup>392</sup>. Risk factors for pancreatic cancer include smoking history, type 2 diabetes, obesity, and a family history of pancreatic cancer or chronic pancreatitis<sup>392</sup>. *BRCA1/2* germline mutation carriers also carry increased risk for pancreatic cancer (4-7% of PDAC patients). In December 2019, the FDA approved a PARP inhibitor (Olaparib/Lynparza) as maintenance therapy for *BRCA1/2*-mutant metastatic PDAC<sup>393</sup>.

The 5-year overall survival (OS) rate (9%) remains dismal for PDAC. The standard of care for local PDAC is surgical resection, often combined with adjuvant chemotherapy or radiotherapy. Surgery currently provides the only curative benefit for this disease, with 5-year OS rates at 37%<sup>392,394</sup>. However, as the majority of PDAC patients are diagnosed with locally advanced or distant metastatic disease, combination chemotherapy (either

FOLFIRINOX or nab-paclitaxel with gemcitabine) is the only treatment option<sup>395</sup>. While combination chemotherapy regimens extends patient survival to 8.5-11.1 months, 5-year OS rates are low (12% for regional disease, 3% for metastatic disease)<sup>392,396,397</sup>. These sobering figures underline that novel therapies for the treatment of pancreatic cancer are urgently needed.

#### 1.5.1. The disease progression and the genetic basis of pancreatic adenocarcinoma

Similar to other cancers arising in the gastrointestinal tract, pancreatic adenocarcinoma is thought to progress through several tumor stages, characterized by increasingly neoplastic and invasive growth. Pancreatic cancer is initiated by the acquisition of oncogenic mutation(s) and loss of tumor suppressor genes in a founding clone, before progressing to precursor lesions. The most common precursor lesions are pancreatic intraepithelial neoplasias (PanINs), although other lesions have been defined (mucinous cystic neoplasms (MCNs), and intraductal papillary mucinous neoplasms (IPMNs))<sup>391,398</sup>. Several stages of PanINs (I-III) have been described, and are associated with increasing neoplastic morphology and disruption of ductal architecture<sup>399</sup>. Progression of PanIN to frank adenocarcinoma is demarcated by local invasion through the ductal basement membrane into the surrounding tissue parenchyma. The final stage in the development of PDAC is metastatic spread to distant tissues.

During the initiation phase, an oncogenic driver mutation transforms cells of the exocrine pancreas. Although PDAC typically arises in the head of the pancreas, the exact cell of origin remains a topic of debate. In fact, multiple lines of experimental evidence

have suggested that ductal, acinar and even endocrine cells can give rise to PDAC under certain chronic inflammatory conditions<sup>400–402</sup>, suggesting that transformative event is highly context-dependent. Acinar cells are thought to be the most permissive to oncogenic transformation, and undergo an acinar-to-ductal metaplasia, possibly driven by extrinsic inflammatory cues<sup>403–405</sup>.

Mathematical models based on mutational analyses of advanced-stage pancreatic cancer patients have estimated that the founding somatically acquired mutation occurs around a median of ~7.1 years (3.3-12.2 years) before the establishment of a PanIN lesion, while development to adenocarcinoma occurs over a period of ~4.3 years (2.3-7.2 years)<sup>406</sup>. Thus, the acquisition of driver mutations is marked by a relatively long latent period prior to becoming fixed in the population through cell division.

*KRAS* mutations are the initiating genetic event in PDAC, and indeed are highly prevalent as the sole founding mutation in early PanIN lesions<sup>407</sup>. Genetic studies have demonstrated that over 90% of PDAC contains activating *KRAS* mutations<sup>408</sup>. *KRAS* mutations occur at several residues, with G12D being most prevalent (41% of *KRAS*-mutated PDAC), followed by G12V (34%), G12R (16%), Q61H (3.9%) and other alleles<sup>409</sup>. Pancreatic cancers can also acquire mutations in different Ras isoforms (*HRAS*, *NRAS*) that may have isoform-specific intracellular signaling outputs<sup>410</sup>. An open question is whether the wild-type *KRAS* allele plays a causal role in oncogenic transformation<sup>409,411</sup>. One report documented the loss of heterozygosity of the wild-type *KRAS* allele, suggesting that it may have tumor-suppressive functions<sup>412</sup>. However, other studies have observed oncogenic roles for wild-type *KRAS*, *NRAS* or *HRAS* in *KRAS*-mutated pancreatic cancer cell lines<sup>413,414</sup>. A second outstanding question that remains

to be answered is how *KRAS* mutations leads to the outgrowth of early lesions, as studies from mouse models have suggestive that *Kras* by itself induces PanIN formation with relatively long latency<sup>415,416</sup>. Indeed, retrospective autopsy studies have revealed that PanIN frequency ranges from 18-28% in otherwise normal individuals<sup>417,418</sup>. The answer for the development of early PanINs may lie in tumor-induced microenvironmental changes, as *Kras* signaling can lead to GM-CSF production, and recruitment of inflammatory IL-17+ CD4+ T cells<sup>419,420</sup>.

While *KRAS* mutations are acquired before the PanIN stages, a number of additional genetic events occur during PanIN progression. Mutational studies by the Cancer Genome Atlas (TCGA) of 150 surgically resected (mostly stage I-III) patient samples revealed that *TP53* (73%), *SMAD4* (32%) and *CDKN2A* (30%) are the most recurrently mutated genes in PDAC, and are frequently co-mutated with *KRAS*<sup>408</sup>. Loss of these three tumor suppressors is well-established in the progression of PDAC (reviewed in <sup>391,421</sup>).

Genetically engineered mouse models such as *LSL-Kras*<sup>G12D/+</sup>; *LSL-Trp53*<sup>R172H/+</sup>; *Pdx-1-Cre* (KPC) mouse have been crucial in evaluating the role of putative oncogenes and tumor suppressor genes in PDAC progression<sup>422,423</sup>. In the KPC model, Cre-mediated recombination of an oncogenic *Kras* allele and a dominant-negative point mutant *Trp53* allele in pancreatic tissue progenitor cells leads to the development of multifocal pancreatic lesions around 10 weeks after birth, and progression to frank adenocarcinoma and distant metastatic disease. Careful examination of this mouse model has led to a “genetic progression” model, where oncogenic *Kras* activation and telomere shortening drives the initial development PanIN I lesions. The loss of *CDKN2A* occurs during the

transition to PanIN II lesions, while *TP53*, *SMAD4* alterations that lead to PanIN III and frank adenocarcinoma<sup>424</sup>. Whether a genetic basis for metastatic spread exists remains an open question, as primary adenocarcinoma and metastatic samples have shown a surprising high degree of overlap in somatic mutations<sup>425,426</sup>. Alternative hypotheses such as an altered epigenetic landscape have been put forward<sup>427</sup>, but remain to be further explored.

In addition to these top four recurrently mutated genes, PDAC samples also contain many less frequently recurrent alterations (<10% of patients). These alterations are associated with diverse biological pathways, such as Kras-MAPK, Wnt, Notch, and TGF- $\beta$  signaling, regulation of the cell cycle, transcriptional control by epigenetic modifiers, and repair of DNA damage<sup>408,421</sup>.

### 1.5.2. The pancreatic tumor microenvironment

Over the course of histopathological disease progression, pancreatic tumors interact extensively with their tumor microenvironment. The PDAC stroma milieu is marked by desmoplasia (a dense fibrotic reaction), poor vascularization, and contains distinct populations of stromal and immune cells. In aggregate, stromal components can account for more than 90% of the total tumor volume<sup>428</sup>.

#### Cancer-associated fibroblasts

Pancreatic stellate cells (PSCs) are myofibroblast-lineage cells that compromise the majority of the stromal compartment in PDAC. In the healthy pancreas, PSCs are located basolateral to acini and in perivascular regions, where they are involved in vitamin



A homeostasis, amylase secretion and preservation of pancreatic tissue integrity<sup>429</sup>. Under certain inflammatory and stress conditions, including in the pancreatic tumor microenvironment, PSCs can become activated, leading to the upregulation of  $\alpha$ -smooth muscle actin ( $\alpha$ -SMA) and fibroblast activation protein- $\alpha$  (FAP- $\alpha$ ). Activated PSCs acquire proliferative capacity, can produce growth factors that stimulate tumor proliferation and invasive motility, and extensively modulate the ECM. PSC-derived ECM components, such as collagen, generate the characteristic desmoplasia observed in PDAC<sup>430</sup>. In the KPC GEMM it was shown that FAP- $\alpha$ + fibroblasts mediate T cell exclusion through the CXCL12 chemokine<sup>431</sup>. Depletion (or pharmacological inhibition) of FAP- $\alpha$ + fibroblasts restored the efficacy of immune checkpoint inhibitor therapy in this model<sup>431</sup>.

However, PSCs are not the only cancer-associated fibroblast population present in PDAC. Rather, CAFs constitute a heterogeneous group of cells that includes mesenchymal stem cells, bone-marrow derived cells, and resident activated fibroblasts<sup>432,433</sup>. Moreover, CAFs are highly plastic and are capable of transdifferentiating into other cell types, such as chondrocytes, adipocytes, myocytes and endothelial cells, which adds further complexity to delineating these populations<sup>432</sup>.

Although CAFs were initially suggested to have pro-tumorigenic roles in PDAC, this view has been challenged more recently. Early *Kras*-mutant lesions secrete abundant Hedgehog (Hh) ligands, which were shown to promote stroma differentiation, and therapeutic resistance to gemcitabine<sup>434–436</sup>. Inhibition of Hh improved vascularization, elevated drug concentrations in the tumor microenvironment and extended overall survival of KPC mice<sup>435</sup>. However, the clinical results with Hh inhibitors were disappointing, and even led to premature trial termination due to decreased survival in

the experimental arm (gemcitabine + IPI-926)<sup>437</sup>. Mechanistic studies with conditional Hh gene knockout, as well as drug studies and CAF depletion studies in GEMMs of PDAC have demonstrated that tumors acquire a more undifferentiated morphology under these settings<sup>438,439</sup>, which may explain their increased aggressive tumor growth. Thus, CAFs may have both tumor promoting functions through the induction of aberrant vasculature, and tumor restraining functions through paracrine maintenance of cancer cell differentiation. However, a number of questions remain to be addressed in this field<sup>432</sup>.

### Tumor-associated macrophages

In addition to a heterogenous population of CAFs, the pancreatic stroma also contains abundant innate and adaptive immune cells. Macrophages are one of the most abundant immune cells in human PDAC, and are also highly prevalent in genetically engineered mouse models. As described in section 1.4.4, macrophage differentiation is a plastic process; the ‘polarization’ of a macrophage is highly dependent on inflammatory factors in the microenvironment. In pancreatic cancers, tumor-associated macrophages have been reported to acquire immunosuppressive markers such as CD86, CD206 (mannose receptor), and IL-10, which are typically associated with a “M2” fate<sup>440</sup>. A number of different tumor-promoting functions have been attributed to TAMs in pancreatic cancer, including driving early tumor cell differentiation (acinar-to-ductal metaplasia)<sup>441–443</sup>, remodeling of the ECM<sup>441,443</sup>, and mediating resistance to gemcitabine<sup>444</sup>. Given the tumor-promoting roles of TAMs, several studies have investigated the impact of macrophage depletion. Inhibition of colony-stimulating factor 1 receptor (CSF-1R), which is involved in macrophage migration and proliferation in peripheral tissues<sup>445</sup>, selectively

reduced M2 TAM numbers, reprogrammed macrophage polarization to a less T cell-suppressive phenotype and enhanced immune checkpoint therapy in an orthotopic model of pancreas cancer<sup>446</sup>. Similar therapeutic responses were observed in the KPC GEMM, where CSF-1R reprogrammed macrophages to enhance local adaptive immune responses, and extended overall survival of these mice<sup>264</sup>. Consistent with a role in promoting tumor invasion, macrophage depletion in KPC mice with clodronate led to a reduction in metastases<sup>447</sup>. Interestingly, pancreatic cancer cells are capable of recruiting macrophages upon metastasis to the liver, which resulted in extensive stromal and fibrotic responses in this distant site<sup>448</sup>. In human PDAC, the presence of CD68+ TAMs in human PDAC is prognostic for an increased risk for metastasis<sup>440,449</sup>. However, absence of TAMs can also lead to decreases in angiogenesis and T cell infiltration<sup>447</sup>, highlighting that TAMs have pleiotropic functions in the TME. This is further illustrated by CD40 agonist therapeutic responses in PDAC mice, which were shown to be macrophage-dependent<sup>450</sup>.

#### Myeloid-derived suppressor cells and tumor-associated neutrophils

In addition to the tumor-promoting roles of TAMs, the PDAC TME is also infiltrated by a number of other myeloid cell types, such as myeloid-derived suppressor cells (MDSCs), and neutrophils. A number of studies have investigated the recruitment of these innate cells to the PDAC TME through chemokine receptors or tumor-derived cytokines.

In the KPC and in an orthotopic pancreatic model, MDSC recruitment is mediated through the secretion of granulocyte-macrophage colony-stimulating factor (GM-CSF)<sup>451,452</sup>. GM-CSF induced the differentiation and proliferation of splenic precursors

into Gr1+CD11b+ cells, which were capable of suppressing T cell function *in vitro*<sup>452,453</sup>. Abrogation of MDSC recruitment through knockdown of GM-CSF expression or neutralization of GM-CSF reduced pancreatic tumor growth<sup>451,452</sup>, and was accompanied by an increase in CD8+ T cell infiltration<sup>451</sup>.

The chemokine receptor CXCR2 is a critical regulator of MDSC and neutrophil migration<sup>454,455</sup>. Genetic deletion of CXCR2 abrogated the seeding of liver metastases and extended survival of KPC mice<sup>456</sup>. Similarly, CXCR2 inhibition in an orthotopic model of PDAC reduced tumor burden by decreasing tumor-associated neutrophil infiltration into the tumor microenvironment<sup>457</sup>. Combination therapy with FOLFIRINOX (the standard of care for metastatic PDAC) led to improvements in the overall survival of KPC tumors, and CCR2 blockade (abrogating TAM recruitment) further enhanced these therapeutic effects<sup>457</sup>.

### T cell infiltration

Several T cell subsets, including effector CD8+ T cells, conventional CD4+ T cells, and T regulatory cells can infiltrate pancreatic tumors<sup>458</sup>. The presence of cytotoxic CD8+ and effector CD4+ tumor infiltrating T cells can be used to stratify patient outcomes<sup>458</sup>. Analyses of TILs isolated from human PDAC samples (including CD8+ T cells and Tregs) revealed expression of co-stimulatory and co-inhibitory receptors (CD137/4-1BB, PD-1, LAG-3, TIM-3, and CD244)<sup>459</sup> and CD45RO<sup>+</sup><sup>460</sup>, suggesting that these T cells are antigen-experienced and may be tumor-reactive.

Within the TME, T cells have been shown to predominantly localize to the tumor stroma (a sign of immune exclusion), possibly caused by ECM-dysregulated chemokine

gradients<sup>459,461</sup>. Observations in PDAC GEMMs indicate that T cell tumor exclusion can be mediated by CXCL12-expressing FAP+ fibroblasts<sup>431,462</sup>. Additionally, CD4+ TIL recruitment may be regulated through Ly6C<sup>low</sup> F4/80+ TAMs<sup>463</sup>. Depletion of TAMs, in combination with CD40 agonists and gemcitabine, is capable of restoring CD4+ and CD8+ T cell infiltration in KPC mice<sup>463</sup>.

Non-canonical  $\gamma\delta$  CD4+ T cells play a pro-tumorigenic role through the secretion of pro-inflammatory IL-17 cytokines, and suppression of adaptive immune responses. Gamma delta T cells have been suggested to be the dominant T cells in human PDAC<sup>460</sup>. PanIN initiation appears to be particularly dependent on these  $\gamma\delta$  CD4+ T cells, as genetic deletion of *IL-17*, *Tcr $\delta$*  or  $\gamma\delta$  T cell depletion led to delayed tumor kinetics in KC mice<sup>420,460</sup>. Pancreatic  $\gamma\delta$  T cells upregulated co-inhibitory ligands (PD-L1, and Galectin-9), which could be therapeutically targeted to reduce growth of orthotopically transplanted KPC tumors<sup>460</sup>.

Tregs can also contribute to IL-17 in the TME by acquiring a ROR $\gamma$ t+Foxp3+ phenotype<sup>464</sup>. In human PDAC, Tregs are actively recruited to the TME and constitute a significant fraction of the T cell infiltrate<sup>465</sup>. Knockdown of *Ccl5* expression in a pancreatic transplant model reduced the migration of CCR5+ Tregs into the TME, and slowed tumor growth<sup>374</sup>. Similarly, depletion of Tregs (by anti-CD25 antibody therapy) in combination with *Kras*<sup>G12D</sup> vaccination led to reduced PanIN formation, and extended overall survival of KPC mice<sup>466</sup>.

### 1.5.3. Immunotherapy in pancreatic cancer

Combination chemotherapy for the treatment of metastatic pancreatic cancer provides limited clinical benefit, and overall patient survival remains poor<sup>395</sup>. Therefore, novel therapeutic agents for the treatment of pancreatic cancer are urgently needed. Immune checkpoint inhibitors (ICIs) have revolutionized cancer therapy over the last decade, demonstrating that targeting the immune system in cancer is safe and can lead to durable, long-lasting anti-tumor responses<sup>5</sup>. Therefore, harnessing the immune system in PDAC may improve therapeutic outcomes for patients with this devastating disease.

#### Antigenicity of PDAC

A critical question in harnessing the immune system for therapeutic use is whether pancreatic tumors contain sufficient (neo)antigens that can elicit T cell responses. Although pancreatic cancer has historically considered to be “antigenically poor” based its relative low overall mutation burden<sup>467</sup>, recent studies have suggested that PDAC can indeed harbor antigens<sup>6,468</sup>. An analysis of the TCGA, and International Cancer Genome Consortium (ICGC) datasets has revealed that almost all patient samples contain neoantigens (ranging from 4-4000 per sample)<sup>468</sup>. Among these, KRAS codon 12 mutations (G12D, and G12V) are the most frequently occurring. Therapeutic benefit with *KRAS*<sup>G12D</sup>-reactive adoptive T cell therapy in a patient carrying the (infrequent) HLA-C\*08:02 allele has been demonstrated<sup>469</sup>, suggesting that KRAS neoantigens could be therapeutically exploited. A study of the neoantigen quality in rare long-term survivors (median survival 6 years) revealed a median of 38 predicted neoantigens per tumor<sup>6</sup>. In this patient cohort, the presence of CD8+ T cell infiltrate and higher neoantigen quantity

stratified patients with a better disease outcome<sup>6</sup>. Intriguingly, peripheral T cell reactivity to PDAC neoepitopes and microbial epitopes was observed in patients with a high neoantigen burden<sup>6</sup>, suggesting that structural resemblance between the two classes (“microbial mimicry”) may drive the particular immunogenic nature of neoantigens in this setting. At least a subset of pancreatic cancer patients thus harbor antigenic tumors that are amenable to immunotherapeutic approaches.

### Clinical landscape of immunotherapy in PDAC

The development of immune checkpoint inhibitors (ICIs) reached a milestone with the approvals of an anti-CTLA-4 antibody (ipilimumab) in 2011, and an anti-PD-1 antibody (pembrolizumab) in 2014. Since these initial approvals, several ICIs have been approved for NSCLC, renal carcinoma, small cell lung cancer (SCLC), triple negative breast cancer, MMR-deficient cancers, Hodgkin’s lymphoma, and other types of cancer<sup>470</sup>.

Unfortunately, these clinical successes have largely failed to translate to pancreatic cancer to date. A number of different ICIs have been investigated as monotherapy or combination therapy for the treatment of metastatic PDAC.

The sole clinical success to date was achieved with pembrolizumab in a clinical “basket” trial enrolling a total of 86 patients with MMR-deficient cancers (colorectal, endometrial, pancreatic, gastric, prostate and a number of other cancers). Although PDAC patient numbers were small (n=8), 2 complete responses (CRs), 3 partial responses (PRs), and 1 stable disease (SD) response were reported. On the basis of the positive outcomes achieved in this trial, the FDA approved pembrolizumab for treatment of MMR-deficient cancers in 2017<sup>471</sup>.

A combination chemoimmunotherapy approach has shown promise in an early phase Ib study, although the data is not yet fully mature. In an interim report investigating gemcitabine+ nab-paclitaxel + a CD40 agonist (APX005M) with or without nivolumab (anti-PD-1), 14 out of 24 (58%) evaluable patients at the cut-off had achieved PRs, while 8 patients achieved disease stabilization<sup>472</sup>. Full results of this trial are highly anticipated.

Two clinical trials have investigated ICI monotherapy in MMR-proficient PDAC patients. A phase II trial conducted in 2010 evaluated anti-CTLA-4 (ipilimumab), but did not observe any responses in the 20 evaluable patients by standard RECIST criteria<sup>473</sup>. However, two patients showed minor responses, and the best responder (30% tumor regression), achieved ~9 months of clinical benefit<sup>473</sup>. A second phase I trial evaluated the safety and tolerability of anti-PD-L1 (BMS-936559) in 14 advanced-stage pancreatic cancer patients, but no objective responses were noted in the trial<sup>474</sup>.

Three clinical studies have investigated ICIs in combination with chemotherapy. A phase I study investigating pembrolizumab plus chemotherapy (gemcitabine + nab-paclitaxel for the PDAC arm) included 11 pancreatic cancer patients<sup>475</sup>. The study only achieved modest efficacy signals, achieving 2 PRs, 6 SDs, 2 PDs in this cohort. Unfortunately, anti-PD-1 did not seem to provide any additional clinical benefit in this setting, as an 18% ORR is similar to gemcitabine + nab-paclitaxel combination therapy. A similar conclusion was drawn from a phase I study investigating ipilimumab plus gemcitabine<sup>476</sup>. In this trial, 3 patients (out of 21 patients) achieved a PR, while 7 patients achieved SDs. The 14% ORR is in line with responses to gemcitabine alone. A third phase I study combined anti-CTLA-4 (tremelimumab) plus gemcitabine, but also reported



modest results (2/26 patients achieving a PR, and 7/27 patients achieving stable disease)<sup>471</sup>.

Four other phase I/II studies have investigated combinations of an ICI with non-chemotherapeutic modalities<sup>477–479</sup>. Unfortunately, therapeutic responses across these different treatment regimens, which included anti-PD-L1 (durvalumab) + stereotactic body radiotherapy (2 PRs), pembrolizumab + acalabrutinib (a BTK inhibitor; 3 PRs), and pembrolizumab + BL-8040 (CXCR4 antagonist; 1 PR) have been limited.

Lastly, a highly anticipated phase II trial comparing anti-PD-L1 (durvalumab) alone or in combination with anti-CTLA-4 (tremelimumab) reported clinical results recently<sup>480</sup>. To date, this is the only trial that has investigated the efficacy combination ICIs in PDAC. While the treatment regimen was generally safe and well-tolerated (14% of patients had grade 3 or higher treatment-related adverse events), only two patients (out of 65 enrolled) achieved PRs<sup>480</sup>. It thus appears that combining these distinct immune checkpoint inhibitors does not improve therapeutic efficacy. A number of other combination immune checkpoint inhibitor therapies remain to be explored for the treatment of metastatic PDAC.

## **1.6. Synopsis**

Cancer immunology has a long and storied history. In this introductory chapter, the roots of this field were traced back to clinical observations made by William Coley in the late 1890s. However, the immunological concepts (e.g. vaccination) employed by Coley date even further back to Edward Jenner, and the practice of variolation during the 18<sup>th</sup> century. While the idea that the immune system is capable of recognizing the body's own cancerous cells has been challenged several times, notably in the late 1920s and the 1970s, these rejections have ultimately proved to be premature. Our understanding of the process of immunosurveillance, as well as the cellular players involved in the anti-tumor immune response, has enabled the clinical application of increasingly sophisticated immunotherapeutic strategies.

The complex, multistep processes involved in the anti-tumor immune response were described in detail in this introductory chapter. Tumor immune responses begin with the release of tumor antigens, which are presented by specialized innate immune cells to the adaptive immune arm in lymphoid tissues. This then triggers the clonal expansion and migration of effector T cells to the tumor microenvironment, and culminates in the killing of cancer cells and the release of new antigens. However, immune responses are often thwarted by a number of tumor-intrinsic mechanisms and tumor-extrinsic factors, which enable tumor proliferation to continue unchecked. Tumors may deregulate antigen presentation, activate oncogenic pathways that lead to exclusion of T cells from the tumor microenvironment, or simply suppress the expression of tumor antigens. The immune system may also shape the tumor by selectively eliminating immunogenic cancer clones,

fueling immune escape of cancer cells that have evolved mechanisms of evading immune cell recognition. Additionally, several immune and non-immune cells may be recruited to the tumor microenvironment that further limit effective anti-tumor immune responses. Finally, T cell proliferation and persistence is inherently self-limited, through the action of immune co-inhibitory receptors that dampen T cell functionality. Indeed, much of the recent clinical successes with immunotherapy has been achieved by counteracting the inhibitory effects of these receptors expressed on T cells, rather than directly therapeutically targeting the tumor.

While there much to celebrate about the widespread impact immunotherapy has made on the clinical practice in many types of hematopoietic and epithelial cancers, pancreatic cancer has largely remained refractory to current immune-based approaches. Pancreatic cancer is driven by the acquisition of defined genetic alterations and undergoes a histopathological progression culminating in invasive adenocarcinomas capable of metastasizing to distant tissue sites. Over the course of pancreatic tumor progression, pancreatic tumors recruit additional (non-)immune cells that contribute to a desmoplastic, immunosuppressive tumor microenvironment.

The unique therapeutic challenge posed by pancreatic cancer is perhaps most clearly illustrated by multiple immunotherapeutic approaches yet to make a clinical impact. A key part of solving this challenge is translation of biological insights gained from preclinical models to effective strategies to combat this devastating disease in the clinic.

Chapter 2 will describe the generation and development of two novel mouse models of pancreatic ductal adenocarcinoma. Extensive characterization of these models uncovered unexpected roles for immunoediting and T cell dysfunction in driving

immuno-evasion in pancreatic cancer, and has revealed potentially clinically actionable therapeutic strategies. Chapter 3 will discuss relevance of these results in the broader context of the cancer immunology field, and concludes with a perspective on the promise of immunotherapy in pancreatic cancer.

## 1.7. References

1. Hanahan, D. & Weinberg, R. A. Hallmarks of cancer: The next generation. *Cell* vol. 144 646–674 (2011).
2. Schreiber, R. D., Old, L. J. & Smyth, M. J. Cancer immunoediting: Integrating immunity's roles in cancer suppression and promotion. *Science (80-. )*. **331**, 1565–1570 (2011).
3. Van Der Bruggen, P. *et al.* A gene encoding an antigen recognized by cytolytic T lymphocytes on a human melanoma. *Science (80-. )*. **254**, 1643–1647 (1991).
4. Leach, D. R., Krummel, M. F. & Allison, J. P. Enhancement of antitumor immunity by CTLA-4 blockade. *Science (80-. )*. **271**, 1734–1736 (1996).
5. Hamid, O. *et al.* Five-year survival outcomes for patients with advanced melanoma treated with pembrolizumab in KEYNOTE-001. *Ann. Oncol.* **30**, 582–588 (2019).
6. Balachandran, V. P. *et al.* Identification of unique neoantigen qualities in long-term survivors of pancreatic cancer. *Nature* **551**, S12–S16 (2017).
7. Piana, R. A Snapshot of Early Immunotherapy - The ASCO Post. <https://www.ascopost.com/issues/october-25-2015/a-snapshot-of-early-immunotherapy/> (2015).
8. Gross, C. P. & Sepkowitz, K. A. The myth of the medical breakthrough: Smallpox, vaccination, and Jenner reconsidered. *Int. J. Infect. Dis.* **3**, 54–60 (1998).
9. Best, M., Neuhauser, D. & Slavin, L. 'Cotton Mather, you dog, dam you! I'll inoculate you with this; with a pox to you': Smallpox inoculation, Boston, 1721. *Quality and Safety in Health Care* vol. 13 82–83 (2004).
10. Riedel, S. Edward Jenner and the History of Smallpox and Vaccination. *Baylor Univ. Med. Cent. Proc.* **18**, 21–25 (2005).
11. Jessy, T. Immunity over inability: The spontaneous regression of cancer. *J. Nat. Sci. Biol. Med.* **2**, 43–49 (2011).
12. Oiseth, S. J. & Aziz, M. S. Cancer immunotherapy: a brief review of the history, possibilities, and challenges ahead. *J. Cancer Metastasis Treat.* **3**, 250 (2017).
13. Kienle, G. S. Fever in Cancer Treatment: Coley's Therapy and Epidemiologic Observations. *Glob. Adv. Heal. Med.* **1**, 92–100 (2012).
14. Coley, W. B. The Treatment of Malignant Tumors by Repeated Inoculations of Erysipelas: With a Report of Ten Original Cases. *J. Am. Med. Assoc.* **XX**, 615–616 (1893).
15. Tsung, K. & Norton, J. A. Lessons from Coley's Toxin. *Surg. Oncol.* **15**, 25–28 (2006).
16. Coley Nauts, H., Swift, W. E. & Coley, B. L. The Treatment of Malignant Tumors by Bacterial Toxins as Developed by the Late William B. Coley, M.D., Reviewed in the Light of Modern Research. *Cancer Res.* **6**, 205–216 (1946).
17. McCarthy, E. F. The toxins of William B. Coley and the treatment of bone and soft-tissue sarcomas. *Iowa Orthop. J.* **26**, 154–158 (2006).
18. Ehrlich, P. Ueber den jetzigen Stand der Karzinomforschung. *Ned. Tijdschr. Geneeskd.* vol. 5 273–290 (1909).

19. Triolo, V. A. Nineteenth Century Foundations of Cancer Research Origins of Experimental Research. *Cancer Res.* **24**, 4–27 (1964).
20. Little, C. C. & Tyzzer, E. E. Further experimental studies on the inheritance of susceptibility to a Transplantable tumor, Carcinoma (J. W. A.) of the Japanese waltzing Mouse. *J. Med. Res.* **33**, 393 (1916).
21. Roopenian, D., Young Choi, E. & Brown, A. The immunogenomics of minor histocompatibility antigens. *Immunol. Rev.* **190**, 86–94 (2002).
22. Scott, O. C. A. Tumor Transplantation and Tumor Immunity: A Personal View. *Cancer Res.* **51**, 757–763 (1991).
23. Woglom, W. H. Immunity to Transplantable Tumours. *Cancer Rev.* **4**, 129–214 (1929).
24. Parish, C. R. Cancer immunotherapy: The past, the present and the future. *Immunol. Cell Biol.* **81**, 106–113 (2003).
25. Thorsby, E. A short history of HLA. *Tissue Antigens* **74**, 101–116 (2009).
26. Gorer, P. A., Lyman, S. & Snell, G. D. Studies on the genetic and antigenic basis of tumour transplantation: Linkage between a histocompatibility gene and ‘ fused ’ in mice. *Proc. R. Soc. B* 499–505 (1948).
27. Billingham, R. E., Brent, L. & Medawar, P. B. ‘Actively acquired tolerance’ of foreign cells. *Nature* **172**, 603–606 (1953).
28. Billingham, R. E., Brent, L. & Medawar, P. B. Quantitative Studies on Tissue Transplantation Immunity. III. Actively Acquired Tolerance. *Philos. Trans. R. Soc. Lond. B. Biol. Sci.* **239**, 357–414 (1956).
29. Simpson, E. Medawar’s legacy to cellular immunology and clinical transplantation: a commentary on Billingham, Brent and Medawar (1956) ‘Quantitative studies on tissue transplantation immunity. III. Actively acquired tolerance’. *Philos. Trans. R. Soc. B Biol. Sci.* **370**, 20140382 (2015).
30. Burnet, F. M. *The Production of Antibodies. A Review and a Theoretical Discussion.* (Macmillan & Co., 1941).
31. Gross, L. Intradermal Immunization of C3H Mice against a Sarcoma That Originated in an Animal of the Same Line. *Cancer Res.* **3**, (1943).
32. Foley, E. J. Antigenic Properties of Methylcholanthrene-induced Tumors in Mice of the Strain of Origin. *Cancer Res.* **13**, 835–837 (1953).
33. Prehn, R. T. & Main, J. M. Immunity to Methylcholanthrene-Induced Sarcomas. **18**, 769–778 (1957).
34. Klein, G., Sjögren, H. O., Klein, E. & Hellstrom, K. E. Demonstration of Resistance against Methylcholanthrene-induced Sarcomas in the Primary Autochthonous Host. *Cancer Res.* **20**, 1561–1572 (1960).
35. Burnet, M. Cancer - A Biological Approach. *Br. Med. J.* 841–847 (1957) doi:10.1136/bmj.1.5023.841.
36. Burnet, F. M. The Concept of Immunological Surveillance. in *Progress in experimental tumor research.* vol. 13 1–27 (Karger Publishers, 1970).
37. Thomas, L. Cellular and humoral aspects of the hypersensitive states. *Cell. Humoral Asp. Hypersensitive States* 529–532 (1959) doi:10.1111/j.0954-6820.1961.tb00220.x.
38. Dunn, G. P., Old, L. J. & Schreiber, R. D. The Three Es of Cancer Immunoediting. *Annu. Rev. Immunol.* **22**, 329–360 (2004).

39. Old, L. J. & Boyse, E. A. Immunology of Experimental Tumors. *Annu. Rev. Med.* **15**, 167–186 (1964).
40. Flanagan, S. P. 'Nude', a new hairless gene with pleiotropic effects in the mouse. *Genet. Res.* **8**, 295–309 (1966).
41. Pantelouris, E. M. Absence of thymus in a mouse mutant. *Nature* vol. 217 370–371 (1968).
42. Stutman, O. Tumor development after 3-methylcholanthrene in immunologically deficient athymic-nude mice. *Science (80-. )*. **183**, 534–536 (1974).
43. Stutman, O. Chemical carcinogenesis in nude mice: Comparison between nude mice from homozygous matings and heterozygous matings and effect of age and carcinogen dose. *J. Natl. Cancer Inst.* **62**, 353–358 (1979).
44. Hewitt, H. B., Blake, E. R. & Walder, A. S. A critique of the evidence for active host defence against cancer, based on personal studies of 27 murine tumours of spontaneous origin. *Br. J. Cancer* **33**, 241–259 (1976).
45. Hunig, T. T-cell function and specificity in athymic mice. *Immunol. Today* **4**, 84–87 (1983).
46. Ikehara, S., Pahwa, R. N., Fernandes, G., Hansen, C. T. & Good, R. A. Functional T cells in athymic nude mice. *Proc. Natl. Acad. Sci. U. S. A.* **81**, 886–888 (1984).
47. Maleckar, J. R. & Sherman, L. A. The composition of the T cell receptor repertoire in nude mice. *J. Immunol.* **138**, 3873–3876 (1987).
48. Chiossone, L., Dumas, P. Y., Vienne, M. & Vivier, E. Natural killer cells and other innate lymphoid cells in cancer. *Nature Reviews Immunology* vol. 18 671–688 (2018).
49. Souza-Fonseca-Guimaraes, F., Cursons, J. & Huntington, N. D. The Emergence of Natural Killer Cells as a Major Target in Cancer Immunotherapy. *Trends Immunol.* **40**, 142–158 (2019).
50. Shimasaki, N., Jain, A. & Campana, D. NK cells for cancer immunotherapy. *Nat. Rev. Drug Discov.* **19**, 200–218 (2020).
51. Ward, J. P., Gubin, M. M., Schreiber, R. D. & States, U. Therapeutically Induced Immune Responses to Cancer. *Adv Immunol.* 1–40 (2016) doi:10.1016/bs.ai.2016.01.001.The.
52. Kaplan, D. H. *et al.* Demonstration of an interferon  $\gamma$ -dependent tumor surveillance system in immunocompetent mice. *Proc. Natl. Acad. Sci. U. S. A.* **95**, 7556–7561 (1998).
53. Smyth, M. J. *et al.* Differential tumor surveillance by natural killer (NK) and NKT cells. *J. Exp. Med.* **191**, 661–668 (2000).
54. Shankaran, V. *et al.* IFN $\gamma$ , and lymphocytes prevent primary tumour development and shape tumour immunogenicity. *Nature* **410**, 1107–1111 (2001).
55. Street, S. E. A., Cretney, E. & Smyth, M. J. Perforin and interferon- $\gamma$  activities independently control tumor initiation, growth, and metastasis. *Blood* **97**, 192–197 (2001).
56. Gowans, J. L., McGregor, D. D. & Cowen, Di. M. Initiation of immune responses by small lymphocytes. *Nature* **196**, 651–655 (1962).
57. Miller, J. F. A. P. Immunological function of the thymus. *Lancet* **278**, 748–749 (1961).
58. Miller, J. F. A. P. Effect of neonatal thymectomy on the immunological

- responsiveness of the mouse. *Proc. R. Soc. London. Ser. B. Biol. Sci.* **156**, 415–428 (1962).
59. Miller, J. F. A. P. Immunological Significance of the Non-Antigenicity of Synthetic. *Nature* **195**, 1318–1319 (1962).
  60. Miller, J. F. A. P., Doak, S. M. A. & Cross, A. M. Role of the Thymus in Recovery of the Immune Mechanism in the Irradiated Adult Mouse. *Exp. Biol. Med.* **112**, 785–792 (1963).
  61. Miller, J. F. A. P. Effect of Thymectomy in Adult Mice on Immunological Responsiveness. *Nature* **208**, 1337–1338 (1965).
  62. Mitchell, G. F. & Miller, J. F. Immunological activity of thymus and thoracic-duct lymphocytes. *Proc. Natl. Acad. Sci. U. S. A.* **59**, 296–303 (1968).
  63. Miller, J. F. & Mitchell, G. F. Cell to cell interaction in the immune response. I. Hemolysin-forming cells in neonatally thymectomized mice reconstituted with thymus or thoracic duct lymphocytes. *J. Exp. Med.* **128**, 801–820 (1968).
  64. Mitchell, G. F. & Miller, J. F. Cell to cell interaction in the immune response. II. The source of hemolysin-forming cells in irradiated mice given bone marrow and thymus or thoracic duct lymphocytes. *J. Exp. Med.* **128**, 821–837 (1968).
  65. Miller, J. F. A. P. & Sprent, J. Thymus-derived cells in mouse thoracic duct lymph. *Nature* **230**, 267–271 (1971).
  66. Boyse, E. A., Miyazawa, M., Aoki, T. & Old, L. J. Ly-A and Ly-B: two systems of lymphocyte isoantigens in the mouse. *Proc. R. Soc. London. Ser. B. Biol. Sci.* **170**, 175–193 (1968).
  67. Raff, M. C. Surface Antigenic Markers for Distinguishing T and B Lymphocytes in Mice. *Transpl. Rev.* **6**, 52–80 (1971).
  68. Kisielow, P. *et al.* Ly antigens as markers for functionally distinct subpopulations of thymus-derived lymphocytes of the mouse. *Nature* **253**, 219–220 (1975).
  69. Cantor, H. & Boyse, E. A. Functional subclasses of T lymphocytes bearing different Ly antigens. I. The generation of functionally distinct T cell subclasses is a differentiative process independent of antigen. *J. Exp. Med.* **141**, 1376–1389 (1975).
  70. Köhler, G. & Milstein, C. Continuous cultures of fused cells secreting antibody of predefined specificity. *Nature* **256**, 495–497 (1975).
  71. Herzenberg, L. A. *et al.* The history and future of the Fluorescence Activated Cell Sorter and flow cytometry: A view from Stanford. in *Clinical Chemistry* vol. 48 1819–1827 (2002).
  72. Mishell, R. I. & Dutton, R. W. Immunization of dissociated spleen cell cultures from normal mice. *J. Exp. Med.* **126**, 423–442 (1967).
  73. Steinman, R. M. & Cohn, Z. A. Identification of a novel cell type in peripheral lymphoid organs of mice: I. Morphology, quantitation, tissue distribution. *J. Exp. Med.* **137**, 1142–1162 (1973).
  74. Steinman, R. M. & Cohn, Z. A. Identification of a novel cell type in peripheral lymphoid organs of mice: II. Functional properties in vitro. *J. Exp. Med.* **139**, 380–397 (1974).
  75. Nussenzweig, M. C., Steinman, R. M., Gutchinov, B. & Cohn, Z. A. Dendritic cells are accessory cells for the development of anti-trinitrophenyl cytotoxic T lymphocytes. *J. Exp. Med.* **152**, 1070–1084 (1980).



76. Nussenzweig, M. C., Steinman, R. M., Witmer, M. D. & Gutchinov, B. A monoclonal antibody specific for mouse dendritic cells. *Proc. Natl. Acad. Sci. U. S. A.* **79**, 161–165 (1982).
77. Steinman, R. M., Gutchinov, B., Witmer, M. D. & Nussenzweig, M. C. Dendritic cells are the principal stimulators of the primary mixed leukocyte reaction in mice. *J. Exp. Med.* **157**, 613–627 (1983).
78. Lecture, N. & Nussenzweig, M. C. *Ralph Steinman and the discovery of dendritic cells.* (2011).
79. Porter, R. R. Chemical structure of  $\gamma$ -globulin and antibodies. *Br. Med. Bull.* **19**, 197–201 (1963).
80. Cunningham, B. A., Pflumm, M. N., Rutishauser, U. & Edelman, G. M. Subgroups of amino acid sequences in the variable regions of immunoglobulin heavy chains. *Proc. Natl. Acad. Sci. U. S. A.* **64**, 997–1003 (1969).
81. Hozumi, N. & Tonegawa, S. Evidence for somatic rearrangement of immunoglobulin genes coding for variable and constant regions. *Proc. Natl. Acad. Sci. U. S. A.* **73**, 3628–3632 (1976).
82. Miller, J. F. A. P. & Sadelain, M. The journey from discoveries in fundamental immunology to cancer immunotherapy. *Cancer Cell* **27**, 439–449 (2015).
83. van Epps, H. L. Rules of engagement: the discovery of MHC restriction. *J. Exp. Med.* **201**, 665 (2005).
84. Zinkernagel, R. M. & Doherty, P. C. Restriction of in vitro T cell-mediated cytotoxicity in lymphocytic choriomeningitis within a syngeneic or semiallogeneic system. *Nature* **248**, 701–702 (1974).
85. Doherty, P. C. & Zinkernagel, R. M. Enhanced immunological surveillance in mice heterozygous at the H-2 gene complex. *Nature* **256**, 50–52 (1975).
86. Doherty, P. C. & Zinkernagel, R. M. A biological role for the major histocompatibility antigens. *Lancet* **305**, 1406–1409 (1975).
87. Townsend, A. R. M. *et al.* The epitopes of influenza nucleoprotein recognized by cytotoxic T lymphocytes can be defined with short synthetic peptides. *Cell* **44**, 959–968 (1986).
88. Bjorkman, P. J. *et al.* The foreign antigen binding site and T cell recognition regions of class I histocompatibility antigens. *Nature* **329**, 512–518 (1987).
89. Hedrick, S. M., Cohen, D. I., Nielsen, E. A. & Davis, M. M. Isolation of cDNA clones encoding T cell-specific membrane-associated proteins. *Nature* **308**, 149–153 (1984).
90. Yoshikai, Y. *et al.* Sequence and expression of transcripts of the human T-cell receptor  $\beta$ -chain genes. *Nature* **312**, 521–524 (1984).
91. Chien, Y. H. *et al.* A third type of murine T-cell receptor gene. *Nature* **312**, 31–35 (1984).
92. Saito, H. *et al.* A third rearranged and expressed gene in a clone of cytotoxic T lymphocytes. *Nature* **312**, 36–40 (1984).
93. Yanagi, Y., Chan, A., Chin, B., Minden, M. & Mak, T. W. Analysis of cDNA clones specific for human T cells and the  $\alpha$  and  $\beta$  chains of the T-cell receptor heterodimer from a human T-cell line. *Proc. Natl. Acad. Sci. U. S. A.* **82**, 3430–3434 (1985).
94. Oettgen, H. C., Terhorst, C., Cantley, L. C. & Rosoff, P. M. Stimulation of the T3-T cell receptor complex induces a membrane-potential-sensitive calcium influx. *Cell*

- 40**, 583–590 (1985).
95. Gold, D. P. *et al.* Isolation of cDNA clones encoding the 20K non-glycosylated polypeptide chain of the human T-cell receptor/T3 complex. *Nature* **324**, 702 (1986).
  96. Morgan, D. A., Ruscetti, F. W. & Gallo, R. Selective in vitro growth of T lymphocytes from normal human bone marrows. *Science (80-. )*. **193**, 1007–1008 (1976).
  97. Dembić, Z. *et al.* Transfer of specificity by murine  $\alpha$  and  $\beta$  T-cell receptor genes. *Nature* **320**, 232–238 (1986).
  98. Van Pel, A. & Boon, T. Protection against a nonimmunogenic mouse leukemia by an immunogenic variant obtained by mutagenesis. *Proc. Natl. Acad. Sci. U. S. A.* **79**, 4718–4722 (1982).
  99. Weon, J. L. & Potts, P. R. The MAGE protein family and cancer. *Current Opinion in Cell Biology* vol. 37 1–8 (2015).
  100. Van Den Eynde, B. J. & Van Der Bruggen, P. T cell defined tumor antigens. *Curr. Opin. Immunol.* **9**, 684–693 (1997).
  101. Koebel, C. M. *et al.* Adaptive immunity maintains occult cancer in an equilibrium state. *Nature* **450**, 903–907 (2007).
  102. Nishimura, H., Minato, N., Nakano, T. & Honjo, T. *Immunological studies on PD-1-deficient mice: implication of PD-1 as a negative regulator for B cell responses.* *International Immunology* vol. 10 (1998).
  103. Chen, D. S. & Mellman, I. Oncology meets immunology: The cancer-immunity cycle. *Immunity* **39**, 1–10 (2013).
  104. Lee, J.-K., Choi, Y.-L., Kwon, M. & Park, P. J. Mechanisms and Consequences of Cancer Genome Instability: Lessons from Genome Sequencing Studies. *Annu. Rev. Pathol. Mech. Dis.* **11**, 283–312 (2016).
  105. Schumacher, T. N., Scheper, W. & Kvistborg, P. Cancer Neoantigens. *Annu. Rev. Immunol.* **37**, 173–200 (2019).
  106. Matsushita, H. *et al.* Cancer exome analysis reveals a T-cell-dependent mechanism of cancer immunoediting. *Nature* **482**, 400–404 (2012).
  107. Linnemann, C. *et al.* High-throughput epitope discovery reveals frequent recognition of neo-antigens by CD4+ T cells in human melanoma. *Nat. Med.* **21**, 81–85 (2015).
  108. van Rooij, N. *et al.* Tumor Exome Analysis Reveals Neoantigen-Specific T-Cell Reactivity in an Ipilimumab-Responsive Melanoma. *J. Clin. Oncol.* **31**, e439–e442 (2013).
  109. Robbins, P. F. *et al.* Mining exomic sequencing data to identify mutated antigens recognized by adoptively transferred tumor-reactive T cells. *Nat. Med.* **19**, 747–752 (2013).
  110. Rizvi, N. A. *et al.* Mutational landscape determines sensitivity to PD-1 blockade in non-small cell lung cancer. *Science (80-. )*. **348**, 124–128 (2015).
  111. Tran, E. *et al.* T-Cell Transfer Therapy Targeting Mutant KRAS in Cancer. *N. Engl. J. Med.* **375**, 2255–2262 (2016).
  112. Lo, W. *et al.* Immunologic Recognition of a Shared p53 Mutated Neoantigen in a Patient with Metastatic Colorectal Cancer. (2019) doi:10.1158/2326-6066.CIR-18-0686.
  113. Kenter, G. G. *et al.* Vaccination against HPV-16 oncoproteins for vulvar

- intraepithelial neoplasia. *N. Engl. J. Med.* **361**, 1838–1847 (2009).
114. Stevanović, S. *et al.* Complete regression of metastatic cervical cancer after treatment with human papillomavirus-targeted tumor-infiltrating T cells. *J. Clin. Oncol.* **33**, 1543–1550 (2015).
  115. Kelderman, S. & Kvistborg, P. Tumor antigens in human cancer control. *Biochim. Biophys. Acta - Rev. Cancer* **1865**, 83–89 (2016).
  116. Gotter, J., Brors, B., Hergenroth, M. & Kyewski, B. Medullary Epithelial Cells of the Human Thymus Express a Highly Diverse Selection of Tissue-specific Genes Colocalized in Chromosomal Clusters. *J. Exp. Med.* **199**, 155–166 (2004).
  117. Galluzzi, L., Buqué, A., Kepp, O., Zitvogel, L. & Kroemer, G. Immunogenic cell death in cancer and infectious disease. *Nature Reviews Immunology* vol. 17 97–111 (2017).
  118. Galluzzi, L. *et al.* Molecular mechanisms of cell death: Recommendations of the Nomenclature Committee on Cell Death 2018. *Cell Death and Differentiation* vol. 25 486–541 (2018).
  119. Kroemer, G., Galluzzi, L., Kepp, O. & Zitvogel, L. Immunogenic Cell Death in Cancer Therapy. *Annu. Rev. Immunol.* **31**, 51–72 (2013).
  120. Gardner, A. & Ruffell, B. Dendritic Cells and Cancer Immunity. *Trends in Immunology* vol. 37 855–865 (2016).
  121. Domogalla, M. P., Rostan, P. V., Raker, V. K. & Steinbrink, K. Tolerance through education: How tolerogenic dendritic cells shape immunity. *Frontiers in Immunology* vol. 8 1764 (2017).
  122. Kaldjian, E. P., Gretz, J. E., Anderson, A. O., Shi, Y. & Shaw, S. *Spatial and molecular organization of lymph node T cell cortex: a labyrinthine cavity bounded by an epithelium-like monolayer of fibroblastic reticular cells anchored to basement membrane-like extracellular matrix.* *International Immunology* vol. 13 (2001).
  123. Blattman, J. N. *et al.* Estimating the precursor frequency of naive antigen-specific CD8 T cells. *J. Exp. Med.* **195**, 657–664 (2002).
  124. Krummel, M. F., Bartumeus, F. & Gérard, A. T cell migration, search strategies and mechanisms. *Nature Reviews Immunology* vol. 16 193–201 (2016).
  125. Courtney, A. H., Lo, W. L. & Weiss, A. TCR Signaling: Mechanisms of Initiation and Propagation. *Trends in Biochemical Sciences* vol. 43 108–123 (2018).
  126. Love, P. E. & Hayes, S. M. ITAM-mediated signaling by the T-cell antigen receptor. *Cold Spring Harbor perspectives in biology* vol. 2 a002485 (2010).
  127. Huang, J. *et al.* A Single peptide-major histocompatibility complex ligand triggers digital cytokine secretion in CD4<sup>+</sup> T Cells. *Immunity* **39**, 846–857 (2013).
  128. Mariuzza, R. A., Agnihotri, P. & Orban, J. The structural basis of T-cell receptor (TCR) activation: An enduring enigma. *Journal of Biological Chemistry* vol. 295 914–925 (2020).
  129. Malissen, B. & Bongrand, P. Early T Cell Activation: Integrating Biochemical, Structural, and Biophysical Cues. *Annu. Rev. Immunol.* **33**, 539–561 (2015).
  130. Chen, L. & Flies, D. B. Molecular mechanisms of T cell co-stimulation and co-inhibition. *Nature Reviews Immunology* vol. 13 227–242 (2013).
  131. Baumeister, S. H., Freeman, G. J., Dranoff, G. & Sharpe, A. H. Coinhibitory Pathways in Immunotherapy for Cancer. *Annu. Rev. Immunol.* **34**, 539–573 (2016).
  132. van der Woude, L. L., Gorris, M. A. J., Halilovic, A., Figdor, C. G. & de Vries, I. J.

- M. Migrating into the Tumor: a Roadmap for T Cells. *Trends in Cancer* **3**, 797–808 (2017).
133. Masopust, D. & Schenkel, J. M. The integration of T cell migration, differentiation and function. *Nat. Rev. Immunol.* **13**, 309–320 (2013).
  134. Harlin, H. *et al.* Chemokine expression in melanoma metastases associated with CD8 + T-Cell recruitment. *Cancer Res.* **69**, 3077–3085 (2009).
  135. Andersson, Å. *et al.* IL-7 Promotes CXCR3 Ligand-Dependent T Cell Antitumor Reactivity in Lung Cancer. *J. Immunol.* **182**, 6951–6958 (2009).
  136. Muthuswamy, R., Corman, J. M., Dahl, K., Chatta, G. S. & Kalinski, P. Functional reprogramming of human prostate cancer to promote local attraction of effector CD8+ T cells. *Prostate* **76**, 1095–1105 (2016).
  137. Mikucki, M. E. *et al.* Non-redundant requirement for CXCR3 signalling during tumoricidal T-cell trafficking across tumour vascular checkpoints. *Nat. Commun.* **6**, 1–14 (2015).
  138. Carman, C. V. & Martinelli, R. T lymphocyte-endothelial interactions: Emerging understanding of trafficking and antigen-specific immunity. *Front. Immunol.* **6**, (2015).
  139. Castermans, K. & Griffioen, A. W. Tumor blood vessels, a difficult hurdle for infiltrating leukocytes. *Biochimica et Biophysica Acta - Reviews on Cancer* vol. 1776 160–174 (2007).
  140. Carman, C. V. & Springer, T. A. Trans-cellular migration: cell-cell contacts get intimate. *Current Opinion in Cell Biology* vol. 20 533–540 (2008).
  141. Muller, W. A. Mechanisms of Leukocyte Transendothelial Migration. *Annu. Rev. Pathol. Mech. Dis.* **6**, 323–344 (2011).
  142. Leight, J. L., Drain, A. P. & Weaver, V. M. Extracellular Matrix Remodeling and Stiffening Modulate Tumor Phenotype and Treatment Response. *Annu. Rev. Cancer Biol.* **1**, 313–334 (2017).
  143. Walker, C., Mojares, E. & Del Río Hernández, A. Role of extracellular matrix in development and cancer progression. *International Journal of Molecular Sciences* vol. 19 (2018).
  144. Naba, A. *et al.* The matrisome: In silico definition and in vivo characterization by proteomics of normal and tumor extracellular matrices. *Mol. Cell. Proteomics* **11**, (2012).
  145. Henke, E., Nandigama, R. & Ergün, S. Extracellular Matrix in the Tumor Microenvironment and Its Impact on Cancer Therapy. *Frontiers in Molecular Biosciences* vol. 6 (2020).
  146. Salmon, H. *et al.* Matrix architecture defines the preferential localization and migration of T cells into the stroma of human lung tumors. *J. Clin. Invest.* **122**, 899–910 (2012).
  147. Mrass, P. *et al.* Random migration precedes stable target cell interactions of tumor-infiltrating T cells. *J. Exp. Med.* **203**, 2749–2761 (2006).
  148. Boissonnas, A., Fetler, L., Zeelenberg, I. S., Hugues, S. & Amigorena, S. In vivo imaging of cytotoxic T cell infiltration and elimination of a solid tumor. *J. Exp. Med.* **204**, 345–356 (2007).
  149. Dieckmann, N. M. G., Frazer, G. L., Asano, Y., Stinchcombe, J. C. & Griffiths, G. M. The cytotoxic T lymphocyte immune synapse at a glance. *J. Cell Sci.* **129**, 2881–

- 2886 (2016).
150. Stinchcombe, J. C., Majorovits, E., Bossi, G., Fuller, S. & Griffiths, G. M. Centrosome polarization delivers secretory granules to the immunological synapse. *Nature* **443**, 462–465 (2006).
  151. Halle, S. *et al.* In Vivo Killing Capacity of Cytotoxic T Cells Is Limited and Involves Dynamic Interactions and T Cell Cooperativity. *Immunity* **44**, 233–245 (2016).
  152. Strasser, A., Jost, P. J. & Nagata, S. The Many Roles of FAS Receptor Signaling in the Immune System. *Immunity* vol. 30 180–192 (2009).
  153. Martínez-Lostao, L., Anel, A. & Pardo, J. How Do Cytotoxic Lymphocytes Kill Cancer Cells? *Clin. Cancer Res.* **21**, 5047–5056 (2015).
  154. Voskoboinik, I., Whisstock, J. C. & Trapani, J. A. Perforin and granzymes: Function, dysfunction and human pathology. *Nature Reviews Immunology* vol. 15 388–400 (2015).
  155. Garrido, F. *et al.* Natural history of HLA expression during tumour development. *Immunology Today* vol. 14 491–499 (1993).
  156. Ward, P. L., Koeppen, H. K., Hurteau, T., Rowley, D. A. & Schreiber, H. Major Histocompatibility Complex Class I and Unique Antigen Expression by Murine Tumors That Escaped from CD8+ T-Cell-dependent Surveillance. *Cancer Res.* **50**, 3851–3858 (1990).
  157. Khong, H. T. & Restifo, N. P. Natural selection of tumor variants in the generation of ‘tumor escape’ phenotypes. *Nat. Immunol.* **3**, 999–1005 (2002).
  158. Vasmel, W. L. E., Sijts, E. J. A. M., Leupers, C. J. M., Matthews, E. A. & Melief, C. J. M. Primary virus-induced lymphomas evade T cell immunity by failure to express viral antigens. *J. Exp. Med.* **169**, 1233–1254 (1989).
  159. Spiotto, M. T., Rowley, D. A. & Schreiber, H. Bystander elimination of antigen loss variants in established tumors. *Nat. Med.* **10**, 294–298 (2004).
  160. Yee, C. *et al.* Adoptive T cell therapy using antigen-specific CD8+ T cell clones for the treatment of patients with metastatic melanoma: In vivo persistence, migration, and antitumor effect of transferred T cells. *Proc. Natl. Acad. Sci. U. S. A.* **99**, 16168–16173 (2002).
  161. Sotillo, E. *et al.* Convergence of acquired mutations and alternative splicing of CD19 enables resistance to CART-19 immunotherapy. *Cancer Discov.* **5**, 1282–1295 (2015).
  162. Shalabi, H. *et al.* Sequential loss of tumor surface antigens following chimeric antigen receptor T-cell therapies in diffuse large B-cell lymphoma. *Haematologica* vol. 103 e215–e218 (2018).
  163. O’Rourke, D. M. *et al.* A single dose of peripherally infused EGFRvIII-directed CAR T cells mediates antigen loss and induces adaptive resistance in patients with recurrent glioblastoma. *Sci. Transl. Med.* **9**, (2017).
  164. Leone, P. *et al.* MHC Class I Antigen Processing and Presenting Machinery: Organization, Function, and Defects in Tumor Cells. **105**, (2013).
  165. Campoli, M. & Ferrone, S. HLA antigen changes in malignant cells: Epigenetic mechanisms and biologic significance. *Oncogene* vol. 27 5869–5885 (2008).
  166. Paulson, K. G. *et al.* Acquired cancer resistance to combination immunotherapy from transcriptional loss of class I HLA. *Nat. Commun.* **9**, 1–10 (2018).
  167. Gettinger, S. *et al.* Impaired HLA class I antigen processing and presentation as a

- mechanism of acquired resistance to immune checkpoint inhibitors in lung cancer. *Cancer Discov.* **7**, 1420–1435 (2017).
168. Bernal, M., Ruiz-Cabello, F., Concha, A., Paschen, A. & Garrido, F. Implication of the  $\beta$ 2-microglobulin gene in the generation of tumor escape phenotypes. *Cancer Immunology, Immunotherapy* vol. 61 1359–1371 (2012).
  169. Zaretsky, J. M. *et al.* Mutations Associated with Acquired Resistance to PD-1 Blockade in Melanoma. *N. Engl. J. Med.* **375**, 819–829 (2016).
  170. Maleno, I. *et al.* Frequent loss of heterozygosity in the  $\beta$ 2-microglobulin region of chromosome 15 in primary human tumors. *Immunogenetics* **63**, 65–71 (2011).
  171. Kaklamanis, L. *et al.* Loss of major histocompatibility complex-encoded transporter associated with antigen presentation (TAP) in colorectal cancer. *Am. J. Pathol.* **145**, 505–509 (1994).
  172. Chen, H. L. *et al.* A functionally defective allele of TAP1 results in loss of MHC class I antigen presentation in a human lung cancer. *Nat. Genet.* **13**, 210–213 (1996).
  173. Sucker, A. *et al.* Genetic evolution of T-cell resistance in the course of melanoma progression. *Clin. Cancer Res.* **20**, 6593–6604 (2014).
  174. del Campo, A. B. *et al.* Immune escape of cancer cells with beta2-microglobulin loss over the course of metastatic melanoma. *Int. J. Cancer* **134**, 102–113 (2014).
  175. McGranahan, N. *et al.* Allele-Specific HLA Loss and Immune Escape in Lung Cancer Evolution. *Cell* **171**, 1259–1271.e11 (2017).
  176. Gonzalez, H., Hagerling, C. & Werb, Z. Roles of the immune system in cancer: From tumor initiation to metastatic progression. *Genes and Development* vol. 32 1267–1284 (2018).
  177. Mahmoud, S. M. A. *et al.* Tumor-infiltrating CD8+ lymphocytes predict clinical outcome in breast cancer. *J. Clin. Oncol.* **29**, 1949–1955 (2011).
  178. Loi, S. *et al.* Tumor-infiltrating lymphocytes and prognosis: A pooled individual patient analysis of early-stage triple-negative breast cancers. *J. Clin. Oncol.* **37**, 559–569 (2019).
  179. Clemente, C. G. *et al.* Prognostic value of tumor infiltrating lymphocytes in the vertical growth phase of primary cutaneous melanoma. *Cancer* **77**, 1303–1310 (1996).
  180. van Houdt, I. S. *et al.* Favorable outcome in clinically stage II melanoma patients is associated with the presence of activated tumor infiltrating T-lymphocytes and preserved MHC class I antigen expression. *Int. J. Cancer* **123**, 609–615 (2008).
  181. Fu, Q. *et al.* Prognostic value of tumor-infiltrating lymphocytes in melanoma: a systematic review and meta-analysis. *OncolImmunology* vol. 8 (2019).
  182. Ropponen, K. M., Eskelinen, M. J., Lipponen, P. K., Alhava, E. & Kosma, V. Prognostic value of tumour-infiltrating lymphocytes (TILs) in colorectal cancer. *J. Pathol.* **182**, 318–324 (1997).
  183. Naito, Y. *et al.* CD8+ T cells infiltrated within cancer cell nests as a prognostic factor in human colorectal cancer. *Cancer Res.* **58**, 3491–3494 (1998).
  184. Pagès, F. *et al.* Effector Memory T Cells, Early Metastasis, and Survival in Colorectal Cancer. *N. Engl. J. Med.* **353**, 2654–2666 (2005).
  185. Fridman, W. H., Pagès, F., Sauts-Fridman, C. & Galon, J. The immune contexture in human tumours: Impact on clinical outcome. *Nature Reviews Cancer* vol. 12 298–306 (2012).

186. Galon, J., Angell, H. K., Bedognetti, D. & Marincola, F. M. The Continuum of Cancer Immunosurveillance: Prognostic, Predictive, and Mechanistic Signatures. *Immunity* vol. 39 11–26 (2013).
187. Vajdic, C. M. *et al.* Cancer incidence before and after kidney transplantation. *J. Am. Med. Assoc.* **296**, 2823–2831 (2006).
188. Moloney, F. J. *et al.* A population-based study of skin cancer incidence and prevalence in renal transplant recipients. *Br. J. Dermatol.* **154**, 498–504 (2006).
189. Jiang, Y. *et al.* The Incidence of Cancer in a Population-Based Cohort of Canadian Heart Transplant Recipients. *Am. J. Transplant.* **10**, 637–645 (2010).
190. Baccarani, U. *et al.* Comparison of de novo tumours after liver transplantation with incidence rates from Italian cancer registries. *Dig. Liver Dis.* **42**, 55–60 (2010).
191. Silverberg, M. J. *et al.* HIV infection, immunodeficiency, viral replication, and the risk of cancer. *Cancer Epidemiol. Biomarkers Prev.* **20**, 2551–2559 (2011).
192. Silverberg, M. J. *et al.* HiV infection Status, immunodeficiency, and the incidence of Non-Melanoma Skin cancer. **105**, (2013).
193. Rubinstein, P. G., Aboulaflia, D. M. & Zloza, A. Malignancies in HIV/AIDS: From epidemiology to therapeutic challenges. *Aids* **28**, 453–465 (2014).
194. Vesely, M. D., Kershaw, M. H., Schreiber, R. D. & Smyth, M. J. Natural Innate and Adaptive Immunity to Cancer. *Annu. Rev. Immunol.* **29**, 235–271 (2011).
195. Teng, M. W. L. *et al.* Opposing roles for IL-23 and IL-12 in maintaining occult cancer in an equilibrium state. *Cancer Res.* **72**, 3987–3996 (2012).
196. Wu, X. *et al.* Immune microenvironment profiles of tumor immune equilibrium and immune escape states of mouse sarcoma. *Cancer Lett.* **340**, 124–133 (2013).
197. Kataoka, T. *et al.* FLIP prevents apoptosis induced by death receptors but not by perforin/granzyme B, chemotherapeutic drugs, and gamma irradiation. *J. Immunol.* **161**, 3936–42 (1998).
198. Hinz, S. *et al.* Bcl-X(L) protects pancreatic adenocarcinoma cells against CD95- and TRAIL-receptor-mediated apoptosis. *Oncogene* **19**, 5477–5486 (2000).
199. Keane, M. M., Ettenberg, S. A., Lowrey, G. A., Russell, E. K. & Lipkowitz, S. Fas expression and function in normal and malignant breast cell lines. *Cancer Res.* **56**, 4791–4798 (1996).
200. Takahashi, H. *et al.* FAS death domain deletions and cellular FADD-like interleukin 1 $\beta$  converting enzyme inhibitory protein (long) overexpression: Alternative mechanisms for deregulating the extrinsic apoptotic pathway in diffuse large B-cell lymphoma subtypes. *Clin. Cancer Res.* **12**, 3265–3271 (2006).
201. Nusse, R. & Clevers, H. Wnt/ $\beta$ -Catenin Signaling, Disease, and Emerging Therapeutic Modalities. *Cell* vol. 169 985–999 (2017).
202. Spranger, S., Bao, R. & Gajewski, T. F. Melanoma-intrinsic  $\beta$ -catenin signalling prevents anti-tumour immunity. *Nature* **523**, 231–235 (2015).
203. Spranger, S., Dai, D., Horton, B. & Gajewski, T. F. Tumor-Residing Batf3 Dendritic Cells Are Required for Effector T Cell Trafficking and Adoptive T Cell Therapy. *Cancer Cell* **31**, 711-723.e4 (2017).
204. Luke, J. J., Bao, R., Sweis, R. F., Spranger, S. & Gajewski, T. F. WNT/ $\beta$ -catenin pathway activation correlates with immune exclusion across human cancers. *Clin. Cancer Res.* **25**, 3074–3083 (2019).
205. Fruman, D. A. *et al.* The PI3K Pathway in Human Disease. *Cell* vol. 170 605–635

- (2017).
206. Peng, W. *et al.* Loss of PTEN promotes resistance to T cell-mediated immunotherapy. *Cancer Discov.* **6**, 202–216 (2016).
  207. Kortlever, R. M. *et al.* Myc Cooperates with Ras by Programming Inflammation and Immune Suppression. *Cell* **171**, 1301-1315.e14 (2017).
  208. Skoulidis, F. *et al.* STK11/LKB1 mutations and PD-1 inhibitor resistance in KRAS-mutant lung adenocarcinoma. *Cancer Discov.* **8**, 822–835 (2018).
  209. Koyama, S. *et al.* STK11/LKB1 deficiency promotes neutrophil recruitment and proinflammatory cytokine production to suppress T-cell activity in the lung tumor microenvironment. *Cancer Res.* **76**, 999–1008 (2016).
  210. Kitajima, S. *et al.* Suppression of STING associated with lkb1 loss in KRAS-driven lung cancer. *Cancer Discov.* **9**, 34–45 (2019).
  211. Knudsen, E. S. & Witkiewicz, A. K. The Strange Case of CDK4/6 Inhibitors: Mechanisms, Resistance, and Combination Strategies. *Trends in Cancer* vol. 3 39–55 (2017).
  212. Zhang, J. *et al.* Cyclin D-CDK4 kinase destabilizes PD-L1 via cullin 3-SPOP to control cancer immune surveillance. *Nature* **553**, 91–95 (2018).
  213. Jin, X. *et al.* Phosphorylated RB Promotes Cancer Immunity by Inhibiting NF- $\kappa$ B Activation and PD-L1 Expression. *Mol. Cell* **73**, 22-35.e6 (2019).
  214. Goel, S. *et al.* CDK4/6 inhibition triggers anti-tumour immunity. *Nature* **548**, 471–475 (2017).
  215. Schaer, D. A. *et al.* The CDK4/6 Inhibitor Abemaciclib Induces a T Cell Inflamed Tumor Microenvironment and Enhances the Efficacy of PD-L1 Checkpoint Blockade. *Cell Rep.* **22**, 2978–2994 (2018).
  216. Deng, J. *et al.* CDK4/6 inhibition augments antitumor immunity by enhancing T-cell activation. *Cancer Discov.* **8**, 216–233 (2018).
  217. Jerby-Arnon, L. *et al.* A Cancer Cell Program Promotes T Cell Exclusion and Resistance to Checkpoint Blockade. *Cell* **175**, 984-997.e24 (2018).
  218. Bergers, G. & Benjamin, L. E. Tumorigenesis and the angiogenic switch. *Nature Reviews Cancer* vol. 3 401–410 (2003).
  219. Lanitis, E., Irving, M. & Coukos, G. Targeting the tumor vasculature to enhance T cell activity. *Current Opinion in Immunology* vol. 33 55–63 (2015).
  220. Huang, Y. *et al.* Improving immune-vascular crosstalk for cancer immunotherapy. *Nature Reviews Immunology* vol. 18 195–203 (2018).
  221. Krock, B. L., Skuli, N. & Simon, M. C. Hypoxia-Induced Angiogenesis: Good and Evil. *Genes Cancer* **2**, 1117–1133 (2011).
  222. De Palma, M., Biziato, D. & Petrova, T. V. Microenvironmental regulation of tumour angiogenesis. *Nature Reviews Cancer* vol. 17 457–474 (2017).
  223. Potente, M., Gerhardt, H. & Carmeliet, P. Basic and therapeutic aspects of angiogenesis. *Cell* vol. 146 873–887 (2011).
  224. Bellone, M. & Calcinotto, A. Ways to enhance lymphocyte trafficking into tumors and fitness of tumor infiltrating lymphocytes. *Frontiers in Oncology* vol. 3 SEP 231 (2013).
  225. Motz, G. T. *et al.* Tumor endothelium FasL establishes a selective immune barrier promoting tolerance in tumors. *Nat. Med.* **20**, 607–615 (2014).
  226. Green, D. R., Droin, N. & Pinkoski, M. Activation-induced cell death in T cells.



- Immunol. Rev.* **193**, 70–81 (2003).
227. Ferguson, T. A. & Griffith, T. S. A vision of cell death: Fas ligand and immune privilege 10 years later. *Immunol. Rev.* **213**, 228–238 (2006).
  228. Joyce, J. A. & Fearon, D. T. T cell exclusion, immune privilege, and the tumor microenvironment. *Science (80-. )*. **348**, 74–80 (2015).
  229. Kandalafi, L. E., Facciabene, A., Buckanovich, R. J. & Coukos, G. Endothelin B Receptor, a New Target in Cancer Immune Therapy. (2009) doi:10.1158/1078-0432.CCR-08-0543.
  230. Kalluri, R. The biology and function of fibroblasts in cancer. *Nature Reviews Cancer* vol. 16 582–598 (2016).
  231. Liu, T. *et al.* Cancer-associated fibroblasts: An emerging target of anti-cancer immunotherapy. *Journal of Hematology and Oncology* vol. 12 86 (2019).
  232. Lynch, M. D. & Watt, F. M. Fibroblast heterogeneity: implications for human disease. *Journal of Clinical Investigation* vol. 128 26–35 (2018).
  233. David, C. J. & Massagué, J. Contextual determinants of TGF $\beta$  action in development, immunity and cancer. *Nature Reviews Molecular Cell Biology* vol. 19 419–435 (2018).
  234. Donatelli, S. S. *et al.* TGF- $\beta$ -inducible microRNA-183 silences tumor-associated natural killer cells. *Proc. Natl. Acad. Sci. U. S. A.* **111**, 4203–4208 (2014).
  235. Ahmadzadeh, M. & Rosenberg, S. A. TGF- $\beta$ 1 Attenuates the Acquisition and Expression of Effector Function by Tumor Antigen-Specific Human Memory CD8 T Cells. *J. Immunol.* **174**, 5215–5223 (2005).
  236. Broderick, L. & Bankert, R. B. Membrane-Associated TGF- $\beta$ 1 Inhibits Human Memory T Cell Signaling in Malignant and Nonmalignant Inflammatory Microenvironments. *J. Immunol.* **177**, 3082–3088 (2006).
  237. Chakravarthy, A., Khan, L., Bensler, N. P., Bose, P. & De Carvalho, D. D. TGF- $\beta$ -associated extracellular matrix genes link cancer-associated fibroblasts to immune evasion and immunotherapy failure. *Nat. Commun.* **9**, 1–10 (2018).
  238. Mariathasan, S. *et al.* TGF $\beta$  attenuates tumour response to PD-L1 blockade by contributing to exclusion of T cells. *Nature* **554**, 544–548 (2018).
  239. Tauriello, D. V. F. *et al.* TGF $\beta$  drives immune evasion in genetically reconstituted colon cancer metastasis. *Nature* **554**, 538–543 (2018).
  240. Wan, Y. Y. & Flavell, R. A. ‘Yin-Yang’ functions of transforming growth factor- $\beta$  and T regulatory cells in immune regulation. *Immunol. Rev.* **220**, 199–213 (2007).
  241. Byrne, S. N., Knox, M. C. & Halliday, G. M. TGF $\beta$  is responsible for skin tumour infiltration by macrophages enabling the tumours to escape immune destruction. *Immunol. Cell Biol.* **86**, 92–97 (2008).
  242. Takahashi, H. *et al.* Cancer-associated fibroblasts promote an immunosuppressive microenvironment through the induction and accumulation of protumoral macrophages. *Oncotarget* **8**, 8633–8647 (2017).
  243. Comito, G. *et al.* Cancer-associated fibroblasts and M2-polarized macrophages synergize during prostate carcinoma progression. *Oncogene* **33**, 2423–2431 (2014).
  244. Menetrier-Caux, C. *et al.* Inhibition of the Differentiation of Dendritic Cells From CD34+ Progenitors by Tumor Cells: Role of Interleukin-6 and Macrophage Colony-Stimulating Factor. *Blood* **92**, 4778–4791 (1998).

245. Park, S.-J. *et al.* IL-6 Regulates In Vivo Dendritic Cell Differentiation through STAT3 Activation. *J. Immunol.* **173**, 3844–3854 (2004).
246. Chomarat, P., Banchereau, J., Davoust, J. & Palucka, A. K. IL-6 switches the differentiation of monocytes from dendritic cells to macrophages. *Nat. Immunol.* **1**, 510–514 (2000).
247. Alkasalias, T., Moyano-Galceran, L., Arsenian-Henriksson, M. & Lehti, K. Fibroblasts in the tumor microenvironment: Shield or spear? *International Journal of Molecular Sciences* vol. 19 (2018).
248. Acerbi, I. *et al.* Human breast cancer invasion and aggression correlates with ECM stiffening and immune cell infiltration. *Integr. Biol.* **7**, 1120–1134 (2015).
249. Kumar, V., Patel, S., Tcyganov, E. & Gabrilovich, D. I. The Nature of Myeloid-Derived Suppressor Cells in the Tumor Microenvironment. *Trends in Immunology* vol. 37 208–220 (2016).
250. Connolly, M. K. *et al.* Distinct populations of metastases-enabling myeloid cells expand in the liver of mice harboring invasive and preinvasive intra-abdominal tumor. *J. Leukoc. Biol.* **87**, 713–725 (2010).
251. Lesokhin, A. M. *et al.* Monocytic CCR2 + myeloid-derived suppressor cells promote immune escape by limiting activated CD8 T-cell infiltration into the tumor microenvironment. *Cancer Res.* **72**, 876–886 (2012).
252. Huang, B. *et al.* CCL2/CCR2 pathway mediates recruitment of myeloid suppressor cells to cancers. *Cancer Lett.* **252**, 86–92 (2007).
253. Obermajer, N., Muthuswamy, R., Odunsi, K., Edwards, R. P. & Kalinski, P. PGE 2-induced CXCL 12 production and CXCR4 expression controls the accumulation of human MDSCs in ovarian cancer environment. *Cancer Res.* **71**, 7463–7470 (2011).
254. Bronte, V. & Zanovello, P. Regulation of immune responses by L-arginine metabolism. *Nat. Rev. Immunol.* **5**, 641–654 (2005).
255. Yu, J. *et al.* Myeloid-Derived Suppressor Cells Suppress Antitumor Immune Responses through IDO Expression and Correlate with Lymph Node Metastasis in Patients with Breast Cancer. *J. Immunol.* **190**, 3783–3797 (2013).
256. Noman, M. Z. *et al.* PD-L1 is a novel direct target of HIF-1 $\alpha$ , and its blockade under hypoxia enhanced: MDSC-mediated T cell activation. *J. Exp. Med.* **211**, 781–790 (2014).
257. Schlecker, E. *et al.* Tumor-Infiltrating Monocytic Myeloid-Derived Suppressor Cells Mediate CCR5-Dependent Recruitment of Regulatory T Cells Favoring Tumor Growth. *J. Immunol.* **189**, 5602–5611 (2012).
258. Lavin, Y., Mortha, A., Rahman, A. & Merad, M. Regulation of macrophage development and function in peripheral tissues. *Nature Reviews Immunology* vol. 15 731–744 (2015).
259. Mantovani, A., Marchesi, F., Malesci, A., Laghi, L. & Allavena, P. Tumour-associated macrophages as treatment targets in oncology. *Nat. Rev. Clin. Oncol.* **14**, 399–416 (2017).
260. Murray, P. J. Macrophage Polarization. *Annu. Rev. Physiol.* **79**, 541–566 (2017).
261. Linde, N. *et al.* Vascular endothelial growth factor-induced skin carcinogenesis depends on recruitment and alternative activation of macrophages. *J. Pathol.* **227**, 17–28 (2012).
262. Chitu, V. & Stanley, E. R. Colony-stimulating factor-1 in immunity and inflammation.

- Curr. Opin. Immunol.* **18**, 39–48 (2006).
263. Pyonteck, S. M. *et al.* CSF-1R inhibition alters macrophage polarization and blocks glioma progression. *Nat. Med.* **19**, 1264–1272 (2013).
  264. Candido, J. B. *et al.* CSF1R+ Macrophages Sustain Pancreatic Tumor Growth through T Cell Suppression and Maintenance of Key Gene Programs that Define the Squamous Subtype. *Cell Rep.* **23**, 1448–1460 (2018).
  265. Lin, E. Y. & Pollard, J. W. Tumor-associated macrophages press the angiogenic switch in breast cancer. *Cancer Research* vol. 67 5064–5066 (2007).
  266. Yeo, E. J. *et al.* Myeloid wnt7b mediates the angiogenic switch and metastasis in breast cancer. *Cancer Res.* **74**, 2962–2973 (2014).
  267. De Palma, M. *et al.* Tie2 identifies a hematopoietic lineage of proangiogenic monocytes required for tumor vessel formation and a mesenchymal population of pericyte progenitors. *Cancer Cell* **8**, 211–226 (2005).
  268. Wyckoff, J. B. *et al.* Direct visualization of macrophage-assisted tumor cell intravasation in mammary tumors. *Cancer Res.* **67**, 2649–2656 (2007).
  269. Quail, D. F. & Joyce, J. A. Microenvironmental regulation of tumor progression and metastasis. *Nature Medicine* vol. 19 1423–1437 (2013).
  270. Kren, L. *et al.* Production of immune-modulatory nonclassical molecules HLA-G and HLA-E by tumor infiltrating amoeboid microglia/macrophages in glioblastomas: A role in innate immunity? *J. Neuroimmunol.* **220**, 131–135 (2010).
  271. Morandi, F. *et al.* Human neuroblastoma cells trigger an immunosuppressive program in monocytes by stimulating soluble HLA-G release. *Cancer Res.* **67**, 6433–6441 (2007).
  272. Kryczek, I. *et al.* B7-H4 expression identifies a novel suppressive macrophage population in human ovarian carcinoma. *J. Exp. Med.* **203**, 871–881 (2006).
  273. Kuang, D. M. *et al.* Activated monocytes in peritumoral stroma of hepatocellular carcinoma foster immune privilege and disease progression through PD-L1. *J. Exp. Med.* **206**, 1327–1337 (2009).
  274. Bloch, O. *et al.* Gliomas promote immunosuppression through induction of B7-H1 expression in tumor-associated macrophages. *Clin. Cancer Res.* **19**, 3165–3175 (2013).
  275. Doedens, A. L. *et al.* Macrophage expression of hypoxia-inducible factor-1 $\alpha$  suppresses T-cell function and promotes tumor progression. *Cancer Res.* **70**, 7465–7475 (2010).
  276. Noman, M. Z. *et al.* PD-L1 is a novel direct target of HIF-1 $\alpha$ , and its blockade under hypoxia enhanced: MDSC-mediated T cell activation. *J. Exp. Med.* **211**, 781–790 (2014).
  277. Liguori, M. *et al.* Functional TRAIL receptors in monocytes and tumor-associated macrophages: A possible targeting pathway in the tumor microenvironment. *Oncotarget* **7**, 41662–41676 (2016).
  278. Sharda, D. R. *et al.* Regulation of Macrophage Arginase Expression and Tumor Growth by the Ron Receptor Tyrosine Kinase. *J. Immunol.* **187**, 2181–2192 (2011).
  279. Rodriguez, P. C. *et al.* Arginase I production in the tumor microenvironment by mature myeloid cells inhibits T-cell receptor expression and antigen-specific T-cell responses. *Cancer Res.* **64**, 5839–5849 (2004).
  280. Rodriguez, P. C. *et al.* L-Arginine Consumption by Macrophages Modulates the

- Expression of CD3 $\zeta$  Chain in T Lymphocytes. *J. Immunol.* **171**, 1232–1239 (2003).
281. Curiel, T. J. *et al.* Specific recruitment of regulatory T cells in ovarian carcinoma fosters immune privilege and predicts reduced survival. *Nat. Med.* **10**, 942–949 (2004).
  282. Liu, J. *et al.* Tumor-Associated Macrophages Recruit CCR6+ Regulatory T Cells and Promote the Development of Colorectal Cancer via Enhancing CCL20 Production in Mice. *PLoS One* **6**, e19495 (2011).
  283. Adeegbe, D. O. & Nishikawa, H. Natural and induced T regulatory cells in cancer. *Frontiers in Immunology* vol. 4 190 (2013).
  284. Denning, T. L., Wang, Y. C., Patel, S. R., Williams, I. R. & Pulendran, B. Lamina propria macrophages and dendritic cells differentially induce regulatory and interleukin 17-producing T cell responses. *Nat. Immunol.* **8**, 1086–1094 (2007).
  285. Zhu, Y., Yao, S. & Chen, L. Cell Surface Signaling Molecules in the Control of Immune Responses: A Tide Model. *Immunity* vol. 34 466–478 (2011).
  286. Zhang, Q. & Vignali, D. A. A. Co-stimulatory and Co-inhibitory Pathways in Autoimmunity. *Immunity* vol. 44 1034–1051 (2016).
  287. Tivol, E. A. *et al.* Loss of CTLA-4 leads to massive lymphoproliferation and fatal multiorgan tissue destruction, revealing a critical negative regulatory role of CTLA-4. *Immunity* **3**, 541–547 (1995).
  288. Waterhouse, P. *et al.* Lymphoproliferative disorders with early lethality in mice deficient in Ctl $\alpha$ -4. *Science (80-. )*. **270**, 985–988 (1995).
  289. Nishimura, H., Nose, M., Hiai, H., Minato, N. & Honjo, T. *Development of Lupus-like Autoimmune Diseases by Disruption of the PD-1 Gene Encoding an ITIM Motif-Carrying Immunoreceptor.* *Immunity* vol. 11 (1999).
  290. Moskophidis, D., Lechner, F., Pircher, H. & Zinkernagel, R. M. Virus persistence in acutely infected immunocompetent mice by exhaustion of antiviral cytotoxic effector T cells. *Nature* **362**, 758–761 (1993).
  291. Zajac, A. J. *et al.* Viral immune evasion due to persistence of activated T cells without effector function. *J. Exp. Med.* **188**, 2205–2213 (1998).
  292. Wherry, E. J., Blattman, J. N., Murali-Krishna, K., van der Most, R. & Ahmed, R. Viral Persistence Alters CD8 T-Cell Immunodominance and Tissue Distribution and Results in Distinct Stages of Functional Impairment. *J. Virol.* **77**, 4911–4927 (2003).
  293. Fuller, M. J. & Zajac, A. J. Ablation of CD8 and CD4 T Cell Responses by High Viral Loads. *J. Immunol.* **170**, 477–486 (2003).
  294. Swain, S. L., Mckinstry, K. K. & Strutt, T. M. The priming environment can vary Expanding roles for CD4 + T cells in immunity to viruses. (2012) doi:10.1038/nri3152.
  295. Wherry, E. J. *et al.* Molecular Signature of CD8+ T Cell Exhaustion during Chronic Viral Infection. *Immunity* **27**, 670–684 (2007).
  296. Pauken, K. E. *et al.* Epigenetic stability of exhausted T cells limits durability of reinvigoration by PD-1 blockade. *Science (80-. )*. **354**, 1160–1165 (2016).
  297. Sen, D. R. *et al.* The epigenetic landscape of T cell exhaustion. *Science (80-. )*. **354**, 1165–1169 (2016).
  298. Yao, C. *et al.* Single-cell RNA-seq reveals TOX as a key regulator of CD8+ T cell persistence in chronic infection. *Nat. Immunol.* **20**, 890–901 (2019).
  299. Khan, O. *et al.* TOX transcriptionally and epigenetically programs CD8+ T cell

- exhaustion. *Nature* **571**, 211–218 (2019).
300. Alfei, F. *et al.* TOX reinforces the phenotype and longevity of exhausted T cells in chronic viral infection. *Nature* **571**, 265–269 (2019).
  301. Scott, A. C. *et al.* TOX is a critical regulator of tumour-specific T cell differentiation. *Nature* **571**, 270–274 (2019).
  302. Wherry, E. J. T cell exhaustion. *Nature Immunology* vol. 12 492–499 (2011).
  303. Blank, C. U. *et al.* Defining ‘T cell exhaustion’. *Nat. Rev. Immunol.* **19**, 665–674 (2019).
  304. Barber, D. L. *et al.* Restoring function in exhausted CD8 T cells during chronic viral infection. *Nature* **439**, 682–687 (2006).
  305. Ahmadzadeh, M. *et al.* Tumor antigen-specific CD8 T cells infiltrating the tumor express high levels of PD-1 and are functionally impaired. *Blood* **114**, 1537–1544 (2009).
  306. Thommen, D. S. *et al.* Progression of lung cancer is associated with increased dysfunction of T cells defined by coexpression of multiple inhibitory receptors. *Cancer Immunol. Res.* **3**, 1344–1354 (2015).
  307. Baitsch, L. *et al.* Exhaustion of tumor-specific CD8 + T cells in metastases from melanoma patients. *J. Clin. Invest.* **121**, 2350–2360 (2011).
  308. Matsuzaki, J. *et al.* Tumor-infiltrating NY-ESO-1-specific CD8+ T cells are negatively regulated by LAG-3 and PD-1 in human ovarian cancer. *Proc. Natl. Acad. Sci. U. S. A.* **107**, 7875–7880 (2010).
  309. Lu, X. *et al.* Tumor antigen-specific CD8+ T cells are negatively regulated by PD-1 and Tim-3 in human gastric cancer. *Cell. Immunol.* **313**, 43–51 (2017).
  310. Li, J. *et al.* Tumor-infiltrating Tim-3+ T cells proliferate avidly except when PD-1 is co-expressed: Evidence for intracellular cross talk. *Oncoimmunology* **5**, e1200778 (2016).
  311. Zippelius, A. *et al.* Effector Function of Human Tumor-Specific CD8 T Cells in Melanoma Lesions: A State of Local Functional Tolerance. *Cancer Res.* **64**, 2865–2873 (2004).
  312. Li, H. *et al.* Dysfunctional CD8 T Cells Form a Proliferative, Dynamically Regulated Compartment within Human Melanoma. *Cell* **176**, 775-789.e18 (2019).
  313. Schietinger, A. *et al.* Tumor-Specific T Cell Dysfunction Is a Dynamic Antigen-Driven Differentiation Program Initiated Article Tumor-Specific T Cell Dysfunction Is a Dynamic Antigen-Driven Differentiation Program Initiated Early during Tumorigenesis. *Immunity* 1–13 (2016) doi:10.1016/j.immuni.2016.07.011.
  314. Fehlings, M. *et al.* Checkpoint blockade immunotherapy reshapes the high-dimensional phenotypic heterogeneity of murine intratumoural neoantigen-specific CD8+ T cells. *Nat. Commun.* **8**, 1–12 (2017).
  315. Giraldo, N. A. *et al.* Tumor-infiltrating and peripheral blood T-cell immunophenotypes predict early relapse in localized clear cell renal cell carcinoma. *Clin. Cancer Res.* **23**, 4416–4428 (2017).
  316. Thommen, D. S. *et al.* A transcriptionally and functionally distinct pd-1 + cd8 + t cell pool with predictive potential in non-small-cell lung cancer treated with pd-1 blockade. *Nat. Med.* **24**, 994–1004 (2018).
  317. van der Leun, A. M., Thommen, D. S. & Schumacher, T. N. CD8+ T cell states in human cancer: insights from single-cell analysis. *Nature Reviews Cancer* vol. 20

- 218–232 (2020).
318. Miller, B. C. *et al.* Subsets of exhausted CD8+ T cells differentially mediate tumor control and respond to checkpoint blockade. *Nat. Immunol.* **20**, 326–336 (2019).
  319. Kurtulus, S. *et al.* Checkpoint Blockade Immunotherapy Induces Dynamic Changes in PD-1 – CD8 + Tumor-Infiltrating T Cells. *Immunity* **50**, 181-194.e6 (2019).
  320. Siddiqui, I. *et al.* Intratumoral Tcf1 + PD-1 + CD8 + T Cells with Stem-like Properties Promote Tumor Control in Response to Vaccination and Checkpoint Blockade Immunotherapy. *Immunity* **50**, 195-211.e10 (2019).
  321. Singer, M. *et al.* A Distinct Gene Module for Dysfunction Uncoupled from Activation in Tumor-Infiltrating T Cells. *Cell* **166**, 1500-1511.e9 (2016).
  322. Chihara, N. *et al.* Induction and transcriptional regulation of the co-inhibitory gene module in T cells. *Nature* **558**, 454–459 (2018).
  323. Li, J., He, Y., Hao, J., Ni, L. & Dong, C. High Levels of Eomes Promote Exhaustion of Anti-tumor CD8+ T Cells. *Front. Immunol.* **9**, 2981 (2018).
  324. Gibson, H. M. *et al.* Induction of the CTLA-4 Gene in Human Lymphocytes Is Dependent on NFAT Binding the Proximal Promoter. *J. Immunol.* **179**, 3831–3840 (2007).
  325. Egen, J. G. & Allison, J. P. Cytotoxic T lymphocyte antigen-4 accumulation in the immunological synapse is regulated by TCR signal strength. *Immunity* **16**, 23–35 (2002).
  326. Linsley, P. S. *et al.* Coexpression and functional cooperation of CTLA-4 and CD28 on activated T lymphocytes. *J. Exp. Med.* **176**, 1595–1604 (1992).
  327. Stamper, C. C. *et al.* Crystal structure of the B7-1/CTLA-4 complex that inhibits human immune responses. *Nature* **410**, 608–611 (2001).
  328. Schwartz, J. C. D., Zhang, X., Fedorov, A. A., Nathenson, S. G. & Almo, S. C. Structural basis for co-stimulation by the human CTLA-4/B7-2 complex. *Nature* **410**, 604–608 (2001).
  329. Walker, L. S. K. & Sansom, D. M. The emerging role of CTLA4 as a cell-extrinsic regulator of T cell responses. *Nature Reviews Immunology* vol. 11 852–863 (2011).
  330. Qureshi, O. S. *et al.* Trans-endocytosis of CD80 and CD86: A molecular basis for the cell-extrinsic function of CTLA-4. *Science (80-. )*. **332**, 600–603 (2011).
  331. Walker, L. S. K. & Sansom, D. M. Confusing signals: Recent progress in CTLA-4 biology. *Trends in Immunology* vol. 36 63–70 (2015).
  332. Agata, Y. *et al.* Expression of the PD-1 antigen on the surface of stimulated mouse T and B lymphocytes. *International Immunology* vol. 8 <https://academic.oup.com/intimm/article-abstract/8/5/765/693918> (1996).
  333. Sharpe, A. H. & Pauken, K. E. The diverse functions of the PD1 inhibitory pathway. *Nat. Rev. Immunol.* **18**, 153–167 (2018).
  334. Sun, C., Mezzadra, R. & Schumacher, T. N. Regulation and Function of the PD-L1 Checkpoint. *Immunity* vol. 48 434–452 (2018).
  335. Keir, M. E. *et al.* Tissue expression of PD-L1 mediates peripheral T cell tolerance. *J. Exp. Med.* **203**, 883–895 (2006).
  336. Latchman, Y. *et al.* PD-L2 is a second ligand for PD-1 and inhibits T cell activation. *Nat. Immunol.* **2**, 261–268 (2001).
  337. Wei, S. C., Duffy, C. R. & Allison, J. P. Fundamental mechanisms of immune checkpoint blockade therapy. *Cancer Discovery* vol. 8 1069–1086 (2018).

338. Walker, L. S. K. PD-1 and CTLA-4: Two checkpoints, one pathway? *Sci. Immunol.* **2**, (2017).
339. Patsoukis, N. *et al.* PD-1 alters T-cell metabolic reprogramming by inhibiting glycolysis and promoting lipolysis and fatty acid oxidation. *Nat. Commun.* **6**, (2015).
340. Boles, K. S. *et al.* A novel molecular interaction for the adhesion of follicular CD4 T cells to follicular DC. *Eur. J. Immunol.* **39**, 695–703 (2009).
341. Stanietsky, N. *et al.* The interaction of TIGIT with PVR and PVRL2 inhibits human NK cell cytotoxicity. *Proc. Natl. Acad. Sci. U. S. A.* **106**, 17858–17863 (2009).
342. Yu, X. *et al.* The surface protein TIGIT suppresses T cell activation by promoting the generation of mature immunoregulatory dendritic cells. *Nat. Immunol.* **10**, 48–57 (2009).
343. Levin, S. D. *et al.* Vstm3 is a member of the CD28 family and an important modulator of T-cell function. *Eur. J. Immunol.* **41**, 902–915 (2011).
344. Joller, N. *et al.* Cutting Edge: TIGIT Has T Cell-Intrinsic Inhibitory Functions. *J. Immunol.* **186**, 1338–1342 (2011).
345. Joller, N. *et al.* Treg cells expressing the coinhibitory molecule TIGIT selectively inhibit proinflammatory Th1 and Th17 cell responses. *Immunity* **40**, 569–581 (2014).
346. Chauvin, J. M. *et al.* TIGIT and PD-1 impair tumor antigen-specific CD8+ T cells in melanoma patients. *J. Clin. Invest.* **125**, 2046–2058 (2015).
347. Kurtulus, S. *et al.* TIGIT predominantly regulates the immune response via regulatory T cells. *J. Clin. Invest.* **125**, 4053–4062 (2015).
348. Anderson, A. C., Joller, N. & Kuchroo, V. K. Lag-3, Tim-3, and TIGIT: Co-inhibitory Receptors with Specialized Functions in Immune Regulation. *Immunity* vol. 44 989–1004 (2016).
349. Stengel, K. F. *et al.* Structure of TIGIT immunoreceptor bound to poliovirus receptor reveals a cell-cell adhesion and signaling mechanism that requires cis-trans receptor clustering. *Proc. Natl. Acad. Sci. U. S. A.* **109**, 5399–5404 (2012).
350. Anderson, A. C., Joller, N. & Kuchroo, V. K. Lag-3, Tim-3, and TIGIT: Co-inhibitory Receptors with Specialized Functions in Immune Regulation. *Immunity* vol. 44 989–1004 (2016).
351. Johnston, R. J. *et al.* The Immunoreceptor TIGIT Regulates Antitumor and Antiviral CD8+ T Cell Effector Function. *Cancer Cell* **26**, 923–937 (2014).
352. Zhang, Y. *et al.* Genome-wide DNA methylation analysis identifies hypomethylated genes regulated by FOXP3 in human regulatory T cells. *Blood* **122**, 2823–2836 (2013).
353. Fuhrman, C. A. *et al.* Divergent Phenotypes of Human Regulatory T Cells Expressing the Receptors TIGIT and CD226. *J. Immunol.* **195**, 145–155 (2015).
354. Triebel, F. *et al.* LAG-3, a novel lymphocyte activation gene closely related to CD4. *J. Exp. Med.* **171**, 1393–1405 (1990).
355. Workman, C. J. & Vignali, D. A. A. Negative Regulation of T Cell Homeostasis by Lymphocyte Activation Gene-3 (CD223). *J. Immunol.* **174**, 688–695 (2005).
356. Lino, A. C. *et al.* LAG-3 Inhibitory Receptor Expression Identifies Immunosuppressive Natural Regulatory Plasma Cells. *Immunity* **49**, 120-133.e9 (2018).
357. Kisielow, M., Kisielow, J., Capoferri-Sollami, G. & Karjalainen, K. Expression of

- lymphocyte activation gene 3 (LAG-3) on B cells is induced by T cells. *Eur. J. Immunol.* **35**, 2081–2088 (2005).
358. Mao, X. *et al.* Pathological  $\alpha$ -synuclein transmission initiated by binding lymphocyte-activation gene 3. *Science (80-. )*. **353**, (2016).
  359. Gagliani, N. *et al.* Coexpression of CD49b and LAG-3 identifies human and mouse T regulatory type 1 cells. *Nat. Med.* **19**, 739–746 (2013).
  360. Xu, F. *et al.* LSECTin expressed on melanoma cells promotes tumor progression by inhibiting antitumor T-cell responses. *Cancer Res.* **74**, 3418–3428 (2014).
  361. Kouo, T. *et al.* Galectin-3 shapes antitumor immune responses by suppressing CD8 T Cells via LAG-3 and Inhibiting Expansion of Plasmacytoid Dendritic Cells. *Cancer Immunol. Res.* **3**, 412–423 (2015).
  362. Huard, B., Prigent, P., Tournier, M., Bruniquel, D. & Triebel, F. CD4/major histocompatibility complex class II interaction analyzed with CD4- and lymphocyte activation gene-3 (LAG-3)-Ig fusion proteins. *Eur. J. Immunol.* **25**, 2718–2721 (1995).
  363. Wang, J. *et al.* Fibrinogen-like Protein 1 Is a Major Immune Inhibitory Ligand of LAG-3. *Cell* **176**, 334–347.e12 (2019).
  364. Hannier, S., Tournier, M., Bismuth, G. & Triebel, F. CD3/TCR Signaling Activation Gene-3 Molecules Inhibit CD3/TCR Complex-Associated Lymphocyte. *J Immunol* **161**, 4058–4065 (1998).
  365. Zhu, J., Yamane, H. & Paul, W. E. Differentiation of Effector CD4 T Cell Populations. *Annu. Rev. Immunol.* **28**, 445–489 (2010).
  366. Kim, H. J. & Cantor, H. CD4 T-cell subsets and tumor immunity: the helpful and the not-so-helpful. *Cancer immunology research* vol. 2 91–98 (2014).
  367. Togashi, Y., Shitara, K. & Nishikawa, H. Regulatory T cells in cancer immunosuppression — implications for anticancer therapy. *Nature Reviews Clinical Oncology* vol. 16 356–371 (2019).
  368. Wing, K. & Sakaguchi, S. Regulatory T cells exert checks and balances on self tolerance and autoimmunity. *Nature Immunology* vol. 11 7–13 (2010).
  369. Brunkow, M. E. *et al.* Disruption of a new forkhead/winged-helix protein, scurf, results in the fatal lymphoproliferative disorder of the scurfy mouse. *Nat. Genet.* **27**, 68–73 (2001).
  370. Takahashi, T. *et al.* Immunologic self-tolerance maintained by CD25<sup>+</sup> CD4<sup>+</sup> naturally anergic and suppressive T cells: induction of autoimmune disease by breaking their anergic/suppressive state. *International Immunology* vol. 10 (1998).
  371. Thornton, A. M. & Shevach, E. M. CD4<sup>+</sup>CD25<sup>+</sup> immunoregulatory T cells suppress polyclonal T cell activation in vitro by inhibiting interleukin 2 production. *J. Exp. Med.* **188**, 287–296 (1998).
  372. Perez, V. L. *et al.* Induction of peripheral T cell tolerance in vivo requires CTLA-4 engagement. *Immunity* **6**, 411–417 (1997).
  373. Wing, K. *et al.* CTLA-4 control over Foxp3<sup>+</sup> regulatory T cell function. *Science (80-. )*. **322**, 271–275 (2008).
  374. Tan, M. C. B. *et al.* Disruption of CCR5-Dependent Homing of Regulatory T Cells Inhibits Tumor Growth in a Murine Model of Pancreatic Cancer. *J. Immunol.* **182**, 1746–1755 (2009).
  375. Shields, J. D., Kourtis, I. C., Tomei, A. A., Roberts, J. M. & Swartz, M. A. Induction



- of lymphoidlike stroma and immune escape by tumors that express the chemokine CCL21. *Science* (80-. ). **328**, 749–752 (2010).
376. Grossman, W. J. *et al.* Human T regulatory cells can use the perforin pathway to cause autologous target cell death. *Immunity* **21**, 589–601 (2004).
  377. Wilson, J. M. *et al.* The A 2B Adenosine Receptor Impairs the Maturation and Immunogenicity of Dendritic Cells . *J. Immunol.* **182**, 4616–4623 (2009).
  378. Deaglio, S. *et al.* Adenosine generation catalyzed by CD39 and CD73 expressed on regulatory T cells mediates immune suppression. *J. Exp. Med.* **204**, 1257–1265 (2007).
  379. Steinbrink, K., Wöflfl, M., Jonuleit, H., Knop, J. & Enk, A. H. Induction of tolerance by IL-10-treated dendritic cells. *J. Immunol.* **159**, 4772–80 (1997).
  380. Collison, L. W. *et al.* The inhibitory cytokine IL-35 contributes to regulatory T-cell function. *Nature* **450**, 566–569 (2007).
  381. Turnis, M. E. *et al.* Interleukin-35 Limits Anti-Tumor Immunity. *Immunity* **44**, 316–329 (2016).
  382. Jarnicki, A. G., Lysaght, J., Todryk, S. & Mills, K. H. G. Suppression of Antitumor Immunity by IL-10 and TGF- $\beta$ -Producing T Cells Infiltrating the Growing Tumor: Influence of Tumor Environment on the Induction of CD4 + and CD8 + Regulatory T Cells . *J. Immunol.* **177**, 896–904 (2006).
  383. De Simone, M. *et al.* Transcriptional Landscape of Human Tissue Lymphocytes Unveils Uniqueness of Tumor-Infiltrating T Regulatory Cells. *Immunity* **45**, 1135–1147 (2016).
  384. Nishikawa, H. *et al.* Definition of target antigens for naturally occurring CD4+ CD25+ regulatory T cells. *J. Exp. Med.* **201**, 681–686 (2005).
  385. Galon, J. & Bruni, D. Approaches to treat immune hot, altered and cold tumours with combination immunotherapies. *Nature Reviews Drug Discovery* vol. 18 197–218 (2019).
  386. Gajewski, T. F. *et al.* Cancer immunotherapy targets based on understanding the t cell-inflamed versus non-t cell-inflamed tumor microenvironment. in *Advances in Experimental Medicine and Biology* vol. 1036 19–31 (Springer New York LLC, 2017).
  387. Spranger, S. *et al.* Density of immunogenic antigens does not explain the presence or absence of the T-cell-inflamed tumor microenvironment in melanoma. *Proc. Natl. Acad. Sci. U. S. A.* **113**, E7759–E7768 (2016).
  388. Nagarsheth, N., Wicha, M. S. & Zou, W. Chemokines in the cancer microenvironment and their relevance in cancer immunotherapy. *Nature Reviews Immunology* vol. 17 559–572 (2017).
  389. Turley, S. J., Cremasco, V. & Astarita, J. L. Immunological hallmarks of stromal cells in the tumour microenvironment. *Nat. Rev. Immunol.* **15**, 669–682 (2015).
  390. Bonaventura, P. *et al.* Cold tumors: A therapeutic challenge for immunotherapy. *Frontiers in Immunology* vol. 10 (2019).
  391. Hezel, A. F., Kimmelman, A. C., Stanger, B. Z., Bardeesy, N. & DePinho, R. A. Genetics and biology of pancreatic ductal adenocarcinoma. *Genes and Development* vol. 20 1218–1249 (2006).
  392. Siegel, R. L., Miller, K. D. & Jemal, A. Cancer statistics, 2020. *CA. Cancer J. Clin.* **70**, 7–30 (2020).

393. Golan, T. *et al.* Maintenance Olaparib for Germline BRCA-Mutated Metastatic Pancreatic Cancer. *N. Engl. J. Med.* **381**, 317–327 (2019).
394. Tesfaye, A. A., Philip, P. A. & Tesfaye, A. *Adjuvant Treatment of Surgically Resectable Pancreatic Ductal Adenocarcinoma. Clinical Advances in Hematology & Oncology* vol. 17 (2019).
395. Balsano, R., Tommasi, C. & Garajova, I. State of the art for metastatic pancreatic cancer treatment: Where are we now?\*. *Anticancer Research* vol. 39 3405–3412 (2019).
396. Conroy, T. *et al.* FOLFIRINOX versus Gemcitabine for Metastatic Pancreatic Cancer. *N. Engl. J. Med.* **364**, 1817–1825 (2011).
397. Von Hoff, D. D. *et al.* Increased Survival in Pancreatic Cancer with nab-Paclitaxel plus Gemcitabine. *N. Engl. J. Med.* **369**, 1691–1703 (2013).
398. Smith, J. A., Singhi, A. D. & Maitra, A. Precursors to invasive pancreatic cancer. *Gastrointest. Cancer Targets Ther.* **2012**, 19–27 (2012).
399. Hruban, R. H., Wilentz, R. E. & Kern, S. E. Genetic progression in the pancreatic ducts. *American Journal of Pathology* vol. 156 1821–1825 (2000).
400. Xu, Y., Liu, J., Nipper, M. & Wang, P. Ductal vs. acinar? Recent insights into identifying cell lineage of pancreatic ductal adenocarcinoma. *Ann. Pancreat. Cancer* **2**, 11–11 (2019).
401. Fukuda, A. & Takaori, K. Genetics and biology of pancreatic cancer and its precursor lesions: lessons learned from human pathology and mouse models. *Ann. Pancreat. Cancer* **2**, 1–23 (2019).
402. Friedlander, S. Y. G. *et al.* Context-Dependent Transformation of Adult Pancreatic Cells by Oncogenic K-Ras. *Cancer Cell* **16**, 379–389 (2009).
403. Morris IV, J. P., Cano, D. A., Sekine, S., Wang, S. C. & Hebrok, M.  $\beta$ -catenin blocks Kras-dependent reprogramming of acini into pancreatic cancer precursor lesions in mice. *J. Clin. Invest.* **120**, 508–520 (2010).
404. O, J.-P. D. La *et al.* Notch and Kras reprogram pancreatic acinar cells to ductal intraepithelial neoplasia. *Proc. Natl. Acad. Sci.* **105**, 18907–18912 (2008).
405. Habbe, N. *et al.* Spontaneous induction of murine pancreatic intraepithelial neoplasia (mPanIN) by acinar cell targeting of oncogenic Kras in adult mice. *Proc. Natl. Acad. Sci. U. S. A.* **105**, 18913–18918 (2008).
406. Makohon-Moore, A. P. *et al.* Precancerous neoplastic cells can move through the pancreatic ductal system. *Nature* **561**, 201–205 (2018).
407. Kanda, M. *et al.* Presence of somatic mutations in most early-stage pancreatic intraepithelial neoplasia. *Gastroenterology* **142**, 730-733.e9 (2012).
408. Raphael, B. J. *et al.* Integrated Genomic Characterization of Pancreatic Ductal Adenocarcinoma. *Cancer Cell* **32**, 185-203.e13 (2017).
409. Waters, A. M. & Der, C. J. KRAS: The critical driver and therapeutic target for pancreatic cancer. *Cold Spring Harb. Perspect. Med.* **8**, a031435 (2018).
410. Prior, I. A., Lewis, P. D. & Mattos, C. A comprehensive survey of ras mutations in cancer. *Cancer Res.* **72**, 2457–2467 (2012).
411. Zhou, B., Der, C. J. & Cox, A. D. The role of wild type RAS isoforms in cancer. *Seminars in Cell and Developmental Biology* vol. 58 60–69 (2016).
412. Qiu, W. *et al.* Disruption of p16 and activation of kras in pancreas increase ductal adenocarcinoma formation and metastasis in vivo. *Oncotarget* **2**, 862–873 (2011).

413. Lim, K. H., Ancrile, B. B., Kashatus, D. F. & Counter, C. M. Tumour maintenance is mediated by eNOS. *Nature* **452**, 646–649 (2008).
414. Grabocka, E. *et al.* Wild-Type H- and N-Ras Promote Mutant K-Ras-Driven Tumorigenesis by Modulating the DNA Damage Response. *Cancer Cell* **25**, 243–256 (2014).
415. Hingorani, S. R. *et al.* Preinvasive and invasive ductal pancreatic cancer and its early detection in the mouse. *Cancer Cell* **4**, 437–450 (2003).
416. Notta, F., Hahn, S. A. & Real, F. X. A genetic roadmap of pancreatic cancer: Still evolving. *Gut* **66**, 2170–2178 (2017).
417. Cubilla, A. L. & Fitzgerald, P. J. Morphological Lesions Associated with Human Primary Invasive Nonendocrine Pancreas Cancer. *Cancer Res.* **36**, 2690–2698 (1976).
418. Andea, A., Sarkar, F. & Adsay, V. N. Clinicopathological Correlates of Pancreatic Intraepithelial Neoplasia: A Comparative Analysis of 82 Cases With and 152 Cases Without Pancreatic Ductal Adenocarcinoma. *Mod. Pathol.* **16**, 996–1006 (2003).
419. Pylayeva-Gupta, Y., Lee, K. E., Hajdu, C. H., Miller, G. & Bar-Sagi, D. Oncogenic Kras-Induced GM-CSF Production Promotes the Development of Pancreatic Neoplasia. *Cancer Cell* **21**, 836–847 (2012).
420. McAllister, F. *et al.* Oncogenic kras activates a hematopoietic-to-epithelial IL-17 signaling axis in preinvasive pancreatic neoplasia. *Cancer Cell* **25**, 621–637 (2014).
421. Ying, H. *et al.* Genetics and biology of pancreatic ductal adenocarcinoma. *Genes and Development* vol. 30 355–385 (2016).
422. Hingorani, S. R. *et al.* Trp53R172H and KrasG12D cooperate to promote chromosomal instability and widely metastatic pancreatic ductal adenocarcinoma in mice. *Cancer Cell* **7**, 469–483 (2005).
423. Westphalen, C. B. & Olive, K. P. Genetically engineered mouse models of pancreatic cancer. *Cancer Journal (United States)* vol. 18 502–510 (2012).
424. Rhim, A. D. & Stanger, B. Z. Molecular biology of pancreatic ductal adenocarcinoma progression: Aberrant activation of developmental pathways. in *Progress in Molecular Biology and Translational Science* vol. 97 41–78 (Elsevier B.V., 2010).
425. Yachida, S. *et al.* Distant metastasis occurs late during the genetic evolution of pancreatic cancer. *Nature* **467**, 1114–1117 (2010).
426. Makohon-Moore, A. P. *et al.* Limited heterogeneity of known driver gene mutations among the metastases of individual patients with pancreatic cancer. *Nat. Genet.* **49**, 358–366 (2017).
427. Roe, J. S. *et al.* Enhancer Reprogramming Promotes Pancreatic Cancer Metastasis. *Cell* **170**, 875–888.e20 (2017).
428. Neesse, A. *et al.* Stromal biology and therapy in pancreatic cancer. *Gut* vol. 60 861–868 (2011).
429. Schnittert, J., Bansal, R. & Prakash, J. Targeting Pancreatic Stellate Cells in Cancer. *Trends in Cancer* vol. 5 128–142 (2019).
430. Mekapogu, A. R., Pothula, S. P., Pirola, R. C., Wilson, J. S. & Apte, M. V. Multifunctional role of pancreatic stellate cells in pancreatic cancer. *Ann. Pancreat. Cancer* **2**, 10–10 (2019).
431. Feig, C. *et al.* Targeting CXCL12 from FAP-expressing carcinoma-associated

- fibroblasts synergizes with anti-PD-L1 immunotherapy in pancreatic cancer. *Proc. Natl. Acad. Sci. U. S. A.* **110**, 20212–20217 (2013).
432. Neesse, A. *et al.* Stromal biology and therapy in pancreatic cancer: Ready for clinical translation? *Gut* **68**, 159–171 (2019).
  433. Öhlund, D. *et al.* Distinct populations of inflammatory fibroblasts and myofibroblasts in pancreatic cancer. *J. Exp. Med.* **214**, 579–596 (2017).
  434. Bailey, J. M. *et al.* Sonic hedgehog promotes desmoplasia in pancreatic cancer. *Clin. Cancer Res.* **14**, 5995–6004 (2008).
  435. Olive, K. P. *et al.* Inhibition of Hedgehog signaling enhances delivery of chemotherapy in a mouse model of pancreatic cancer. *Science (80-. )*. **324**, 1457–1461 (2009).
  436. Yauch, R. L. *et al.* A paracrine requirement for hedgehog signalling in cancer. *Nature* **455**, 406–410 (2008).
  437. A Study Evaluating IPI-926 in Combination With Gemcitabine in Patients With Metastatic Pancreatic Cancer - Full Text View - ClinicalTrials.gov. <https://clinicaltrials.gov/ct2/show/NCT01130142>.
  438. Özdemir, B. C. *et al.* Depletion of carcinoma-associated fibroblasts and fibrosis induces immunosuppression and accelerates pancreas cancer with reduced survival. *Cancer Cell* **25**, 719–734 (2014).
  439. Rhim, A. D. *et al.* Stromal elements act to restrain, rather than support, pancreatic ductal adenocarcinoma. *Cancer Cell* **25**, 735–747 (2014).
  440. Di Caro, G. *et al.* Dual prognostic significance of tumour-Associated macrophages in human pancreatic adenocarcinoma treated or untreated with chemotherapy. *Gut* **65**, 1710–1720 (2015).
  441. Liou, G. Y. *et al.* Mutant KRAS–induced expression of ICAM-1 in pancreatic acinar cells causes attraction of macrophages to expedite the formation of precancerous lesions. *Cancer Discov.* **5**, 52–63 (2015).
  442. Zhang, Y. *et al.* Myeloid cells are required for PD-1/PD-L1 checkpoint activation and the establishment of an immunosuppressive environment in pancreatic cancer. *Gut* **66**, 124–136 (2017).
  443. Liou, G. Y. *et al.* Macrophage-secreted cytokines drive pancreatic acinar-to-ductal metaplasia through NF-KB and MMPs. *J. Cell Biol.* **202**, 563–577 (2013).
  444. Weizman, N. *et al.* Macrophages mediate gemcitabine resistance of pancreatic adenocarcinoma by upregulating cytidine deaminase. *Oncogene* **33**, 3812–3819 (2014).
  445. Hume, D. A. & MacDonald, K. P. A. Therapeutic applications of macrophage colony-stimulating factor-1 (CSF-1) and antagonists of CSF-1 receptor (CSF-1R) signaling. *Blood* vol. 119 1810–1820 (2012).
  446. Zhu, Y. *et al.* CSF1/CSF1R blockade reprograms tumor-infiltrating macrophages and improves response to T-cell checkpoint immunotherapy in pancreatic cancer models. *Cancer Res.* **74**, 5057–5069 (2014).
  447. Griesmann, H. *et al.* Pharmacological macrophage inhibition decreases metastasis formation in a genetic model of pancreatic cancer. *Gut* **66**, 1278–1285 (2017).
  448. Nielsen, S. R. *et al.* Macrophage-secreted granulins support pancreatic cancer metastasis by inducing liver fibrosis. *Nat. Cell Biol.* **18**, 549–560 (2016).
  449. Kurahara, H. *et al.* Significance of M2-polarized tumor-associated macrophage in

- pancreatic cancer. *J. Surg. Res.* **167**, e211–e219 (2011).
450. Beatty, G. L. *et al.* CD40 agonists alter tumor stroma and show efficacy against pancreatic carcinoma in mice and humans. *Science (80-. )*. **331**, 1612–1616 (2011).
  451. Pylayeva-Gupta, Y., Lee, K. E., Hajdu, C. H., Miller, G. & Bar-Sagi, D. Oncogenic Kras-Induced GM-CSF Production Promotes the Development of Pancreatic Neoplasia. *Cancer Cell* **21**, 836–847 (2012).
  452. Bayne, L. J. *et al.* Tumor-Derived Granulocyte-Macrophage Colony-Stimulating Factor Regulates Myeloid Inflammation and T Cell Immunity in Pancreatic Cancer. *Cancer Cell* **21**, 822–835 (2012).
  453. Stromnes, I. M. *et al.* Targeted depletion of an MDSC subset unmask pancreatic ductal adenocarcinoma to adaptive immunity. *Gut* **63**, 1769–1781 (2014).
  454. Highfill, S. L. *et al.* Disruption of CXCR2-mediated MDSC tumor trafficking enhances anti-PD1 efficacy. *Sci. Transl. Med.* **6**, 237ra67-237ra67 (2014).
  455. Eash, K. J., Greenbaum, A. M., Gopalan, P. K. & Link, D. C. CXCR2 and CXCR4 antagonistically regulate neutrophil trafficking from murine bone marrow. *J. Clin. Invest.* **120**, 2423–2431 (2010).
  456. Steele, C. W. *et al.* CXCR2 Inhibition Profoundly Suppresses Metastases and Augments Immunotherapy in Pancreatic Ductal Adenocarcinoma. *Cancer Cell* **29**, 832–845 (2016).
  457. Nywening, T. M. *et al.* Targeting both tumour-associated CXCR2+ neutrophils and CCR2+ macrophages disrupts myeloid recruitment and improves chemotherapeutic responses in pancreatic ductal adenocarcinoma. *Gut* **67**, 1112–1123 (2018).
  458. Carstens, J. L. *et al.* Spatial computation of intratumoral T cells correlates with survival of patients with pancreatic cancer. *Nat. Commun.* **8**, (2017).
  459. Stromnes, I. M., Hulbert, A., Pierce, R. H., Greenberg, P. D. & Hingorani, S. R. T-cell Localization, Activation, and Clonal Expansion in Human Pancreatic Ductal Adenocarcinoma. *Cancer Immunol. Res.* **5**, 978–991 (2017).
  460. Daley, D. *et al.*  $\gamma\delta$  T Cells Support Pancreatic Oncogenesis by Restraining  $\alpha\beta$  T Cell Activation. *Cell* **166**, 1485-1499.e15 (2016).
  461. Hartmann, N. *et al.* Prevailing role of contact guidance in intrastromal T-cell trapping in human pancreatic cancer. *Clin. Cancer Res.* **20**, 3422–3433 (2014).
  462. Ene-Obong, A. *et al.* Activated pancreatic stellate cells sequester CD8+ T cells to reduce their infiltration of the juxtatumoral compartment of pancreatic ductal adenocarcinoma. *Gastroenterology* **145**, 1121–1132 (2013).
  463. Beatty, G. L. *et al.* Exclusion of T Cells From Pancreatic Carcinomas in Mice Is Regulated by Ly6Clow F4/80+ Extratumoral Macrophages. *Gastroenterology* **149**, 201–210 (2015).
  464. Chellappa, S. *et al.* Regulatory T cells that co-express ROR $\gamma$ t and FOXP3 are pro-inflammatory and immunosuppressive and expand in human pancreatic cancer. *Oncoimmunology* **5**, (2016).
  465. Liyanage, U. K. *et al.* Prevalence of Regulatory T Cells Is Increased in Peripheral Blood and Tumor Microenvironment of Patients with Pancreas or Breast Adenocarcinoma. *J. Immunol.* **169**, 2756–2761 (2002).
  466. Keenan, B. P. *et al.* A listeria vaccine and depletion of t-regulatory cells activate immunity against early stage pancreatic intraepithelial neoplasms and prolong

- survival of mice. *Gastroenterology* **146**, 1784 (2014).
467. Lawrence, M. S. *et al.* Mutational heterogeneity in cancer and the search for new cancer-associated genes. *Nature* **499**, 214–218 (2013).
  468. Bailey, P. *et al.* Exploiting the neoantigen landscape for immunotherapy of pancreatic ductal adenocarcinoma. *Sci. Rep.* **6**, 1–8 (2016).
  469. Tran, E. *et al.* T-Cell Transfer Therapy Targeting Mutant KRAS in Cancer. *N. Engl. J. Med.* **375**, 2255–2262 (2016).
  470. Singh, S. *et al.* Immune checkpoint inhibitors: a promising anticancer therapy. *Drug Discovery Today* vol. 25 223–229 (2020).
  471. Aglietta, M. *et al.* A phase I dose escalation trial of tremelimumab (CP-675,206) in combination with gemcitabine in chemotherapy-naïve patients with metastatic pancreatic cancer. *Ann. Oncol.* (2014) doi:10.1093/annonc/mdu205.
  472. O'Hara, M. H. *et al.* Abstract CT004: A Phase Ib study of CD40 agonistic monoclonal antibody APX005M together with gemcitabine (Gem) and nab-paclitaxel (NP) with or without nivolumab (Nivo) in untreated metastatic ductal pancreatic adenocarcinoma (PDAC) patients. in *Cancer Research* vol. 79 CT004–CT004 (American Association for Cancer Research (AACR), 2019).
  473. Royal, R. E. *et al.* Phase 2 trial of single agent Ipilimumab (anti-CTLA-4) for locally advanced or metastatic pancreatic adenocarcinoma. *J. Immunother. (Hagerstown, Md. 1997)* **33**, 828–833 (2010).
  474. Brahmer, J. R. *et al.* Safety and activity of anti-PD-L1 antibody in patients with advanced cancer. *N. Engl. J. Med.* **366**, 2455–2465 (2012).
  475. Weiss, G. J. *et al.* A phase Ib study of pembrolizumab plus chemotherapy in patients with advanced cancer (PembroPlus). *Br. J. Cancer* **117**, 33–40 (2017).
  476. Kamath, S. D. *et al.* Ipilimumab and Gemcitabine for Advanced Pancreatic Cancer: A Phase Ib Study. *Oncologist* **25**, e808–e815 (2020).
  477. Overman, M. *et al.* Randomized phase II study of the Bruton tyrosine kinase inhibitor acalabrutinib, alone or with pembrolizumab in patients with advanced pancreatic cancer. *J. Immunother. Cancer* **8**, (2020).
  478. Bockorny, B. *et al.* BL-8040, a CXCR4 antagonist, in combination with pembrolizumab and chemotherapy for pancreatic cancer: the COMBAT trial. *Nat. Med.* 1–8 (2020) doi:10.1038/s41591-020-0880-x.
  479. Xie, C. *et al.* Immune Checkpoint Blockade in Combination with Stereotactic Body Radiotherapy in Patients with Metastatic Pancreatic Ductal Adenocarcinoma. *Clin. Cancer Res.* **26**, 2318–2326 (2020).
  480. O'Reilly, E. M. *et al.* Durvalumab with or Without Tremelimumab for Patients with Metastatic Pancreatic Ductal Adenocarcinoma: A Phase 2 Randomized Clinical Trial. *JAMA Oncol.* **5**, 1431–1438 (2019).

## 2. TIGIT-based therapy induces potent anti-tumor responses in pancreatic cancer

William A Freed-Pastor<sup>1,2‡</sup>, **Laurens J Lambert**<sup>1,3‡</sup>, Zackery A Ely<sup>1,3</sup>, Nimisha B Pattada<sup>1</sup>, Kim L Mercer<sup>1,8</sup>, George Eng<sup>1,4</sup>, Ana P Garcia<sup>1</sup>, Arjun Bhutkar<sup>1</sup>, Jason M Schenkel<sup>1,5</sup>, Lin Lin<sup>1</sup>, William M Rideout III<sup>1</sup>, Roderick T Bronson<sup>1</sup>, Peter MK Westcott<sup>1</sup>, William L Hwang<sup>1,6,7</sup>, Toni Delorey<sup>7</sup>, Devan Phillips<sup>7</sup>, Omer H Yilmaz<sup>1,3,4</sup>, Aviv Regev<sup>1,3,7,8</sup>, Tyler Jacks<sup>1,3,8\*</sup>

<sup>1</sup> David H. Koch Institute for Integrative Cancer Research, Massachusetts Institute of Technology, Cambridge, MA 02139, USA

<sup>2</sup> Department of Medical Oncology, Dana-Farber Cancer Institute, Boston, MA, USA

<sup>3</sup> Department of Biology, Massachusetts Institute of Technology, Cambridge, MA 02139, USA

<sup>4</sup> Department of Pathology, Massachusetts General Hospital, Boston, MA 02114, USA

<sup>5</sup> Department of Pathology, Brigham and Women's Hospital, Boston, MA 02115, USA

<sup>6</sup> Department of Radiation Oncology, Massachusetts General Hospital, Boston, MA 02114, USA

<sup>7</sup> Broad Institute of MIT and Harvard, Cambridge, MA 02142, USA

<sup>8</sup> Howard Hughes Medical Institute, Massachusetts Institute of Technology, Cambridge, MA 02139, USA

\*Corresponding author

‡These authors contributed equally to this work

Author contributions

W.F.P., L.J.L. and T.J. conceived of, designed and directed the study; W.F.P., L.J.L., N.B.P., A.P.G., K.L.M., performed all types of experiments reported in the study; Z.A.E. conducted all scRNA-seq bioinformatic analyses. A.B. conducted TCGA bioinformatic analyses. G.E., O.H.Y. provided patient samples and provided conceptual advice; W.F.P., L.L., N.B.P. performed murine surgeries; G.E., R.T.B. provided pathology expertise; W.F.P., A.P.G., W.M.R. conducted ESC targeting and chimera generation; W.L.H., T.D., D.P. performed scRNA-seq. J.M.S., P.M.K.W., O.H.Y., A.R. and A.B. provided conceptual advice; W.F.P., L.J.L. and T.J. wrote the manuscript with comments from all authors.

## **2.1 Abstract**

Pancreatic adenocarcinoma (PDAC) carries a dismal prognosis and remains largely recalcitrant to immune checkpoint blockade<sup>1-3</sup>. Recent sequencing efforts have demonstrated that the majority of human PDAC contains predicted high affinity neoantigens<sup>4,5</sup>, despite harboring a relatively low mutational burden<sup>6</sup>. Human PDAC is also characterized by CD8<sup>+</sup> tumor-infiltrating lymphocytes (TILs) expressing multiple co-inhibitory receptors, consistent with T cell dysfunction<sup>7</sup>. However, our understanding of the full range of molecular and cellular mechanisms underlying immune evasion in PDAC remains incomplete. Here we demonstrate, using two novel preclinical models of neoantigen-expressing PDAC, that antigen-specific CD8<sup>+</sup> TILs become progressively dysfunctional and facilitate immune evasion in a distinct subset of tumors. Both autochthonous and organoid-based approaches faithfully recapitulate immune editing and/or clearance, consistent with prior studies<sup>4,8</sup>. However, in contrast to observations in



tumors derived from monolayer cell lines<sup>8</sup>, these models uncover a significant subset of neoantigen-expressing pancreatic tumors that successfully evade immune clearance, despite eliciting an antigen-specific immune response. Using multiparameter flow cytometry and single-cell transcriptomic profiling, we observe multiple classes of CD8<sup>+</sup> TILs with markers of dysfunction in murine PDAC, and identify analogous CD8<sup>+</sup> TIL populations in human PDAC. Additionally, we demonstrate that combinatorial targeting of TIGIT/PD-1/CD40 can reinvigorate an effective anti-tumor immune response. This detailed characterization of antigen-specific CD8<sup>+</sup> TILs offers important insights into immune evasion in PDAC, which may be leveraged for rational combination immunotherapy to combat this devastating disease.

## 2.2 Main results

### 2.2.1 Preclinical modeling of immunogenic pancreatic cancer

To model the subset of PDAC patients with predicted high affinity neoantigens, we adapted retrograde pancreatic duct delivery<sup>9</sup> of lentiviruses that did or did not express a defined neoantigen in conjunction with existing Cre/LoxP-regulated genetically engineered mouse models (Figure 1a,b). Pancreatic tumors were induced in either immune-competent *Kras*<sup>LSL-G12D/+</sup>; *Trp53*<sup>fl/fl</sup> (KP) or immune-deficient (KP + CD8 $\alpha$  depletion) mice using lentiviral vectors that expressed Cre recombinase alone ('Cre') or Cre in addition to the T cell antigens (OVA<sub>257-264</sub> [SIINFEKL] and OVA<sub>323-339</sub>) fused to the carboxy terminus of mScarlet<sup>10</sup> ('mScarletSIIN'). Retrograde ductal instillation of Cre-expressing lentivirus led to histologically confirmed pancreatic intraepithelial neoplasia (PanIN)/PDAC formation in ~90% of immune-deficient or immune-competent animals by

9 weeks post-initiation (Extended Data Figure 1a). Similarly, 88% of immune-deficient animals transduced with lentivirus expressing mScarletSIIN developed histologically confirmed PanIN/PDAC by 9 weeks post-initiation (Extended Data Figure 1a). Importantly, 100% of these tumor-bearing animals retained mScarlet positivity within PanIN/PDAC lesions (Figure 1c,e and Extended Data Figure 1a,c). In contrast, less than 50% of immune-competent animals transduced with lentivirus expressing mScarletSIIN developed PanIN/PDAC by 9 weeks post-initiation, suggesting that antigen-expressing cells were cleared by CD8<sup>+</sup> T cells during tumor development (Figure 1d,f and Extended Data Figure 1a). Of those tumors that did ultimately develop in immune-competent animals transduced with mScarletSIIN, 80% exhibited lack of tumor-associated mScarlet fluorescence, as determined by both fluorescence stereomicroscopy and immunohistochemical analysis (Figure 1d,f and Extended Data Figure 1c), highly suggestive of immune editing. Of note, a subset (~10%) of immune-competent animals transduced with mScarletSIIN developed macroscopic tumors that retained mScarlet positivity, suggestive of immune evasion (Figure 1d,f and Extended Data Figure 1c). No differences in tumor burden was observed in animals transduced with Cre or mScarletSIIN lentivirus, with or without CD8 $\alpha$ -depletion (Extended Data Figure 1b). Delivery of mScarletSIIN induced a robust CD8<sup>+</sup> T cell response that facilitated the tracking and immunophenotyping of antigen-specific (CD44<sup>hi</sup>H-2K<sup>b</sup>-SIINFEKL<sup>+</sup> [hereafter referred to as 'CD44<sup>hi</sup>Tetramer<sup>+</sup>']) CD8<sup>+</sup> T cells both peripherally and within the tumor microenvironment (Figure 1g-i). Intriguingly, we observed that antigen-specific CD8<sup>+</sup> TILs isolated from 'immune evasive' tumors displayed co-expression of multiple co-inhibitory receptors, suggestive of T cell dysfunction (CD44<sup>hi</sup>Tetramer<sup>+</sup>PD1<sup>+</sup>TIGIT<sup>+</sup> (Extended Data

Figure 1d). However, the rarity of these 'immune evasive' autochthonous tumors precluded a more extensive analysis of T cell phenotypes in this model.

# Figure 1

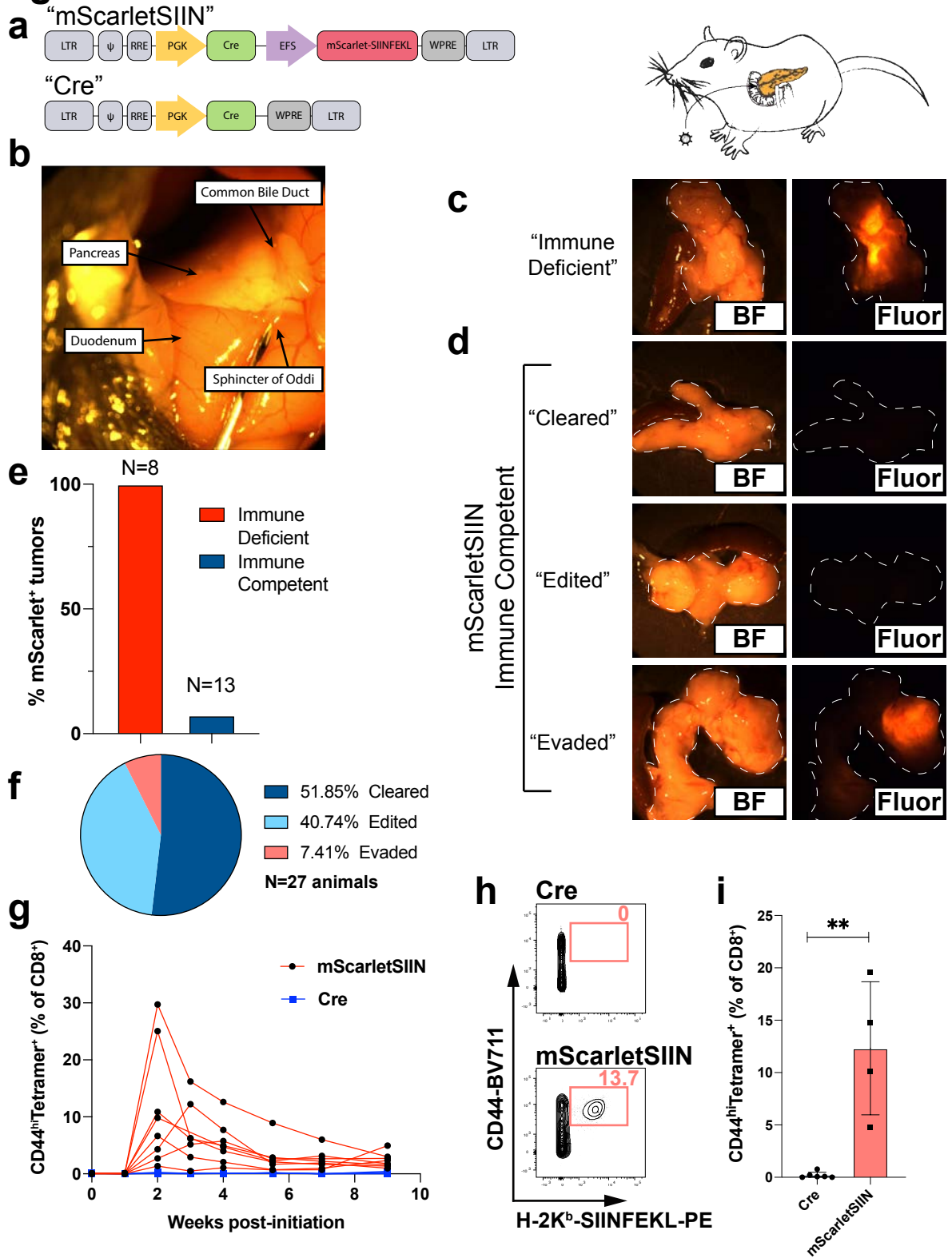


**Figure 1. Divergent tumor and antigenic outcomes in autochthonous immunogenic pancreatic cancer.**

**a**, Lentiviral vectors used to generate immunogenic ('mScarletSIIN') and control ('Cre') autochthonous PDAC. **b**, Retrograde pancreatic duct instillation of lentivirus. **c**, Brightfield (left) and fluorescence stereomicroscopic (right) images of representative 9-week tumors generated using mScarletSIIN in CD8 $\alpha$ -depleted animals. **d**, Brightfield (left) and fluorescence stereomicroscopic (right) images of representative tumor and antigenic outcomes ("cleared", "edited", "evaded") using mScarletSIIN in immune-competent animals. **e**, Percent of mScarlet-positive tumors as assessed by fluorescence stereomicroscopy at 9 weeks post-initiation (n=8 immune-deficient; n=13 immune-competent). **f**, Quantification of tumor and antigenic outcomes in mScarletSIIN immune-competent animals (n=27). **g**, Longitudinal tracking of antigen-specific (CD44<sup>hi</sup>Tetramer<sup>+</sup>) CD8<sup>+</sup> T cells in the peripheral blood of Cre (n=6) and mScarletSIIN (n=8) animals. **h**, Representative flow cytometric plots and **i**, quantification of CD44<sup>hi</sup>Tetramer<sup>+</sup> (gated on single cells/live/CD8<sup>+</sup> lymphocytes) within early-stage (3 week) pancreatic lesions (scatter dot plots; mean +/- SD). Statistical analyses: **i**, two-sided Mann-Whitney test (\*\* P<0.01).

**2.2.2 Immune evasive pancreatic tumors retain antigen expression and presentation**

As immune editing in cancer can occur through epigenetic silencing or genetic deletion of the locus containing the neoantigen<sup>11</sup>, we developed a genetic approach in which SIINFELK, linked to mScarlet on a polycistronic transcript, was knocked into the *Hipp11* safe harbor locus<sup>12</sup> using CRISPR/Cas9-assisted homology-directed repair (HDR) (Figure 2a). Following PCR and Southern blot validation of correctly targeted KP murine embryonic stem cell (mESC) clones (Extended Data Figure 2), we derived a homozygous-targeted pancreatic organoid line from chimeric animals, which maintained robust and uniform mScarletSIIN expression *ex vivo* ('KP;H11-SIIN') (Figure 2b and Extended Data Figure 2). Consistent with our observations in autochthonous immunogenic pancreatic cancer, orthotopic transplantation of genetically-defined KP;H11-SIIN pancreatic organoids into immune-deficient recipients resulted in 100% mScarlet-positive tumor formation after 8 weeks (Figure 2c). Conversely, orthotopic transplantation into immune-competent recipients resulted in 40% immune clearance (mScarlet-negative and histologically normal pancreas; termed 'non-progressor') and 50% immune evasion (mScarlet-positive macroscopic tumor; termed 'progressor'). However, we observed no incidence of macroscopic tumors that had lost antigen

expression, as assessed by stereomicroscopy, immunohistochemical staining and tumor-derived organoid culture (Figure 2d-e, Extended Data Figure 3a,b and Extended Data Figure 4a). In addition, we observed a subset (10%) of immune-competent recipients that retained small areas of mScarlet-positivity in the absence of macroscopic tumor formation (termed 'intermediate'), potentially reflective of a state of immune equilibrium (Figure 2d,e). In line with this hypothesis, we observed that progressor tumors were significantly smaller than tumors that were never exposed to an immune selective pressure ( $P < 0.01$ , Mann-Whitney), potentially suggestive of a prior state of immune equilibrium before ultimate immune escape (Figure 2f). We longitudinally tracked the antigen-specific CD8<sup>+</sup> T cell response in animals transplanted with either KP (no neoantigen) or KP;H11-SIIN pancreatic organoids and demonstrate that only KP;H11-SIIN recipients mount a SIINFEKL-specific CD8<sup>+</sup> T cell response. Furthermore, the magnitude and kinetics of the peripheral response (peaking at 3 weeks post-initiation) are indistinguishable between non-progressor and progressor animals ( $P = n.s.$ , Mann-Whitney; Extended Data Figure 3c). Immunohistochemical and flow cytometric analyses of late-stage progressor tumors revealed an ongoing CD8<sup>+</sup> T cell response, with some intratumoral areas displaying T cell exclusion and others with a high degree of infiltration (Extended Data Figure 3a,d).

In order to characterize the potential mechanisms of immune escape employed by progressor tumors, we re-derived pancreatic tumor organoids from both progressor and immune-deficient animals for *ex vivo* characterization (Extended Data Figure 4). After purifying the malignant compartment through Nutlin-3a selection (see *Methods*), we performed flow cytometry to characterize surface expression of MHC Class I (H-2K<sup>b</sup>, H-

2D<sup>b</sup>), MHC Class II and PD-L1 on tumor-derived organoids and assayed their responsiveness to interferon- $\gamma$  stimulation. None of the progressor tumors exhibited loss of antigen expression, H-2K<sup>b</sup> MHC Class I expression or interferon- $\gamma$  sensitivity by this assay (Figure 2g, Extended Data Figure 4a-d). To further establish that progressor tumor cells retained full capacity to process and present the SIINFEKL neoantigen on their cell surface, we established an organoid/CD8<sup>+</sup> T cell co-culture system. Progressor or immune-deficient tumor-derived organoids were co-embedded in a three-dimensional extracellular matrix with activated 'OT-I' CD8<sup>+</sup> T cells (transgenic for a TCR specific for SIINFEKL in the context of H-2K<sup>b</sup>)<sup>13</sup>. Both progressor and immune-deficient organoids underwent T cell-dependent killing across multiple effector: target (E:T) ratios (Figure 2h and Extended Data Figure 4e,f), further demonstrating that progressor tumors retain antigen expression and antigen presentation capacity. Additionally, these results suggest that progressor tumors might employ non-cell autonomous mechanisms to mediate immune escape *in vivo*.

To characterize the tumor immune microenvironment of progressor tumors, we performed multiparameter flow cytometric analysis of CD45<sup>+</sup> immune cell subsets, isolated directly from KP;H11-SIIN progressor tumors or KP tumors. In line with observations from both human PDAC and the 'KPC' mouse model of PDAC<sup>14,15</sup>, we observed a strong myeloid predominance (neutrophils/macrophages) and a paucity of dendritic cells in both KP and KP;H11-SIIN tumors (Extended Data Figure 5). While there was considerable inter-tumoral heterogeneity, no reproducible differences were found between KP;H11-SIIN and KP tumors in terms of relative abundance of neutrophils (CD11b<sup>+</sup>Ly6G<sup>+</sup>), macrophages (F4/80<sup>+</sup>CD64<sup>+</sup>), monocytes (CD11b<sup>+</sup>Ly6C<sup>+</sup>), B cells

(CD19<sup>+</sup>MHCII<sup>+</sup>), dendritic cells (CD11c<sup>+</sup>MHCII<sup>+</sup>) or dendritic cell subsets (cDC1 [XCR1<sup>+</sup>] or cDC2 [CD172a<sup>+</sup>]) (Extended Data Figure 5).



# Figure 2

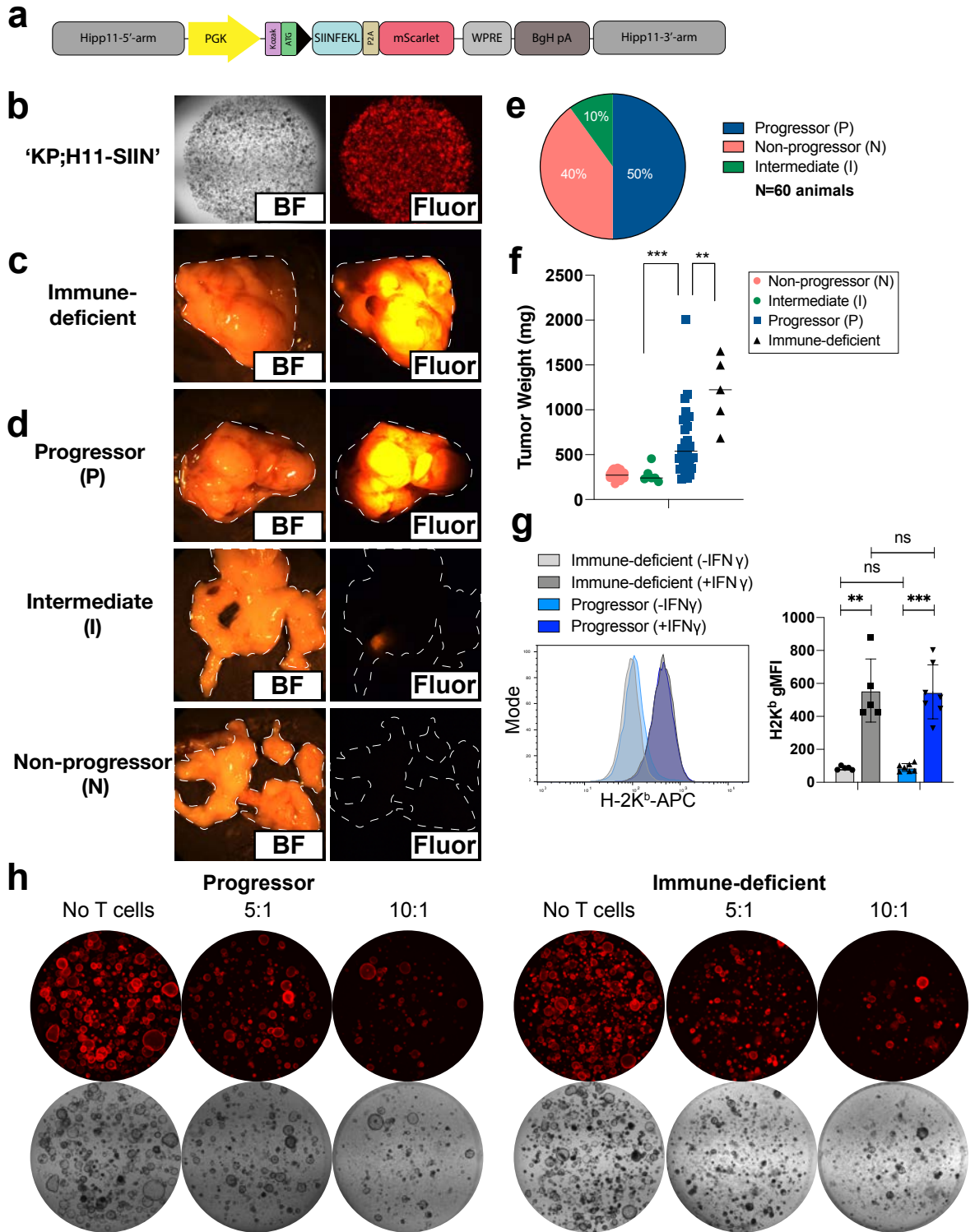


**Figure 2. Orthotopic transplant of immunogenic organoids offers a robust platform to assess immune clearance and immune evasion in the same tissue and antigenic context.**

**a**, 'Hipp11-mScarletSIIN' genomic locus after CRISPR/Cas9-assisted homology-directed repair and Cre recombination. **b**, Brightfield (left) and fluorescent (right) images of *Kras*<sup>G12D/+</sup>; *Trp53*<sup>-/-</sup>; *Hipp11*<sup>mScarletSIIN</sup> ('KP;H11-SIIN') pancreatic organoids. Brightfield (left) and fluorescence stereomicroscopic (right) images of representative 8-week tumors following orthotopic transplantation of KP;H11-SIIN pancreatic organoids into **c**, immune-deficient (*Rag2*<sup>-/-</sup>) animals or **d**, immune-competent animals, depicting the range of tumor and antigenic outcomes in this context ('progressor', 'intermediate', 'non-progressor'). **e**, Quantification of tumor and antigenic outcomes 8-9.5 weeks post-orthotopic transplantation of KP;H11-SIIN pancreatic organoids into immune-competent animals (n=60). **f**, Tumor/pancreas weights 8-9.5 weeks post-orthotopic transplantation of KP;H11-SIIN pancreatic organoids (n=5 *Rag2*<sup>-/-</sup>; n=24 'non-progressor'; n=6 'intermediate', n=30 'progressor'; horizontal bars represent median). **g**, Flow cytometric profiling of surface MHC-I (H-2K<sup>b</sup>) on tumor-derived pancreatic organoids from progressor (n=7) or immune-deficient (n=5) animals with or without interferon- $\gamma$  stimulation, representative histogram (left) or geometric mean fluorescence intensity (gMFI) scatter plots (mean +/- SD; right). **h**, Representative images of Day 5 tumor-derived pancreatic organoids from progressor or immune-deficient animals either in the absence (no T cells) or presence of pre-activated OT-I CD8<sup>+</sup> T cells at 5:1 or 10:1 Effector:Target (E:T) ratios. Statistical analyses: **f,g**, two-sided Mann-Whitney test (n.s. P=non-significant, \*\* P<0.01, \*\*\* P<0.001).

### 2.2.3 Multiple classes of antigen-specific CD8<sup>+</sup> TILs within immune evasive pancreatic tumors

To further elucidate potential mechanisms of immune evasion, we performed single-cell transcriptomic profiling (scRNA-seq)<sup>16</sup> on antigen-specific (CD8<sup>+</sup>CD44<sup>hi</sup>Tetramer<sup>+</sup>) TILs isolated from progressor tumors. After quality control filtering (see *Methods*), we clustered 482 antigen-specific CD8<sup>+</sup> TILs and computed differential gene expression between four distinct clusters (Figure 3a and Extended Data Figure 6b-e). Differential gene expression between transcriptomic clusters suggested distinct cell states within the antigen-specific CD8<sup>+</sup> T cell compartment (Figure 3b). The largest cluster (cluster 0) was enriched for several genes associated with both CD8<sup>+</sup> T cell activation and/or exhaustion (*Pdcd1*, *Havcr2*, *Lag3*, *Tox*, *Gzmb*) (Figure 3d and Extended Data Figure 6c). A smaller cluster (cluster 3) was enriched for hallmarks of CD8<sup>+</sup> T regulatory cells (*Klra6*, *Klra7*, *Ly6c2*) (Figure 3c and Extended Data Figure 6e), previously described in both autoimmunity<sup>17,18</sup> and cancer<sup>19</sup>. Two clusters (clusters 1 and

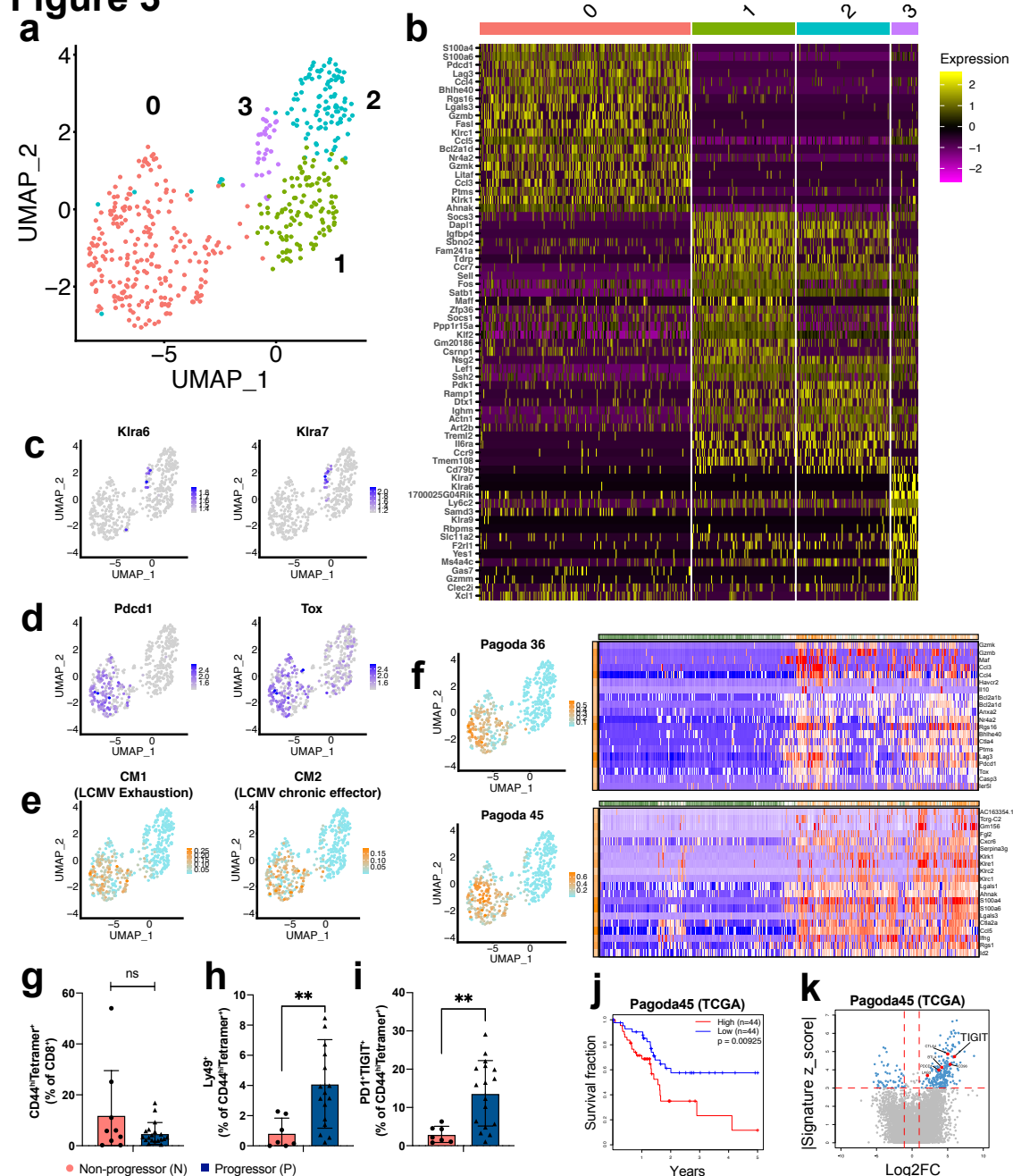
2) were enriched for markers of naïve/memory CD8<sup>+</sup> T cells (*Sell*, *Ccr7*, *Klf2*, *Tcf7*), potentially reflecting one or more aberrant memory-like cell states (Extended Data Figure 6d). To further characterize this data, we generated and plotted scores for gene modules (see *Methods*) derived from CD8<sup>+</sup> T cells in defined cell states from both acute and chronic lymphocytic choriomeningitis virus (LCMV)<sup>20</sup> and B16 melanoma<sup>19</sup>. Intriguingly, cluster 0 was enriched for ‘T cell exhaustion’ as well as ‘chronic effector’ signatures, previously identified in a viral model of T cell dysfunction<sup>20</sup> (Figure 3e and Extended Data Figure 7a-b). Likewise, the mixed ‘activation/dysfunction’ gene module previously identified in B16 melanoma<sup>19</sup> was overrepresented in cluster 0 (Extended Data Figure 7c). Additionally, clusters 1 and 2 expressed a transcriptional program with a high degree of overlap with the ‘naïve/memory’ gene module from B16 melanoma<sup>19</sup> (Extended Data Figure 7c), but interestingly also shared overlap with an effector-biased module from acute LCMV<sup>20</sup> (‘AM13’; Extended Data Figure 7b), further suggestive of an aberrant memory-like program. We then employed flow cytometric profiling to validate the presence of these cell populations within antigen-specific CD8<sup>+</sup> TILs. Consistent with the hypothesis that most antigen-specific CD8<sup>+</sup> TILs are dysfunctional within progressor tumors, we observed a decrease in their proliferative capacity (marked by Ki67<sup>+</sup>) (Extended Data Figure 8c). Both CD44<sup>hi</sup>Tetramer<sup>+</sup>PD1<sup>+</sup>TIGIT<sup>+</sup> and CD44<sup>hi</sup>Tetramer<sup>+</sup>Ly49<sup>+</sup> populations were disproportionately represented in late-stage progressor tumors compared to non-progressors (Figure 3g-i and Extended Data Figure 8a,b). As co-expression of co-inhibitory receptors is thought to distinguish a more dysfunctional phenotype from activation<sup>21,22</sup>, we sought to examine antigen-specific CD8<sup>+</sup> TILs from early-stage intermediate and progressor tumors (week 5). We observed

increased co-expression of PD1<sup>+</sup>TIGIT<sup>+</sup>, PD1<sup>+</sup>TIM3<sup>+</sup>, and PD1<sup>+</sup>LAG3<sup>+</sup> in intermediate and progressor tumors (Extended Data Figure 8a,b), suggesting that the acquisition of a dysfunctional phenotype may occur early in tumor development<sup>22</sup>. In order to more deeply characterize these antigen-specific CD8<sup>+</sup> TILs, we employed Pathway and Gene Set Overdispersion Analysis (PAGODA)<sup>23</sup> to derive *de novo* gene set signatures from scRNA-seq data. This identified three gene set signatures that overlaid clusters 1 and 2 (Pagoda30) and cluster 0 (Pagoda36, Pagoda45) (Figure 3f and Extended Data Figure 7e), further highlighting the heterogeneity within the antigen-specific CD8<sup>+</sup> T cell compartment in immune evasive tumors.

To determine if human PDAC harbors analogous classes of CD8<sup>+</sup> T cells, we took two parallel approaches. First, we isolated and performed flow cytometry on CD8<sup>+</sup> TILs from freshly resected pancreatic adenocarcinoma specimens. Of the 13 specimens tested, 9 had sufficient (>200) CD8<sup>+</sup> TILs for further immunophenotyping. In line with previous reports<sup>7</sup>, we demonstrate that the majority (64-96%) of CD8<sup>+</sup> TILs are antigen-experienced (CD45RO<sup>+</sup>TCF1<sup>lo</sup>) and are similarly enriched for co-expression of multiple co-inhibitory receptors (PD1<sup>+</sup>TIGIT<sup>+</sup>, PD1<sup>+</sup>LAG3<sup>+</sup>, and PD1<sup>+</sup>TIM3<sup>+</sup>), suggestive of a state of T cell dysfunctionality in the tumor microenvironment (Extended Data Figure 9a-c).

Next, we explored the prognostic value of our *de novo* gene signatures in the human pancreatic cancer (PAAD) cohort from the Cancer Genome Atlas (TCGA)<sup>24</sup>. Individual patient tumors were stratified according to their bulk RNA-seq gene expression correlation with Pagoda30, Pagoda36, and Pagoda45 gene modules. We observed no prognostic impact of Pagoda30 (*data not shown*), whereas high-scoring patients (upper quartile, n=44), whose gene expression profiles correlated with either

Pagoda36 or Pagoda45, exhibited significantly worse survival compared to patients whose gene expression profiles were least correlated with the respective signatures (lower quartile, n=44) (Figure 3j and Extended Data Figure 9d). Furthermore, we utilized TCGA gene expression data to elucidate transcriptomic signatures that distinguish high-versus low-scoring patient cohorts and to query co-inhibitory receptor expression in relation to our *de novo* gene signatures. As Pagoda36 is defined by expression of genes canonically associated with T cell exhaustion, it is perhaps not surprising that we observed a strong correlation of multiple co-inhibitory receptors with the Pagoda36 signature (Extended Data Figure 9e). Interestingly, *TIGIT* expression in human PDAC was the most highly correlated co-inhibitory receptor to both Pagoda45 and Pagoda36 transcriptomic signatures (Figure 3k and Extended Data Figure 9e), suggesting that TIGIT may represent a critical immune checkpoint in human PDAC.

**Figure 3****Figure 3. Distinct classes of antigen-specific CD8<sup>+</sup> TILs isolated from immune evasive PDAC.**

**a**, UMAP projection of scRNA-seq of CD8<sup>+</sup>CD44<sup>hi</sup>Tetramer<sup>+</sup> TILs from progressor tumors. **b**, Heatmap of differentially expressed genes between clusters with selected genes highlighted. UMAP projections of the gene expression for **c**, *Klra6* (Ly49F), *Klra7* (Ly49G2). **d**, *Pdcd1* (PD-1), *Tox* (Tox). **e**, UMAP projections of the gene module expression for "LCMV T cell exhaustion" (CM1) and "LCMV T cell chronic effector" (CM2). **f**, Heatmap and UMAP projections of the expression for Pagoda signatures (Pagoda36, Pagoda45). **g**, CD8<sup>+</sup> TIL analysis of late-stage (week 9.5) non-progressor or progressor animals. **h**, CD44<sup>hi</sup>Tetramer<sup>+</sup>Ly49F/G2<sup>+</sup> CD8<sup>+</sup> TILs **i**, CD44<sup>hi</sup>Tetramer<sup>+</sup>PD1<sup>+</sup>TIGIT<sup>+</sup> CD8<sup>+</sup> TILs in late-stage (week 9.5) non-progressor or progressor animals (**g-i**, gated on single/lymphocytes/CD45<sup>+</sup>, live, all three scatter plots showing mean +/- SD). **j**, Kaplan-Meier survival analysis of upper ("High", red) and lower ("Low", blue) quartile TCGA PAAD patients (n=44 each) stratified by expression correlation with the murine-derived Pagoda45 gene signature. **k**, All genes ranked by absolute z-score in the human TCGA PAAD gene signature between most and least Pagoda45-correlated cohorts (y-axis) compared to the magnitude of their fold change (x-axis, log2 fold change (Log2FC) of most/least correlated cohort expression). Selected co-inhibitory receptors highly upregulated in most-correlated tumors are highlighted in red. Statistical analyses: **g-i**, two-sided Mann-Whitney test (n.s. P=non-significant, \*\* P<0.01), **j**, log-rank test (P=0.00925).

#### 2.2.4 TIGIT-directed combination immunotherapy as a novel therapeutic approach in PDAC

While CTLA-4 and/or PD-L1 inhibition have failed to show clinical benefit in human PDAC<sup>1-3</sup>, recent reports have highlighted the clinical promise of combining anti-PD-1 antibodies with CD40 agonistic antibodies and cytotoxic chemotherapy<sup>25</sup>. In order to rationally guide possible combination immunotherapies in PDAC, we queried protein expression of the canonical ligands for co-inhibitory receptors (PD-L1 [PD-1], Galectin 9 [TIM3], CD155/PVR [TIGIT])<sup>26</sup>, using human PDAC tissue microarrays<sup>27,28</sup>. Consistent with prior reports<sup>29</sup>, we observed little to no expression of PD-L1 in human PDAC, whereas both Galectin 9 and CD155/PVR were expressed at “high/medium” levels on 40% and 50% of tumors, respectively (Figure 4a,b).

Given the elevated expression of CD155 in human PDAC and the strong correlation of *TIGIT* gene expression with Pagoda36 and Pagoda45, we evaluated TIGIT-directed combination immunotherapy as a novel therapeutic approach for PDAC. Following orthotopic transplantation of KP;H11-SIIN pancreatic organoids into immune-competent animals and confirmation of tumor establishment and progression (at 6 weeks post-initiation), animals were randomized by baseline tumor volume to an isotype control arm or one of five therapeutic arms (anti-PD-1, anti-TIGIT, anti-PD-1 + CD40 agonist, anti-TIGIT + CD40 agonist, anti-TIGIT + anti-PD-1 + CD40 agonist) for treatment over 4 weeks (Figure 4c). As expected, isotype control-treated tumors grew unabated (Figure 4d,e), as assessed by serial high-resolution ultrasound imaging. Consistent with clinical observations, anti-PD-1 monotherapy had no appreciable impact on tumor progression (0% objective response rate [ORR]) (Figure 4d,f). Similarly, both anti-TIGIT monotherapy

(0% ORR) and anti-TIGIT + CD40 agonist (9% ORR) demonstrated minimal clinical efficacy (Figure 4d,g,i). In line with the early clinical promise of anti-PD-1 + CD40 agonist antibodies observed in clinical trials<sup>25</sup>, we observed an 18% ORR with anti-PD-1 + CD40 agonist therapy (Figure 4d,h). Excitingly, in triple therapy-treated animals (anti-TIGIT + anti-PD-1 + CD40 agonist), we observed an increase in objective response and disease control rates (40% ORR, 70% DCR) with 20% durable complete responses (CR) (Figure 4d,j). Notably, all therapeutic arms were well tolerated as assessed by body status and weight (Extended Data Figure 10). After completion of the predefined treatment period, many initial responders rapidly progressed. However, complete responders remained durable following therapy discontinuation [ongoing CRs >12 weeks after stopping therapy at the time of data cut-off] (Extended Data Figure 10). This implies that continuous therapy may be required for all but complete responders to achieve durable benefit. Because all three of these targets have therapeutic monoclonal antibodies in clinical development or are already approved for clinical use, anti-TIGIT+anti-PD-1+CD40 agonist combination immunotherapy may represent a promising approach for rapid clinical evaluation.



# Figure 4

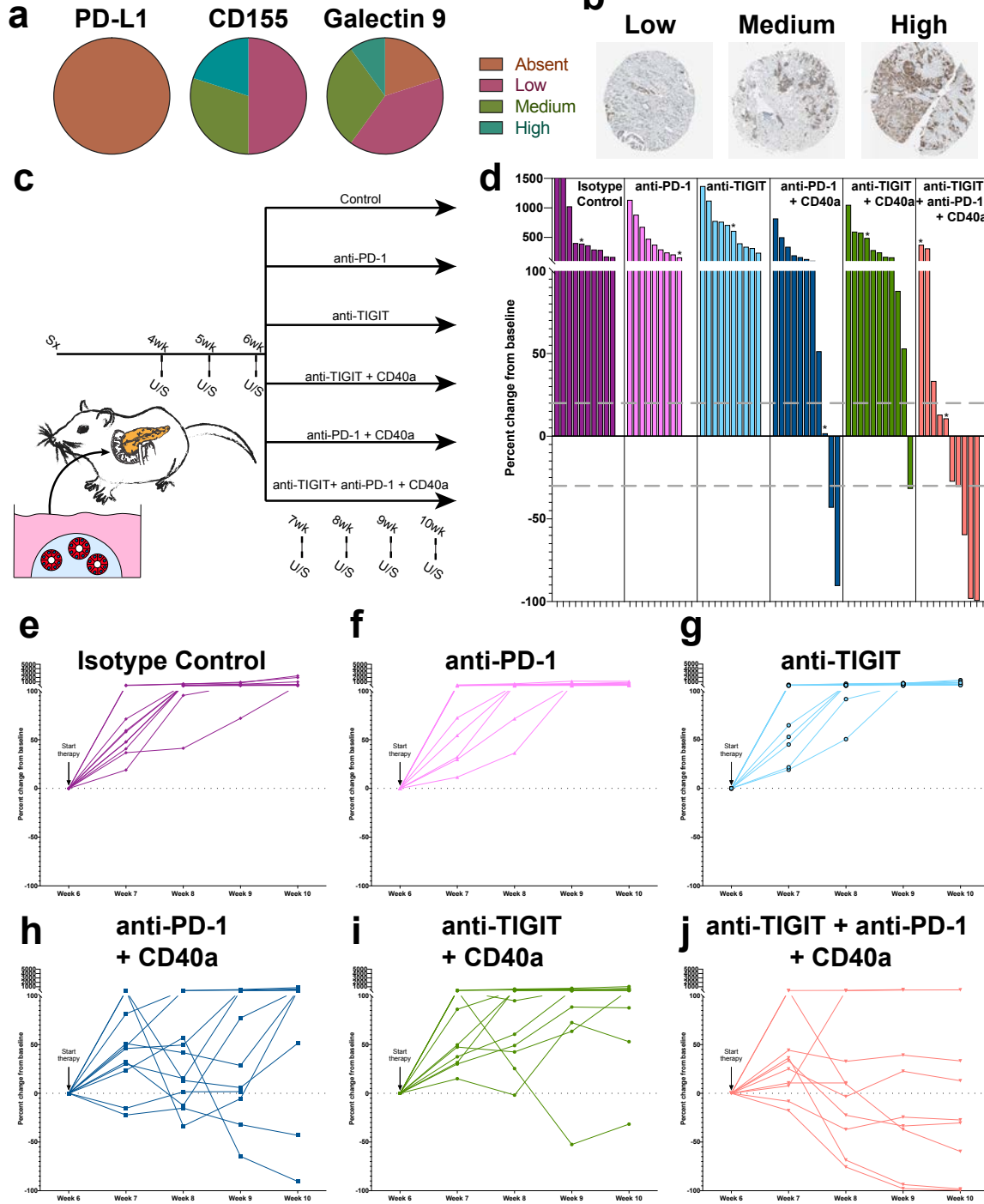


**Figure 4. TIGIT-targeting combination immunotherapy reinvigorates T cells to elicit anti-tumor responses.**

**a**, Quantification of ligand expression (PD-L1, CD155, Galectin 9) on human pancreatic cancer tissue microarrays (Image credit: Human Protein Atlas; image/gene/data available from v19.22.proteinatlas.org). **b**, Representative images of 'Low', 'Medium', 'High'-expressing CD155/PVR human PDAC (Image credit: Human Protein Atlas; image/gene/data available from v19.22.proteinatlas.org; <https://www.proteinatlas.org/ENSG0000073008-PVR/pathology/pancreatic+cancer#Quantity>). **c**, Schematic of preclinical trial design (n=9-11 per arm). **d**, Waterfall plots of treatment response after 4 weeks of therapy. **e-j**, Spider plots of treatment response during therapy. \*represents animal that died prior to 4-week analysis. U/S = ultrasound.

## 2.3 Discussion

While pancreatic tumorigenesis is initiated by genetic events, the tumor immune microenvironment plays an instrumental role in shaping tumor progression. Our present study using two orthogonal preclinical models of neoantigen-expressing pancreatic cancer reveals that PDAC undergoes all three phases of immunosurveillance<sup>30</sup>. Notably, this stands in contrast to a recent report using an antigen-expressing PDAC model that lacks detectable immune editing/clearance and paradoxically displays accelerated tumor progression as a consequence of antigen expression<sup>15</sup>. Future studies will be needed to address the potential role of model-specific differences in these results. Importantly, our data reveal that a subset of pancreatic cancer evades immune clearance despite continued expression of a high affinity neoantigen, and furthermore suggest that immune evasion in pancreatic cancer can be non-cell autonomous. Additionally, using high-resolution profiling, we uncovered multiple subsets of antigen-specific CD8<sup>+</sup> TILs within immune-evasive tumors. This highlights an underappreciated heterogeneity within the antigen-specific TIL compartment, including cells in an exhausted state, chronic-effector state, memory-like state, and a state reminiscent of CD8<sup>+</sup> T regulatory cells well-described in autoimmunity<sup>17</sup>.

Immune modulation has emerged as a promising therapeutic strategy for numerous tumor types. However, it is likely that tissue of origin, histologic subtype and/or genetic alterations might dictate disparate mechanisms of immune evasion<sup>31,32</sup>. Here we uncover a unique dependency on the TIGIT/CD155 axis, when targeted in conjunction with PD-1+CD40, for continued immune evasion in PDAC. As CD155/PVR has been reported to be upregulated by oncogenic KRAS<sup>33</sup>, it is tempting to speculate that the

TIGIT/CD155 axis might represent a critical immune checkpoint in additional KRAS-driven tumors. While our data implicates additional immune checkpoints for preclinical evaluation, combinatorial targeting of TIGIT/PD-1/CD40 represents a promising approach for rapid clinical translation.

## **2.4 Acknowledgements**

We thank the entire Jacks laboratory with specific thanks to N. Sacks, A. Jaeger, M. Burger and D. Canner for helpful discussions and technical assistance. We thank K. Yee, J. Teixeira, K. Anderson, M. Magendantz for administrative support. This work was supported by the Howard Hughes Medical Institute, NCI Cancer Center Support Grant P30-CA1405, the Lustgarten Foundation Pancreatic Cancer Research Laboratory at MIT, DFHCC SPORE in Gastrointestinal Cancer Career Enhancement Award (W.F.P.), the Stand Up To Cancer-Lustgarten Foundation Pancreatic Cancer Interception Translational Cancer Research Grant (Grant Number: SU2C-AACR-DT25-17, W.F.P, T.J.) and the Stand Up To Cancer Golden Arrow Early Career Scientist Award (GA-6182, W.F.P.). Stand Up To Cancer is a program of the Entertainment Industry Foundation. Research grants are administered by the American Association for Cancer Research, the scientific partner of SU2C. We thank the Koch Institute Swanson Biotechnology Center for technical support, specifically the Flow Cytometry, Histology, Preclinical Modeling, Imaging & Testing and Integrative Genomics & Bioinformatics core facilities.

## 2.5 Methods

### Mice

All animal studies described in this study were approved by the MIT Institutional Animal Care and Use Committee. All animals were maintained on a pure C57BL/6J genetic background. Generation of *Kras*<sup>LSL-G12D/+</sup> and *p53*<sup>flox/flox</sup> mice has previously been described<sup>34,35</sup>. *OT-I* TCR transgenic mice have been previously described<sup>13</sup>.

### Lentiviral constructs

“Lenti-PGK-Cre” and “Lenti-PGK-Cre-EFS-mScarletSIIN” were generated using gBlocks (IDT) and Gibson assembly<sup>36</sup>. Detailed cloning strategies and primer sequences are available on request. All vectors with detailed maps and sequences will be deposited into Addgene.

### Molecular cloning of targeting vector and CRISPR/Cas9-assisted targeting of H11;SIIN

The “H11-mScarletSIIN” targeting vector was generated using gBlocks (IDT) and Gibson assembly<sup>36</sup>. “U6-sgfiller-eCas9-T2A-BlastR” was generated using Gibson assembly. In order to insert sgRNAs, the vector was digested with FastDigest Esp3I (Thermo Fisher) and ligated with BsmBI-compatible annealed oligonucleotides. sgRNAs were designed using Benchling<sup>37</sup>, which was also used to predict potential off-target sites. All vectors with detailed maps and sequences will be deposited into Addgene.

### mESC line generation

“KP\*1”, a C57BL/6J *Kras*<sup>LSL-G12D/+</sup>; *Trp53*<sup>flox/flox</sup> (KP) murine embryonic stem cell line, was generated by crossing a hormone-primed C57BL/6J *Trp53*<sup>flox/flox</sup> female with a C57BL/6J *Kras*<sup>LSL-G12D/+</sup>; *Trp53*<sup>flox/flox</sup> male. At 3.5 days post-coitum, blastocysts were flushed from the uterus, isolated, and cultured on a mouse embryonic fibroblast (MEF) feeder layer in ESC media+LIF+2i [Knockout DMEM (Gibco), 15% FBS (Hyclone), 1% NEAA (Sigma-Aldrich), 2 mM Glutamine (Gibco), 0.1 mM β-mercaptoethanol (Sigma-Aldrich) 50 IU Penicillin, 50 IU Streptomycin, 1000 U/mL LIF (Amsbio), 3 μM CHIR99021 (AbMole), 1 μM PD0325901(AbMole)]. After 5-7 days in culture the outgrown inner cell mass was isolated, trypsinized and re-plated on a fresh MEF layer. ES cell lines were genotyped for *Kras*<sup>LSL-G12D/+</sup>; *Trp53*<sup>flox/flox</sup>, and *Zfy* (Y-chromosome specific). Primer sequences available upon request. ES cell lines were tested for pluripotency by injection into host blastocysts from albino mice to generate chimeric mice.

### **ESC targeting**

Briefly, DNA mixes (1:1 mix of “U6-H11sg-eCas9-T2A-BlastR”: “H11-mScarletSIIN” targeting vector) were ethanol precipitated prior to DNA (1 μg) transfection of approximately 3\*10<sup>5</sup> KP\*1 mESCs in a gelatin-coated 24-well plate using Lipofectamine 2000 (Thermo Fisher) according to the manufacturer instructions. mESCs were selected with Blasticidin (6 μg/mL) for 2 days, starting 36 hr post-transfection before low-density replating on MEF feeder lines in the absence of Blasticidin. Large mESC colonies were manually picked using a stereomicroscope, expanded and evaluated for correct integration using PCR with primers spanning both 5’ and 3’ homology arms (primer sequences available on request). Correct clones by PCR evaluation were evaluated

using Southern blot analysis. Briefly, genomic DNA was digested with NsiI-HF (NEB) overnight. Digestions were electrophoresed on 0.7% agarose gels and blotted to Amersham Hybond XL nylon membranes (GE Healthcare). Samples were probed with <sup>32</sup>P-labeled “H11 5’ external”, “H11 3’ external” and “internal” probes applied in Church buffer<sup>38</sup> (annotated in Extended Data Figure 2; probe sequences available on request).

Correctly targeted clones were injected into albino C57BL/6J blastocysts. Chimerism was assessed by coat color. Pancreatic organoids were isolated from chimeric animals and “donor” organoids were purified from the host pancreas using 72 hr of puromycin (6 µg/mL) selection (leveraging the presence of the puromycin resistance gene within the LSL cassette upstream of *KRAS*<sup>G12D</sup>)<sup>34</sup>.

### **Lentiviral production/titering**

Lentiviral plasmids and packaging vectors were prepared by using endo-free maxiprep kits (QIAGEN). Lentiviruses were produced by co-transfection of HEK-293 cells with lentiviral constructs plus packaging vectors: PsPax2 (psPAX2 was a gift from Didier Trono (Addgene plasmid # 12260 ; <http://n2t.net/addgene:12260> ; RRID:Addgene\_12260) and Pmd2.G (pMD2.G was a gift from Didier Trono (Addgene plasmid # 12259 ; <http://n2t.net/addgene:12259> ; RRID:Addgene\_12259). Viral supernatant was harvested 48 and 72 hr post-transfection, filtered through a 0.45 µm filter, and concentrated by ultracentrifugation (25,000 rpm for 2 hr at 4°C). Concentrated virus was resuspended in Opti-MEM (Gibco) and lentiviral aliquots were frozen and stored at -80°C. Lentiviruses were titered in Green-Go cells as previously described<sup>39</sup>.

## **Retrograde pancreatic duct delivery**

Retrograde pancreatic duct instillation of lentivirus has been previously described<sup>9</sup>. We adapted this technique in a number of ways. Briefly, the ventral abdomen was depilated (using clippers or Nair) 1-2 days prior to surgery. Animals were anesthetized with Isoflurane and the surgical area was disinfected with alternating Betadine/Isopropyl alcohol. A small skin incision was made in the anterior abdomen (~2-3 cm midline incision extending caudally from the xiphoid process). A subsequent incision was made through the linea alba and incision edges were secured in place with a Colibri retractor. The remainder of the procedure was conducted under a Nikon stereomicroscope. A moistened (with sterile 0.9% saline) sterile cotton swab was used to gently move the left lobe of the liver cranially towards the diaphragm. A second moistened sterile cotton swab was used to gently reposition the colon/small intestine into the right lower abdominal quadrant, until the duodenum was visualized. The duodenum was similarly gently repositioned (still in the abdominal cavity) using moistened cotton swabs until the pancreas, common bile duct and sphincter of Oddi were well visualized (Figure 1b). The common bile duct and cystic duct were gently separated from the portal vein and hepatic artery using blunt dissection with Moria forceps. A microclip was placed on the cystic duct to prevent influx of the viral particles into the liver or gallbladder, forcing the viral vector retrograde through the pancreatic duct. To infuse the viral vector, the common bile duct was cannulated with a 30G needle at the level of the sphincter of Oddi. Virus (150  $\mu$ L) was injected over the course of 30 sec. Gently pressure was applied at the sphincter of Oddi upon needle exit. Subsequently, the microclip and Colibri retractor were removed. The peritoneum was closed using running 4-0 Vicryl sutures. The cutis and fascia were

closed using simple interrupted 4-0 Vicryl sutures. The entire procedure was conducted on a circulating warm water heating blanket to prevent intra-operative hypothermia. All mice received pre-operative analgesia with Buprenorphine-SR and post-operative subcutaneous warmed 0.9% normal saline and were followed post-operatively for any signs of discomfort or distress.

For retrograde pancreatic ductal instillation, male mice (aged 3-6 weeks) and female mice (aged 3-8 weeks) were transduced with 250K TU (transducing units, see viral titering) in serum-free media (Opti-MEM; Gibco).

For experiments involving CD8 $\alpha$  depletion, animals were dosed with CD8 $\alpha$ -depleting antibody (BioXCell, Clone 2.43, 200  $\mu$ g/mouse, dosed i.p every 3-4 days) beginning one day prior to surgery.

### **Organoid generation and characterization**

Pancreatic organoid isolation and propagation has been previously described<sup>40</sup>. Briefly, for genetically-defined pancreatic organoids, pancreata were manually dissected from genetically engineered mice of the desired genotype. Pancreata were then manually minced with razor blades and dissociated in pancreas digestion buffer [1x PBS, 125 U/mL collagenase IV (Worthington)] for 20 min at 37°C. Cell suspensions were filtered through 70  $\mu$ m filters, washed with 1x PBS and centrifuged with slow deceleration. Cell pellets were resuspended in 100% growth-factor reduced Matrigel (Corning) and solidified at 37°C. Cells were subsequently cultured in organoid complete media (minor modifications from previously described formulations<sup>40</sup>, see details below) and monitored for organoid outgrowth. Organoids were passaged with TrypLE Express (Life Technologies) for at



least 4 passages to purify the ductal component prior to *Cre* recombinase-mediated recombination. For recombination, organoids were spininfected with adenoviral (Ad-CMV-Cre; University of Iowa Viral Vector Core Facility) at a MOI >100 to ensure 100% recombination. All organoids were genotyped both prior to and following Ad-CMV-Cre to ensure proper recombination.

Tumor-derived pancreatic organoids were isolated following the same procedure as above with the exception of 30 min in pancreas digestion buffer. Tumor-derived organoids were passaged at least four times prior to experimental manipulation to remove contaminating cell types. P53 deficient organoids were selected via resistance to Nutlin-3a (10  $\mu$ M, Sigma-Aldrich). Pancreatic organoids were maintained in culture for <20 passages.

### **Pancreatic Organoid Complete Media**

The media for pancreatic organoids was formulated based on L-WRN cell conditioned media (L-WRN CM)<sup>41</sup>. Briefly, L-WRN CM was generated by collecting 8 days of supernatant from the L-WRN cells, grown in Advanced DMEM/F12 (Gibco) supplemented with 20% fetal bovine serum (Hyclone), 2 mM GlutaMAX, 100 units/mL of penicillin, 100  $\mu$ g/mL of streptomycin, and 0.25  $\mu$ g/mL amphotericin. L-WRN CM was diluted 1:1 in Advanced DMEM/F12 (Gibco) and supplemented with additional RSPO-1 conditioned media (10% v/v), generated using Cultrex HA-R-Spondin1-Fc 293T Cells. The following molecules were also added to the growth media: B27 (Gibco), 1  $\mu$ M N-acetylcysteine (Sigma-Aldrich), 10  $\mu$ M nicotinamide (Sigma-Aldrich), 50 ng/mL EGF (Novus Biologicals), 500 nM A83-01 (Cayman Chemical), 10  $\mu$ M SB202190 (Cayman Chemical), and 500 nM

PGE2 (Cayman Chemical). Wnt activity of the conditioned media was assessed and normalized between batches via luciferase reporter activity of TCF/LEF activation (Enzo Leading Light Wnt reporter cell line).

### **T cell culture**

OT-I splenocytes were harvested from C57BL/6J *OT-I;Rag2<sup>-/-</sup>* transgenic mice, and spleens were mashed through 70  $\mu\text{m}$  filters. Red blood cells were lysed with ACK buffer for 2 min before cell suspension neutralization with PBS and pelleted for plating. Splenocytes were counted and adjusted to  $1 \times 10^6$  cells/mL in T cell medium [RPMI 1640 (Corning) supplemented with 10% heat-inactivated FBS, 20 mM HEPES (Gibco), 1 mM Sodium Pyruvate (Thermo Fisher), 2 mM L-Glutamine (Gibco), 50  $\mu\text{M}$   $\beta$ -mercaptoethanol (Gibco), 1x NEAA (Sigma), 0.5x Pen/Strep (Gibco) with 10 ng/mL hIL-2 (Peprotech) and 1  $\mu\text{M}$  SIINFEKL peptide (Anaspec)]. Splenocytes were activated for 24 hr at 37°C in a tissue culture incubator, before manual CD8 $\alpha^+$  isolation according to the manufacturer instructions (Milteny Biotec). OT-I T cells were subsequently expanded 4-6 days in T cell medium with 10 ng/mL hIL-2 prior to organoid co-culture.

### **Organoid + CD8<sup>+</sup> T cell co-culture and imaging**

Pancreatic organoids (day 5-7 in culture) were dissociated using TrypLE Express (Life Technologies) and single cell suspensions were generated by vigorous resuspension. Activated OT-I CD8<sup>+</sup> T cells (see above) and organoid cell numbers were determined by manual hemocytometer cell counting, and T cells:organoids were mixed at defined effector:target ratios. Matrigel was then added (5  $\mu\text{L}$  per well in 96w plates for Incucyte

live cell imaging; 20-50 uL per well for culture in 24-well plates; final 85% Matrigel) before solidification at 37°C. Cells were cultured in complete organoid medium supplemented with 10 ng/mL hIL-2 (PeproTech). Incucyte images of co-cultures were acquired every 4 hr (BF/RFP channels) for 6-11 days for Incucyte live cell imaging or imaged at Day 5-7 for larger cultures.

### **Orthotopic transplantation**

Orthotopic transplantation of organoids was performed with minor modifications to previously reported protocols for orthotopic transplantation of pancreatic monolayer cell lines<sup>42</sup>. Briefly, animals were anesthetized using Isoflurane, the left subcostal region was depilated (using clippers or Nair) and the surgical area was disinfected with alternating Betadine/Isopropyl alcohol. A small (~2 cm) skin incision was made in the left subcostal area and the spleen was visualized through the peritoneum. A small incision (~2 cm) was made through the peritoneum overlying the spleen and the spleen and pancreas were exteriorized using ring forceps. A 30G needle was inserted into the pancreatic parenchyma parallel to the main pancreatic artery and 100 µL (containing  $1.25 \times 10^5$  organoid cells in 50% PBS + 50% Matrigel) was injected into the pancreatic parenchyma. Successful injection was visualized by formation of a fluid-filled region within the pancreatic parenchyma without leakage. The pancreas/spleen were gently internalized, and the peritoneal and skin layers were sutured independently using 4-0 Vicryl sutures. All mice received pre-operative analgesia with Buprenorphine-SR and were followed post-operatively for any signs of discomfort or distress. Organoid/Matrigel mixes

were kept on ice throughout the entirety of the procedure to prevent solidification prior to injection.

For orthotopic transplantation, syngeneic mice (aged 4-10 weeks) were transplanted. Male pancreatic organoids were only transplanted back into male recipients.

### **Small rodent ultrasound**

Quantification of murine pancreatic tumors by high resolution ultrasound has been previously described<sup>43</sup>. Briefly, animals were anesthetized using Isoflurane and the lateral and ventral abdominal areas were depilated using Nair. Sterile 0.9% saline (1 mL) was administered by i.p. injection prior to imaging to improve visualization of the pancreas. Animals were imaged using the Vevo3100/LAZRX ultrasound and photoacoustic imaging system (Fujifilm-Visualsonics). Animals were placed on the imaging platform in the supine position and a layer of ultrasound gel was applied over the entirety of the abdominal area. The ultrasound transducer (VisualSonics 550S) was placed on the abdomen orthogonal to the plane of the imaging platform. Landmark organs, such as the kidney, spleen, and liver, were identified in order to define the area of the pancreas. The transducer was set at the scanning midpoint of the normal pancreas or pancreatic tumor and a 3D image of 10-20 mm, depending on tumor size, at a Z- slice thickness of 0.04 mm. Three-dimensional (3D) images were uploaded to the Vevo Lab Software. The volumetric analysis function was used to define the tumor border at various Z-slices through the entirety of the tumor and derive the final calculated tumor volume.

### **Preclinical trial**

For preclinical trials, age and sex-matched recipient *C57BL/6J* mice were purchased from The Jackson Laboratory (JAX). Orthotopic transplantation was performed as described above. Mice were monitored for tumor development at 4, 5, 6 weeks post-initiation using high-resolution ultrasound (as described above) to confirm tumor establishment and interval growth. Animals with established tumors (baseline 10-220 mm<sup>3</sup> by 6 weeks post-initiation) were randomized by tumor burden within 24 hr of baseline imaging to either control or experimental treatment arms. Researchers performing health checks, ultrasound imaging and interpretation were blinded to cohort allocation. Isotype (control) arm consisted of 200 µg/mouse Rat IgG2a (BioXCell; Clone 2A3) + 100 µg/mouse Mouse IgG1 (BioXCell; Clone MOPC-21). Experimental arms consisted of anti-PD1<sup>44</sup> (BioXCell; Clone 29F.1A12; Rat IgG2a; 200 µg/mouse, dosed i.p. every 2-3 days), anti-TIGIT<sup>45</sup> (Absolute Antibody; Clone 1B4; Mouse IgG1; 100 µg/mouse, dosed i.p. every 2-3 days), CD40 agonist<sup>46</sup> (BioXCell; Clone FGK4.5/FGK45; Rat IgG2a; 100 µg/mouse, dosed i.p. once every 4 weeks) monotherapy or combination therapy as described in the text. Animals were treated for 4 weeks and weekly weights and ultrasound imaging was performed as described.

### **Tissue and blood collection for flow cytometry of murine PDAC**

Pancreatic tumor-bearing animals were euthanized by cervical dislocation, prior to whole organ dissection (pancreas, spleen), tumor imaging and collection in RPMI 1640 supplemented with 1% heat-inactivated FBS. Pancreas tumors were finely minced with scissors in MACS C tubes (Miltenyi Biotec), and digested for 30 min at 37°C with gentle agitation in 5 mL digestion buffer [1x HBSS (Gibco), 1 mM HEPES (Gibco), 1% heat-

inactivated FBS, 125 U/mL collagenase IV (Worthington), 40 U/mL DNaseI, grade II (Roche)]. Pancreas tumors were processed on a gentleMACS Octo Dissociator using the “*m\_spleen\_04*” program. Digestion buffer was neutralized with 5 mL heat-inactivated FBS, washed with PBS, and filtered through 70 µm filters. Single cell suspensions were pelleted at 1500 rpm with slow deceleration, and transferred to 96-well round-bottom plates for flow cytometric staining.

Spleen samples were mashed through 70 µm filters, collected in RPMI 1640 supplemented with 1% heat-inactivated FBS and pelleted. Red blood cells were lysed with ACK buffer for 2 min before cell suspension neutralization with PBS, pelleted for plating and transferred to 96-well round-bottom plates for flow cytometric staining.

Peripheral blood (100-200 µL) for longitudinal tracking of T cells or prior to euthanasia was collected by retroorbital bleeding and added to 4% sodium citrate (50 µL) to prevent clotting. Red blood cells were lysed in two rounds with ACK buffer for 2 min before cell suspension neutralization with PBS. Single cell suspensions were transferred to 96-well round-bottom plates for flow cytometric staining.

### **Tissue processing for flow cytometry of human PDAC**

Freshly resected human pancreatic adenocarcinoma specimens were transferred in RPMI 1640 on ice to the laboratory. Pancreas tumors were finely minced with scissors in MACS C tubes, and processed as described above for murine PDAC. Human PBMCs from IRB-consented healthy individuals (StemCell) were thawed, washed with PBS and immediately stained for flow cytometry. All studies using human specimens were

approved by the Massachusetts General Hospital Institutional Review Board and conducted according to the principles expressed in the Declaration of Helsinki.

### **Processing for flow cytometry of pancreatic organoids**

Pancreatic organoids were grown as described above. Prior to isolation, organoids were treated with interferon-gamma (10 ng/mL; PeproTech) for 48-72 hr prior to analysis. Organoids were dissociated using TrypLE (10 min to minimize cleavage of surface proteins) washed with PBS, and filtered through 70 µm filters. Single cell suspensions were pelleted at 2000 rpm and transferred to 96-well round-bottom plates for flow cytometric staining.

### **Antibodies and flow cytometry**

Fluorochrome-conjugated antibodies directed against the following mouse antigens were used for analysis by flow cytometry: CD4-Alexa Fluor 647 (RM4-5, 1:400, BioLegend); CD4-BUV737 (RM4-5, 1:400, BD Biosciences); CD8a-BUV395 (53-6.7, 1:400, BD Biosciences); CD8a-BV421 (53-6.7, 1:400, BioLegend); CD8a-BV785 (53-6.7, 1:400, BioLegend); CD11b-BV605 (M1/70, 1:200, BioLegend); CD11b-PE-Cy7 (M1/70, 1:1400, BioLegend); CD11c-PE-Cy7 (N418, 1:400, Invitrogen); CD19-BUV395 (1D3, 1:200, BD Biosciences); CD44-BV605 (IM7, 1:400, BioLegend); CD44-BV711 (IM7, 1:200, BioLegend); CD44-FITC (IM7, 1:200, Invitrogen); CD45-APC (30-F11, 1:400, Invitrogen); CD45-BV786 (30-F11, 1:400, BioLegend); CD64-BV421 (X54-5/7.1, 1:200, BioLegend); CD172a-FITC (P84, 1:400, BioLegend); EpCam-PE-Cy7 (G8.8, 1:200, BioLegend); F4/80-APC (BM8, 1:200, BioLegend); H-2Db-FITC (28-14-8, 1:400, Invitrogen); H-2Kb-

APC (AF6-88.5, 1:400, BioLegend); LAG3-FITC (C9B7W, 1:200, Invitrogen); Ly-6C-PerCP-Cy5.5 (HK1.4, 1:200, BioLegend); Ly-6G-Alexa Fluor 700 (1A8, 1:400, BioLegend); Ly49F-BV421 (HBF-719, 1:100, BD Biosciences); Ly49G2-FITC (4D11, 1:100, Invitrogen); MHC-II (I/A-I/E)-BV711 (M5/114.15.2, 1:600, BioLegend); PD-1-BV510 (29F.1A12, 1:400, BioLegend); PD-L1-BV421 (10F.9G2, 1:100, BioLegend); TIGIT-PerCP-Cy5.5 (GIGD7, 1:200, Invitrogen); TIM3-BV605 (RMT3-23, 1:200, BioLegend); XCR1-PE (ZET, 1:400, BioLegend). For H-2Kb-SIINFEKL tetramer staining, monomer was purchased from the NIH Tetramer Core Facility and tetramerized with Streptavidin-PE in-house.

The following fluorochrome-conjugated antibodies against human surface antigens were used (all 1:40): CD3-BUV805 (UCHT1, BD Biosciences); CD8-BUV737 (SK1, BD Biosciences); CD45RO-BUV395 (UCHL1, BD Biosciences); LAG3-PE/Dazzle 594 (11C3C65, BioLegend); PD-1-BV510 (EH12.1, BD Biosciences); TIGIT-PE-Cy7 (MBSA43, Invitrogen); TIM3-BV711 (7D3, BD Biosciences).

Prior to surface staining, cell pellets were resuspended in Live/Dead dye (Ghost Dye Red 780, Tonbo Biosciences or Zombie Aqua Fixable Viability Dye, BioLegend) diluted 1:1000 in PBS on ice for 20 min in the dark. Surface staining was performed on cells in PBS with 1% heat-inactivated FBS on ice for 30 min in the dark. Cell pellets were fixed overnight in 1x fixation buffer (eBioscience), prior to permeabilization and intracellular staining for 1 hr in the dark at RT with the following antibodies: anti-human FoxP3-Alexa Fluor 700 (PCH101, 1:20, Invitrogen); Ki-67-Alexa Fluor 700 (B56, 1:200, BD Biosciences), Ki-67-BV786 (B56, 1:100, BD Biosciences); TCF-1-Alexa Fluor 647 (C63D9, 1:250, Cell Signaling Technologies). Samples were acquired on BD LSR II or



LSR Fortessa machines, cell sorting was performed on a BD Aria IIIu. FACS data was analyzed using Flowjo v10 software (BD).

For flow cytometric immunophenotyping, samples with less than 100 CD8<sup>+</sup> cells or less than 50 CD44<sup>hi</sup>Tetramer<sup>+</sup> cells within a given cell population were not considered for further sub-setting of these populations.

### **Immunohistochemistry and pathology review**

Isolated pancreas and spleen tissues were preserved overnight in zinc formalin fixative, transferred to 70% EtOH and processed for paraffin embedding. Four (4)  $\mu$ m paraffin sections were cut for Hematoxylin & Eosin staining and IHC. For IHC, upon dewaxing, antigen retrieval was performed in a 10 mM citrate buffer (pH 6) for 5 min at 125°C. Slides were cooled to room temperature and washed with TBS + 0.1% Tween-20 (Sigma-Aldrich). Slides were incubated with Endogenous Peroxidase Block (Dako) for 30 min and blocked with normal horse serum (Vector Labs) for 1 hr. Slides were incubated with primary antibody [rabbit anti-RFP (Rockland, 1:400), rat anti-CK19 (Troma-III, DSHB, 1:200)] overnight at 4°C and with the corresponding anti-species HRP-conjugated secondary antibody (Vector Labs) for 30 min at RT. Slides were developed with DAB Peroxidase Substrate Kit (Vector Labs).

For CD8 $\alpha$  and CD4 co-staining, slides were dewaxed, and antigen retrieval was performed in 10 mM citrate buffer (pH 6). Slides were blocked with Bloxall Endogenous Peroxidase and Alkaline Phosphatase Block and normal horse serum (all Vector Labs). Slides were incubated with primary rabbit anti-CD8 $\alpha$  antibody (Abcam EPR21769, 1:1000) overnight at 4°C and with secondary Alkaline phosphatase anti-Rabbit IgG for 30

min at RT. Slides were then developed with Vector Black Alkaline phosphatase substrate (Vector Labs) and blocked again with Bloxall and normal horse serum. Slides were incubated with primary rabbit anti-CD4 (Abcam EPR19514, 1:400) for 3 hr at RT and secondary HRP conjugated anti-Rabbit antibody for 30 min. Slides were developed with HRP VINA Green Chromogen (Biocare Medical). All histologic diagnoses were confirmed with a pathologist (R.T.B.) specialized in rodent pathology.

### **Single-cell RNA sequencing**

Sorted cells were washed three times in 1x PBS (calcium and magnesium free) containing 0.04% w/v BSA, and then quantified and titrated to a final concentration of approximately 300 cells/ $\mu$ L. Using the Chromium Single Cell 3' Solution (v3) according to manufacturer's instructions, approximately 2000-5000 cells were partitioned into Gel Beads in Emulsion (GEMs) with cell lysis and barcoded reverse transcription of mRNA into cDNA, followed by amplification, enzymatic fragmentation, 5' adaptor ligation and unique sample index attachment. The recovery rate was ~800 cells per sample after filtering for quality control. Sample libraries were sequenced on the HiSeq X Version 2.5 (Illumina) with the following read configuration: Read1 28 cycles, Read2 96 cycles, Index read 8 cycles.

### **Single-cell RNA sequencing analysis**

#### *Data processing, cell clustering, and differential expression analysis*

Raw sequencing data were processed using Cell Ranger, version 3.0.2, and sequencing reads were aligned to the mm10 reference mouse transcriptome (version 3.0.0). After processing, including filtering barcodes with less than 500 UMIs or those with more than

10% of reads matching the mitochondrial genome, Cell Ranger reported 545 cell-associated barcodes and detected 15,065 genes. Cells lacking expression of *Cd3e* and *Cd8a* were discarded. After this, low-quality cells with less than 100 detected genes were filtered out, and cells exceeding the 97th percentile for number of detected genes were excluded to remove probable doublets. The resulting matrix used for downstream analyses was defined by 482 cells and 15,065 genes.

Data normalization and scaling, variable feature selection, cell clustering, and differential gene expression analysis was performed using Seurat, version 3.1.4<sup>47</sup>. Data were normalized by total expression per cell and scaled using a factor of 10,000 and log transformed (natural scale). The top 2,000 variable genes were selected using Seurat's default "vst" method. The expression of these genes was then scaled and centered, and these genes were then used for all downstream analysis. Principal component analysis (PCA) was then performed for dimensionality reduction, and the first 30 principal components were selected using the elbow method heuristic as guidance.

A *k*-nearest neighbor graph (KNN, *k*=20) was constructed in PC space using the top 30 principal components. Four clusters were detected using the Louvain method of community detection (default parameters and resolution = 0.54)<sup>48</sup>. Data was visualized using the Uniform Manifold Approximation and Projection (UMAP) algorithm implemented in Seurat<sup>49,50</sup>. Default parameters were used, with the following exceptions: the method parameter ("umap-learn") and the metric parameter ("correlation"). Differential gene expression between clusters was assessed using the default Wilcoxon Rank Sum test.

### *Gene Module Analysis*

Seurat's AddModuleScore function (control parameter = 8) was used to calculate gene module scores for all cells. For this analysis, gene sets were derived from previously published gene modules. For datasets providing human gene modules, a custom R script was generated to retrieve corresponding mouse orthologs from Ensembl with the biomaRt package (version 2.42.0)<sup>51,52</sup>. A Ly49<sup>+</sup>CD8<sup>+</sup> T cell module score was also derived from bulk RNA-seq data<sup>18</sup> available on the Gene Expression Omnibus (GEO; accession number: GSE130975). For these data, the raw count matrix was downloaded and processed using DESeq2<sup>53</sup>, version 1.26.0. Specifically, differential gene expression was evaluated between the Ly49<sup>+</sup>CD8<sup>+</sup> (n = 3 replicates) and the Ly49<sup>-</sup>CD8<sup>+</sup> (n = 3 replicates) conditions. The top 126 differentially expressed genes with log<sub>2</sub> fold change > 3 (all with adjusted  $P \ll 0.01$ ) were selected for the Ly49<sup>+</sup>CD8<sup>+</sup> gene module. The cells in our scRNA-seq dataset were then scored for this module using the method described above.

To derive *de novo* gene modules from our scRNA-seq dataset, the Pathway and Gene Set Overdispersion Analysis (PAGODA)<sup>23</sup> framework from the SCDE package (version 2.14.0) was used. The analysis was performed starting with the raw counts for the same 482 cells that remained after filtering in the previous analysis. The knn error model was fit using min.count.threshold = 2 and k = ncol(cd/4), where "cd" represented the matrix after clean.counts was performed with default parameters. Gene expression magnitudes were then normalized with trim = 3/ncol(cd) and max.adj.var=5. *De novo* gene modules were then determined using trim = 7.1/ncol(varinfo\$mat) and n.clusters = 50 and otherwise default parameters for the pagoda.gene.clusters function. The top three *de novo* gene sets (modules 30, 36, and 45) with the highest over-dispersion Z score (adjusted for multiple hypotheses) that best distinguished the cellular subpopulations

defined by SCDE were selected, and all cells were scored for these modules in Seurat as described above.

## **TCGA analysis**

### *Human Pancreatic Adenocarcinoma gene expression analysis*

Gene expression profiles for human Pancreatic Adenocarcinoma (PAAD) patient primary tumors (n=178) were obtained from the TCGA repository<sup>24</sup> ([tcga-data.nci.nih.gov/tcga](http://tcga-data.nci.nih.gov/tcga)). *De novo* murine gene sets (Pagoda36 and Pagoda45) identified by PAGODA<sup>23</sup> (described above) were used to score these human gene expression profiles of individual tumors using ssGSEA<sup>54</sup>. Mouse gene symbols were translated to human orthologs using homology information from the Mouse Genome Informatics database (MGI, [informatics.jax.org](http://informatics.jax.org)). Tumors were stratified based on standardized ssGSEA scores (z-scores). Tumors with the most correlated (high scoring cohort,  $z > 1.5$ ) and least correlated (low scoring cohort,  $z < -1.5$ ) expression profiles were selected for unsupervised transcriptomic analysis. A high-resolution signature discovery approach (Independent Component Analysis, ICA<sup>55</sup>) was employed to analyze the transcriptomes of these high and low-scoring cohorts to characterize changes in gene expression profiles, as described previously<sup>56–58</sup>. Briefly, this unsupervised blind source separation technique was used on this discrete count-based expression dataset to elucidate statistically independent and biologically relevant signatures. ICA is a signal processing and multivariate data analysis technique in the category of unsupervised matrix factorization methods<sup>55</sup>. The R implementation of the core JADE algorithm (Joint Approximate Diagonalization of Eigenmatrices)<sup>59–61</sup> was used. Statistical significance of

signatures distinguishing the two human patient cohorts was assessed using the Mann-Whitney-Wilcoxon test ( $\alpha = 0.05$ ) and the top human gene signature corresponding to each Pagoda module was selected ( $p=3.1e-07$  for Pagoda36;  $p=0.00023$  for Pagoda45). Each of these human PAAD signatures identifies up- and down-regulated genes between the high- and low-scoring patient cohorts where patients were stratified by ssGSEA scores derived using the corresponding Pagoda geneset. A volcano plot was used to illustrate the magnitude of fold-change (X-axis) versus the human signature score (Y-axis) for all genes. All signature analyses were conducted in the R Statistical Programming language ([www.r-project.org](http://www.r-project.org)).

#### *Human clinical data analysis*

Human PAAD RNA-seq gene expression profiles of primary tumors ( $n=178$ ) and relevant clinical data were obtained from TCGA. Genes with the highest adjusted variance (score  $> 2$ ) per Pagoda murine expression module (Pagoda36: 17 genes, Pagoda45: 21 genes) were selected as driver genes and translated to human symbols using homology information from MGI ([informatics.jax.org](http://informatics.jax.org)). Human gene expression profiles were scored using ssGSEA for each of these driver genesets, as described above. Patients were stratified based on standardized ssGSEA scores and Kaplan-Meier survival analyses were conducted to compare high-scoring patients (top quartile,  $n=44$ ) with low-scoring patients (bottom quartile,  $n=44$ ) and significance was assessed using the log-rank test. Survival analyses were conducted using the survival package in R. The log-rank test was used in the 'survdif' call to assess the difference between Kaplan-Meier estimates of survival.

## **Statistical Analyses**

All graphs and statistical analyses were generated with GraphPad Prism 8 or in R as described above. The following statistical tests were used in this study: (1) Two-sided Mann-Whitney test was performed in GraphPad Prism 8. (2) Log-rank test was performed as described above in R.

## 2.6 References

1. Royal, R. E. *et al.* Phase 2 trial of single agent Ipilimumab (anti-CTLA-4) for locally advanced or metastatic pancreatic adenocarcinoma. *J. Immunother. (Hagerstown, Md. 1997)* **33**, 828–833 (2010).
2. Brahmer, J. R. *et al.* Safety and activity of anti-PD-L1 antibody in patients with advanced cancer. *N. Engl. J. Med.* **366**, 2455–2465 (2012).
3. O'Reilly, E. M. *et al.* Durvalumab with or Without Tremelimumab for Patients with Metastatic Pancreatic Ductal Adenocarcinoma: A Phase 2 Randomized Clinical Trial. *JAMA Oncol.* **5**, 1431–1438 (2019).
4. Balachandran, V. P. *et al.* Identification of unique neoantigen qualities in long-term survivors of pancreatic cancer. *Nature* **551**, S12–S16 (2017).
5. Bailey, P. *et al.* Exploiting the neoantigen landscape for immunotherapy of pancreatic ductal adenocarcinoma. *Sci. Rep.* **6**, 1–8 (2016).
6. Lawrence, M. S. *et al.* Mutational heterogeneity in cancer and the search for new cancer-associated genes. *Nature* **499**, 214–218 (2013).
7. Stromnes, I. M., Hulbert, A., Pierce, R. H., Greenberg, P. D. & Hingorani, S. R. T-cell Localization, Activation, and Clonal Expansion in Human Pancreatic Ductal Adenocarcinoma. *Cancer Immunol. Res.* **5**, 978–991 (2017).
8. Evans, R. A. *et al.* Lack of immunoediting in murine pancreatic cancer reversed with neoantigen. *JCI insight* **1**, (2016).
9. Chiou, S. H. *et al.* Pancreatic cancer modeling using retrograde viral vector delivery and in vivo CRISPR/Cas9-mediated somatic genome editing. *Genes Dev.* **29**, 1576–1585 (2015).



10. Bindels, D. S. *et al.* MScarlet: A bright monomeric red fluorescent protein for cellular imaging. *Nat. Methods* **14**, 53–56 (2016).
11. DuPage, M., Mazumdar, C., Schmidt, L. M., Cheung, A. F. & Jacks, T. Expression of tumour-specific antigens underlies cancer immunoediting. *Nature* **482**, 405–409 (2012).
12. Hippenmeyer, S. *et al.* Genetic mosaic dissection of Lis1 and Ndel1 in neuronal migration. *Neuron* **68**, 695–709 (2010).
13. Hogquist, K. A. *et al.* T cell receptor antagonist peptides induce positive selection. *Cell* **76**, 17–27 (1994).
14. Zhu, Y. *et al.* Tissue-Resident Macrophages in Pancreatic Ductal Adenocarcinoma Originate from Embryonic Hematopoiesis and Promote Tumor Progression. *Immunity* **47**, 323-338.e6 (2017).
15. Hegde, S. *et al.* Dendritic Cell Paucity Leads to Dysfunctional Immune Surveillance in Pancreatic Cancer. *Cancer Cell* **37**, 289-307.e9 (2020).
16. Zheng, G. X. Y. *et al.* Massively parallel digital transcriptional profiling of single cells. *Nat. Commun.* **8**, 1–12 (2017).
17. Kim, H. J. *et al.* CD8<sup>+</sup> T regulatory cells express the Ly49 class I MHC receptor and are defective in autoimmune prone B6-Yaa mice. *Proc. Natl. Acad. Sci. U. S. A.* **108**, 2010–2015 (2011).
18. Saligrama, N. *et al.* Opposing T cell responses in experimental autoimmune encephalomyelitis. *Nature* **572**, 481–487 (2019).
19. Singer, M. *et al.* A Distinct Gene Module for Dysfunction Uncoupled from Activation in Tumor-Infiltrating T Cells. *Cell* **166**, 1500-1511.e9 (2016).

20. Doering, T. A. *et al.* Network Analysis Reveals Centrally Connected Genes and Pathways Involved in CD8+ T Cell Exhaustion versus Memory. *Immunity* **37**, 1130–1144 (2012).
21. Chihara, N. *et al.* Induction and transcriptional regulation of the co-inhibitory gene module in T cells. *Nature* **558**, 454–459 (2018).
22. Schietinger, A. *et al.* Tumor-Specific T Cell Dysfunction Is a Dynamic Antigen-Driven Differentiation Program Initiated Early during Tumorigenesis. *Immunity* **45**, 389–401 (2016).
23. Fan, J. *et al.* Characterizing transcriptional heterogeneity through pathway and gene set overdispersion analysis. *Nat. Methods* **13**, 241–244 (2016).
24. Raphael, B. J. *et al.* Integrated Genomic Characterization of Pancreatic Ductal Adenocarcinoma. *Cancer Cell* **32**, 185-203.e13 (2017).
25. Vonderheide, R. H. CD40 Agonist Antibodies in Cancer Immunotherapy. *Annu. Rev. Med.* **71**, 47–58 (2020).
26. Anderson, A. C., Joller, N. & Kuchroo, V. K. Lag-3, Tim-3, and TIGIT: Co-inhibitory Receptors with Specialized Functions in Immune Regulation. *Immunity* vol. 44 989–1004 (2016).
27. Uhlen, M. *et al.* A pathology atlas of the human cancer transcriptome. *Science* (80-. ). **357**, (2017).
28. Uhlen, M. *et al.* Tissue-based map of the human proteome. *Science* (80-. ). **347**, 1260419–1260419 (2015).
29. Yarchoan, M. *et al.* PD-L1 expression and tumor mutational burden are independent biomarkers in most cancers. *JCI Insight* **4**, (2019).

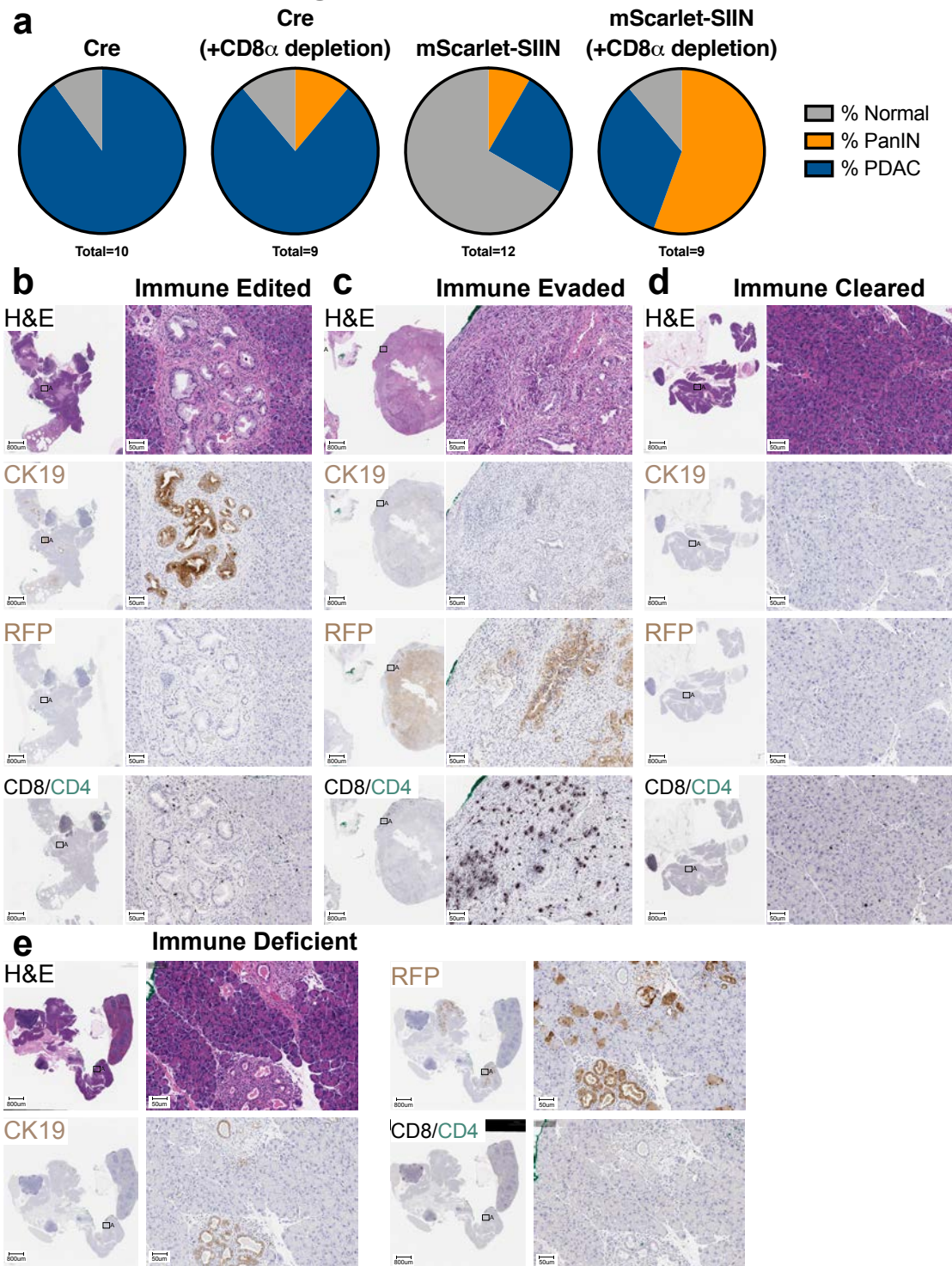
30. Dunn, G. P., Old, L. J. & Schreiber, R. D. The Three Es of Cancer Immunoediting. *Annu. Rev. Immunol.* **22**, 329–360 (2004).
31. Johnson, B. A., Yarchoan, M., Lee, V., Laheru, D. A. & Jaffee, E. M. Strategies for Increasing Pancreatic Tumor Immunogenicity. *Clin. Cancer Res. An Off. J. Am. Assoc. Cancer Res.* **23**, 1656–1669 (2017).
32. Wellenstein, M. D. & de Visser, K. E. Cancer-Cell-Intrinsic Mechanisms Shaping the Tumor Immune Landscape. *Immunity* vol. 48 399–416 (2018).
33. Ikeda, W. *et al.* TAGE4/nectin-like molecule-5 heterophilically trans-interacts with cell adhesion molecule nectin-3 and enhances cell migration. *J. Biol. Chem.* **278**, 28167–28172 (2003).
34. Jackson, E. L. *et al.* Analysis of lung tumor initiation and progression using conditional expression of oncogenic K-ras. *Genes Dev.* **15**, 3243–3248 (2001).
35. Marino, S., Vooijs, M., Van Der Gulden, H., Jonkers, J. & Berns, A. Induction of medulloblastomas in p53-null mutant mice by somatic inactivation of Rb in the external granular layer cells of the cerebellum. *Genes Dev.* **14**, 994–1004 (2000).
36. Gibson, D. G. *et al.* Enzymatic assembly of DNA molecules up to several hundred kilobases. *Nat. Methods* **6**, 343–345 (2009).
37. Benchling [Biology Software]. (2019). Retrieved from <https://benchling.com>.
38. Church, G. M. & Gilbert, W. Genomic sequencing. *Proc. Natl. Acad. Sci. U. S. A.* **81**, 1991–1995 (1984).
39. Sánchez-Rivera, F. J. *et al.* Rapid modelling of cooperating genetic events in cancer through somatic genome editing. *Nature* **516**, 428–431 (2014).
40. Boj, S. F. *et al.* Organoid models of human and mouse ductal pancreatic cancer.

- Cell* **160**, 324–338 (2015).
41. VanDussen, K. L., Sonnek, N. M. & Stappenbeck, T. S. L-WRN conditioned medium for gastrointestinal epithelial stem cell culture shows replicable batch-to-batch activity levels across multiple research teams. *Stem Cell Res.* **37**, 101430 (2019).
  42. Kim, M. P. *et al.* Generation of orthotopic and heterotopic human pancreatic cancer xenografts in immunodeficient mice. *Nat. Protoc.* **4**, 1670–1680 (2009).
  43. Sastra, S. A. & Olive, K. P. Quantification of Murine Pancreatic Tumors by High Resolution Ultrasound. *Methods Mol. Biol.* **980**, (2013).
  44. Liang, S. C. *et al.* Regulation of PD-1, PD-L1, and PD-L2 expression during normal and autoimmune responses. *Eur. J. Immunol.* **33**, 2706–2716 (2003).
  45. Dixon, K. O. *et al.* Functional Anti-TIGIT Antibodies Regulate Development of Autoimmunity and Antitumor Immunity. *J. Immunol. (Baltimore, Md. 1950)* **200**, 3000–3007 (2018).
  46. Rolink, A., Melchers, F. & Andersson, J. The SCID but not the RAG-2 gene product is required for S $\mu$ -S $\epsilon$  heavy chain class switching. *Immunity* **5**, 319–330 (1996).
  47. Butler, A., Hoffman, P., Smibert, P., Papalexi, E. & Satija, R. Integrating single-cell transcriptomic data across different conditions, technologies, and species. *Nat. Biotechnol.* **36**, 411–420 (2018).
  48. De Meo, P., Ferrara, E., Fiumara, G. & Provetti, A. Generalized Louvain method for community detection in large networks. in *International Conference on Intelligent Systems Design and Applications, ISDA* 88–93 (2011). doi:10.1109/ISDA.2011.6121636.

49. McInnes, L., Healy, J., Saul, N. & Großberger, L. UMAP: Uniform Manifold Approximation and Projection Software • Review • Repository • Archive. (2018) doi:10.21105/joss.00861.
50. Becht, E. *et al.* Dimensionality reduction for visualizing single-cell data using UMAP. *Nat. Biotechnol.* **37**, 38–47 (2019).
51. Durinck, S., Spellman, P. T., Birney, E. & Huber, W. Mapping identifiers for the integration of genomic datasets with the R/ Bioconductor package biomaRt. *Nat. Protoc.* **4**, 1184–1191 (2009).
52. Durinck, S. *et al.* BioMart and Bioconductor: a powerful link between biological databases and microarray data analysis. *Bioinformatics* **21**, 3439–40 (2005).
53. Love, M. I., Huber, W. & Anders, S. Moderated estimation of fold change and dispersion for RNA-seq data with DESeq2. *Genome Biol.* **15**, 550 (2014).
54. Barbie, D. A. *et al.* Systematic RNA interference reveals that oncogenic KRAS-driven cancers require TBK1. *Nature* **462**, 108–112 (2009).
55. Hyvärinen, A. & Oja, E. Independent component analysis: Algorithms and applications. *Neural Networks* **13**, 411–430 (2000).
56. Muzumdar, M. D. *et al.* Survival of pancreatic cancer cells lacking KRAS function. *Nat. Commun.* **8**, 1–19 (2017).
57. Li, C. M. C. *et al.* Foxa2 and Cdx2 cooperate with Nkx2-1 to inhibit lung adenocarcinoma metastasis. *Genes Dev.* **29**, 1850–1862 (2015).
58. Romero, R. *et al.* Keap1 loss promotes Kras-driven lung cancer and results in dependence on glutaminolysis. *Nat. Med.* **23**, 1362–1368 (2017).
59. Rutledge, D. N. & Jouan-Rimbaud Bouveresse, D. Independent Components

- Analysis with the JADE algorithm. *TrAC - Trends in Analytical Chemistry* vol. 50 22–32 (2013).
60. Biton, A. *et al.* Independent Component Analysis Uncovers the Landscape of the Bladder Tumor Transcriptome and Reveals Insights into Luminal and Basal Subtypes. *Cell Rep.* **9**, 1235–1245 (2014).
61. Miettinen, J., Nordhausen, K. & Taskinen, S. Blind source separation based on joint diagonalization in R: The packages JADE and BSSasymp. *J. Stat. Softw.* **76**, 1–31 (2017).

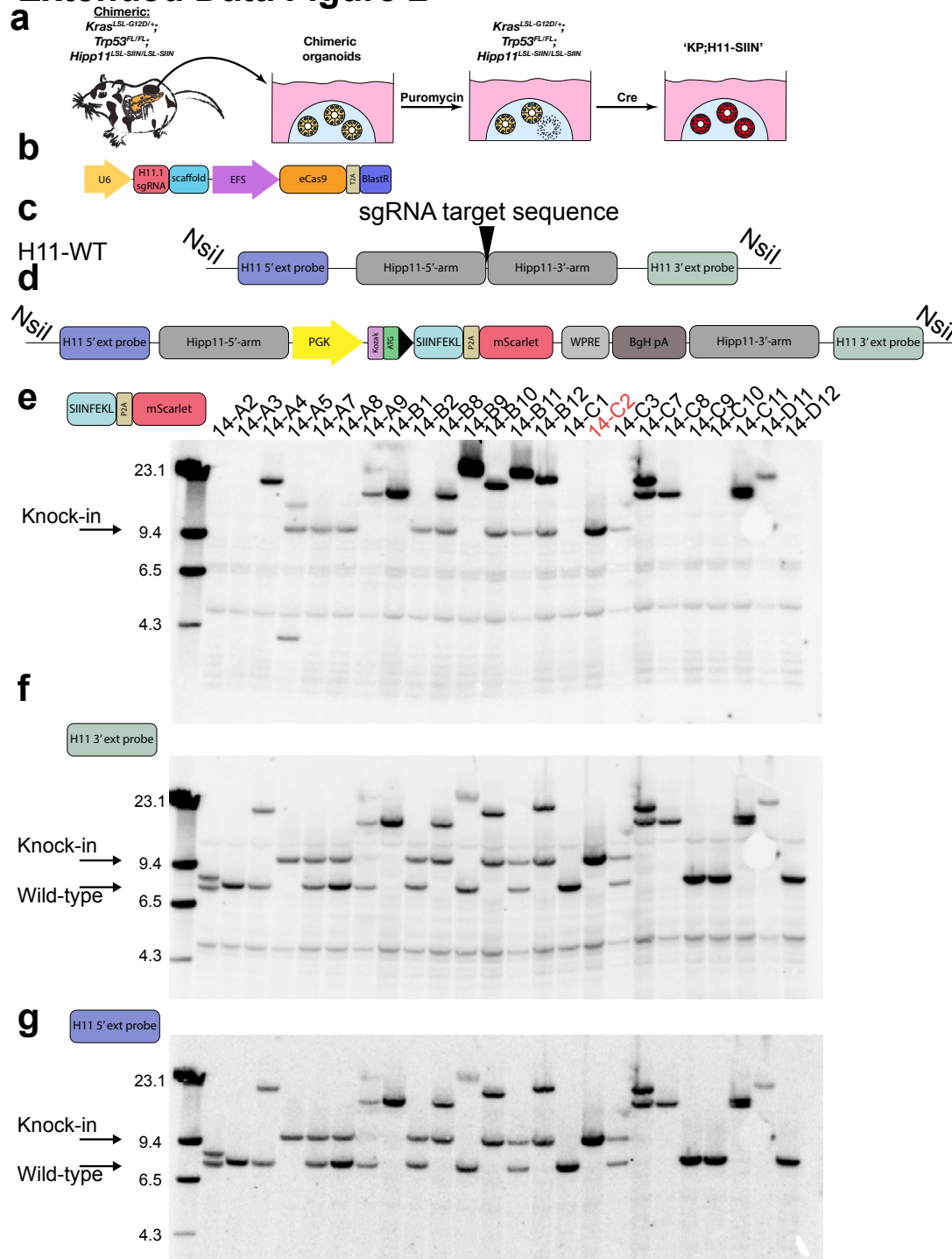
# Extended Data Figure 1



## Extended Data Figure 1

**a**, Quantification of histologic breakdown of control (Cre) or immunogenic (mScarletSIIN) autochthonous animals, with or without CD8 $\alpha$  depletion, at 9 weeks post-initiation (n=9-12 animals per condition). All histologic diagnoses were confirmed by a pathologist specializing in rodent pathology (R.T.B.). **b-e**, Hematoxylin and eosin (H&E) and immunohistochemical staining for cytokeratin 19 (CK19), mScarlet (RFP), CD8 $\alpha$  (CD8) and/or CD4 (CD4) on representative images for **b**, immune-edited **c**, immune-evaded **d**, immune-cleared **e**, immune-deficient animals.

## Extended Data Figure 2

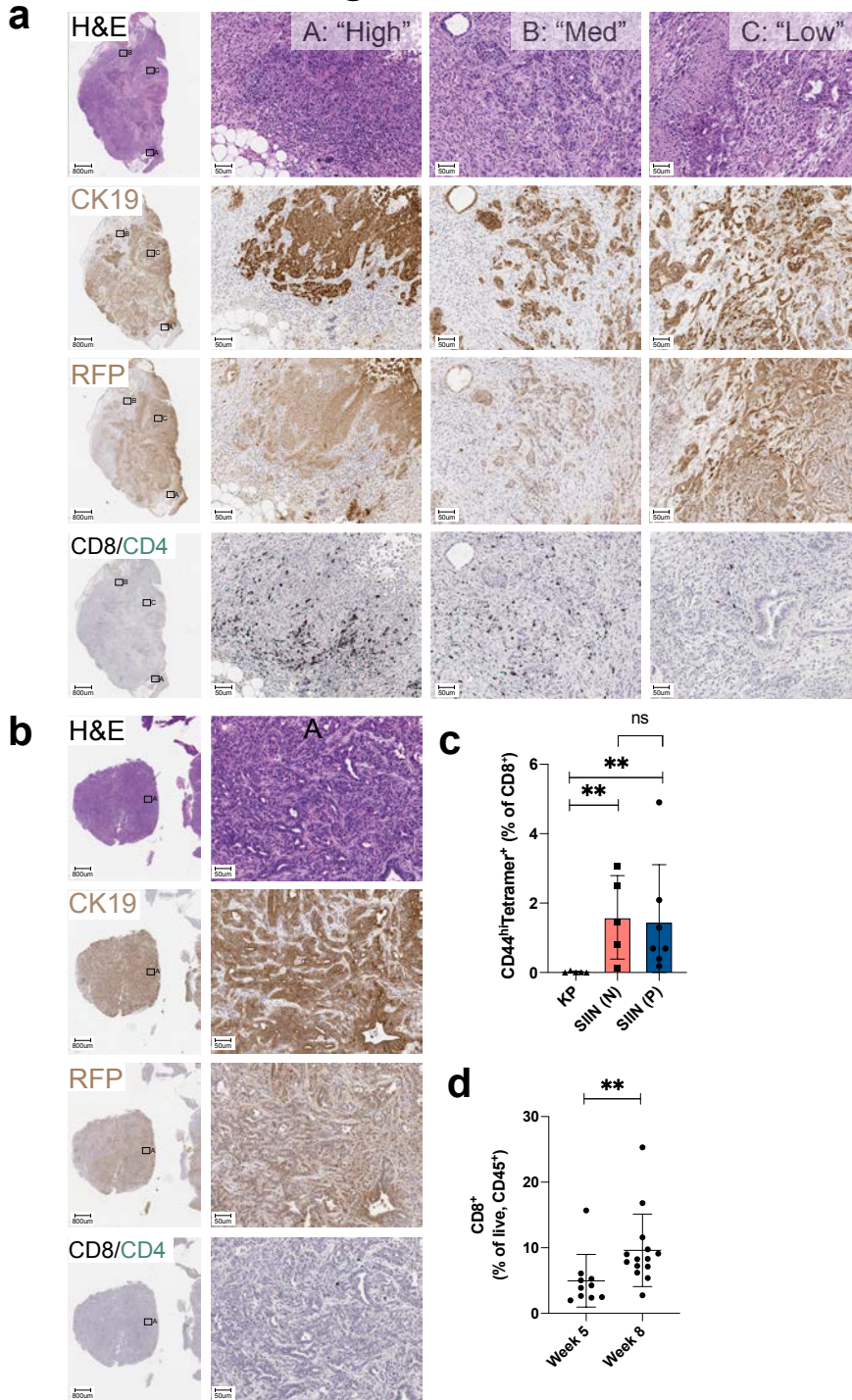


### Extended Data Figure 2

**a**, Experimental schematic depicting chimera generation, isolation of organoids, purification of mESC-derived organoids and Cre-mediated recombination of alleles. Schematics of **b**, “U6-sgRNA-EFS-eCas9-P2A-Blast” **c**, *Hipp11* wild-type genomic locus, **d**, extended *H11-SIIN* genomic locus (with southern blot probes annotated) following successful knock-in and recombination. Southern blot validation of *NsiI* digested genomic DNA from mESC clones using **e**, internal probe, **f**, 3' external probe, **g**, 5' external probe (probes depicted graphically next to each blot). Highlighted in red is the clone ‘14-C2’ which was a homozygous targeted clone used to generate ‘KP;H11-SIIN’ genetically-defined pancreatic organoids.



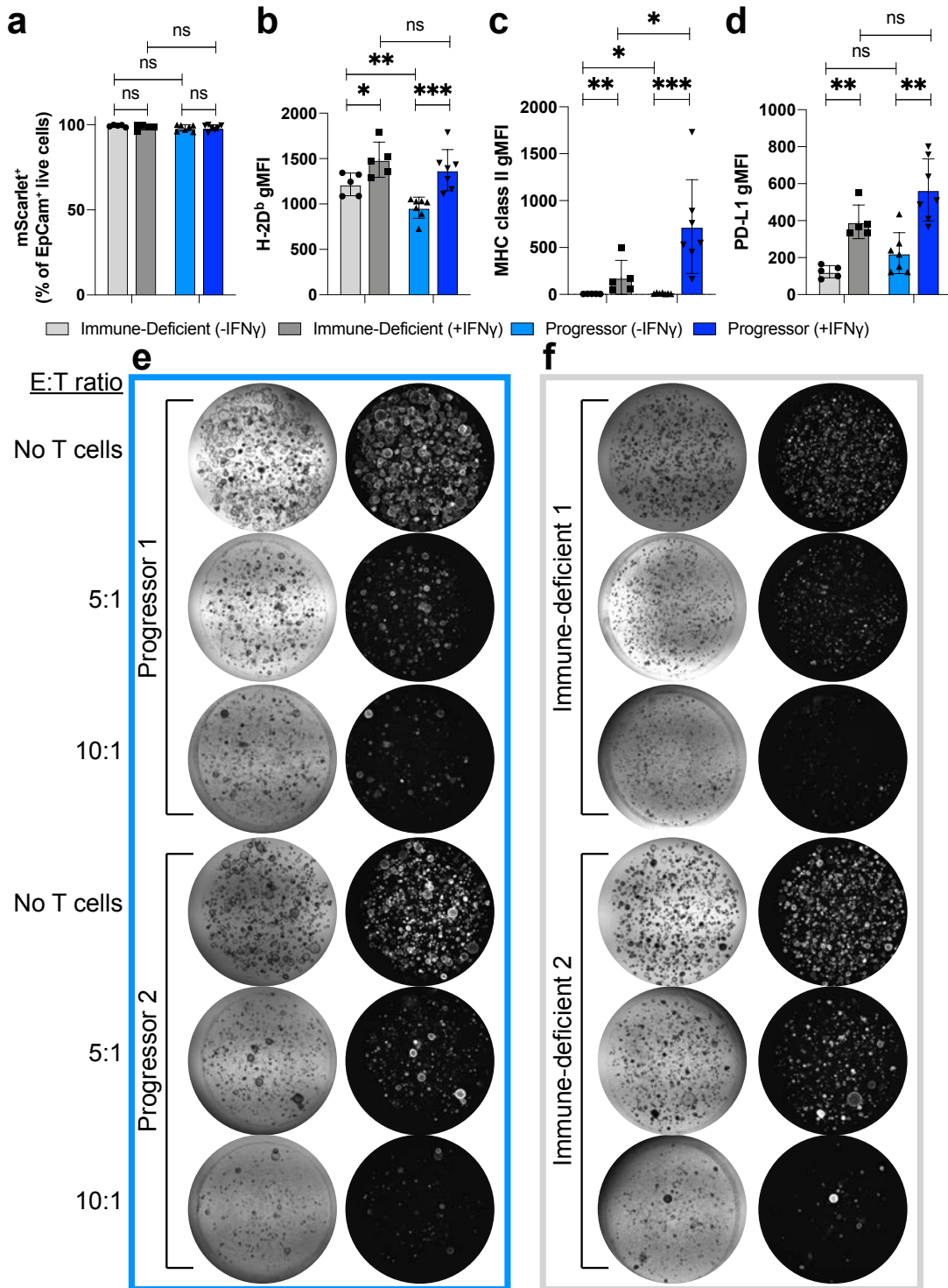
## Extended Data Figure 3



### Extended Data Figure 3

Hematoxylin and eosin (H&E) and immunohistochemical staining for cytokeratin 19 (CK19), mScarlet (RFP), CD8 $\alpha$  (CD8) and/or CD4 (CD4) on representative images for **a**, progressor with high-magnification images for representative areas of “high”, “medium” (“med”) or “low” CD8<sup>+</sup> T cell infiltration or **b**, immune-deficient animals. **c**, Flow cytometric assessment of CD44<sup>hi</sup>Tetramer<sup>+</sup>CD8<sup>+</sup> T cells during peak response in peripheral blood at 3 weeks post-initiation (scatter plots showing mean  $\pm$  SD). **d**, Flow cytometric analysis of CD8<sup>+</sup> T lymphocytes (% of live, CD45<sup>+</sup>) in progressor tumors at 5 and 8 weeks post-initiation (scatter plots showing mean  $\pm$  SD). Statistical analyses: **c,d**, two-sided Mann-Whitney test (\*\*  $P < 0.01$ ).

## Extended Data Figure 4

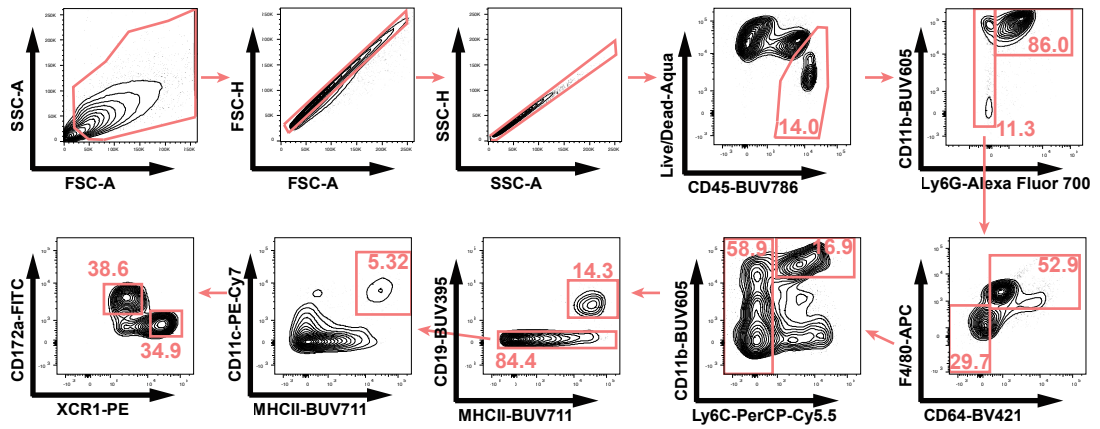


### Extended Data Figure 4

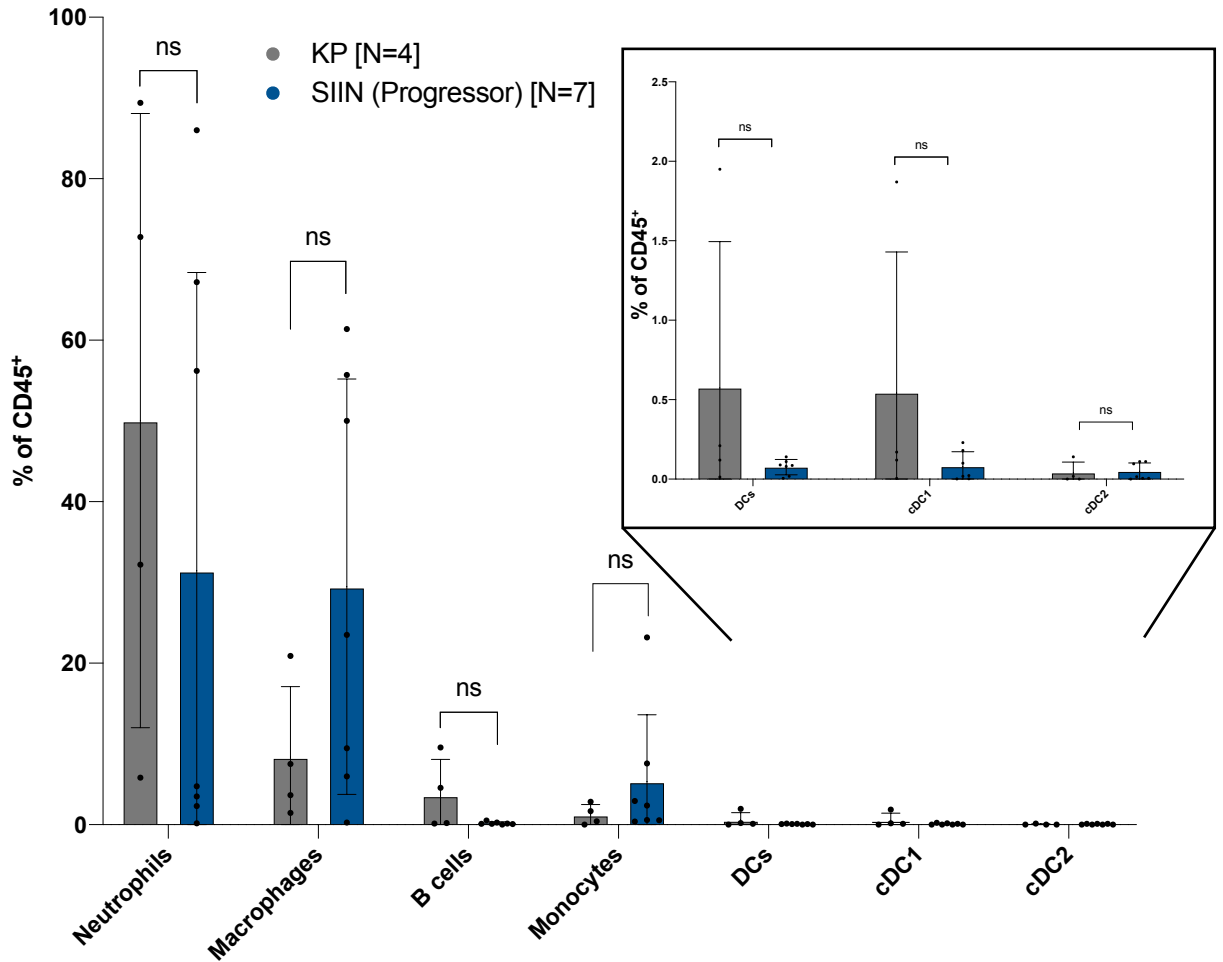
Flow cytometric assessment of **a**, mScarlet-positivity **b**, MHC-I (H-2D<sup>b</sup>) **c**, MHC-II (I-A/I-E) and **d**, PD-L1 surface expression on pancreatic tumor-derived organoids from progressor (n=7) or immune deficient (n=5) animals (all four scatter plots showing mean +/- SD). **e-f**, Representative images of Day 5 pancreatic tumor-derived organoids from progressor or immune-deficient animals either in the absence (no T cells) or presence of pre-activated OT-I CD8<sup>+</sup> T cells at 5:1 or 10:1 E:T ratios. Statistical analyses: **a-d**, two-sided Mann-Whitney test (n.s. P=non-significant, \* P < 0.05, \*\* P < 0.01, \*\*\* P < 0.001).

# Extended Data Figure 5

**a**



**b**

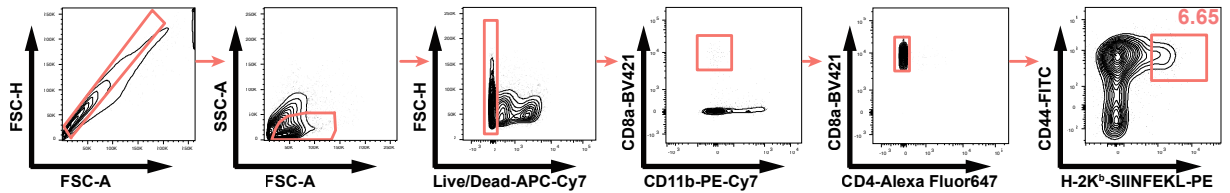


## Extended Data Figure 5

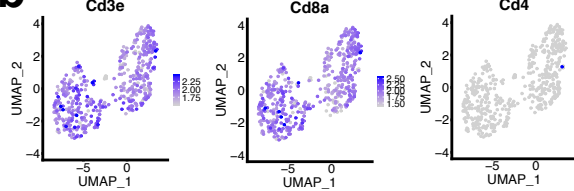
**a**, Gating strategy and **b**, Flow cytometric quantification of innate and adaptive (non-T cell) CD45<sup>+</sup> immune populations from KP (n=4) and KP;H11-SIIN progressor tumors (n=7) (scatter plots showing mean  $\pm$  SD). Statistical analyses: **b**, two-sided Mann-Whitney test (n.s., P = non-significant).

# Extended Data Figure 6

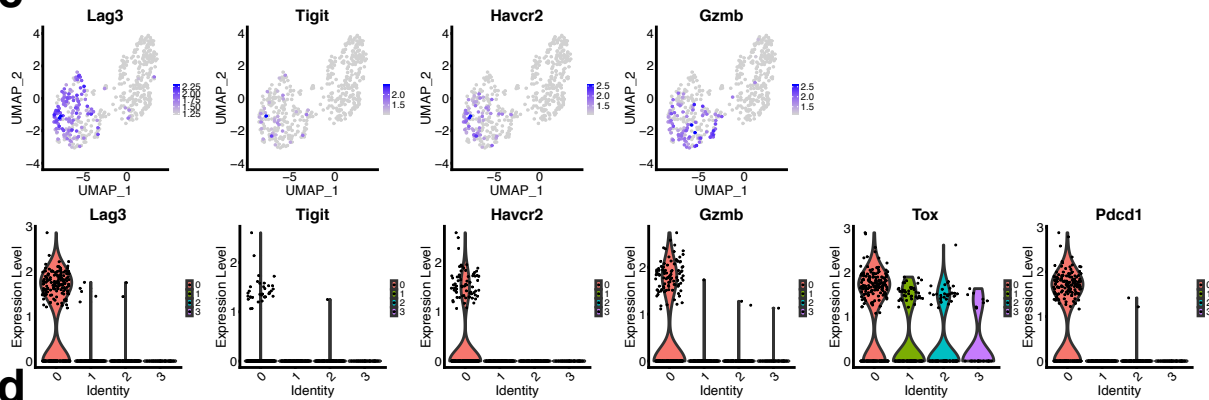
**a**



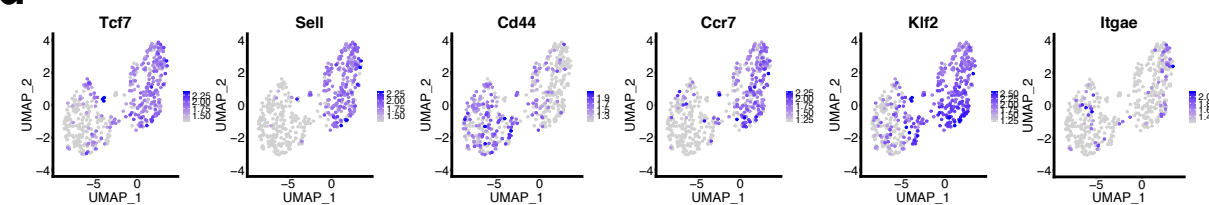
**b**



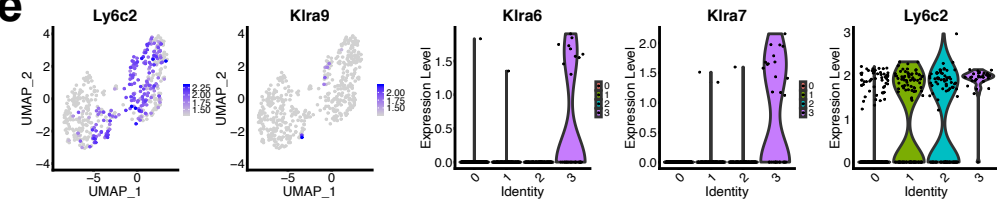
**c**



**d**



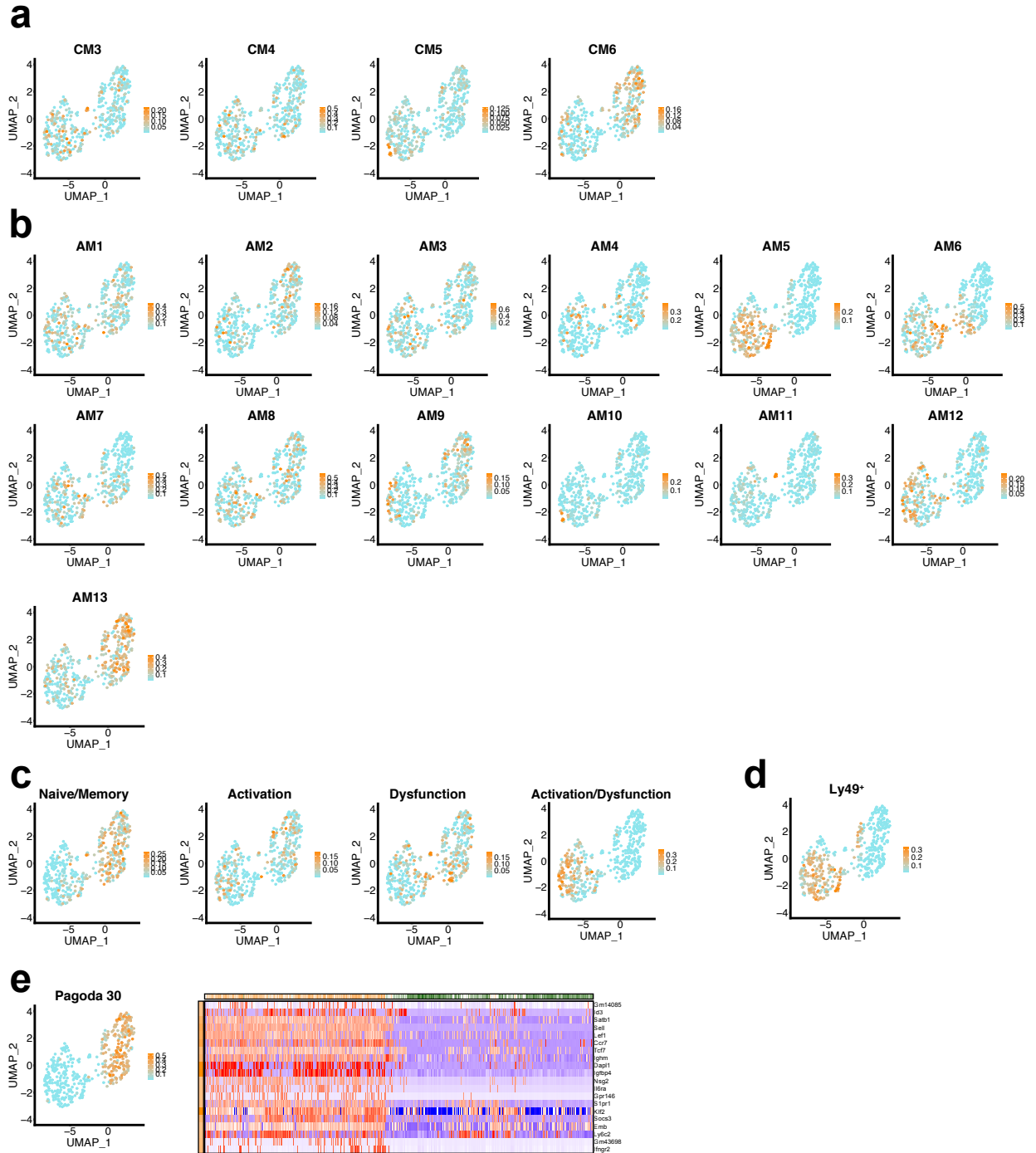
**e**



## Extended Data Figure 6

**a**, Sorting strategy for CD44<sup>hi</sup>Tetramer<sup>+</sup> CD8<sup>+</sup> TILs from progressor tumors for scRNA-Seq analysis. UMAP projections of the gene expression for **b**, quality controls: *Cd3e* (CD3), *Cd8a* (CD8 $\alpha$ ), *Cd4* (CD4). **c**, UMAP projections of the gene expression (top) and violin plots (bottom) for selected genes associated with cluster 0: *Lag3* (LAG3), *Tigit* (TIGIT), *Havcr2* (TIM3), *Pcd1* (PD-1), *Tox* (TOX), *Gzmb* (Granzyme B). **d**, UMAP projections of the gene expression for selected genes associated with clusters 1,2,3: *Tcf7* (TCF1), *Sell* (CD62L), *Cd44* (CD44), *Ccr7* (CCR7), *Klf2* (KLF2), *Itgae* (CD103). **e**, UMAP projections of the gene expression and violin plots for selected genes associated with cluster 3: *Ly6c2* (Ly6c), *Klr9* (Ly49I), *Klr6* (Ly49F), *Klr7* (Ly49G2).

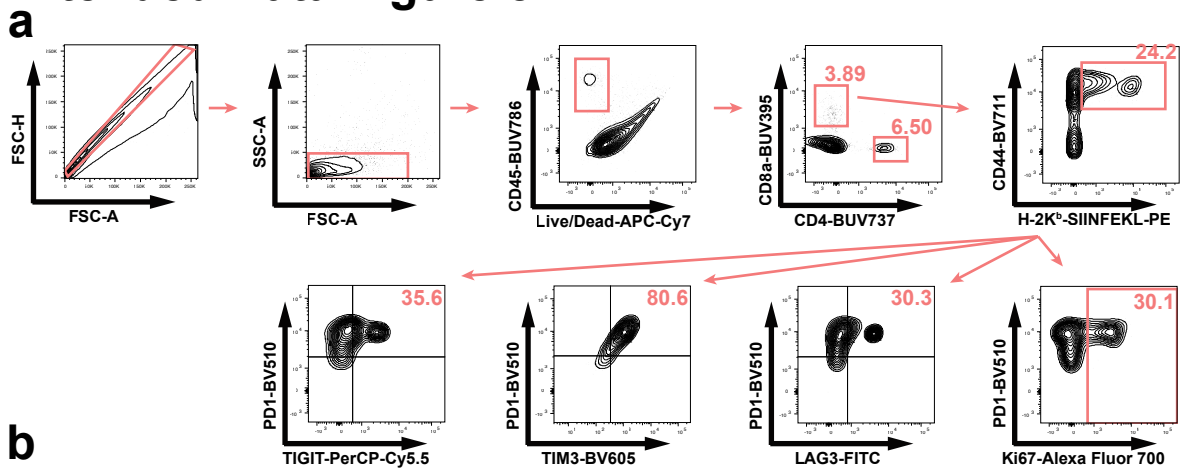
# Extended Data Figure 7



## Extended Data Figure 7

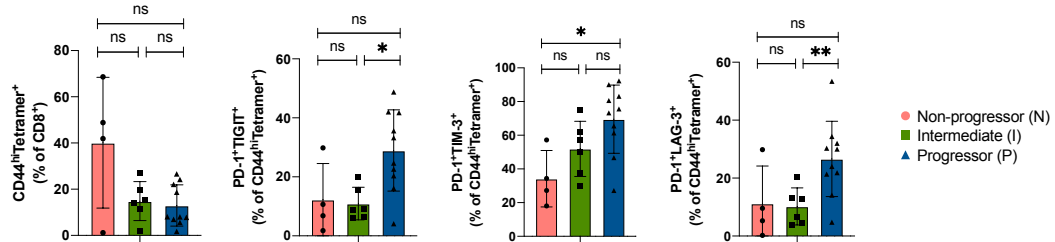
UMAP projections of the gene module expression for all remaining modules from **a**, chronic LCMV<sup>20</sup>, **b**, acute LCMV<sup>20</sup>, **c**, B16 melanoma<sup>19</sup>, **d**, Ly49<sup>+</sup> <sup>18</sup>. **e**, Heatmap and UMAP projection of the gene signature expression of Pagoda30.

# Extended Data Figure 8

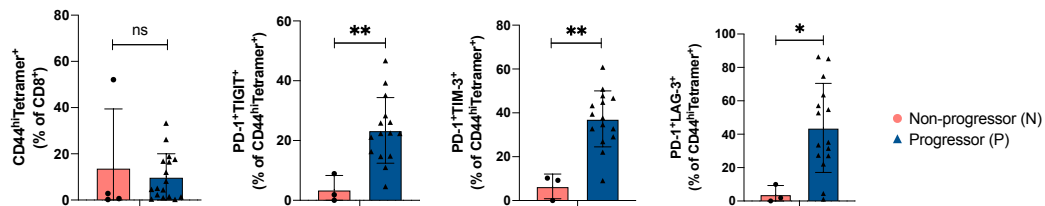


**b**

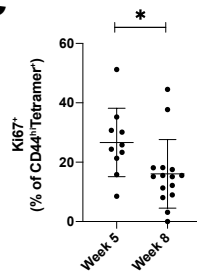
Week 5



Week 8



**c**

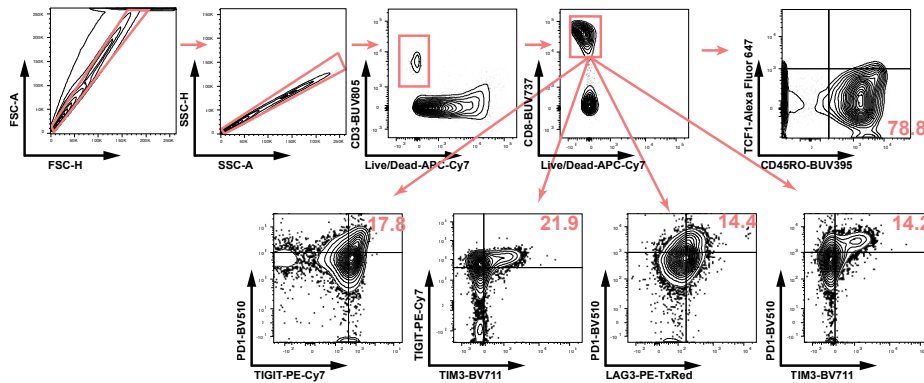


## Extended Data Figure 8

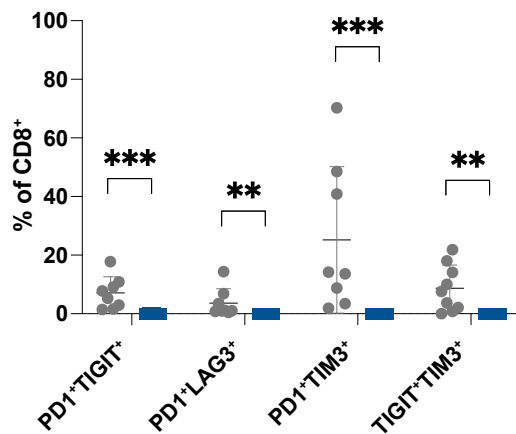
**a**, Gating strategy for immunophenotyping of CD44<sup>hi</sup>Tetramer<sup>+</sup> CD8<sup>+</sup> TILs **b**, Week 5 (top) and week 8 (bottom) analysis of CD44<sup>hi</sup>Tetramer<sup>+</sup> CD8<sup>+</sup> TILs from orthotopically transplanted KP;H11-SIIN pancreatic organoids (gated as illustrated in **a**). **c**, Ki67<sup>+</sup> population of CD44<sup>hi</sup>Tetramer<sup>+</sup> CD8<sup>+</sup> TILs from progressor tumors at defined times following tumor initiation (scatter plot showing mean +/- SD). Statistical analyses: **b,c**, two-sided Mann-Whitney test (n.s., P=non-significant, \* P < 0.05, \*\* P < 0.01).

## Extended Data Figure 9

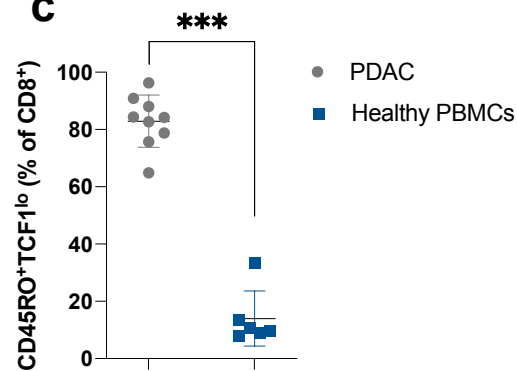
**a**



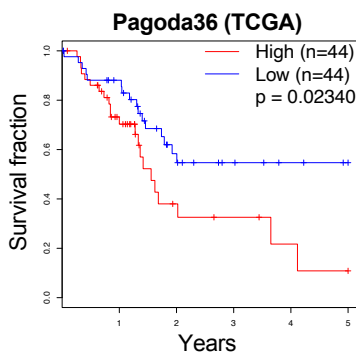
**b**



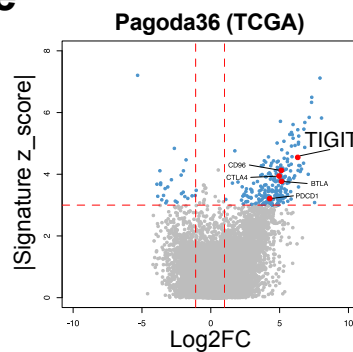
**c**



**d**



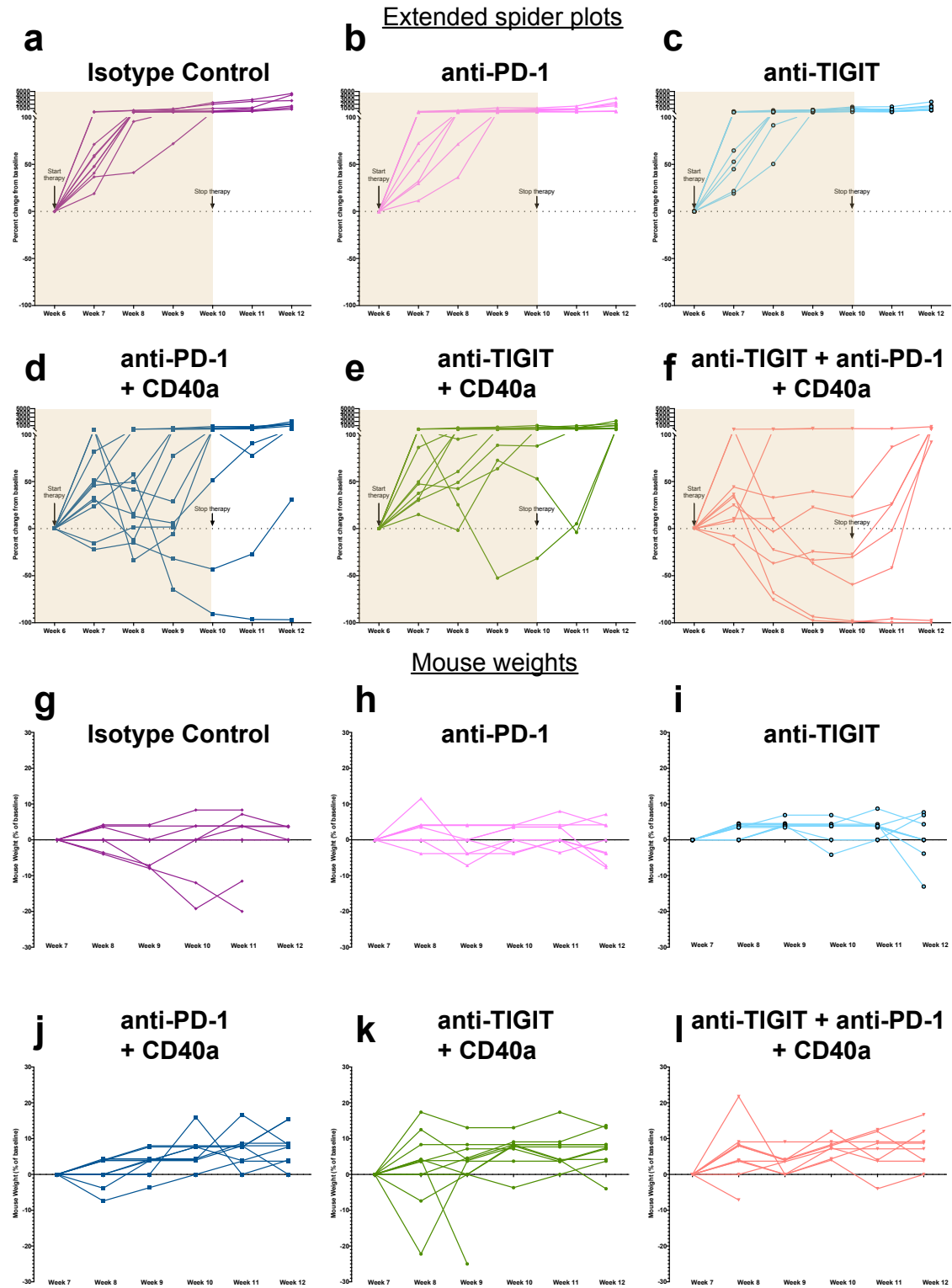
**e**



### Extended Data Figure 9

**a**, Gating strategy for immunophenotyping of CD8<sup>+</sup> TILs from human PDAC resections **b**, Quantification of co-inhibitory receptor co-expression on CD8<sup>+</sup> T cells from healthy peripheral blood mononuclear cells (PBMCs) or human PDAC resection (gated as illustrated in **a**; scatter plots showing mean +/- SD). **c**, Quantification of antigen-experienced (CD45RO<sup>+</sup>TCF1<sup>lo</sup>) CD8<sup>+</sup> TILs (scatter plots showing mean +/- SD). **d**, Kaplan-Meier survival analysis of upper ("High", red) and lower ("Low", blue) quartile TCGA PAAD patients (n=44 each) stratified by expression correlation with the murine-derived Pagoda36 gene signature. **e**, All genes ranked by their absolute z-score in the human TCGA PAAD gene signature between most and least Pagoda36-correlated cohorts (y-axis) compared to the magnitude of their fold change (x-axis, log<sub>2</sub> fold change (Log<sub>2</sub>FC) of most/least-correlated cohort expression). Selected co-inhibitory receptors highly upregulated in most-correlated tumors are highlighted in red. Statistical analyses: **b,c**, two-sided Mann-Whitney test (\*\* P < 0.01, \*\*\* P < 0.001). **d**, log-rank test (p = 0.0234)

# Extended Data Figure 10



## Extended Data Figure 10

**a-f**, Longitudinal tracking during and following therapy by small rodent ultrasound imaging with therapy start/stop times indicated (spider plot through week 10 opacified; data depicted in Figure 4e-j). **g-l**, Mouse weights during and following therapy.



### 3. Discussion

The work presented in this thesis has focused on gaining a deeper understanding of the dynamics between the immune system and pancreatic tumor progression. I have described the development of two novel, orthogonal mouse models of pancreatic cancer: an “immunogenic” *Kras*<sup>G12D/+</sup>; *Tp53*<sup>fl/fl</sup>-driven autochthonous GEMM where lentiviral instillation in the pancreatic duct induces neoantigen expression of the SIINFEKL antigen, and a *Kras*<sup>G12D</sup>; *Tp53*<sup>fl/fl</sup> organoid-based transplantation model stably expressing the SIINFEKL antigen from the *H11* genetic locus. Both models faithfully recapitulate disease progression from early pancreatic intraepithelial neoplastic (PanIN) lesions to malignant pancreatic ductal adenocarcinoma (PDAC), and distant metastatic disease. These mouse models were leveraged to longitudinally characterize the T cell response in the tumor microenvironment, as well as uncover an immunosuppressive axis that promotes tumor immune escape in PDAC. In the next sections, I will discuss the implications of these findings for our understanding of immunoediting, T cell dysfunction, and the clinical translatability of novel combination immunotherapies.

#### **3.1. Genetically engineered mouse models offer unique insights into tumor immunoediting**

Seminal work from Bob Schreiber and colleagues over the last two decades has led to the definition of the ‘cancer immunoediting’ process<sup>1,2</sup>. During cancer immunoediting, tumor-immune interactions undergo three phases: elimination, equilibrium, and escape. The immune system recognizes and eliminates antigenic tumor cells early in neoplastic growth. If the immune response is unable to completely eradicate

malignant cells from the body, the immune response enters a state of equilibrium with the (dormant) tumor, where constant selective immune pressure can drive adaptive processes in the tumor. As a result, tumors may lose antigenicity or establish immunoevasive mechanisms, which ultimately allows immune escape.

Work from our laboratory has deepened the understanding of the cancer immunoediting process by extending these findings from murine transplant models to autochthonous models. Consistent with the results in MCA-induced sarcoma models reported by Schreiber and others, autochthonous SIINFEKL-expressing sarcoma tumors undergo extensive immunoediting by T cells<sup>3</sup>. Immunoediting of these tumors leads to delayed emergence of antigen-negative tumors. In contrast, autochthonous SIINFEKL-expressing tumors arising in different tissue context, the lung, are capable of evading a strong immune response while maintaining antigenicity<sup>4</sup>. As the genetic drivers and antigens are identical in these models, this suggests that tissue origin and microenvironment play an instrumental role in shaping anti-tumor immunity. Indeed, detailed characterization of the tumor microenvironment has revealed a tumor-promoting role for the microbiome through  $\gamma\delta$  T cells<sup>5</sup>, and a role for T regulatory cells in restraining anti-tumor T cell responses to lung adenocarcinomas<sup>6,7</sup>. Additionally, immune responses in lung tumors can be potentially be restimulated through the engagement of NK cells<sup>8</sup>.

As the KPC GEMM does not allow investigation of tumor-specific T cell responses in the pancreatic microenvironment, we adapted an elegant surgical technique developed by Monte Winslow (a former postdoc in our laboratory) and colleagues at Stanford to initiate autochthonous *Kras*<sup>G12D/+</sup>, *Tp53*<sup>fl/fl</sup> ("KP") pancreatic tumors with a defined model neoantigen (SIINFEKL)<sup>9</sup>.

To our knowledge, this is the first demonstration that autochthonous pancreatic tumors are immunoedited by the CD8<sup>+</sup> T cell response. Furthermore, our work demonstrates that a subset of autochthonous tumors is capable of evading a robust tumor-specific T cell response while maintaining antigenicity. These results are consistent with observations in murine sarcoma transplant and autochthonous tumor models, where antigen loss precedes the clonal outgrowth of tumors<sup>3,10,11</sup>.

It should also be noted that a different immunogenic GEMM of pancreatic cancer was recently published by the DeNardo group<sup>12</sup>. While their model used a similar genetic background as the present study, importantly Cre-expression is controlled of the pancreas-specific *p48* locus and the ovalbumin-IRES-GFP model antigens are under tetracycline-inducible control of the *Rosa26* locus (denoted as “KPC-OG”). Interestingly, OG antigen expression accelerated PDAC progression through pro-inflammatory, pathogenic CD4<sup>+</sup> (T<sub>H</sub>17) T cell responses. In contrast to the results reported here, Hegde *et al.* found no evidence for immunoediting in their model, and late-stage PDAC tumors maintained GFP<sup>12</sup>. A number of factors could account for the differing results observed. First, KPC-OG drives the expression of full-length ovalbumin, while in the present study a truncated ovalbumin sequence encompassing SIINFEKL was used. Full-length ovalbumin contains a MHC II-restricted epitope (e.g. OVA<sub>323-339</sub>)<sup>13</sup>, which may explain the pathogenic CD4<sup>+</sup> T cell response in KPC-OG mice. It would be interesting to test if the immunoediting observed in our autochthonous tumor is influenced by a CD4<sup>+</sup> T cell response. Second, while Hegde *et al.* position their germline encoded OG antigen as a true neoantigen (i.e. not subjected to thymic tolerance), they use a vaccination and transplantation approach to argue that SIINFEKL-specific T cell responses are unaffected

in KPC-OG. However, prior results from our laboratory have demonstrated that it is possible to “break” tolerance against germline, self-antigen ( $R26^{LSL-LSIY/+}$ ) through tumor vaccination<sup>14</sup>, which raises the possibility that the OG antigen may be partially tolerized (and therefore leads to the thymic deletion of high-affinity SIINFEKL-specific CD8 T cells). A critical test of this concept is assessing whether Ovalbumin-IRES-GFP expression can be detected in the thymus, and crossing KPC-OG with transgenic TCR-recognizing SIINFEKL (“OT-I”) mice<sup>15</sup>; a decrease of peripheral OT-I T cells in the latter experiment would demonstrate that thymic tolerance is operational. Lastly, it may be helpful to investigate these model-specific differences by crossing the OG allele into the autochthonous model described here, as this may lead to new insights how nature of antigen influences tumor progression.

#### A model for immunoediting during pancreatic tumorigenesis

The kinetics and peak expansion of the antigen-specific T cell compartment suggest that immunoediting in SIINFEKL-expressing autochthonous tumors may occur relatively early during tumor development. At three weeks post-initiation, pancreatic lesions are unlikely to have progressed to adenocarcinomas and T-cell mediated immunoediting may thus be a feature of the PanIN stage. The observed lack of tumor burden differences between unedited (CD8-depleted) tumors and edited tumors further suggests that early immunoediting may have minimal effects on the progression of PanIN to adenocarcinoma.

These results suggest a model where rapid immune pressure after oncogenic transformation forces tumor evolution down divergent paths (**Figure 1a**).

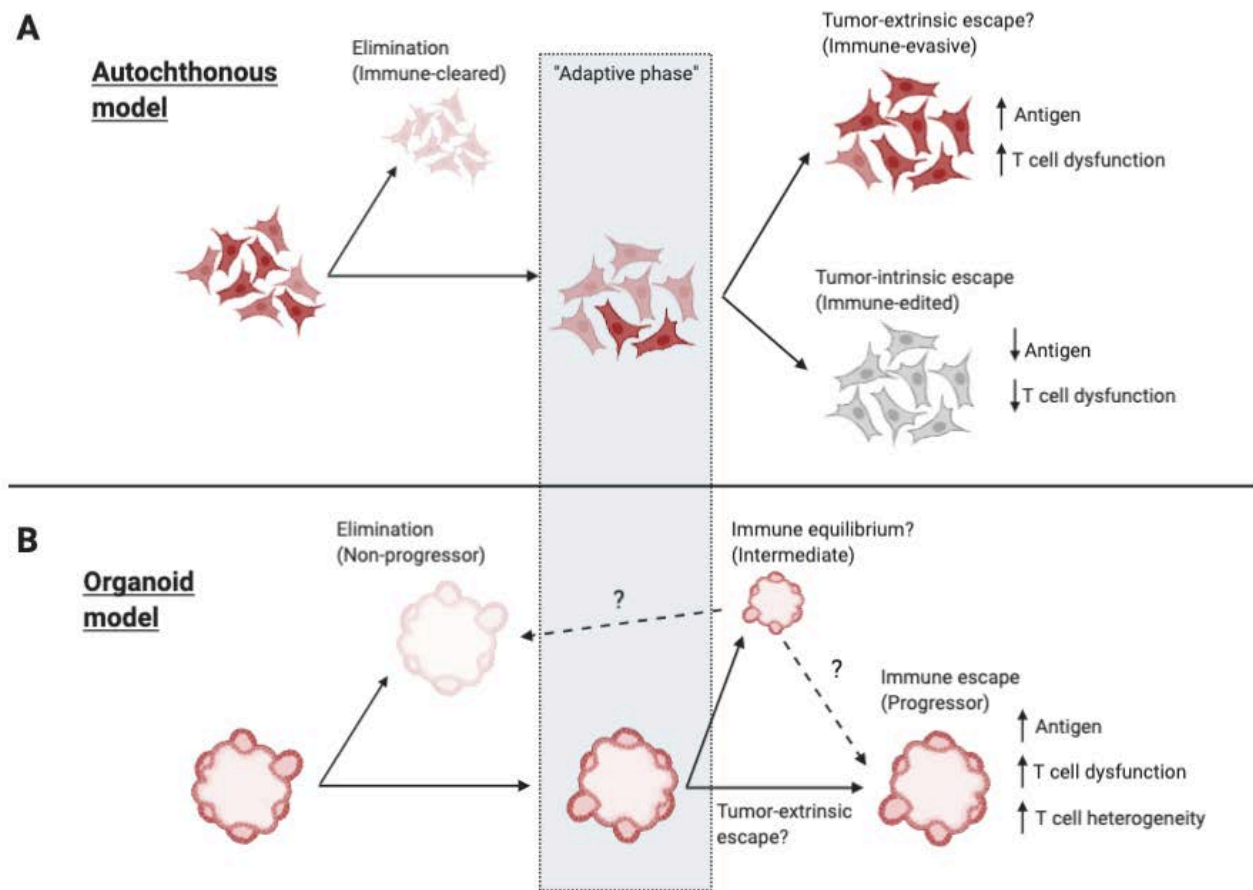


**Figure 1: Model for tumor-immune dynamics in autochthonous and organoid tumor models of pancreatic cancer.** (Created with Biorender.com)

In the first path, pancreatic lesions are unable to escape immune detection and T cell-mediated cytotoxicity, leading rapid to the removal of these clones (manifesting as “immune-cleared” phenotypes). Thus, these lesions do not progress beyond the “elimination” phase of immunoediting. Prior work has identified a crucial role for type I interferons in tumor elimination of H31m1 (sarcoma) and B16.F10 (melanoma) models<sup>16,17</sup>. It would be very interesting to investigate if a similar IFN- $\alpha/\beta$  and CD8 $\alpha$ +CD103+ (cross-presenting) dendritic cells axis is operational in early immunosurveillance of pancreatic cancer as well.

In the second path of the model, tumors are able to adapt to immune pressure, leading to further branching in tumor evolution. The majority of these tumors adapt by deregulation of antigen expression (manifesting as “immune-edited”), which then allows them to rapidly escape immune detection. An open question is the molecular mechanism that leads to antigen downregulation. Two mechanisms to explain the loss of tumor antigenicity could be envisioned. First, low SIINFEKL-expressing cancer cell clones may become selected and preferentially establish tumors. Lentiviral constructs can integrate in many regions of the genome<sup>18</sup>, which creates a population of initiating cancer cells with varying expression levels of antigen expression. Certain “hypoimmunogenic” clones may then subsequently evade immune detection and establish tumors lesions. Second, cancer cells may actively repress antigen expression, which also allows for the formation of immunoedited tumors. Although this needs to be experimentally validated, treatment of immunoedited sarcoma lines with 5-aza-2'-deoxycytidine (a DNA methylation inhibitor) was capable of restoring antigen expression<sup>3</sup>. Antigen loss could thus be mediated through the active epigenetic silencing of the lentiviral integration locus.

A subset of immune-adapting tumors is unable to deregulate antigen expression, and instead develops distinct (and possibly tumor-extrinsic) mechanisms to escape immune responses. Although the relative rarity of these immunoevasive tumors precluded us from mechanistically defining immune escape, immunophenotyping of one tumor revealed that antigen-specific CD8+ T cells were marked by the co-expression of co-inhibitory receptors, suggesting that these TILs may become dysfunctional in the tumor. T cell dysfunction is thought to be driven by chronic antigen exposure in the TME<sup>19</sup>. While it is possible that tumor escape in this setting involves a dysfunctional T cell response, it

remains to be determined whether direct tumor-CD8+ T cell interactions or additional immunosuppressive cells in the microenvironment play causal roles in mediating tumor immune escape.

### **3.2. Outlook – the potential of autochthonous models and outstanding questions**

The results obtained with the autochthonous GEMM described in this thesis highlight a number of key strengths of autochthonous tumor models. These models can be leveraged to study many biological aspects of tumor progression that may be lacking in other cancer model systems, for example in xenograft or cell line transplantation models. By initiating oncogenic transformation in single (or a focal number of) cells, autochthonous tumors faithfully model the entire histopathological disease progression from pancreatic intraepithelial neoplasias (PanIN) to locally invasive pancreatic ductal adenocarcinoma (PDAC), and even distant metastatic disease (in advanced-stage tumors). This offers an opportunity to interrogate the impact and role of oncogenic pathways on both primary tumor progression as well as metastatic spread, and indeed this work is ongoing in our laboratory. In contrast, xenograft or transplantation models rely on a single (bolus) injection of fully transformed cancer cells, which may only accurately model biological aspects of end-stage disease. Autochthonous models also allow for the investigation of the endogenous interactions between a developing tumor and the immune cells recruited to the tumor microenvironment. The autochthonous GEMM developed here closely recapitulated the characteristics of the human pancreatic tumor microenvironment, including dense stromal-rich areas with poor vasculature, and

extensive tissue fibrosis. While the present data has focused exclusively on the role of CD8+ T cells in immunoediting, this model is well-suited to explore the impact of other immune cells on tumor progression.

An outstanding question is the role of CD4+ T cells and NK cells during immunoediting responses in pancreatic tumors. Results in CD8-depleted SIINFEKL-expressing autochthonous tumors show that, while antigen expression is maintained, the majority of these “tumors” are histologically still in PanINs stages. In contrast, the vast majority of (non-SIINFEKL expressing) Cre tumors were adenocarcinomas, suggesting a tumor delay in SIINFEKL-expressing tumors, even in absence of CD8+ T cells. It is possible that CD4+ T cells through the skewing of T cell response or by acquisition of effector functions<sup>20</sup>, or alternatively, NK cells contribute to tumor control in these autochthonous tumors<sup>21</sup>. Combined CD8+CD4 or CD8+NK depletion may offer additional insights and possibly reveal a degree of functional redundancy between these immune cell types.

This immunogenic autochthonous model may also enable more extensive, phenotypic characterization of the antigen-specific T cell response. In contrast to the autochthonous *Kras*<sup>G12D/+</sup>; *Trp53*<sup>R172H/+</sup>; *Pdx-1-Cre* (“KPC”) model developed in 2005<sup>22</sup>, tumors can be initiated in the adult murine pancreas and model antigens can be introduced at will. The immunobiology of KPC tumors has been extensively investigated<sup>23</sup>, including detailed characterization of the CD8+ T cell infiltrate. Indeed, therapeutic effects achieved with treatment regimens involving combination chemoimmunotherapy in KPC mice suggest that CD8+ T cell responses are involved in this model<sup>24</sup>. However, the nature of antigens recognized by T cells in these models are unknown, thus precluding



further study of antigen-specific T cell response. In contrast, our autochthonous model enables facile longitudinal tracking of the antigen-specific T cell response. This has allowed both investigation of the early kinetics of the SIINFEKL-reactive T cell response, as well as detailed profiling of tumor-responding T cells. This system is easily adapted to accommodate different antigens or to explore the effect of a polyclonal population of neoantigens. These questions are important to consider as human PDAC is likely to harbor neoantigens with varying MHC I affinity<sup>25,26</sup>.

### **3.3. Organoid tumor immune escape may be mediated by tumor-extrinsic mechanisms of immune evasion**

The “immunogenic” tumor organoid system described in this thesis enabled more rapid elucidation of mechanisms of tumor immune escape, while still facilitating longitudinal tracking of the tumor-specific CD8+ T cell response. Transplantation of these organoids in syngeneic, immunocompetent C57BL/6J mice unexpectedly gave rise to two divergent antigenic phenotypes that were termed “progressor” and “non-progressor”, and a third intermediary state (**Figure 1b**). Below, I will discuss a number of implications that these results have on our understanding of immunoediting and immunoevasion of PDAC tumors.

#### **Lack of antigen downregulation in tumor organoids**

While autochthonous tumors are capable of escaping immune clearance through the loss of antigen expression, this mechanism does not appear to operate in tumor organoids. It is possible that the homozygous integration of the SIINFEKL allele into the *H11* locus poses an increased barrier to rapid downregulation of antigen expression, as this “safe harbor” locus is known to drive relatively stable gene expression across murine tissue types<sup>27</sup>. Additionally, homozygous integration of the allele may further safeguard against loss of heterozygosity of antigen presentation, which has been observed at the HLA locus (e.g. in human NSCLC)<sup>28</sup>.

#### Possible immune equilibrium state in intermediate tumor organoids

As the burden of intermediate tumors was indistinguishable from normal, “non-progressed” pancreatic tumor tissues, it is possible that these tumors were captured in a state of immune equilibrium. While many aspects of immune equilibrium biology remain unexplored<sup>29</sup>, experimental evidence indicates that equilibrium is associated with a quiescent cellular state, decreased reduced proliferation (Ki67), and increased apoptotic markers (TUNEL+ staining)<sup>30</sup>. Importantly, these dormant lesions are infiltrated by T cells, B220+ cells and macrophages<sup>30</sup>, suggesting that local immune activity controls these lesions. This is further functionally supported by studies demonstrating that removal of immune pressure (CD8 and CD4 depletion, or IFN- $\gamma$  neutralization) leads to rapid tumor outgrowth<sup>30</sup>. It would be interesting to explore if intermediate tumors are similarly restrained by (antigen-specific) T cell responses. Additionally, the presence of a FACS-sortable cellular marker (mScarlet) may allow for extensive transcriptional profiling of this

tumor phenotype, and establish whether these lesions are undergoing regression or active immune escape.

#### Pancreatic tumors may escape immune elimination through T cell dysfunction

Our results argue that progressor tumors did not escape immune elimination through the loss of antigenicity, deregulation of antigen presentation or the IFN- $\gamma$  pathway, which are established clinical resistance mechanisms to immune checkpoint inhibitor therapy<sup>31</sup>. Furthermore, tumor-derived progressor organoids did not develop intrinsic apoptotic resistance to T cell-mediated cytotoxicity<sup>32,33</sup>, and in fact, were rapidly killed by antigen-specific CD8+ T cells in coculture assays.

Instead, antigen-specific activated CD8+ T cells upregulated multiple co-inhibitory receptors and progressively lost proliferative capacity in progressor tumors. Moreover, tumor-specific CD8+ T cells acquired transcriptional programs that shared extensive overlap with published gene expression signatures derived from exhausted T cells in chronic LMCV<sup>34</sup> and dysfunctional intratumoral T cells in B16 melanoma<sup>35</sup>. Collectively, the data suggest that antigen-specific T cells become progressively dysfunctional over the course of pancreatic tumor progression.

A number of follow-up experiments would further strengthen the conclusion that tumor-specific CD8+ T cells become dysfunctional in organoid tumors. Dysfunctional T cells have impaired effector function (IFN- $\gamma$ , TNF- $\alpha$ , IL-2 production) and degranulation capacity (CD107a surface marker positivity)<sup>36</sup>; and indeed, experimental assessment of T cell functionality in progressor tumors is in progress. A lack of proliferative capacity and *in vivo* persistence characteristic for dysfunctional CD8+ T cells can be validated by

adoptive transfer of antigen-specific TILs into congenically marked naïve hosts and challenging these naïve hosts with SIINFEKL-expressing tumors. This approach has recently been used to demonstrate that progenitor dysfunctional intratumoral CD8<sup>+</sup> T cells are more persistent than terminal dysfunctional intratumoral CD8<sup>+</sup> T cells<sup>37</sup>. Additionally, it would be interesting to compare *in vivo* persistence and tumor control of dysfunctional CD8<sup>+</sup> T cells isolated at different stages of PDAC progression to establish whether TILs become progressively dysfunctional.

Collectively, the maintenance of tumor antigen and the acquisition of T cell dysfunctionality suggests that tumor organoid persistence drives SIINFEKL-specific T cell progressive dysfunctionality, and ultimately, a failure to control tumor growth.

An open question is whether tumor antigen persistence directly drives T cell dysfunction, or whether additional (immune) cells in the tumor microenvironment may impair anti-tumor T cell responses. The former model would be in line with a previous report from Schietinger *et al.*, utilizing a tamoxifen-inducible, autochthonous liver cancer model that expresses SV40 large T antigen (Tag) as a self-antigen<sup>19</sup>. Pre-malignant lesions in these autochthonous liver tumors rapidly induced a fixed, hyporesponsive state in Tag-specific CD8<sup>+</sup> T cells that was maintained by persistent antigen exposure. It would be interesting to compare the transcriptional profiles of early CD8<sup>+</sup> effector T cells in our organoid tumor model with the core dysfunctional program that was elucidated in the SV40-expressing liver model to test whether any core gene signatures are shared, regardless of tumor tissue localization and antigen specificity.

Although no obvious differences in the innate immune composition were found, our current data do not conclusively rule out the involvement of innate immune, stromal or T regulatory cells in driving T cell dysfunctionality during organoid tumor immune escape. In particular, TIGIT<sup>+</sup> regulatory T cells have been shown to be more activated, and suppressive cells than TIGIT<sup>-</sup> regulatory T cells in murine B16.F10 and MC38 models<sup>38</sup>. Furthermore, genetic loss of TIGIT on Tregs, but not on CD8<sup>+</sup> T cells, delayed B16.F10 tumor growth<sup>38</sup>, suggesting that Tregs actively regulated anti-tumor immunity in the melanoma model. It will be worthwhile to further immunophenotype immune cell populations in progressor tumor lesions (potentially with a focus on TIGIT) to understand their relative contribution to CD8<sup>+</sup> T cell dysfunctionality, and tumor immune escape. Elegant genetic knockout approaches as described by Kurtulus *et al.*, may also further be applied in the organoid model to dissect the contribution of different immune cells to the efficacy observed with anti-TIGIT therapy. Collectively, these approaches may elucidate into how T cell function is governed by the composition of the tumor microenvironment.

#### **3.4. Transcriptional profiling of the antigen-specific T cell compartment revealed heterogeneous effector states**

Unexpectedly, we observed considerable transcriptional heterogeneity in the anti-tumor T cell response, despite the uniform expression of a high-affinity MHC class I neoantigen (10 nM for H-2K<sup>b</sup>)<sup>39</sup> and the progressive outgrowth of tumors. Protein expression of *Pdcd-1* (PD-1), *Hacvr-3* (TIM-3), and *Lag-3* genes (cluster 0 markers), and *Klra6* (Ly49F) and *Klra7* (Ly49G) (cluster 3 markers) was experimentally validated by flow

cytometry, indicating that phenotypically distinct CD8<sup>+</sup> T cell populations are present in the tumor microenvironment.

Computational analyses (PAGODA, and gene signature mapping) revealed more intracluster heterogeneity in the exhausted T cell population, as both exhaustion and chronic effector signatures mapped to the same cluster in our dataset. These data raise the idea that this population may reflect a “spectrum” of T cell functionality in the tumor microenvironment. It is possible that chronic effector T cells may still exert (some) degree of tumor control, while more exhausted T cells have acquired a more terminal, dysfunctional cellular fate. It would be interesting to leverage adoptive transfer and tumor challenge experiments described above to further dissect the functionality and *in vivo* persistence of these potentially distinct cell populations.

Additionally, our scRNA-sequencing dataset also revealed the presence of a uniquely marked cluster (3) by the Ly49 cell-surface receptors. Ly49 proteins (and their human homologs, killer inhibitory receptors) have established roles in NK licensing<sup>40</sup>. Recently, a population of regulatory CD8<sup>+</sup> T cells has been described in a murine experimental model of multiple sclerosis<sup>41</sup>. Interestingly, these Ly49<sup>+</sup>CD8<sup>+</sup> T cells were antigen-specific, and suppressed CD4<sup>+</sup> T cells *in vitro* through perforin-mediated killing<sup>41</sup>. However, antigen-specific Ly49<sup>+</sup>CD8<sup>+</sup> T cells have not been reported in tumor models. It would therefore be very interesting to further establish the functional relevance of this population of Ly49<sup>+</sup>CD8<sup>+</sup> T cells through adoptive transfer of co-mixed antigen-specific T cells (effector CD8<sup>+</sup> T cells + Ly49<sup>+</sup>CD8<sup>+</sup> T cells) and through *in vitro* T cell co-culture assays.

### **3.5. Outlook – The future of immunotherapy in pancreatic ductal adenocarcinoma through the lens of genetically engineered mouse models**

Although pancreatic cancer has long been regarded as “immunologically silent”, recent advances in our understanding of this complex disease have overturned that dogma. Computational analyses of PDAC antigenicity have revealed that pancreatic tumors indeed carry antigens that may be recognized by the human immune system<sup>25,26</sup>. This is also supported by histological and flow cytometric studies demonstrating the presence of activated, dysfunctional tumor-infiltrating lymphocytes in human PDAC<sup>42</sup>, including the characterization presented in this thesis. Furthermore, at least a subset of PDAC (MMR-deficient) patients can already derive clinical benefit from currently approved immunotherapies<sup>43</sup>, demonstrating that this disease is not inherently resistant to immune-targeted therapies. Lastly, exceptional long-term survivors of PDAC appear to carry a unique set of high quality neoantigens capable of stimulating robust, clonal T cell responses<sup>26</sup>, suggesting at least a subset of patients harbor highly tumor-reactive T cells.

Unfortunately, despite the widespread clinical efficacy of immune checkpoint inhibitors in many solid and hematopoietic cancers, MMR-proficient pancreatic ductal adenocarcinoma has largely remained refractory to immune checkpoint monotherapy and combination immune therapy. This is certainly not due to a lack of clinical effort in the field; as described in the introduction of this thesis, numerous combinations of immunomodulatory therapeutics have been investigated for the treatment of metastatic PDAC.

A theme that emerges from this thesis is that further clinical development can be driven by novel biological insights made in murine mouse models of cancer. To this end,

we have developed and characterized novel immunogenic genetically engineered mouse models of PDAC. Although many facets of the anti-tumor T cell response in these models remain to be explored, our preclinical studies reinforce that the biology of the pancreatic tumor microenvironment can guide rational design of novel immunotherapeutic strategies. A deeper understanding of the immunoevasive mechanisms employed by tumors will enable application of clinical strategies with increased sophistication. I am hopeful that armed with these biological insights, we can improve the lives of pancreatic cancer with curative immunotherapies.



### 3.6. References

1. Dunn, G. P., Old, L. J. & Schreiber, R. D. The Three Es of Cancer Immunoediting. *Annu. Rev. Immunol.* **22**, 329–360 (2004).
2. Schreiber, R. D., Old, L. J. & Smyth, M. J. Cancer immunoediting: Integrating immunity's roles in cancer suppression and promotion. *Science (80-. )*. **331**, 1565–1570 (2011).
3. DuPage, M., Mazumdar, C., Schmidt, L. M., Cheung, A. F. & Jacks, T. Expression of tumour-specific antigens underlies cancer immunoediting. *Nature* **482**, 405–409 (2012).
4. DuPage, M. *et al.* Endogenous T cell responses to antigens expressed in lung adenocarcinomas delay malignant tumor progression. *Cancer Cell* **19**, 72–85 (2011).
5. Jin, C. *et al.* Commensal Microbiota Promote Lung Cancer Development via  $\gamma\delta$  T Cells. *Cell* **176**, 998-1013.e16 (2019).
6. Joshi, N. S. *et al.* Regulatory T Cells in Tumor-Associated Tertiary Lymphoid Structures Suppress Anti-tumor T Cell Responses. *Immunity* 1–12 (2015) doi:10.1016/j.immuni.2015.08.006.
7. Li, A. *et al.* IL-33 Signaling Alters Regulatory T Cell Diversity in Support of Tumor Development. *Cell Rep.* **29**, 2998-3008.e8 (2019).
8. Schmidt, L. *et al.* Enhanced adaptive immune responses in lung adenocarcinoma through natural killer cell stimulation. doi:10.1073/pnas.1904253116.
9. Chiou, S. H. *et al.* Pancreatic cancer modeling using retrograde viral vector delivery and in vivo CRISPR/Cas9-mediated somatic genome editing. *Genes Dev.* **29**, 1576–1585 (2015).
10. Shankaran, V. *et al.* IFN $\gamma$ , and lymphocytes prevent primary tumour development and shape tumour immunogenicity. *Nature* **410**, 1107–1111 (2001).
11. Matsushita, H. *et al.* Cancer exome analysis reveals a T-cell-dependent mechanism of cancer immunoediting. *Nature* **482**, 400–404 (2012).
12. Hegde, S. *et al.* Dendritic Cell Paucity Leads to Dysfunctional Immune Surveillance in Pancreatic Cancer. *Cancer Cell* **37**, 289-307.e9 (2020).
13. Mcfarland, B. J., Sant, A. J., Lybrand, T. P. & Beeson, C. Ovalbumin(323-339) Peptide Binds to the Major Histocompatibility Complex Class II I-A d Protein Using Two Functionally Distinct Registers †. (1999) doi:10.1021/bi991393l.
14. Cheung, A. F., DuPage, M. J. P., Dong, H. K., Chen, J. & Jacks, T. Regulated expression of a tumor-associated antigen reveals multiple levels of T-cell tolerance in a mouse model of lung cancer. *Cancer Res.* **68**, 9459–9468 (2008).
15. Hogquist, K. A. *et al.* T cell receptor antagonist peptides induce positive selection. *Cell* **76**, 17–27 (1994).
16. Fuertes, M. B. *et al.* Host type I IFN signals are required for antitumor CD8+ T cell responses through CD8 $\alpha$ + dendritic cells. *J. Exp. Med.* **208**, 2005–2016 (2011).
17. Diamond, M. S. *et al.* Type I interferon is selectively required by dendritic cells for immune rejection of tumors. *J. Exp. Med.* **208**, 1989–2003 (2011).
18. Lewinski, M. K. *et al.* Retroviral DNA integration: Viral and cellular determinants of

- target-site selection. *PLoS Pathog.* **2**, 0611–0622 (2006).
19. Schietinger, A. *et al.* Tumor-Specific T Cell Dysfunction Is a Dynamic Antigen-Driven Differentiation Program Initiated Early during Tumorigenesis. *Immunity* **45**, 389–401 (2016).
  20. Juno, J. A. *et al.* Cytotoxic CD4 T cells-friend or foe during viral infection? *Frontiers in Immunology* vol. 8 (2017).
  21. Böttcher, J. P. *et al.* NK Cells Stimulate Recruitment of cDC1 into the Tumor Microenvironment Promoting Cancer Immune Control. *Cell* **172**, 1022-1037.e14 (2018).
  22. Hingorani, S. R. *et al.* Trp53R172H and KrasG12D cooperate to promote chromosomal instability and widely metastatic pancreatic ductal adenocarcinoma in mice. *Cancer Cell* **7**, 469–483 (2005).
  23. Lee, J. W., Komar, C. A., Bengsch, F., Graham, K. & Beatty, G. L. Genetically engineered mouse models of pancreatic cancer: The KPC model (LSL-KrasG12D/+;LSL-Trp53R172H/+;Pdx-1-Cre), its variants, and their application in immuno-oncology drug discovery. *Curr. Protoc. Pharmacol.* **2016**, 14.39.1-14.39.20 (2016).
  24. Byrne, K. T. & Vonderheide, R. H. CD40 Stimulation Obviates Innate Sensors and Drives T Cell Immunity in Cancer. *Cell Rep.* **15**, 2719–2732 (2016).
  25. Bailey, P. *et al.* Exploiting the neoantigen landscape for immunotherapy of pancreatic ductal adenocarcinoma. *Sci. Rep.* **6**, 1–8 (2016).
  26. Balachandran, V. P. *et al.* Identification of unique neoantigen qualities in long-term survivors of pancreatic cancer. *Nature* **551**, S12–S16 (2017).
  27. Tasic, B. *et al.* Site-specific integrase-mediated transgenesis in mice via pronuclear injection. *Proc. Natl. Acad. Sci. U. S. A.* **108**, 7902–7907 (2011).
  28. McGranahan, N. *et al.* Allele-Specific HLA Loss and Immune Escape in Lung Cancer Evolution. *Cell* **171**, 1259-1271.e11 (2017).
  29. Teng, M. W. L., Swann, J. B., Koebel, C. M., Schreiber, R. D. & Smyth, M. J. Immune-mediated dormancy: an equilibrium with cancer. *J. Leukoc. Biol.* **84**, 988–993 (2008).
  30. Koebel, C. M. *et al.* Adaptive immunity maintains occult cancer in an equilibrium state. *Nature* **450**, 903–907 (2007).
  31. Kalbasi, A. & Ribas, A. Tumour-intrinsic resistance to immune checkpoint blockade. *Nat. Rev. Immunol.* **20**, 25–39 (2020).
  32. Kataoka, T. *et al.* FLIP prevents apoptosis induced by death receptors but not by perforin/granzyme B, chemotherapeutic drugs, and gamma irradiation. *J. Immunol.* **161**, 3936–42 (1998).
  33. Hinz, S. *et al.* Bcl-X(L) protects pancreatic adenocarcinoma cells against CD95- and TRAIL-receptor-mediated apoptosis. *Oncogene* **19**, 5477–5486 (2000).
  34. Doering, T. A. *et al.* Network Analysis Reveals Centrally Connected Genes and Pathways Involved in CD8+ T Cell Exhaustion versus Memory. *Immunity* **37**, 1130–1144 (2012).
  35. Singer, M. *et al.* A Distinct Gene Module for Dysfunction Uncoupled from Activation in Tumor-Infiltrating T Cells. *Cell* **166**, 1500-1511.e9 (2016).
  36. Wherry, E. J. T cell exhaustion. *Nature Immunology* vol. 12 492–499 (2011).
  37. Miller, B. C. *et al.* Subsets of exhausted CD8+ T cells differentially mediate tumor

- control and respond to checkpoint blockade. *Nat. Immunol.* **20**, 326–336 (2019).
38. Kurtulus, S. *et al.* TIGIT predominantly regulates the immune response via regulatory T cells. *J. Clin. Invest.* **125**, 4053–4062 (2015).
  39. Karandikar, S. H. *et al.* Identification of epitopes in ovalbumin that provide insights for cancer neoepitopes. *JCI Insight* **4**, (2019).
  40. Rahim, M. M. A. *et al.* Ly49 receptors: Innate and adaptive immune paradigms. *Frontiers in Immunology* vol. 5 145 (2014).
  41. Saligrama, N. *et al.* Opposing T cell responses in experimental autoimmune encephalomyelitis. *Nature* **572**, 481–487 (2019).
  42. Stromnes, I. M., Hulbert, A., Pierce, R. H., Greenberg, P. D. & Hingorani, S. R. T-cell Localization, Activation, and Clonal Expansion in Human Pancreatic Ductal Adenocarcinoma. *Cancer Immunol. Res.* **5**, 978–991 (2017).
  43. Le, D. T. *et al.* Evaluation of ipilimumab in combination with allogeneic pancreatic tumor cells transfected with a GM-CSF gene in previously treated pancreatic cancer. *J. Immunother.* **36**, 382–389 (2013).

## Appendix I

### Progressor tumors are sensitive to adoptive cell therapy

Laurens J Lambert<sup>1,2‡</sup>, William A Freed-Pastor<sup>1,3‡</sup>, Tyler Jacks<sup>1,2,4\*</sup>

1 David H. Koch Institute for Integrative Cancer Research, Massachusetts Institute of Technology, Cambridge, MA 02139, USA

2 Department of Biology, Massachusetts Institute of Technology, Cambridge, MA 02139, USA

3 Department of Medical Oncology, Dana-Farber Cancer Institute, Boston, MA, USA

2 Department of Biology, Massachusetts Institute of Technology, Cambridge, MA 02139, USA

4 Howard Hughes Medical Institute, Massachusetts Institute of Technology, Cambridge, MA 02139, USA

\*Corresponding author

‡These authors contributed equally to this work

#### Author contributions

L.J.L., W.F.P., and T.J. conceived of, designed and directed the study; L.J.L., W.F.P. performed all types of experiments reported in the study; L.J.L. wrote this appendix.

## Abstract

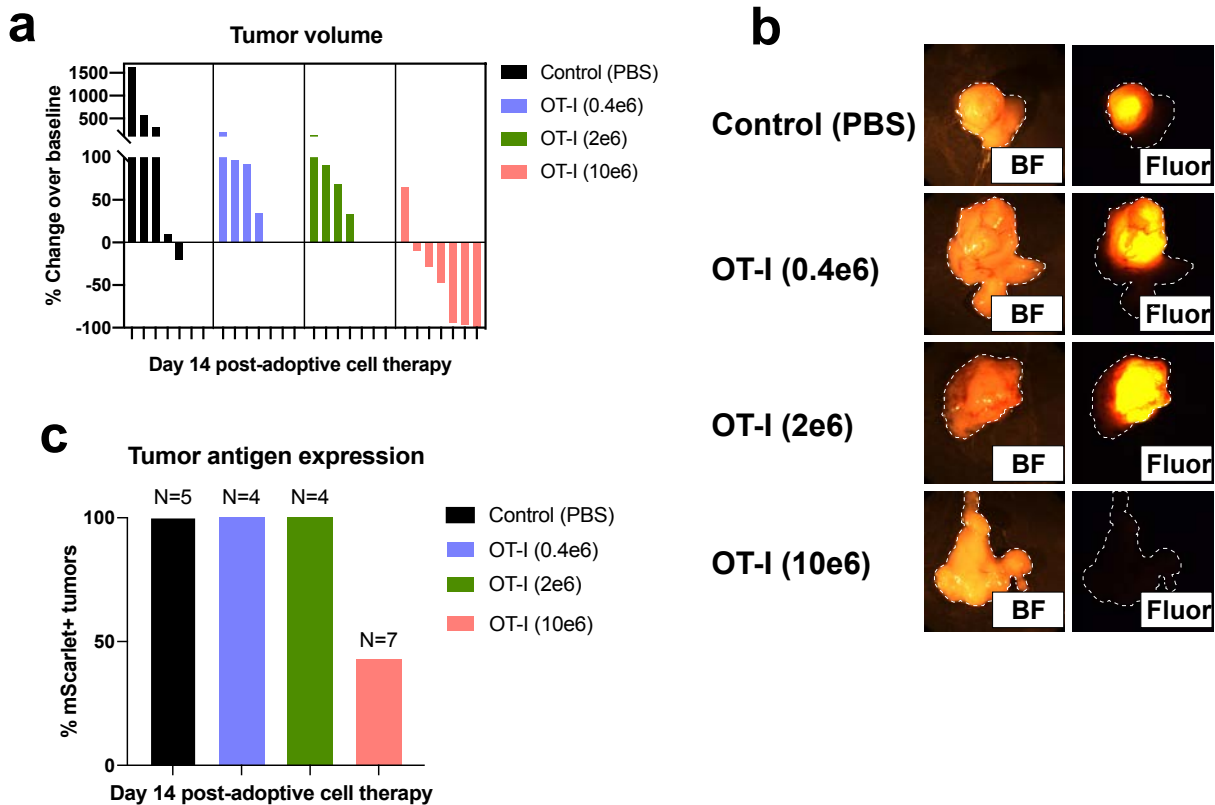
Over the past decade, cancer immunotherapies have achieved durable responses in many types of solid and hematological tumors. However, mismatch-proficient pancreatic ductal adenocarcinoma (PDAC) has remained largely refractory to immune-based therapeutic approaches<sup>1-3</sup>. In a previous study, we described the development of a neoantigen-expressing organoid-based preclinical model to investigate the molecular and cellular mechanisms that drive immune evasion in PDAC (Freed-Pastor, Lambert *et al.*, unpublished). Here we demonstrate that this preclinical organoid system remains sensitive to adoptive T cell therapy. These findings position this model system as a preclinical platform to further investigate T cell-centric approaches for the treatment of PDAC.

## Main text

To further characterize the sensitivity of a previously described neoantigen-expressing organoid-based pancreatic adenocarcinoma (PDAC) system (Freed-Pastor, Lambert *et al.*, unpublished) to adoptive cell therapy, the following approach was taken.

*Kras*<sup>LSL-G12D/+</sup>; *Trp53*<sup>fl/fl</sup>; *H11mScarletSIIN* (*KP*; *H11-SIN*) pancreatic organoids were first orthotopically transplanted into immune-competent mice and tumor growth was monitored by small rodent ultrasound. Tumors that demonstrated increase in volume over two successive ultrasound scans at week 4 and 5 post-transplantation were then subjected to adoptive cell therapy treatment. Tumor-bearing mice were randomized to either control treatment (PBS; n=5), or treatment with pre-activated with transgenic TCR-recognizing SIINFEKL (“OT-I”) T cells<sup>4</sup> at varying doses ( $0.4 \times 10^6$  T cells (n=4);  $2 \times 10^6$  T

cells (n=4); or  $10 \times 10^6$  T cells (n=7)). As expected, progressor tumors in the control treatment arm continued to grow unabated (**Appendix Figure 1a**). In the treatment arm, progressor tumors treated with low dose or intermediate doses of OT-I largely continued to grow, albeit at a slower rate compared to control progressor tumors. Strikingly, high dose OT-I treatment led to robust tumor regression in the majority of animals (6/7; ~86%). Consistent with these observations, tumor antigen expression was maintained in control and low- and intermediate-dose progressor tumors, while only a minority of progressor tumors had demonstrable tumor antigen expression in the high-dose OT-I treatment arm (3/7; ~43%; **Appendix Figure 1b,c**). Together, these results suggest that a sufficiently robust anti-tumor T cell response can effectively control tumor growth.



**Appendix Figure 1: Adoptive cell transfer (ACT) of pre-activated OT-I CD8<sup>+</sup> T cells leads to rapid tumor regression in previously progressing tumors.** **a**, Waterfall plots of treatment response assessed by rodent ultrasound after transfer of preactivated OT-I CD8<sup>+</sup> T cells (T cell dose in brackets). **b**, Representative images of brightfield (left) and fluorescent (right) images of *Kras*<sup>G12D/+</sup>; *Trp53*<sup>-/-</sup>; *Hipp1*<sup>mScarletSIIN</sup> ('KP;H11-SIIN') pancreatic tumor organoids at 2 weeks post-ACT. **c**, Tumor antigen expression as assessed by mScarlet fluorescence upon necropsy.

## Discussion

Adoptive cell therapy (ACT) has shown tremendous clinical promise in hematological malignancies<sup>5-7</sup>. While a number of clinical studies have investigated ACT in pancreatic cancer<sup>8-12</sup>, clinical responses have been limited. Our observations that adoptively transferred T cells elicit robust pancreatic tumor regressions in a dose-dependent manner are therefore notable, particularly since the endogenous T cell response is incapable of controlling tumor growth. These results suggest that immune evasion in pancreatic tumors may be overcome with sufficiently robust T cell priming and expansion. Furthermore, the model system described here presents a unique opportunity

to dissect the molecular and cellular mechanisms that limit the efficacy of ACT in PDAC. Leveraging these insights will be crucial for the development of novel, potent T-cell centric therapeutic strategies.

## Methods

### Mice

All animal studies described in this study were approved by the MIT Institutional Animal Care and Use Committee. All animals were maintained on a pure C57BL/6J genetic background. *OT-I* TCR transgenic mice have been previously described<sup>4</sup>.

### Progressor organoid generation and characterization

The generation of the parental *Kras*<sup>LSL-G12D/+</sup>;*Trp53*<sup>fl/fl</sup>;*H11mScarletSIIN* (*KP*; *H11-SIIN*) pancreatic organoid line has been previously described (Freed-Pastor, Lambert *et al.*, unpublished). Briefly, progressor pancreatic organoids were isolated by manually dissecting pancreata from mice with established *KP*;*H11-SIIN* tumors. Pancreata were manually minced with razor blades and dissociated in pancreas digestion buffer [1x PBS, 125 U/mL collagenase IV (Worthington)] for 30 min at 37°C. Cell suspensions were filtered through 70 µm filters, washed with 1x PBS and centrifuged with slow deceleration. Cell pellets were resuspended in 100% growth-factor reduced Matrigel (Corning) and solidified at 37°C. Cells were subsequently cultured in organoid complete media (minor modifications from previously described formulations<sup>13</sup> see details below) and monitored for organoid outgrowth. Organoids were passaged with TrypLE Express (Life Technologies) for at least 4 passages to remove contaminating cell types. P53 deficient



organoids were selected via resistance to Nutlin-3a (10  $\mu$ M, Sigma-Aldrich). Pancreatic organoids were maintained in culture for <20 passages before orthotopic transplantation into C57BL6/J mice.

### **Pancreatic Organoid Complete Media**

The media for pancreatic organoids was formulated based on L-WRN cell conditioned media (L-WRN CM)<sup>14</sup>. Briefly, L-WRN CM was generated by collecting 8 days of supernatant from the L-WRN cells, grown in Advanced DMEM/F12 (Gibco) supplemented with 20% fetal bovine serum (Hyclone), 2 mM GlutaMAX, 100 units/mL of penicillin, 100  $\mu$ g/mL of streptomycin, and 0.25  $\mu$ g/mL amphotericin. L-WRN CM was diluted 1:1 in Advanced DMEM/F12 (Gibco) and supplemented with additional RSPO-1 conditioned media (10% v/v), generated using Cultrex HA-R-Spondin1-Fc 293T Cells. The following molecules were also added to the growth media: B27 (Gibco), 1  $\mu$ M N-acetylcysteine (Sigma-Aldrich), 10  $\mu$ M nicotinamide (Sigma-Aldrich), 50 ng/mL EGF (Novus Biologicals), 500 nM A83-01 (Cayman Chemical), 10  $\mu$ M SB202190 (Cayman Chemical), and 500 nM PGE2 (Cayman Chemical). Wnt activity of the conditioned media was assessed and normalized between batches via luciferase reporter activity of TCF/LEF activation (Enzo Leading Light Wnt reporter cell line).

### **Orthotopic transplantation**

Orthotopic transplantation of organoids was performed with minor modifications to previously reported protocols for orthotopic transplantation of pancreatic monolayer cell lines<sup>15</sup>. Briefly, animals were anesthetized using Isoflurane, the left subcostal region

was depilated (using clippers or Nair) and the surgical area was disinfected with alternating Betadine/Isopropyl alcohol. A small (~2 cm) skin incision was made in the left subcostal area and the spleen was visualized through the peritoneum. A small incision (~2 cm) was made through the peritoneum overlying the spleen and the spleen and pancreas were exteriorized using ring forceps. A 30G needle was inserted into the pancreatic parenchyma parallel to the main pancreatic artery and 100  $\mu$ L (containing  $1.25 \times 10^5$  organoid cells in 50% PBS + 50% Matrigel) was injected into the pancreatic parenchyma. Successful injection was visualized by formation of a fluid-filled region within the pancreatic parenchyma without leakage. The pancreas/spleen were gently internalized, and the peritoneal and skin layers were sutured independently using 4-0 Vicryl sutures. All mice received pre-operative analgesia with Buprenorphine-SR and were followed post-operatively for any signs of discomfort or distress. Organoid/Matrigel mixes were kept on ice throughout the entirety of the procedure to prevent solidification prior to injection.

For orthotopic transplantation, syngeneic mice (aged 4-10 weeks) were transplanted. Male pancreatic organoids were only transplanted back into male recipients.

### **T cell culture and transfer**

OT-I splenocytes were harvested from C57BL/6J *OT-I;Rag2<sup>-/-</sup>* transgenic mice, and spleens were mashed through 70  $\mu$ m filters. Red blood cells were lysed with ACK buffer for 2 min before cell suspension neutralization with PBS and pelleted for plating. Splenocytes were counted and adjusted to  $1 \times 10^6$  cells/mL in T cell medium [RPMI 1640 (Corning) supplemented with 10% heat-inactivated FBS, 20 mM HEPES (Gibco), 1 mM

Sodium Pyruvate (Thermo Fisher), 2 mM L-Glutamine (Gibco), 50  $\mu$ M  $\beta$ -mercaptoethanol (Gibco), 1x NEAA (Sigma), 0.5x Pen/Strep (Gibco) with 10 ng/mL hIL-2 (Peprotech) and 1  $\mu$ M SIINFEKL peptide (Anaspec)]. Splenocytes were activated for 24 hr at 37°C in a tissue culture incubator, before manual CD8 $\alpha^+$  isolation according to the manufacturer instructions (Milteny Biotec). OT-I T cells were subsequently expanded 4-6 days in T cell medium with 10 ng/mL hIL-2 prior to organoid co-culture before adoptive T cell transfer at varying dose of T cells ( $0.4 \times 10^6$ ,  $2 \times 10^6$  or  $10 \times 10^6$  T cells).

### **Small rodent ultrasound**

Quantification of murine pancreatic tumors by high resolution ultrasound has been previously described<sup>16</sup>. Briefly, animals were anesthetized using Isoflurane and the lateral and ventral abdominal areas were depilated using Nair. Sterile 0.9% saline (1 mL) was administered by intraperitoneal injection prior to imaging to improve visualization of the pancreas. Animals were imaged using the Vevo3100/LAZRX ultrasound and photoacoustic imaging system (Fujifilm-Visualsonics). Animals were placed on the imaging platform in the supine position and a layer of ultrasound gel was applied over the entirety of the abdominal area. The ultrasound transducer (VisualSonics 550S) was placed on the abdomen orthogonal to the plane of the imaging platform. Landmark organs, such as the kidney, spleen, and liver, were identified in order to define the area of the pancreas. The transducer was set at the scanning midpoint of the normal pancreas or pancreatic tumor and a 3D image of 10-20 mm, depending on tumor size, at a Z- slice thickness of 0.04 mm. Three-dimensional (3D) images were uploaded to the Vevo Lab

Software. The volumetric analysis function was used to define the tumor border at various Z-slices through the entirety of the tumor and derive the final calculated tumor volume.

### **Statistical Analyses**

All graphs and statistical analyses were generated with GraphPad Prism 8. The two-sided Mann-Whitney test was performed in GraphPad Prism

### **Acknowledgments**

We thank the entire Jacks laboratory for helpful discussions. We thank K. Yee, J. Teixeira, K. Anderson, M. Magendantz for administrative support. This work was supported by the Howard Hughes Medical Institute, NCI Cancer Center Support Grant P30-CA1405, the Lustgarten Foundation Pancreatic Cancer Research Laboratory at MIT, DFHCC SPORE in Gastrointestinal Cancer Career Enhancement Award (W.F.P.), the Stand Up To Cancer-Lustgarten Foundation Pancreatic Cancer Interception Translational Cancer Research Grant (Grant Number: SU2C-AACR-DT25-17, W.F.P, T.J.) and the Stand Up To Cancer Golden Arrow Early Career Scientist Award (GA-6182, W.F.P.). Stand Up To Cancer is a program of the Entertainment Industry Foundation. Research grants are administered by the American Association for Cancer Research, the scientific partner of SU2C. We thank the Koch Institute Swanson Biotechnology Center for technical support, specifically the Flow Cytometry, Histology, Preclinical Modeling, Imaging & Testing and Integrative Genomics & Bioinformatics core facilities.

## References

1. Royal, R. E. *et al.* Phase 2 trial of single agent Ipilimumab (anti-CTLA-4) for locally advanced or metastatic pancreatic adenocarcinoma. *J. Immunother. (Hagerstown, Md. 1997)* **33**, 828–833 (2010).
2. Brahmer, J. R. *et al.* Safety and activity of anti-PD-L1 antibody in patients with advanced cancer. *N. Engl. J. Med.* **366**, 2455–2465 (2012).
3. O'Reilly, E. M. *et al.* Durvalumab with or Without Tremelimumab for Patients with Metastatic Pancreatic Ductal Adenocarcinoma: A Phase 2 Randomized Clinical Trial. *JAMA Oncol.* **5**, 1431–1438 (2019).
4. Hogquist, K. A. *et al.* T cell receptor antagonist peptides induce positive selection. *Cell* **76**, 17–27 (1994).
5. Maude, S. L. *et al.* Tisagenlecleucel in children and young adults with B-cell lymphoblastic leukemia. *N. Engl. J. Med.* **378**, 439–448 (2018).
6. Neelapu, S. S. *et al.* Axicabtagene ciloleucel CAR T-cell therapy in refractory large B-Cell lymphoma. *N. Engl. J. Med.* **377**, 2531–2544 (2017).
7. Wang, M. *et al.* KTE-X19 CAR T-Cell therapy in relapsed or refractory mantle-cell lymphoma. *N. Engl. J. Med.* (2020) doi:10.1056/NEJMoa1914347.
8. Thistlethwaite, F. C. *et al.* The clinical efficacy of first-generation carcinoembryonic antigen (CEACAM5)-specific CAR T cells is limited by poor persistence and transient pre-conditioning-dependent respiratory toxicity. *Cancer Immunol. Immunother.* **66**, 1425–1436 (2017).
9. Smaglo, B. G. *et al.* A phase I trial targeting advanced or metastatic pancreatic cancer using a combination of standard chemotherapy and adoptively transferred

- nonengineered, multiantigen specific T cells in the first-line setting (TACTOPS). *J. Clin. Oncol.* **38**, 4622–4622 (2020).
10. Beatty, G. L. *et al.* Activity of Mesothelin-Specific Chimeric Antigen Receptor T Cells Against Pancreatic Carcinoma Metastases in a Phase 1 Trial. *Gastroenterology* **155**, 29–32 (2018).
  11. Beatty, G. L. *et al.* Mesothelin-specific chimeric antigen receptor mRNA-engineered T cells induce anti-tumor activity in solid malignancies. *Cancer Immunol. Res.* **2**, 112–120 (2014).
  12. Haas, A. R. *et al.* Phase I Study of Lentiviral-Transduced Chimeric Antigen Receptor-Modified T Cells Recognizing Mesothelin in Advanced Solid Cancers. *Mol. Ther.* **27**, 1919–1929 (2019).
  13. Boj, S. F. *et al.* Organoid models of human and mouse ductal pancreatic cancer. *Cell* **160**, 324–338 (2015).
  14. VanDussen, K. L., Sonnek, N. M. & Stappenbeck, T. S. L-WRN conditioned medium for gastrointestinal epithelial stem cell culture shows replicable batch-to-batch activity levels across multiple research teams. *Stem Cell Res.* **37**, 101430 (2019).
  15. Kim, M. P. *et al.* Generation of orthotopic and heterotopic human pancreatic cancer xenografts in immunodeficient mice. *Nat. Protoc.* **4**, 1670–1680 (2009).
  16. Sastra, S. A. & Olive, K. P. Quantification of Murine Pancreatic Tumors by High Resolution Ultrasound. *Methods Mol. Biol.* **980**, (2013).

